THE UNIVERSITY OF HULL

Antiferroelectric and Ferroelectric Smectic C

Side Chain Liquid Crystal Polymers

Being a Thesis submitted for the Degree of Doctor of Philosophy

at the University of Hull

by

Steven Pringle BSc (Hons)

(Coventry University)

September 1996

PAGE NUMBERING AS ORIGINAL

Summary of Thesis submitted for the Degree of Doctor of Philosophy

by Steven Pringle, BSc (Hons)

Antiferroelectric and Ferroelectric Smectic C Side Chain Liquid Crystal Polymers

Chirality in liquid crystals has been of increasing interest over the past twenty five years. More recently interesting results have been obtained in the area of chiral smectic liquid crystals with the discovery of Twist Grain Boundary (TGB), antiferroelectric and ferrielectric liquid crystal phases.

The thesis is concerned mainly with the investigation into the incidence of novel smectic phases in Side Chain Liquid Crystal Polymers (SCLCPs), and the effect structural variation has on the appearance of these phases.

A study of the effect of lateral fluoro substitution in the rigid core of the molecule on the formation of chiral smectic C phases showed how the position of the fluoro substituent affected the thermal stability of the polymeric material. This study also led to the discovery of an antiferroelectric-like structure in a polymer containing an achiral, swallow-tailed terminal chain.

The thesis also describes an "odd / even" effect when altering the length of the flexible spacer connecting the polymer backbone to the rigid core of the side chain; a polymer with a flexible spacer containing an odd number of carbon atoms exhibits an antiferroelectric phase and the corresponding analogue with an even number of carbon atoms in the flexible spacer exhibits a ferroelectric phase.

The effect of altering the moiety which connects the polymer backbone to the flexible spacer is also examined. Polymers which contain an ether functionality as the linking moiety retain their antiferroelectric properties. However, in

polymers where the linking group is a "reverse ester", a smectic C phase was not observed.

The final structural feature examined in this thesis involved an examination of the effect of changing the substituent on the polymer backbone. It was found that in polymers where the linking group was an ether moiety, or a reversed ester, increasing the size and polarity of the backbone substituent did not alter the phase sequence, but the liquid crystal phase was thermally stabilised. In polymers where the backbone was linked by an ester group, markedly increasing the polarity of the backbone substituent caused the resulting SCLCP to become more glass-like; the mesophase was thermally stabilised and gave poor alignment of the side chains.

ACKNOWLEDGEMENTS

ACKNOWLEDGEMENTS

There have been many people who, over the course of the past three or so years, have supported, influenced, persuaded, cajoled, or simply downright bullied me into not only completing the work in this thesis, but also in completing the writing of this thesis. The following few paragraphs are dedicated to those who have 'helped' me along the way.

Firstly my sincerest gratitude and heartfelt thanks must go to my supervisor Dr Kenneth J. Toyne, for his (often) frank discussions over the three years. My thanks also go to Prof. John W. Goodby for offering me the chance to begin this work, and to DERA / RSRE at Malvern for providing the financial backing.

My thanks go also to the academic staff connected with the Hull Liquid Crystal Group, Dr Mike Hird, Dr David Lacey and Dr Peter Styring for all their valuable discussions, and to Mrs B Worthington, Mr R. Knight and Mr A.D. Roberts for providing spectral analysis of the final compounds and intermediates. A big thankyou must go to all members of Hull University Liquid Crystal Group (past and present), but especially to Dr Alan Hall, Dr Steve Lock and Dr Rachel Tuffin for their useful synthetic discussions. A special thankyou goes to Dr Rob Lewis, Mr Greg Cross, Mr Tim Mann and Dr Alex Seed who helped enormously in matters of chemistry and non-chemistry alike.

Over the past three years I have come into contact with a huge amount of people. The following few are by no means everyone, but are thanked for their friendship, support and kind words of encouragement when the chips were up or down. A special thanks to Andrew McGowan for being a great friend over the past few years.

Without the love and support of my family I simply would not be where I am today. For this, and for everything you've ever done for me I save my greatest thankyou until last. To my parents Bill and Marilyn, thank you. To my brother Chris, thanks. Finally to my grandparents George and Phyllis, thank you for everything. Without these 5 people I could never have completed this mammoth task.

CONTENTS

CONTENTS

CHAPTER 1
INTRODUCTION

INTRODUCTION

1.1 GENERAL INTRODUCTION

In 1888 Austrian botanist Friedrich Reinitzer prepared a number of cholesteryl esters which upon characterisation displayed a peculiar phenomenon when heated. With cholesteryl benzoate (Figure 1.1), Reinitzer observed that the material melted to a milky fluid at 145 °C and then on further heating this milky fluid became clear at 178 °C.[1]
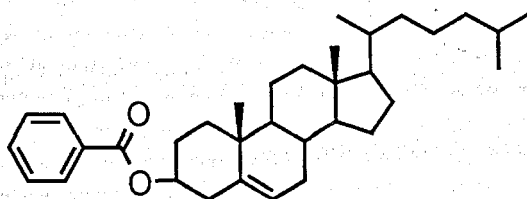
Figure 1.1 - Cholesteryl benzoate

Reinitzer sent a sample of cholesteryl benzoate to the German physicist Otto Lehmann. Lehmann observed that the milky fluid, when viewed through crossed polarisers, appeared (like a solid) brightly coloured and thus he concluded that he was dealing with "very soft crystals" which he christened *fliessende krystalle* (flowing crystals).[2]

By 1920, Vorländer and colleagues had synthesised the liquid crystalline material, ethyl *p*-azoxybenzoate which showed a smectic phase between 114 and 120 °C (Figure 1.2), and Friedel was carrying out optical studies on liquid crystals. Friedel identified the milky fluid observed by Reinitzer and Lehmann as a "phase" which was different from both the crystal phase and the liquid phase and as a result of detailed optical studies determined three different liquid crystal phases; the *Smectic* (S), the *Nematic* (N) and the *Cholesteric* (Ch) phases.[3]
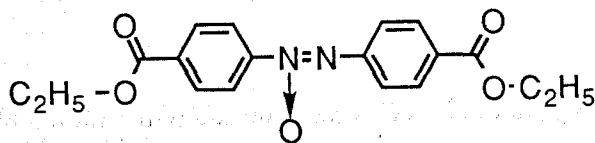
Figure 1.2 - Structure of the Smectic Liquid Crystal Ethyl *p*-azoxybenzoate

Both of the examples given above show the generation of a mesophase by a temperature change; addition of a solvent to a compound can also generate a mesophase (see section 1.2).

In 1963 Fergason produced a novel method for measuring temperature using the colour change of cholesteric liquid crystal phases and in the same year Williams reported the first electrooptical effects in nematic liquid crystals.[4] In 1968 Heilmeier showed that a thin layer of nematic liquid crystal showed a characteristic scattering under an applied voltage and he subsequently invented a new display device using this phenomenon.[5]

In 1971 Schadt and Helfrich, designed a new display configuration called the "Twisted Nematic Mode". This mode has been used widely for many types of liquid crystal display device[6] and is the most commonly used operating principle in current displays with improvements to this device still being achieved.[7] However, other displays which use different liquid crystals and different operating principles, such as ferroelectric displays have also been developed.[8]

1.2 CLASSIFICATION OF LIQUID CRYSTALS[9]

Liquid crystals are divided into *thermotropic* liquid crystals and *lyotropic* liquid crystals, which can be classified and subdivided as shown in Figure 1.3.
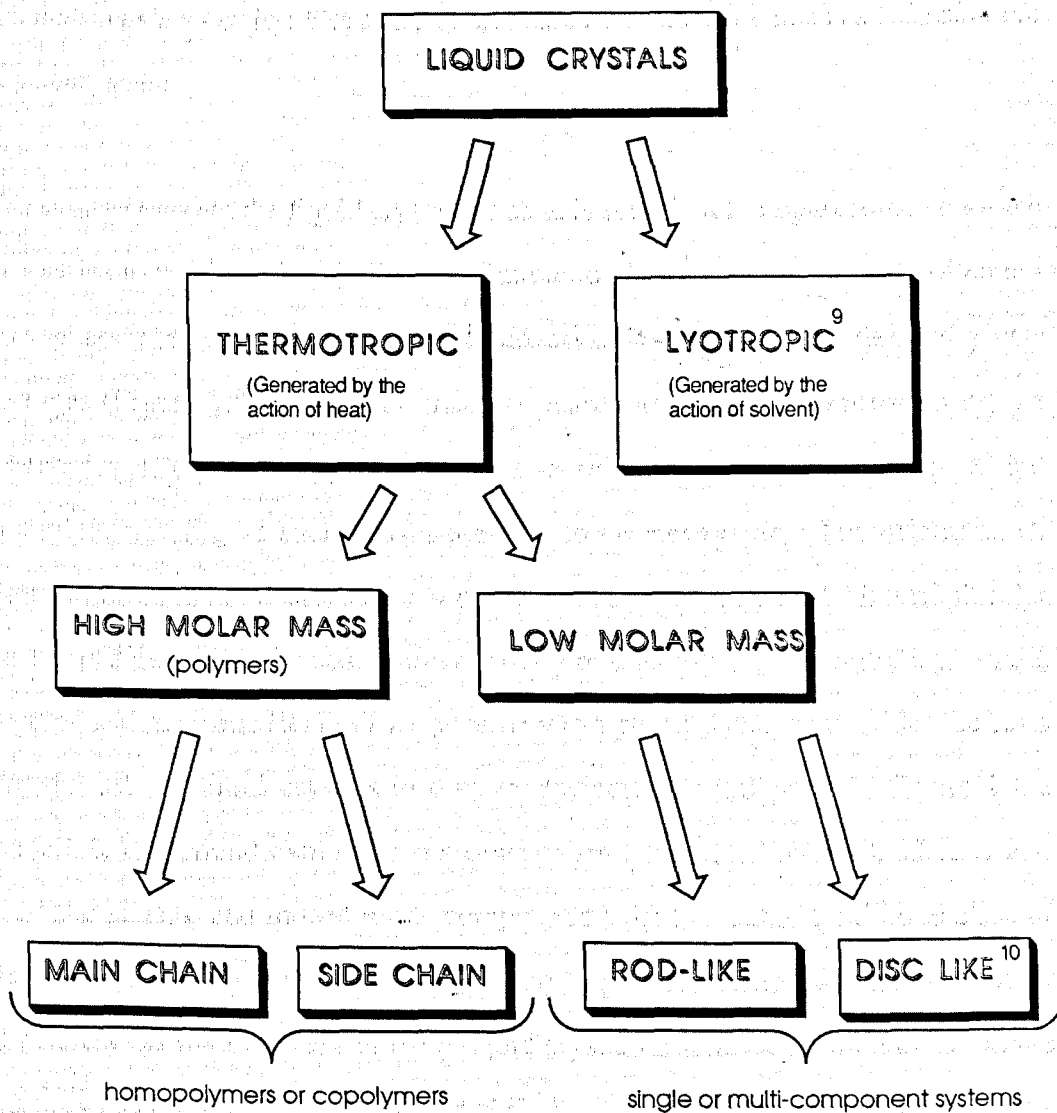
Figure 1.3 - Sub-Classification of Liquid Crystal Systems.[11]

As this thesis is concerned with high molar mass liquid crystals,[12] in particular those displaying the smectic C phase and its subphases, the other classes of liquid crystals will not be discussed further.

1.3 CALAMITIC THERMOTROPIC LIQUID CRYSTAL PHASES

In the following sections the liquid crystalline properties of molecules which have elongated molecular structures are discussed. The shapes of these molecules are referred to as lath- or rod-like and exhibit phases that are sometimes called *calamitic* liquid crystals.

The ordering within the liquid crystalline state is sufficient to impart some solid-like properties to the fluid, but the forces of attraction between molecules are often not strong enough to prevent flow. Liquid crystals undergo well defined phase changes (Figure 1.4) giving intermediate phases, referred to as *mesophases*; the phenomenon of liquid crystallinity is also referred to as *mesomorphism* and materials which give such phases are said to be *mesogenic*. The orientational association of the molecules is only partial and, as the nature of the intermolecular forces is delicately balanced, liquid crystals are sensitive to temperature, pressure, electric and magnetic fields. This sensitivity to a physical change provides the basis for the use of liquid crystals in display devices. As indicated in Figure 1.4 a calamitic compound exhibiting mesomorphism need not show both smectic and nematic phases, and indeed many compounds exist that exhibit only one class of mesophase. Transition temperatures from liquid crystal mesophase to another liquid crystal mesophase, and from liquid crystal mesophase to solid or liquid are usually clearly defined. However in some instances, the temperature at which the transition occurs is reduced, for example, when the compound is cooled from the nematic or smectic to the solid; this is due to a supercooling effect.
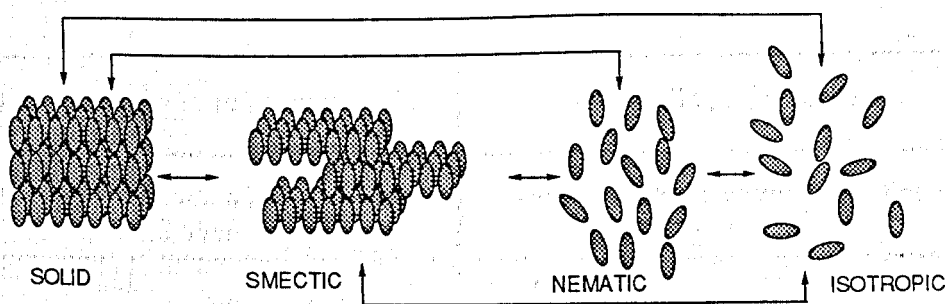
Figure 1.4 - Transitions between Solid, Liquid Crystalline and Isotropic Phases

1.3.1 The Smectic Phase[13]

Smectic phases are lamellar in nature (with the exception of the crystal D phase which has a structure consisting of a cubic close packing arrangement of molecules). Many structural variants of the smectic phase are known and are indicated with subscripts to the letter S (*i.e.* S_A, S_B, S_C *etc.*) (see Table 1.1) with the classes dependent upon how the molecules are arranged in the smectic lamellae, the tilt angle of the molecules with respect to the vertical to the lamellar planes, and upon the degree of correlation with the layers and from layer to layer. It should be noted that the layers need not be rigidly defined or planar and indeed the layers are best regarded as density waves running throughout the system. Currently the S_A, S_B, S_C, S_I and S_F phases are regarded as true liquid crystals and the crystal B, E, J and K (indicated by a letter, *i.e.* B) are considered as soft crystals.[13]

Liquid Crystal Smectics			Crystal Type Smectics		
Type	Order within a Layer	Tilt	Type	Order within a Layer	Tilt
S_A	No	No	B	Yes	No
$S_{B(hexatic)}$	Yes	No	E	Yes	No
S_C	No	Yes	G, J	Yes	Yes
S_F	Yes	Yes	H, K	Yes	Yes
S_I	Yes	Yes			

Table 1.1 Smectic Polymorphic types[13]

1.3.2 The Nematic Phase

The nematic phase is an anisotropic liquid, with the molecules showing only a statistically parallel arrangement of the molecular long axes. The nematic phase is considerably less viscous than the smectic phase, and can be substantially oriented by surface forces. In thin sections between glass slides, the ordered pattern that is established at the surface may be extended across the section.

The cholesteric phase (Ch or N*) is a helical nematic phase (Figure 1.5) with the twist arising from the optically active nature of the chiral molecules. The helicoidal twist of the structure, characterised by a pitch (typically of the order 0.2-2 μm) rotates the electric vector of polarised light as it traverses the mesophase.

1.3.3 Chirality in Liquid Crystals

Chirality in liquid crystals has a unique position; in fact the first material found to exhibit liquid crystal properties was an optically active derivative of cholesterol (Figure 1.1). Chiral liquid crystals can exhibit many properties. Some of these properties are described in the following pages.

1.3.3.1 Cholesteric and Blue Phases

In the cholesteric mesophase (N*) the lath-like molecules pack so as to create a helical macrostructure in a direction perpendicular to their long axes (Figure 1.5). This macrostructure is itself optically active and so the mesophase structure also exhibits its own optical activity, or form chirality.

Molecules

Spiralling Orientational
Order of the Molecules

Half Pitch Length
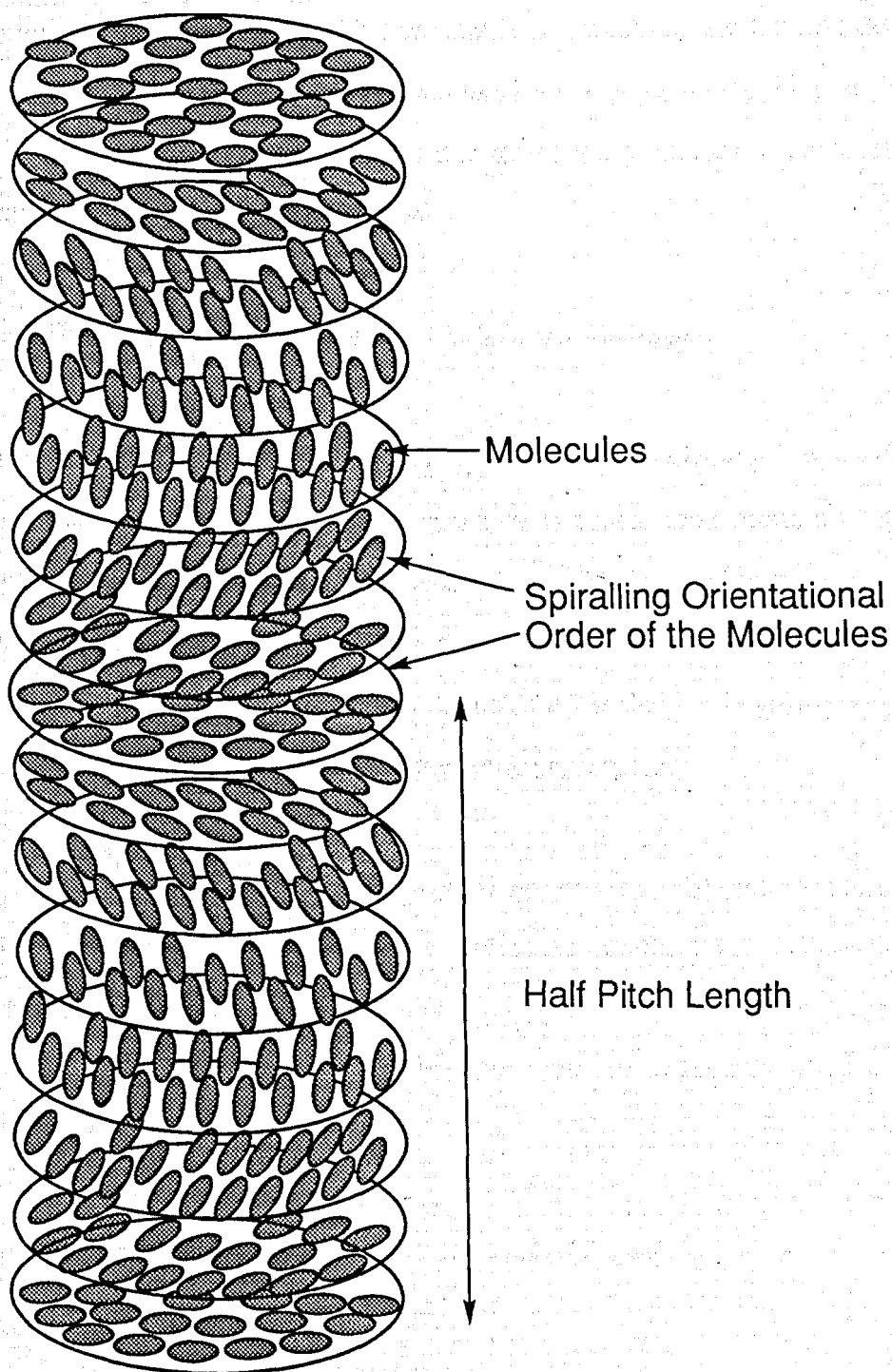
Figure 1.5 - The Cholesteric Phase

If we consider a similar situation where the twist in the orientational order of the
molecules in the cholesteric phase can also occur in a second direction in the plane
perpendicular to the long axis of the molecules, then two helices are formed with
their axes perpendicular to one another in a plane at right angles to the direction of

the long axis of the molecule. This phenomenon was discovered during detailed studies of the optical changes which occur on clearing to the isotropic liquid. These phases were named blue phases (BP) due to the early examples discovered by Coates and Gray[14] being coloured blue.

1.3.3.2 Ferroelectric, Ferrielectric and Antiferroelectric Phases

When a smectic C phase is composed of optically active molecules it will exhibit a helical macrostructure. The helical structure is based upon rotation of the tilt direction of individual layers of the phase about an axis normal to the layer planes on passing from layer to layer. When the helix is unwound the molecules within the layers orientate themselves so that the tilt of the molecules in adjacent layers is the same and the molecules exhibit ferroelectric properties.

Antiferroelectric properties in liquid crystal systems is a fairly recent discovery.[15] In the antiferroelectric S_C* phase the molecules in adjacent layers are tilted in opposite directions. A similar structure is proposed for the ferrielectric S_C* phase however in the ferrielectric phase the distribution of oppositely tilted layers is unequal over the entire system.[16]

Ferroelectric, antiferroelectric and ferrielectric phases are explained further in sections 1.5, 1.6 and 1.6.4 respectively.

1.4 IDENTIFICATION OF MESOPHASES

Smectic, nematic and cholesteric mesophases can usually be distinguished by their optical (*i.e.*, polarised light microscopy),[13,14] miscibility, rheological, diffractive (*e.g.*, X-ray) and thermodynamic (*e.g.*, DSC) properties. The mesophases are most easily identified by using a polarising microscope, since the different phases frequently have recognisably distinct microscopic textures. Examples are the focal-conic, fan-shaped or polygonal textures of smectics (S_A), *schlieren* textures (S_C), and mosaic textures (S_B).[12] A bright satin-like texture is often observed when the nematic phase is viewed between crossed polarisers, although the nematic phase, in common with some smectic phases, also shows a *schlieren* texture consisting of dark brushes, radiating from and ending at points, which form distorted crosses.

The identity of mesophases may be confirmed by miscibility studies. If two mesogenic compounds mix to form a continuous series of solutions showing the same mesophase, then the phases of the two compounds are of the same type. Miscibility studies also allow the latent smectic and nematic tendencies to be assessed for compounds not actually showing mesophases. *Virtual* transition temperatures may be obtained for a compound (X) by studying its mixtures with a suitable host, and assuming near ideal solution behaviour, by performing a linear extrapolation to 100% of X. Such virtual transitions are not observed directly, unlike *enantiotropic* transitions (observed on heating or cooling) and *monotropic* transitions (observed on supercooling of the isotropic phase or a mesophase to below the melting point).

X-ray or neutron diffraction is a useful technique, and is sometimes the only way of identifying the molecular arrangement in the phase and hence the nature of the mesophase type. Thus, X-ray diffraction indicates that the S_C phase has a tilted arrangement of molecules within its layers, whereas the S_A mesophase has an

orthogonal arrangement of the molecules; it also shows that the arrangement of the molecules in the S_A and S_C layers is positionally disordered whereas that in the S_B and E layers is much more ordered. X-ray diffraction also allows the determination of the layer thickness in smectics.

Differential Thermal Analysis (DTA) and Differential Scanning Calorimetry (DSC) allow the determination of the enthalpies of transition (ΔH), *e.g.*, for S_A-N, N-I *etc.*, which are sometimes characteristic for a particular transition, and this information may help in the identification of the mesophases involved. Enthalpies are obtained by DTA by placing the sample in an aluminium pan and heating at a uniform rate. The sample temperature is then monitored by means of a thermocouple and compared with the temperature of a reference, such as an empty pan, which is subjected to the same linear heating. As the temperature of the heating block is raised at a constant rate the sample temperature and that of the reference will be the same until a change in the sample takes place. If the change is exothermic the sample temperature will exceed the reference temperature for a short period. If the change is endothermic sample temperature will temporarily lag behind the reference temperature. These temperature differences are recorded and transmitted to a chart recorder or data station where they are recorded as peaks. A third type of change can be detected. Since the heat capacities of the sample and the reference are different the temperature difference which occurs between the sample and the reference is never actually zero, therefore a change in heat capacity such as that associated with a glass transition will cause a shift in the baseline of the chart recorder.

The temperature difference between the sample and the reference measured by DTA is quantitative and relatively uninformative. To overcome this drawback DSC is used. When a temperature difference between the sample and reference is detected the energy input to either the reference or the sample is increased in order to

maintain both at the same temperature. The thermograms obtained are similar to those obtained by DTA, however the peaks obtained represent the amount of electrical energy supplied to the system and therefore the area under the peaks will be proportional to the change in enthalpy which occurred. Calibration of the instrument will allow the heat capacity of the sample to be calculated in a quantitative manner.

Any single method for identifying mesophases can be misleading and generally it is best to use several methods in combination.

1.5 FERROELECTRIC LIQUID CRYSTALS

1.5.1 Introduction to Ferroelectric Liquid Crystals

Ferroelectricity in crystals has been known since 1921,[18] but ferroelectricity in liquid crystal phases is a relatively recent phenomenon. Meyer *et al.*[19] demonstrated, using an elegant symmetry argument, that the smectic C phase (or any tilted smectic) when composed of optically active molecules should be ferroelectric. Using (*S*)-2-methylbutyl (4-decyloxybenzylidene)-4-aminocinnamate (**DOBAMBC**) (Figure 1.6), they were able to obtain a dielectric hysteresis loop indicating the presence of a spontaneous polarisation (Ps) in the chiral smectic C phase.

$$C_{10}H_{21}O - \text{benzene} - \overset{H}{\underset{}{C}}{=}N - \text{benzene} - \overset{H}{\underset{}{C}}{=}\overset{H}{\underset{}{C}} - \overset{O}{\underset{}{C}} - O - CH_2\overset{*}{C}HC_2H_5 \ (CH_3)$$

DOBAMBC

$$K \xrightarrow{76} S_C{}^* \xrightarrow{93} S_A \xrightarrow{117} Iso\ ^\circ C$$
$$S_C{}^* \xrightarrow{61} S_I{}^*$$
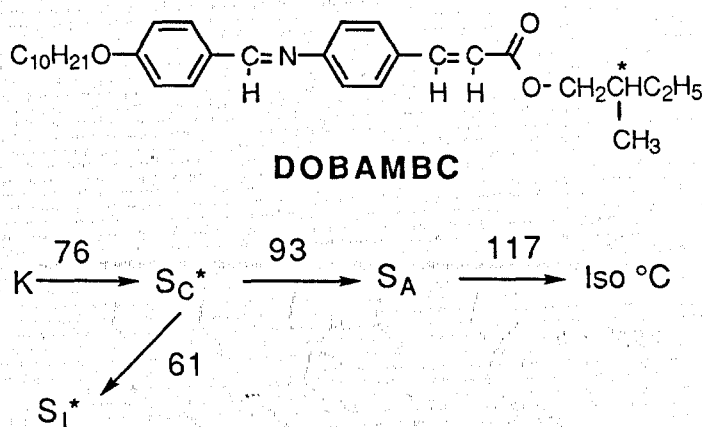
Figure 1.6 - Structure and Transition Temperatures (°C) of DOBAMBC

1.5.2 Symmetry in the Smectic C Phase

If we consider the symmetry for the smectic C phase made up from non optically active molecules (for a guide to the structure of a smectic C phase see Table 1.1), with the molecules arranged in layers having their long axes tilted at an angle θ with

respect to the normal to the layer plane, then the symmetry elements present are a mirror plane, a two-fold axis of rotation and a centre of symmetry. Therefore the symmetry for a non-chiral smectic C phase is C_{2h} (Figure 1.7).
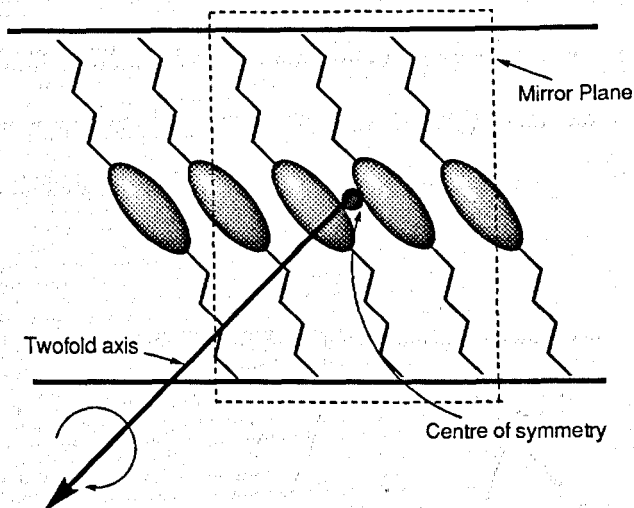
Figure 1.7. - Symmetry of the Smectic C phase
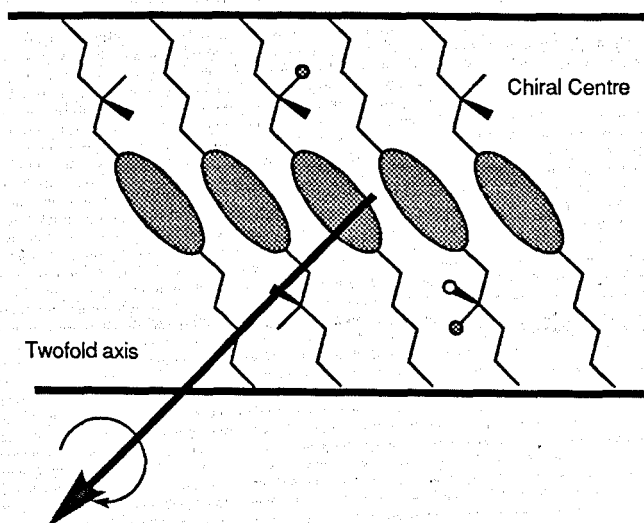
Figure 1.8 - Symmetry of the Smectic C* phase

When this phase is composed of optically active molecules the symmetry elements are reduced to a single two-fold axis parallel to the layer planes and normal to the

vertical planes thus reducing the symmetry to C_2 (Figure 1.8) and causing an imbalance with respect to the dipoles along the C_2 axis.[19]

We can represent an asymmetric molecule by a fish with only one eye[20] (Figure 1.9), with a dipole pointing out of the eye along the y axis; then as the fish prefer to be oriented as shown, there is a two-fold axis in the y direction and it is along this direction that the polarisation develops.
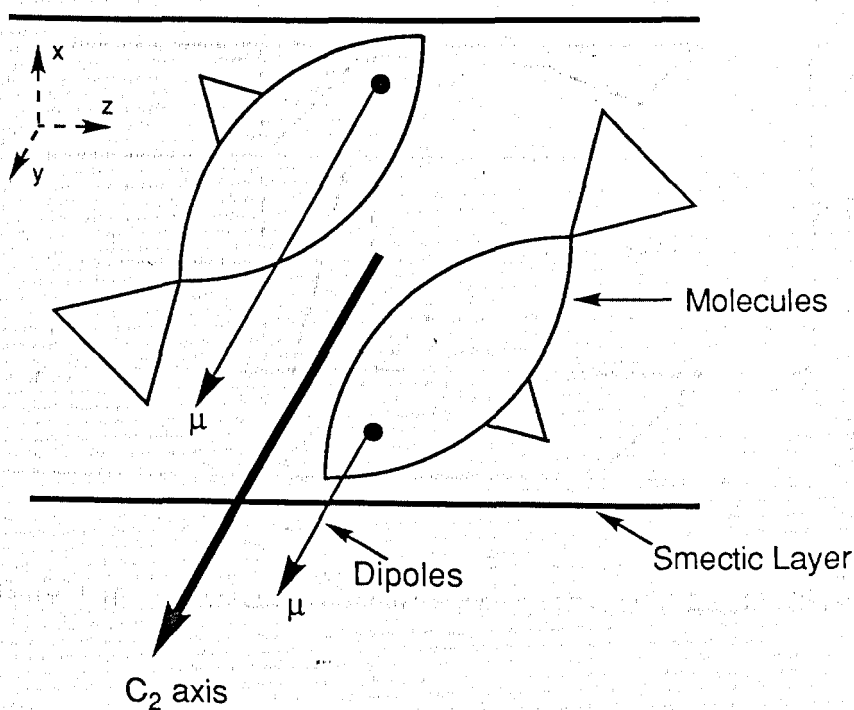
Figure 1.9 - Reduced Symmetry in the Smectic C* Phase

1.5.3 Polarisation Direction

The polarisation is a vector quantity and can point in one of two directions, in our constrained system, and thus a material can have one of two possible spontaneous polarisation directions associated with it[21] (Figure 1.10). The direction is dependent, to a certain extent, on the absolute spatial configuration of the molecule; that is, the (R) and (S) isomers have opposite polarisation directions.
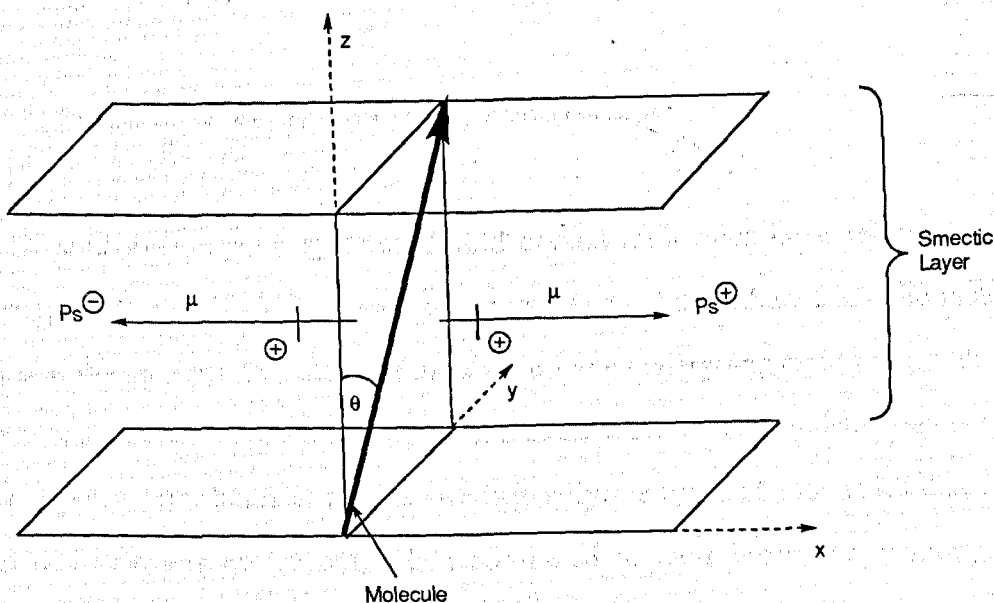
Figure 1.10 - Spontaneous Polarisation Direction in Liquid Crystals

Attempts have been made to relate the absolute spatial configuration of the molecule to the direction of Ps (Figure 1.11) in a similar way to that which Gray and McDonnell used for helical structures (*i.e.* cholesteric systems),[22] with the following relationships found to have some use in S$_C$* liquid crystals.

Sed P (-) +*l*, *Sol P* (+) +*l*, *Sod P* (-) -*l*, *Sel P* (+) -*l*

Red P (-) -*l*, *Rol P* (+) -*l*, *Rod P* (-) +*l*, *Rel P* (+) +*l*

Figure 1.11 - Relationship between Absolute Spatial Configuration and Spontaneous Polarisation[22]

where (*R*) or (*S*) is the absolute spatial configuration, *o* or *e* is the parity, *l* or *d* is the screw direction of the helix, *P*(+) or *P*(-) is the polarisation direction and *-I* or *+I* is the inductive effect of the off axis substituent at the chiral centre. This relationship has been shown to work well for simple molecules but is not accurate for more complex structures.[23]

The fact that such simple correlations exist, however, shows that the microscopic and macroscopic properties of these materials are closely related.

1.5.4 Magnitude of Spontaneous Polarisation

Compared to inorganic systems, liquid crystal molecules have relatively low spontaneous polarisations. These lower values can be attributed to three factors. Firstly, the liquid crystalline molecules are usually undergoing rapid reorientational motion about their molecular long axes, thus only the time dependent alignment of the dipoles contributes to the Ps. Additionally the types of molecules that form ferroelectric phases are not, when compared to their inorganic counterparts, particularly polar. Finally, as the phases are fluid, the molecules can in some cases relax easily after being poled in applied fields.

From a reduction in symmetry it can be deduced that the magnitude of Ps is dependent on the tilt angle θ,[24] the size of the dipole at the chiral centre, and the extent of freedom of rotation the chiral centre has about the molecular long axis. These properties are linked and can be used to describe how the dipole at the chiral centre is coupled to the lateral molecular dipole.

If we consider the following homologous series of compounds[25] (Figure 1.12), we can see that as n increases so the motion of the chiral centre about the molecular long axis decreases.

$$C_8H_{17}-C(=O)-O--C(=O)-O-\overset{*}{\underset{CH_3}{CH}}-C_nH_{2n+1}$$
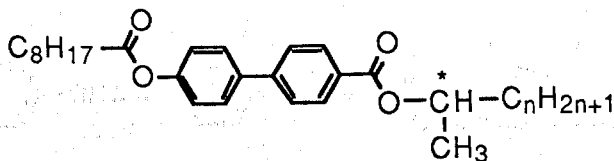
n	P_s ($nC\ cm^{-2}$)
2	7.7
3	32
4	30.7
5	48.8
6	42.2

Figure 1.12 - Effect of Terminal Chiral Chain Length on Spontaneous Polarisation

These results show that for n = 2 the maximum value for P_s is 7.7 nC cm^{-2}, however for n = 5 the value increases almost sevenfold.

As can be seen for the compounds shown in Figure 1.13,[26] the spontaneous polarisation is increased by increasing the dipoles associated with the chiral centre, either by changing the lateral substituent at the chiral centre or by moving the chiral centre closer to the molecule's core

Ps / nC cm^{-2}

$C_{10}H_{21}O$—⬡—CH=N—⬡—CH=CH—C(=O)—O–CH$_2$CHC$_2$H$_5$ | CH$_3$ 5

$C_{10}H_{21}O$—⬡—CH=N—⬡—CH=CH—C(=O)—O–CHC$_2$H$_5$ | CH$_3$ 45

$C_{10}H_{21}O$—⬡—CH=N—⬡—CH=CH—C(=O)—O–CH$_2$CHC$_2$H$_5$ | Cl   40
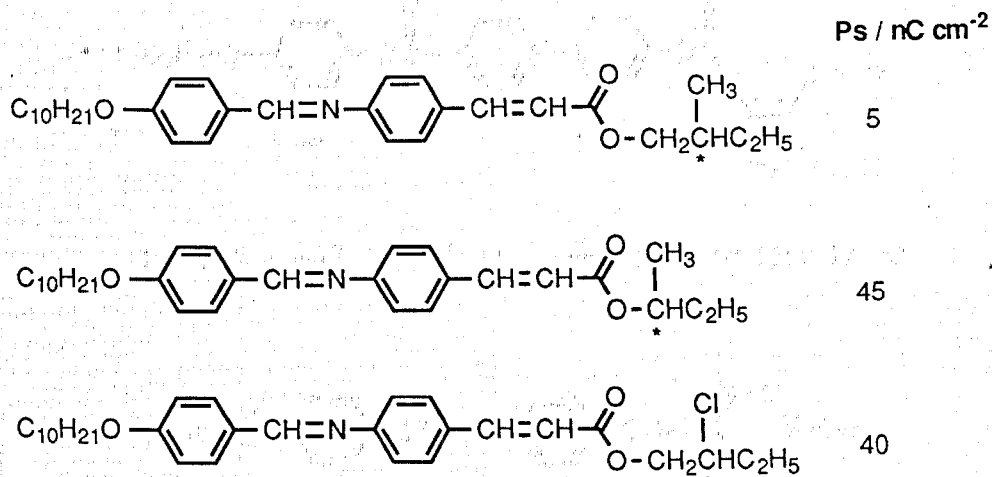
**Figure 1.13 - Effect of Increasing the Dipole at the Chiral
Centre on the Spontaneous Polarisation**

The polarisation also increases dramatically when the motion of the chiral centre is
trapped by steric hindrance of substituents further down the terminal chain (Figure
1.14).[27]

Ps / nC cm^{-2}

$C_7H_{15}O$—⬡⬡—O—C(=O)—CHCH$_2$CHCH$_3$ | Cl | CH$_3$ 80

$C_7H_{15}O$—⬡⬡—O—C(=O)—CHCHCH$_2$CH$_3$ | Cl | CH$_3$ 250
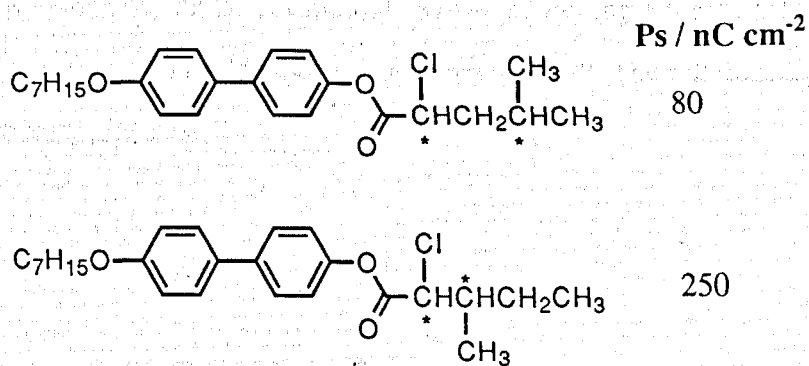
**Figure 1.14 - Effect of Trapping the Motion of the Chiral
Centre on Spontaneous Polarisation**

Further restriction of the motion of the chiral centre can be achieved by having two
chiral centres[28, 29] linked in a carbocyclic ring (Figure 1.15).
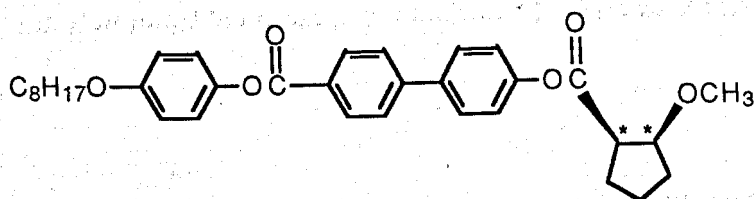
$$Ps = 260 \text{ nC cm}^{-2} \qquad K \quad 54.1 \quad SmC^* \quad 92.8 \quad N^* \quad 161.0 \quad Iso \;°C$$
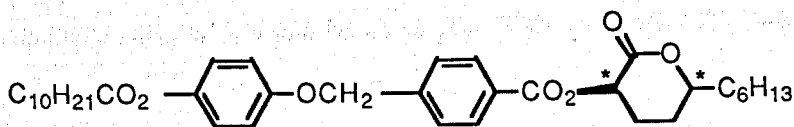
$$Ps = 320 \text{ nC cm}^{-2} \qquad K \quad 108 \quad SmC^* \quad 116 \quad Iso \;°C$$

Figure 1.15 - Spontaneous Polarisation and Transition Temperatures of Ferroelectric Liquid Crystals having Two Chiral Centres

Initially there was considerable interest in increasing the magnitude of the spontaneous polarisation of compounds as the switching time of a ferroelectric liquid crystal was inversely proportional to this value.[30] The relationship is shown in the following equation,

$$\tau \approx \eta / P . E$$

where τ is the reorientational time, η is the viscosity, P is the spontaneous polarisation and E is the applied electric field. It was proposed that the polarisation should be increased in order to reduce the switching time.

More recently low concentrations (*i.e., ca.* 10%) of dopants which are not necessarily liquid crystalline[31] but which have large spontaneous polarisations, have been used in achiral host materials with smectic C phases. These mixtures have lower reorientational viscosities and polarisations than the optically active

material alone, and give switching times in the region of 1-10 μs which are suitable for video rate displays.

1.5.5 Dependence of Spontaneous Polarisation on Temperature

Spontaneous polarisation has been shown to be temperature dependent according to the following expression which can be used as a guide to predict the behaviour of the polarisation,

$$P_S = P_O (T_C - T)^\beta$$

where P_S is the magnitude of the spontaneous polarisation at a temperature T, P_O is a constant for the material, T_C is the smectic A to smectic C* transition temperature and β is an exponent which theoretically should equal 0.5.[32] Figure 1.16 shows a typical plot of spontaneous polarisation against temperature for the ferroelectric material (R)-1-methylpropyl-4-octanoyloxybiphenyl-4'-carboxylate.
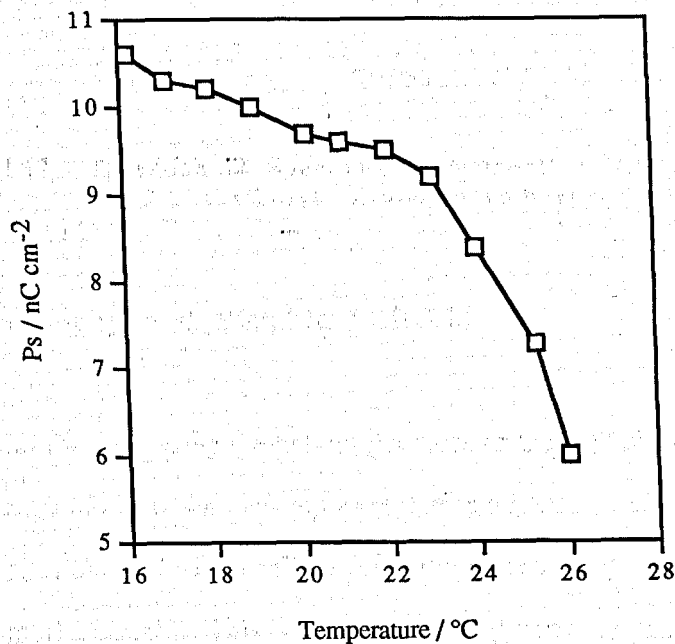
Figure 1.16 - Typical Plot of Spontaneous Polarisation vs Temperature for a Ferroelectric Material

Unusual results can sometimes occur for the dependence of Ps on temperature, *e.g.* (*S*)-2-methylbutyl 4'-nonyloxybiphenyl-4-carboxylate[33] has a negative polarisation direction (see also Figure 1.10) at high temperatures, but as the temperature falls then the direction of the polarisation inverts and becomes positive at lower temperatures (Figure 1.17).
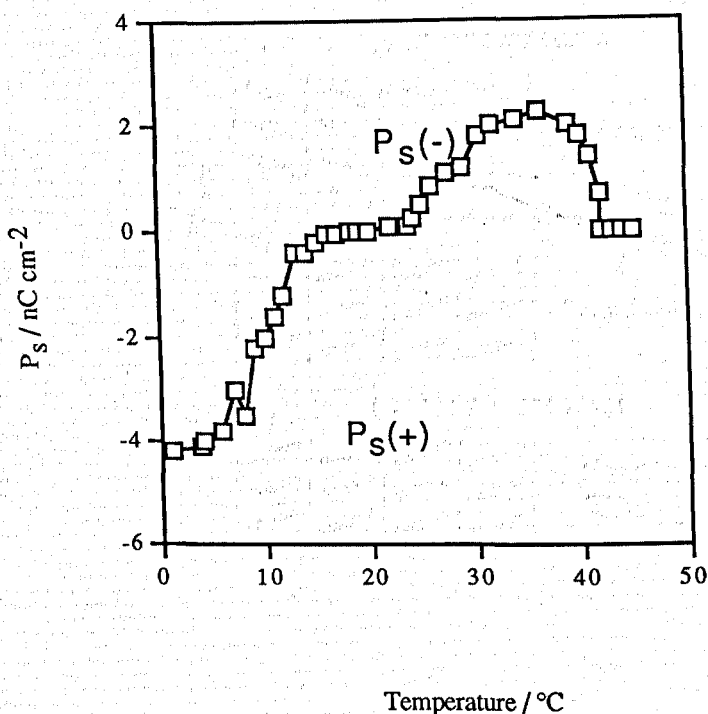
Figure 1.17 - Inversion of Spontaneous Polarisation Direction of (*S*)-2-methylbutyl 4'-nonyloxybiphenyl-4-carboxylate

1.5.6 Ferroelectricity and Bistable Switching

In 1980 a method for unwinding the helical structure of the S_C^* phase was revealed by Clark and Lagerwall[34] when they reported that in a homogeneously aligned cell (*i.e.*, the director is parallel to the cell surface) the helix is unwound when the cell thickness is small enough. This surface-stabilised ferroelectric liquid crystal (SSFLC) can have a net polarisation and inversion of this polarisation can be observed by inverting the polarity of an applied DC voltage (Figure 1.18).
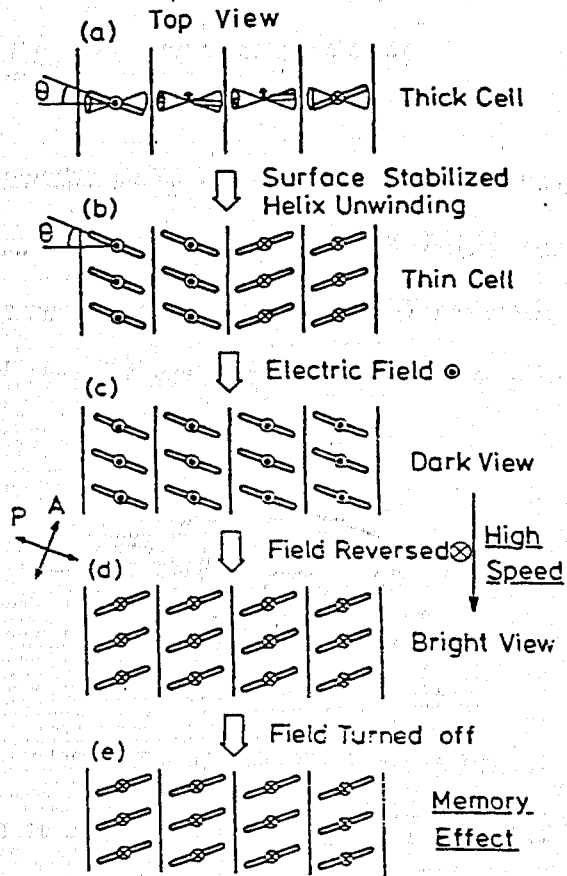
Figure 1.18 - Bistable Switching as proposed by Clark and Lagerwall[34]

1.6 ANTIFERROELECTRIC AND FERRIELECTRIC LIQUID CRYSTAL PHASES

1.6.1 Antiferroelectricity and Tristate Switching

The phenomena of antiferroelectricity and ferrielectricity have been observed in chiral smectic C phases.[35-38] As recently as 1988, Hiji[15] and Furukawa[39] independently reported some unusual behaviour in the ferroelectric material 4-(1-methylheptyloxycarbonyl)phenyl 4'-octyloxybiphenyl-4-carboxylate (MHPOBC) (Figure 1.19).
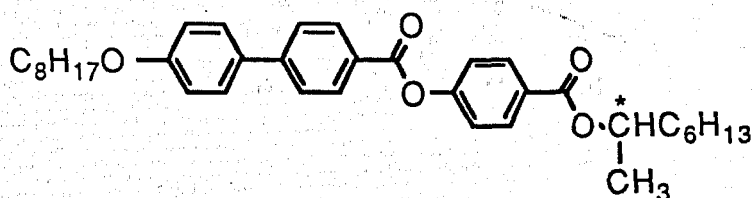
Iso 156.0 S$_A$ 122.0 S$_{C\alpha}$* 120.7 S$_C$* 119.0 S$_{C\gamma}$* 118.3 S$_{C_A}$* 66.0 S$_I$ (anti) 30.0 K °C

Figure 1.19 - Structure and Transition Temperatures (°C) of MHPOBC

Hiji reported, in addition to the bistable state, the appearance of a third state at a certain temperature in electric field studies. Furukawa reported that this state had a clear D.C. threshold behaviour. Chandani et al.[40] proposed a practical application of this tristate switching in a device, with switching between the third state and one of the bistable states showing hysteresis and a sharp threshold (Figure 1.20).

From Figure 1.20 [where FO represents the ferroelectric state, AF represents the antiferroelectric phase, FI represents the ferrielectric state, and (+) or (-) represent the direction of the spontaneous polarisation] we can see that the bistable and tristable switching corresponds to changes in molecular orientation. That is, bistable switching occurs when the material reorients from FO(+) ⟺ FO(-), tristable switching occurs via the reorientation of FO(+) ⟺ AF ⟺ FO(-), and tetrastable switching occurs through FO(+) ⟺ FI(+) ⟺ FI(-) ⟺ FO(-).
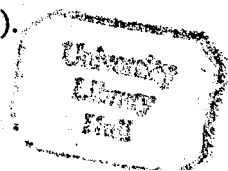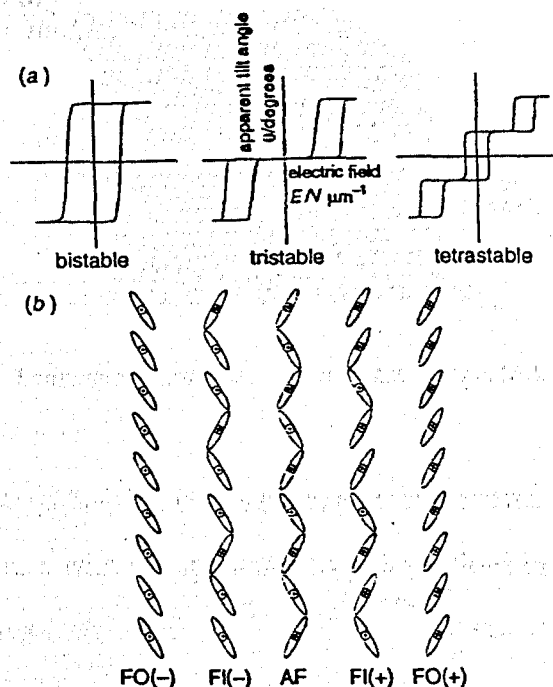
Figure 1.20 - Hysteresis and Molecular Orientation in bistable, tristable & tetrastable states

1.6.2 Discovery of Antiferroelectric Order

In 1989 it was found by using DSC[41, 42] and miscibility studies[41] that this third state was a totally new phase. At the phase transition from the ferroelectric smectic C^* phase to this new state, small peaks were observed in DSC studies, similar to the S_A - S_C^* transition. Miscibility studies of racemic **MHPOBC** with a racemic standard compound [4-(2-methylbutyloxy)phenyl 4'-octyloxybiphenyl-4-carboxylate] showed that this new phase existed between the S_C and S_I but was not miscible with the S_{Bhex} phase.

The proposed structure of this new, antiferroelectric phase, designated S_{CA}^* (where the subscript A refers to the antiferroelectric nature of the phase) can be seen in Figure 1.21.
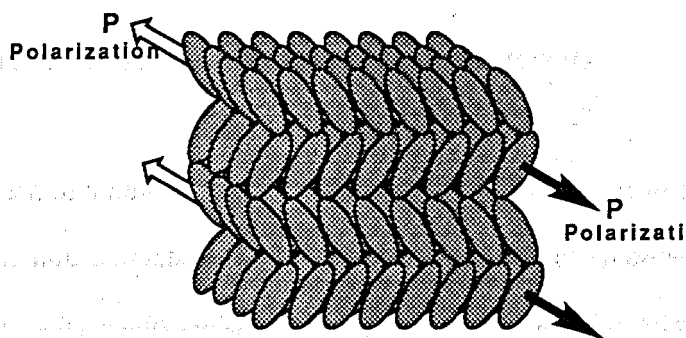
Figure 1.21 - Proposed Structure of the Antiferroelectric Phase

The molecules in the neighbouring layers tilt in almost the same direction in space but in the opposite sense, with the spontaneous polarisations in the neighbouring layers thereby cancelling each other.

Confirmation of this structure has been further enhanced by the conoscopic observations reported by Gorecka et al.[43] By studying (S)-**MHPOBC** they found that in the ferroelectric range, the uniaxial profile at 0 V changed to a biaxial profile on application of an electric field and that the centre of the conoscopic figure moved to one side as the field voltage is increased [due to (S)-**MHPOBC** having a positive spontaneous polarisation]. On reducing the temperature into the antiferroelectric range no centre shift is observed on application of a voltage, suggesting the absence of a spontaneous polarisation. This result is consistent with the alternating structure shown in Figure 1.21.

X-Ray diffraction studies performed by Suzuki et al.[44] on (R)-MHPOBC have shown a thermal hysteresis effect i.e., on cooling the compound a chevron structure is formed by the molecules in the S_{CA}* phase. On heating a bookshelf structure is obtained. It should be noted that this thermal hysteresis is only observed when the cooling process is carried out to below 65 °C and that when the temperature on cooling does not reach 65 °C and the material is heated then the chevron structure remains.

1.6.3 Antiferroelectric Liquid Crystalline Materials

Due to the advent of a new type of electrooptic device[45], interest in the synthesis of antiferroelectric liquid crystalline materials has considerably increased over recent years. Several important relationships between molecular structure and the appearance of the smectic C_A* phase have been established.

1.6.3.1 The Chiral Centre

Most S_{CA}* materials have similar structures around the chiral centre as can be seen in Figure 1.22. Structures (a)[15] and (b)[46] are suitable for obtaining the S_{CA}* phase whereas (c) and (d) are generally unsuitable.
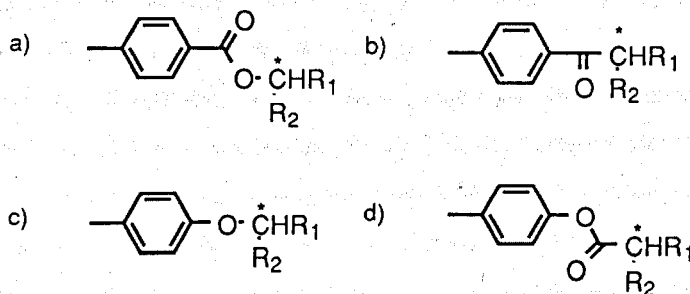
Figure 1.22 - Favourable [(a) and (b)] and Unfavourable [(c) and (d)] Structures around the Chiral Centre for the Appearance of an Antiferroelectric Structure

1.6.3.2 Direction of Ester Groups

It is generally important that ester groups within the molecule are aligned in a certain direction.

In general the ester groups in a liquid crystalline molecule which displays an antiferroelectric mesophase are 'pointed' towards the chiral centre [*i.e.* Figure 1.23(g)]. Molecules in which one of the ester groups 'point' away from the chiral centre generally do not exhibit an antiferroelectric mesophase [i.e.Figure 1.32 (h)]. Ester moieties which are pointed in this direction can be termed *reverse esters*. For example compounds (e), (g) and (i) in Figure 1.23 exhibit the $S_{CA}*$ phase whereas the isomeric compounds (f), (h) and (j), which contain a reversed ester, do not.[15, 46, 47]

(e)

Iso 136 S$_A$ 108 S$_C$* 49 S$_{CA}$*

(f)

Iso 132 S$_A$ 100 S$_C$*

(g)

Iso 145.2 S$_A$ 115 S$_C$* 103 S$_{CA}$*

(h)

Iso 101.3 S$_A$ 92.0 S$_C$*

(i)

Iso 137 S$_A$ 115 S$_C$* 96 S$_{CA}$*

(j)

Iso 105 S$_A$ 102 S$_C$*
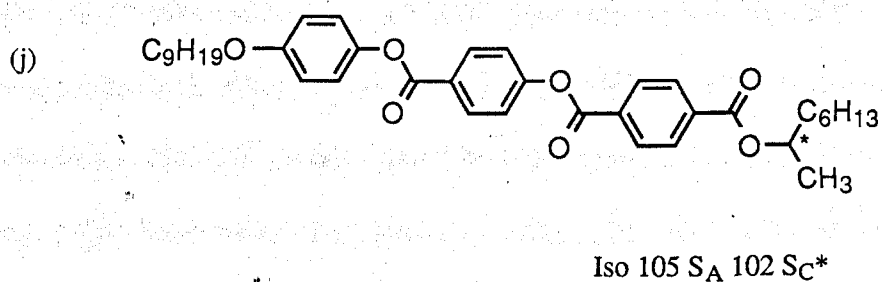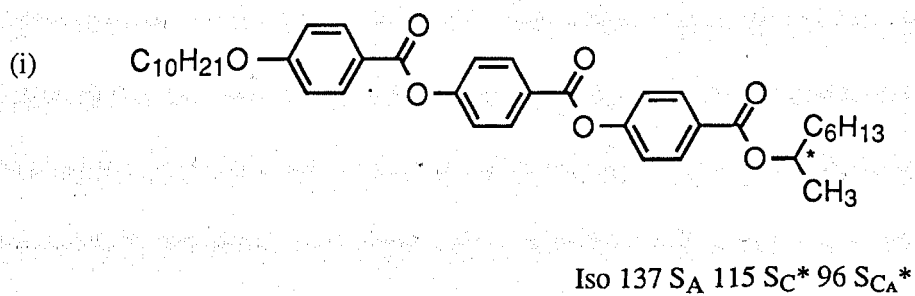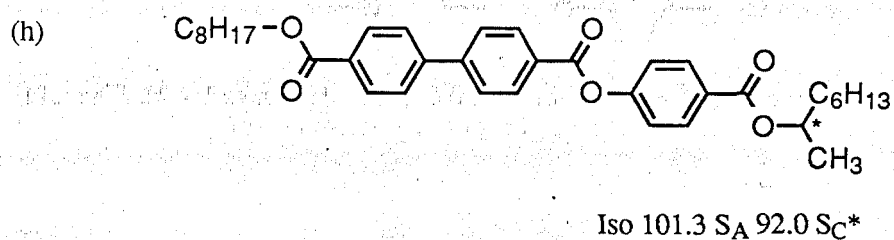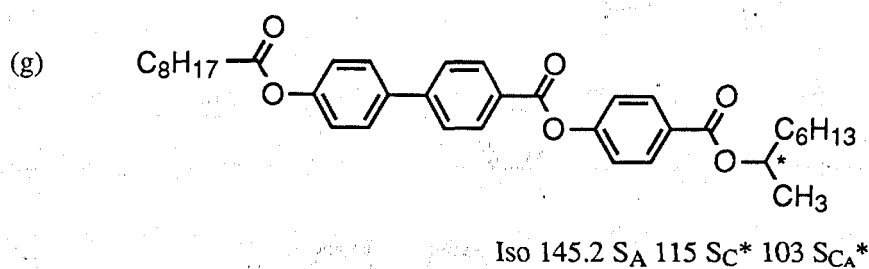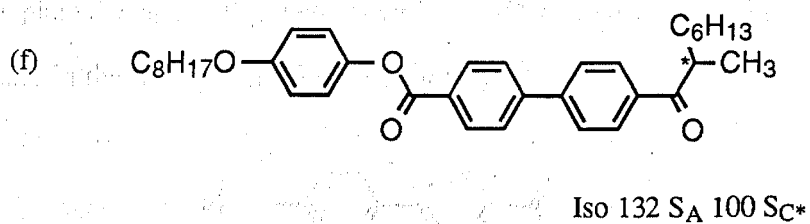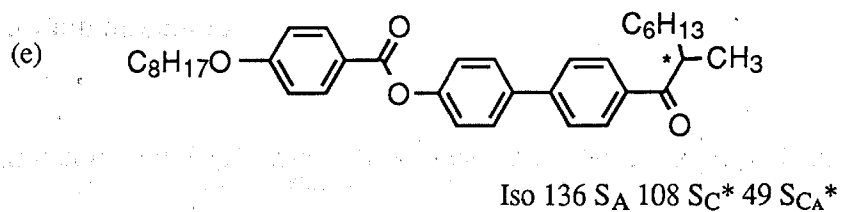
Figure 1.23 - Structures and Transition Temperatures (°C) of Ferroelectric and Antiferroelectric Liquid Crystals

1.6.3.3 Core Structures

The most common S_{CA}^* materials possess three phenyl rings, with an ester group in the core region as shown in Figure 1.24. However it is possible to replace one of the phenyl rings with a heterocyclic ring[48] and still retain the antiferroelectric structure in the mesophase [Figure 1.24 (m)].
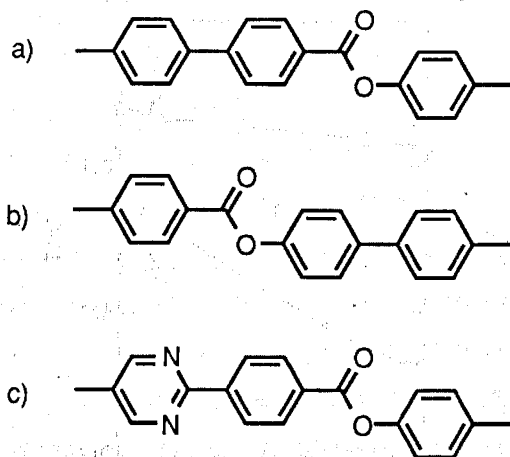
Figure 1.24 - Favourable Core Structures for the Appearance of an Antiferroelectric Liquid Crystal Phase

1.6.4 Ferrielectric Liquid Crystals

The antiferroelectric liquid crystal **MHPOBC** (Figure 1.19) shows not only the S_C^* and S_{CA}^* phases but also certain subphases in the S_C^* region which were noted by Fukui et al.[42] by DSC measurements. Further work was performed by Chandani et al.[41] and Takezoe et al.[49] who produced the following phase diagram.
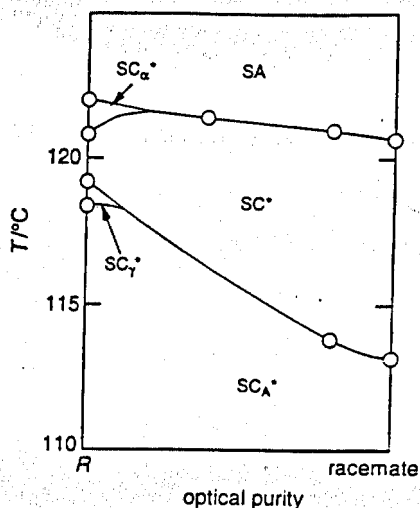
Figure 1.25 - Binary Phase Diagram of Transition Temperatures vs Enantiomeric Excess in MHPOBC

The subphases detailed were tentatively assigned as the $S_{C\alpha}^*$, $S_{C\beta}^*$ and $S_{C\gamma}^*$ phases in their order of occurrence at decreasing temperature. The $S_{C\beta}^*$ phase was subsequently identified as the ordinary S_C^* ferroelectric phase.

By observing the conoscopic figures of the various phases under an applied electric field, Gorecka et al.[43] concluded that the $S_{C\gamma}^*$ phase is a ferrielectric phase and was found to have an apparent tilt angle and polarisation intermediate to those of the ferroelectric and antiferroelectric phases. The $S_{C\gamma}^*$ phase has been assigned the structure exemplified in Figure 1.26 which shows a greater number of layers having a specific tilt direction than those having the opposite tilt direction.
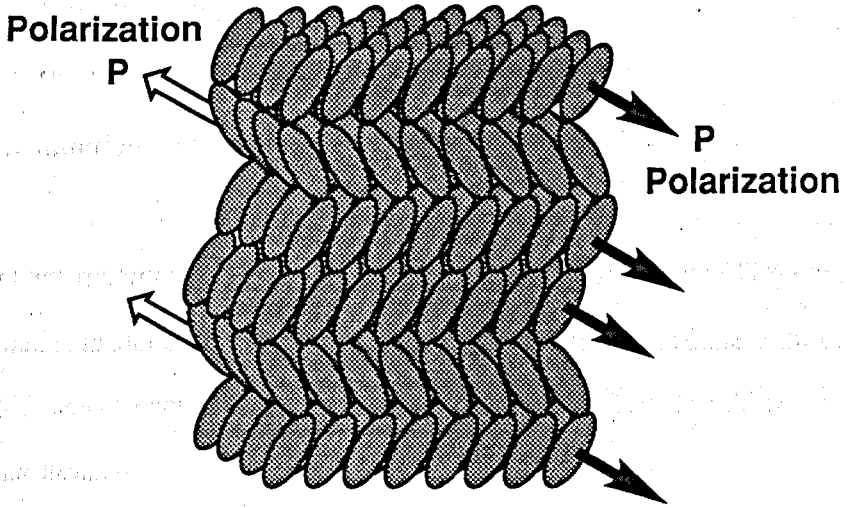
Figure 1.26 - The Structure of a Ferrielectric Phase

1.7 POLYMERS AND POLYMER KINETICS

1.7.1 Introduction

Polymers are macromolecules built up by the linking together of large numbers of much smaller molecules. These small molecules which combine with each other are called *monomers* and the reactions in which they combine are termed *polymerisations*.

1.7.2 Step and Chain Polymerisation

When a polymerisation reaction takes place it usually occurs in one of two distinct ways leading to one of two different types of polymer which were initially classified by Carothers in 1929[50] as *condensation* and *addition* polymers. Condensation polymers were classified as those formed from the reaction of two polyfunctional monomers, the reaction of which involves the elimination of a small molecule *e.g.*, a reaction between a diamine and a diacid. An example of this is the reaction between hexamethylenediamine and adipic acid, to form poly(hexamethylene adipamide) or Nylon 6,6 (Figure 1.27).

$$n \ H_2N\text{-}(CH_2)_6\text{-}NH_2 \quad + \quad n \ HOOC\text{-}(CH_2)_4COOH$$

$$\downarrow$$

$$H\text{---}\left(NH\text{-}(CH_2)_6\text{-}NHCO\text{-}(CH_2)_4\text{-}CO\right)_n\text{---}OH \quad + \quad (2n\text{-}1) \ H_2O$$
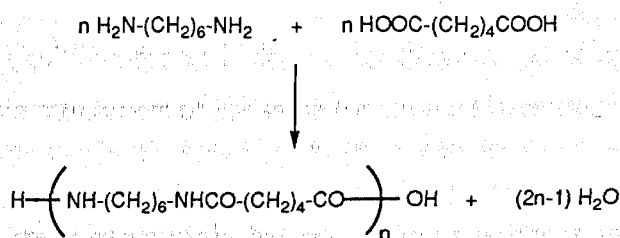
Figure 1.27 - Formation of Nylon 6,6 *via* a Condensation reaction

Addition polymers were classified by Carothers as those formed from monomers without the loss of a small molecule and the majority of addition polymers are formed from vinyl monomers which are forced to react with each other *e.g.*,

$$n\ CH_2=CHY \longrightarrow \left(CH_2-CHY\right)_n$$
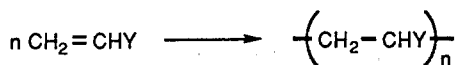
With the development of polymer science, Carothers' original classifications were found to be inadequate. For example, poly(urethanes) are formed by the reaction of diols with diisocyanates without the elimination of a small molecule, *i.e.*,

$$n\ HO-X-OH\ +\ n\ OCN-Y-NCO$$

$$HO\left(X-O\underset{O}{\overset{\parallel}{C}}NHYNH\underset{O}{\overset{\parallel}{C}}O\right)_n XO\underset{O}{\overset{\parallel}{C}}NHYNCO$$
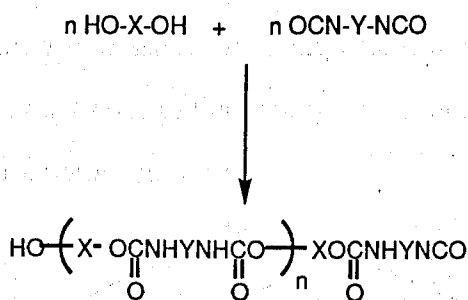
Using Carothers' original classification, poly(urethanes) would be classified as addition polymers since the polymer repeat unit has the same net weight as the monomer. However the polyurethanes are structurally more similar to condensation polymers.

To avoid this confusion polymers have been re-classified into *step* and *chain* polymers, with step polymers being those where the polymer is formed by the step-wise alternating addition of two different monomeric molecules to form a polymer. Chain polymers are defined as those where the polymer is formed from the reaction of two monomers of the same (or similar) structure.

There are three main structural shapes in which polymer molecules can be produced. Polymers can be classified as *linear, branched,* or *crosslinked* (see Figure 1.28). Polymers in which the monomer molecules are linked together in one continuous length to form the polymer are termed linear polymers. Branched polymers can be formed in both step and chain polymerisations and are compounds in which there are side branches of linked polymer molecules

protruding from various points along the polymer chain. The branched polymer can be comb-like with either long (A) or short (B) branches. When there is extensive branching the polymer can have a dendritic structure in which there are branches protruding from other branches, *i.e.*, branched branches (C). The branching of polymers usually has a large effect on many of their properties, the most significant being the decrease in crystallinity (due to a decrease in packing ability) as the branching increases. It is important to point out that the term 'branched polymer' does not refer to linear polymers containing side groups which are simply part of the monomer structure.
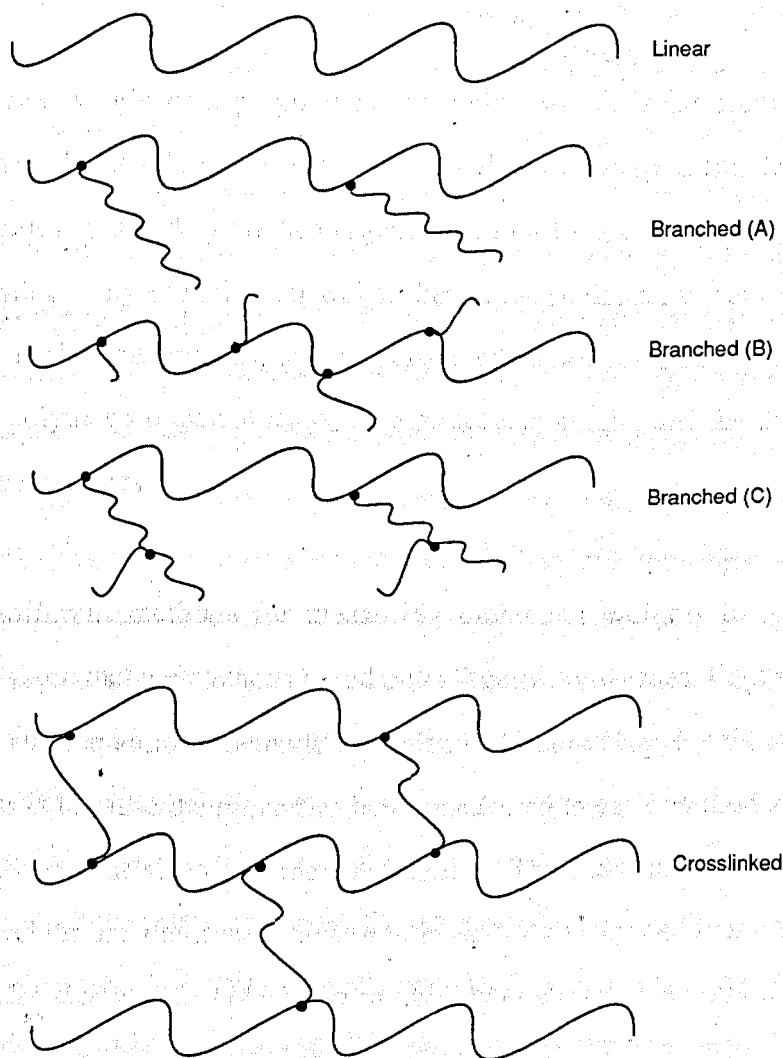
Figure 1.28 - Structure of linear, branched and crosslinked polymers

When polymers are produced in such a way that the polymer molecules are linked together at points other than their ends, the polymers are said to be crosslinked. Crosslinking can be made to occur during polymerisation by using the appropriate set of monomers, or after polymerisation has taken place by various chemical reactions. The number of crosslinks can be varied to give lightly or highly crosslinked polymers. When the number of crosslinks is sufficiently high a three-dimensional network polymer is produced.

1.7.3 Polymers and Molecular Weight

The molecular weight of a polymer is something which is different from the molecular weight of a low molar mass molecule. Polymers differ from small sized molecules in that they are heterogeneous in molecular weight. The reason for this polydispersity of molecular weight lies in the statistical variations present in the polymerisation process, and therefore when we look at the molecular weight of a polymer we look at its average molecular weight, and the distribution of its different weights.

There are different methods for measuring molecular weights in a polymer sample, and these include methods based on colligative properties, light scattering or viscosity and the various methods used give different values for the molecular weight. This is because the properties being measured in each method are biased towards the different sized polymer molecules. The most important types of molecular weight are the *number average molecular weight* ($\overline{M}n$), the *weight average molecular weight* ($\overline{M}w$) and the *viscosity average molecular weight* ($\overline{M}v$).

The number average molecular weight is determined by the measurement of colligative properties such as osmotic pressure, freezing point depression *etc.*

$\overline{M}n$ is defined as the total weight, w, of all the molecules in a polymer sample divided by the total number of molecules present. Thus $\overline{M}n$ is defined by

$$\overline{M}n = \frac{w}{\sum N_x} = \frac{\sum N_x.M_x}{\sum N_x} \qquad \text{... (1)}$$

where the summations are over all the different sizes of polymer molecules from $x = 1$ to $x = \infty$ and N_x is the number of molecules whose weight is M_x. Equation (1) can therefore be written as

$$\overline{M}n = \sum \underline{N}_x.M_x \qquad \text{... (2)}$$

where $\underline{N}_x$ is the mole fraction (or number fraction) of molecules of size M_x.

The weight average molecular weight $\overline{M}w$ can be obtained from light scattering measurements and is defined as

$$\overline{M}w = \sum w_x.M_x \qquad \text{... (3)}$$

where w_x is the weight fraction of molecules whose weight is M_x.

The viscosity average molecular weight, $\overline{M}v$ is obtained from viscosity measurements and is defined by

$$\overline{M}v = \left[\sum w_x.M_x \right]^{1/a} = \left[\frac{\sum N_x.M_x^{a+1}}{\sum N_x.M_x} \right]^{1/a} \qquad \text{... (4)}$$

where a is a constant. The viscosity average molecular weight and the weight average molecular weight are equal when a=1, however $\overline{M}v$ is usually almost always less than $\overline{M}w$ since a is usually in the range of 0.5 - 0.9.

To characterise a polymer sample with reasonable accuracy more than one molecular weight is usually required. For a polydisperse polymer $\overline{M}w > \overline{M}v > \overline{M}n$ and a typical polymer sample has a molecular weight distribution as shown in Figure 1.29.
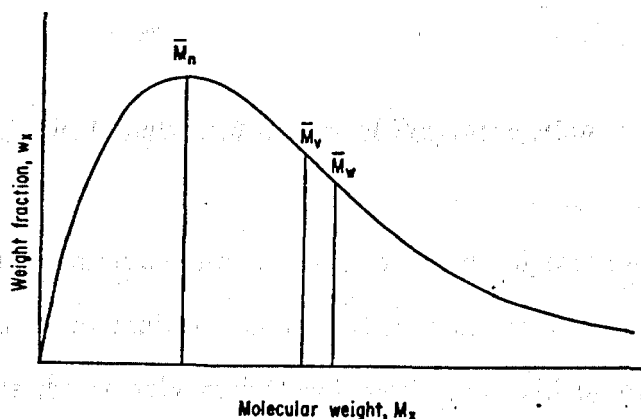
Figure 1.29 - Dispersion of Molecular Weights in a Polymer Sample

For most practical purposes a polymer is characterised by measuring $\overline{M}n$ and $\overline{M}w$ (as $\overline{M}v$ is a close approximation of $\overline{M}w$ - usually within 10%). The ratio of these two molecular weights is known as the *polydispersity* (γ) of the polymer and is dependent on the width of the distribution curve as shown in Figure 1.29.

The determination of the molecular weight distribution of a polymer sample by conventional fractionation techniques is time consuming. A quicker and efficient method which allows the molecular weight distribution to be determined in a fraction of the time is gel permeation chromatography (GPC). GPC separates the polymer samples into fractions according to their molecular size by means of a sieving action. This is achieved using a non-ionic stationary phase of packed spheres whose pore size can be controlled (often beads of cross-linked polystyrene). With a wide distribution of pore sizes in any support gel a separation into molecular size is obtained because the larger molecules dissolved in the solvent carrier cannot diffuse into the pores and are rapidly eluted, while the smaller ones penetrate further with decreasing size and are retarded

correspondingly. Thus the larger molecules leave the column first and the small ones last because they travel a much longer path.[51]

1.7.4 Kinetic Chain Length and Degree of Polymerisation

Polymerisation of unsaturated monomers by chain polymerisation can occur in one of three ways - by radical, anionic and cationic processes. However for the purposes of this thesis only radical polymerisation will be discussed. Chain polymerisation is initiated in unsaturated compounds by a reactive species I* produced from some compound I, which is termed the initiator, *i.e.*

$$I \longrightarrow I^*$$
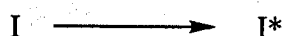
This reactive species then adds to a monomer molecule by homolytically opening the pi bond to form a new radical, and the process is repeated as successive monomer molecules are added.

Radical chain polymerisation can be considered as a chain reaction consisting of three steps - *initiation*, *propagation* and *termination*. The initiation step is considered to contain two reactions. The first of these reactions is the homolytic dissociation of an initiator species to yield a pair of radicals,

$$I \xrightarrow{k_d} 2R \cdot \qquad \qquad ... (5)$$

where k_d is the rate constant for the initiator dissociation. The second part of the initiation reaction involves the addition of this radical to a monomer molecule thus,

$$R \cdot + M \xrightarrow{k_i} M_1 \cdot \qquad \qquad ... (6)$$
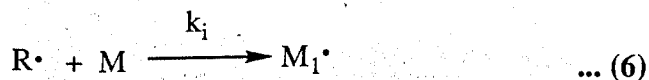
where M represents the monomer molecule and k_i is the rate constant for the initiation step.

Propagation of the polymer chain then proceeds with $M_1 \cdot$ adding to a further monomer molecule, which is in turn followed by successive additions , *i.e.*

$$M_1^{\bullet} + M \xrightarrow{k_p} M_2^{\bullet}$$

$$M_2^{\bullet} + M \xrightarrow{k_p} M_3^{\bullet}$$

$$M_3^{\bullet} + M \xrightarrow{k_p} M_4^{\bullet}$$
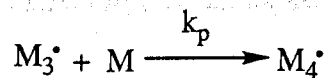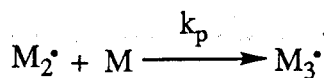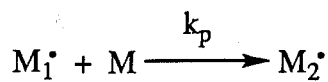
or in general terms

$$M_n^{\bullet} + M \xrightarrow{k_p} M_{n+1}^{\bullet} \qquad \ldots (7)$$
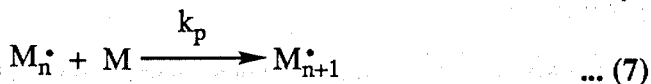
where k_p is the rate constant for propagation. At some point the propagating polymer chain stops growing and the termination process can occur in one of two ways. The first is where two radicals come together and form a polymer *via* a *combination* (or *coupling*) reaction, *i.e.*,
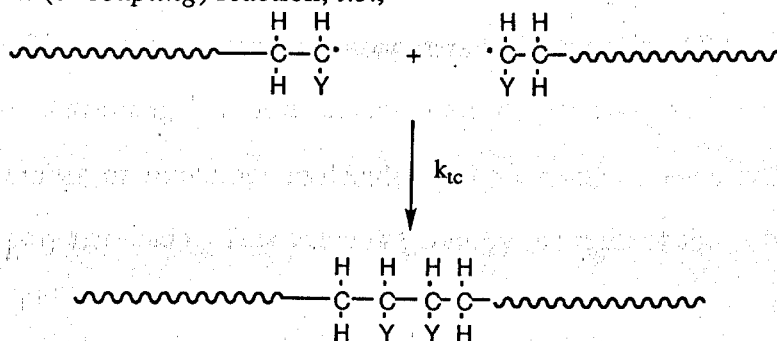
More rarely, termination occurs *via* a disproportionation reaction where a hydrogen radical that is β to a radical centre is transferred to another radical centre resulting in the formation of two polymer molecules - one saturated and the other unsaturated.
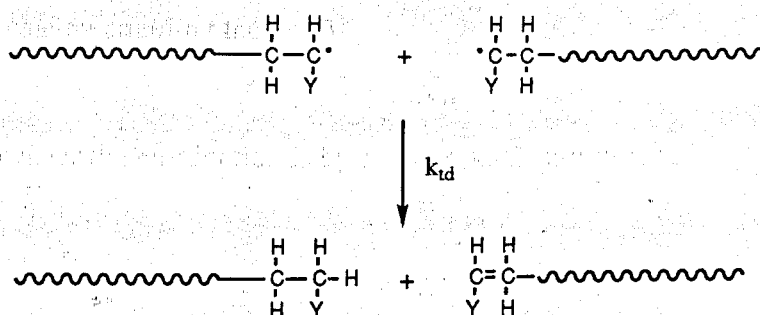
The two different modes of termination can be represented in general terms by

$$M_n^{\bullet} + M_m^{\bullet} \xrightarrow{k_{tc}} M_{n+m} \qquad \ldots (8)$$

and
$$M_n^\bullet + M_m^\bullet \xrightarrow{k_{td}} M_nH + M_m(\text{-}H) \qquad \text{... (9)}$$
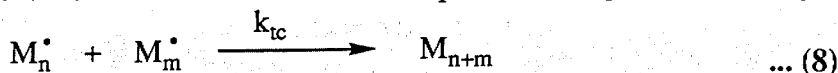
where k_{tc} and k_{td} are the rate constants for termination and combination respectively. The termination step can also be expressed in a combined fashion by

$$M_n^\bullet + M_m^\bullet \xrightarrow{k_t} \text{Dead Polymer} \qquad \text{... (10)}$$
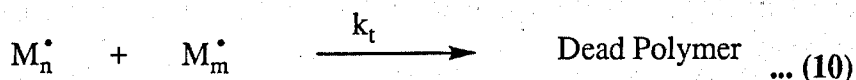
where the mode of termination is not expressed and

$$k_t = k_{tc} + k_{td} \qquad \text{... (11)}$$

If we consider each radical formed in the initiation process, and its subsequent propagation to form a polymer chain, then clearly not all of the radicals formed will react with the same number of monomers to form chains of the same length. The *kinetic chain length*, ν of a radical chain polymerisation is defined as the average number of monomer molecules polymerised by each radical which initiates a polymer chain. This value is given by the ratio of the polymerisation rate to the initiation rate or the termination rate (as under steady state conditions the two are equal).

The kinetic chain length of a polymer can be related to its *number average degree of polymerisation*, $\overline{X}n$. The degree of polymerisation is defined as the number of monomer molecules contained in a polymer molecule. If the propagating radicals terminate by coupling then

$$\overline{X}n = 2\nu \qquad \text{... (12)}$$

If, however the termination is by a disproportionation reaction then

$$\overline{X}n = \nu \qquad \text{... (13)}$$

We can also relate the number average degree of polymerisation to the number average molecular weight by

$$\overline{M}n = M_o.\overline{X}n \qquad \text{... (14)}$$

where M_0 is the weight of the monomer.

1.8 LIQUID CRYSTAL POLYMERS (LCPs)

Liquid crystal polymers (LCPs) are high molecular mass polymeric materials which exhibit mesomorphism. Traditionally two main classes of thermotropic LCPs have been identified, these being main chain and side chain (MCLCPs and SCLCPs respectively). However, more recently, other variants have been identified such as combined LCPs[52, 53] and the rigid rod types as described by Watanabe et al.[54]

1.8.1 Main Chain Liquid Crystal Polymers (MCLCPs)

MCLCPs are those where the mesogenic moiety is contained within the polymer backbone. These polymers can be separated into two types, those that do not contain a flexible spacer linkage and those that do (see Figure 1.30).
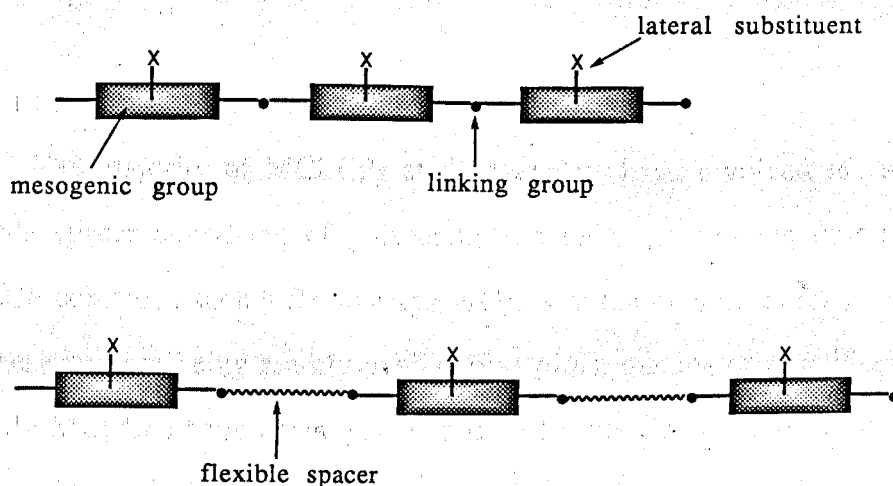
Figure 1.30 - Main Chain LCPs Without and With Flexible Spacer Groups

The incorporation of a flexible alkyl chain in the polymer backbone has the effect of markedly improving solubility and lowering transition temperatures in comparison with the rigid-rod type of polymer with comparable composition.[55]

Rigid-rod polymers may however be modified in other ways to improve their processability, and these polymers are receiving increased attention.[56]

In addition to the use of a flexible spacer, other methods can be used to reduce the transition temperatures of MCLCPs; these approaches include

(a) use of substituents,

(b) addition of a unit to cause dissymmetry of the main chain by copolymerising mesogenic units of different shapes (frustrated chain packing), and

(c) copolymerising non-linear non-mesogenic units.[57]

All of these methods can reduce transition temperatures without adversely affecting the range over which the mesophase occurs[52, 57], but the majority of work concerning MCLCPs has been concerned with the use of flexible spacer units for this purpose.

1.8.1.1 Flexible Spacers in MCLCPs

The majority of MCLCPs studied to date have involved the use of a flexible spacer consisting of polymethylene units (indeed the first reported MCLCP contained such a flexible spacer[58]), with the monomers (or precursors) for these spacers being readily available as diols, diacids or dihalides. More recently MCLCPs have been synthesised where the flexible spacer consists of poly(ethylene oxide) or polysiloxane segments.

1.8.1.2 Mesogenic Groups in MCLCPs

The term *mesogenic group* refers to the part of the polymer chain that is composed of the rigid, linear segments. The mesogenic group usually consists of at least two aromatic (or alicyclic) rings connected at the *p*- positions by a short, rigid link which maintains the linear arrangements of the rings. This enables a rigid element to be formed which has an overall length substantially greater than

the diameter of the aromatic group. Linking groups used include imino, azo, azoxy, ester, and *trans* vinylene groups, as well as a direct single bond link between aromatic rings such as biphenyl and terphenyl units.

1.8.2 Side Chain Liquid Crystal Polymers (SCLCPs)

Side chain LCPs consist essentially of two components, the mesogenic moieties and the polymer main chain to which they are attached. A variety of different polymer main chains are available, and these can be prepared by the three different types of polymerisation specified in Table 1.2.
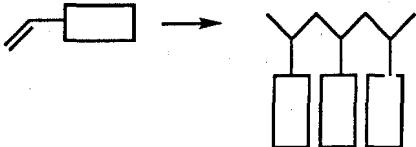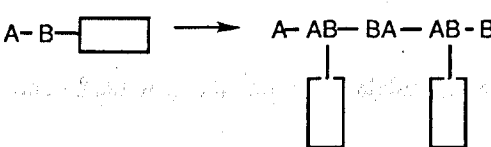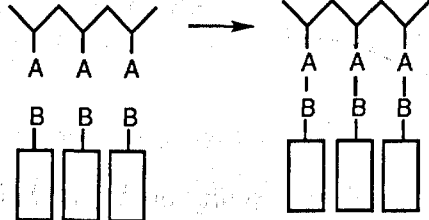
PRINCIPLES		EXAMPLES
Addition Polymerisation		Poly(meth)acrylates Polystyrene derivatives
Condensation Polymerisation		Polyester
Modification of Polymers		Polysiloxane

Table 1.2 - Synthesis of Mesogenic SCLCPs

The most convenient method of synthesis of SCLCPs is to synthesise a mesogenic molecule containing a reactive site capable of undergoing addition polymerisation. A second possibility is to introduce into the low molecular weight mesogen a reactive group capable of undergoing a polycondensation reaction. In this way polymers containing hetero atoms in the backbone can be synthesised. A third synthetic route starts with reactive polymers which can be modified to mesogenic side chain polymers by using a suitable reactive mesogen molecule. An example of this type is the smooth addition of vinyl substituted mesogenic monomers to poly[oxy(methylsilene)], Figure 1.31.
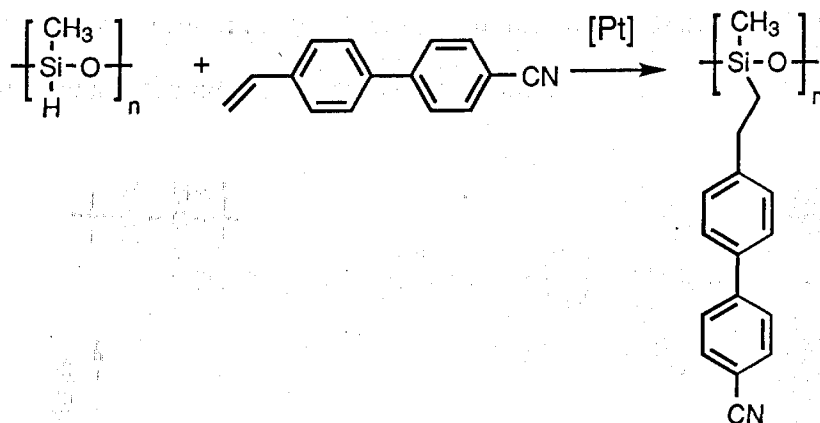
Figure 1.31 - Substituted Mesogenic poly[oxy(methylsilene)]

1.8.2.1 Flexible Spacers in SCLCPs[59]

In the isotropic liquid state a polymer will tend to adopt a statistical chain conformation that hinders anisotropic orientation of the mesogenic side chains and this, coupled with steric hindrance between the pendant groups prevents mesogenic order. In general, polymers which contain a flexible spacer linking the main chain to the pendant mesogenic group often form a mesophase whereas polymers where the pendant mesogenic group is directly attached to the polymer main chain do not exhibit mesomorphism.[59] The flexible spacer decouples motions of the main chain and side chain, and alleviates steric hindrance. Under these conditions the mesogenic side chains can be anisotropically ordered in the fluid state even though the polymer main chain tends to adopt a statistical chain conformation. Consequently variation of the spacer length should clearly influence the liquid crystal order of the side chain.

1.8.2.2 Variation of the Nature of the Mesogenic Group

If a rod-like mesogenic low molar mass molecule is substituted at its ends by an alkyl chain a systematic change in behaviour is observed (see Figure 1.32) as the length of the alkyl chain is increased. If the value for m is small, nematic phases

are observed, but with increasing length of the substituent a smectic phase becomes stable and the nematic phase is suppressed.[60, 61]
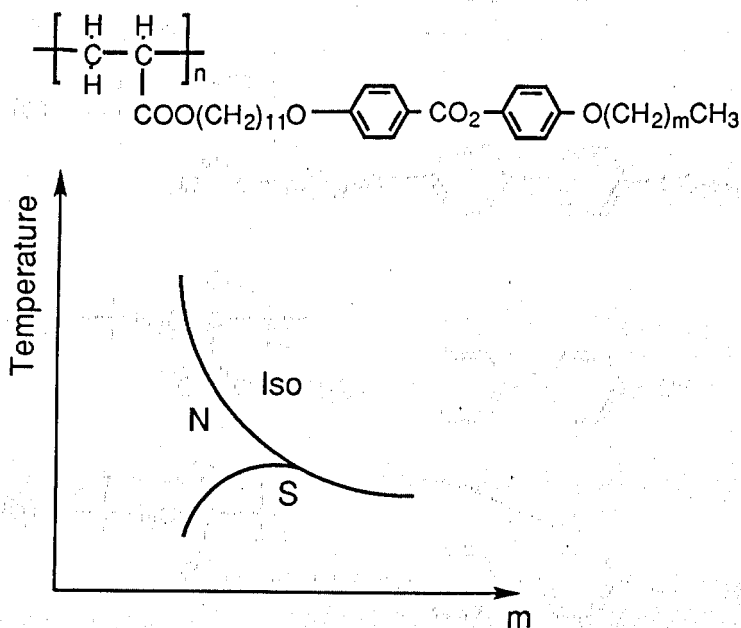
Figure 1.32 - Schematic Phase Behaviour of a Mesogen in Relation to the Chain Length of the Terminal Group

As the flexible spacer in a SCLCP partially decouples the main chain from the side chain it should be expected for polymers that variation of the length of substituents on the mesogenic side chains will also change the nature of the mesophase. Examination of Table 1.3 shows that increasing the length of the flexible spacer has the effect of reducing the transition temperatures. Increasing the length of the terminal substituent has an analogous effect to that in a low molecular weight system, *i.e.* with increasing terminal chain length there is an increased tendency to form a smectic phase.

(n)

(o)

(p)

(q)
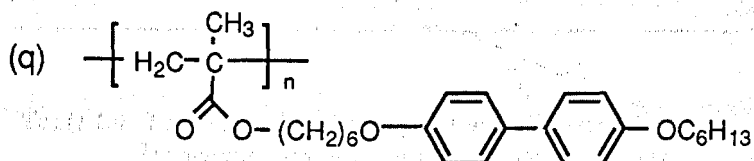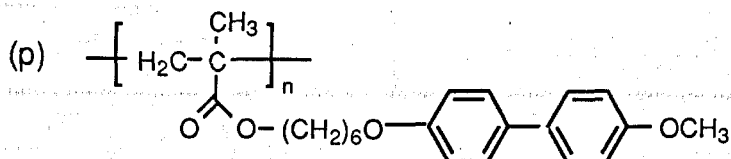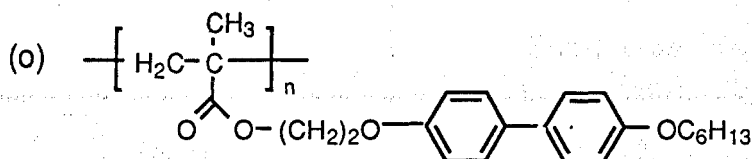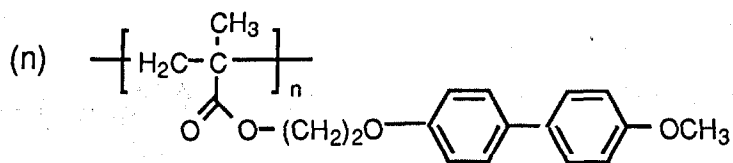
Compound No.	Transition Temperatures	ΔH [LC - Iso] (J g^{-1})
(n)	g 96 N 121 Iso	2.3
(o)	g 137 S 178 Iso	11.5
(p)	g 36 N 101 Iso	2.3
(q)	g 27 S 101 Iso	14.0

Table 1.3 - Transition Temperatures (°C) of SCLCPs with Varying Length of Substituents and Spacer in the Mesogenic Moiety

A similar effect is observed if the length of the rigid core of the mesogenic group is increased; Table 1.4 shows how the thermal stability of the mesophase is affected by increasing the length of the rigid core.
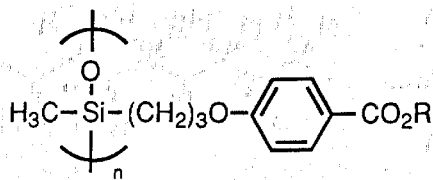
R	Phase Transitions
—OCH$_3$	g 15 N 61 Iso
—OCH$_3$	K 139 N 319 Iso
—OCH$_3$	K 200 N 360 Iso

Table 1.4 - Influence of the Length of the Mesogen on the Phase Transition Temperatures (°C) of Polysiloxanes[63]

1.8.2.3 Effect of Tacticity on Phase Transitions

When a polymer forms from a monomer, it is possible for the monomer to add to the propagating chain in a variety of ways (*i.e.*, head-to-head, head-to-tail, or tail-to-tail). These possibilities lead to the polymer chains produced having a differing structure or *tacticity*. The three types of tacticity are *atactic, isotactic* and *syndiotactic*, as shown in Figure 1.33.
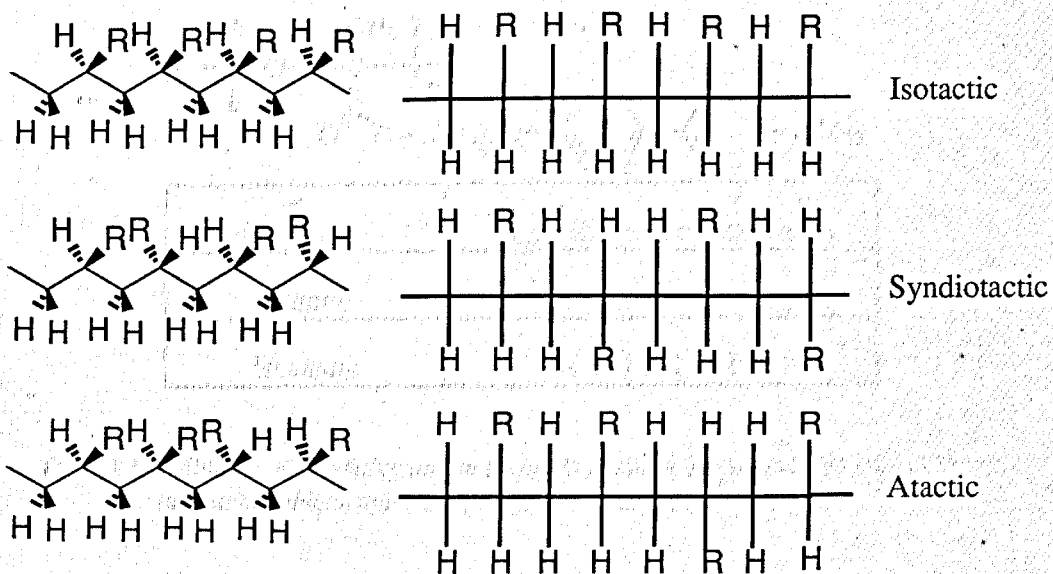
Figure 1.33 - Tacticity in Polymers

It is known in conventional polymers that the type of tacticity has an effect on thermal properties such as the glass transition temperature; *e.g.* for poly(methyl methacrylate) (PMMA) the T_g value for the isotactic polymer is 45-57 °C and for the syndiotactic form it is 112-125 °C. Therefore, judging from these results, the tacticity of a liquid crystal polymer backbone would be expected to shift the temperature range of stability of the mesophase corresponding to the shift of T_g. Results consistent with this view are those of Newmann *et al.*[63] and Hahn *et al.*[64]

The results of Hahn *et al.*[64] are shown in Table 1.5 and in contrast to poly(4-biphenyl acrylate) with no spacer, the melting temperature of the isotactic polymer is higher than that of the atactic polymer, while the isotropization temperature is only slightly higher in the isotactic polymer. However, consistent with poly(4-biphenyl acrylate) and as expected, the thermal stability of the isotactic polymer's mesophase is therefore depressed. It can therefore be deduced from this that polymer tacticity influences the crystalline phase more than the liquid crystalline phases.
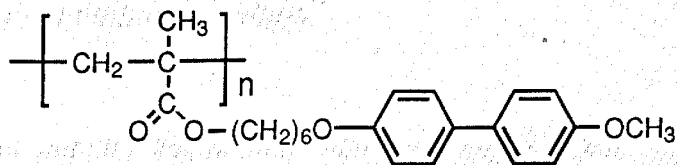
Tacticity	Transition Temperatures
Atactic	K 117 S 127-131 Iso
Isotactic	K 131 S 135 Iso

Table 1.5- Influence of Tacticity on the Phase Transition Temperatures (°C) of Poly[6-(4'-methoxybiphenyl-4-oxy)hexyl] methacrylate[64]
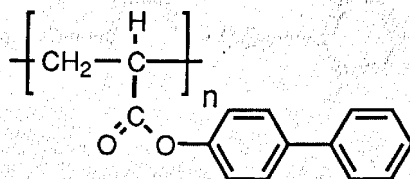
Tacticity	Transition Temperatures
Atactic	g 110 S 280 Iso
Isotactic	g 110 S 233 Iso

Table 1.6 - Influence of Tacticity on the Phase Transitions Temperatures (°C) of Poly(4-biphenyl acrylate)[64]

The type of mesophase produced will depend upon the tacticity only if the polymer backbone directly influences the packing of the mesogenic side chains because of steric hindrance. Even in the case of directly linked mesogenic side chains, Newmann *et al.*[63] did not find any influence of tacticity on the packing of the mesogenic side chains.

1.8.2.4 Influence of Molecular Weight

In general, the transformation of a liquid-crystal monomer to a SCLCP by polymerisation has the effect of stabilising the mesophase and this is illustrated by the values shown in Table 1.7. For system (r), the monomer is not mesogenic, whereas the polymer is nematic. In system (s), the nematic monomer yields a more highly ordered smectic polymer and the transition to the isotropic phase occurs at a higher temperature. For system (t), both monomer and polymer exhibit smectic and nematic phases but once again, the phase transition temperatures are raised.

(r)

(s)

(t)
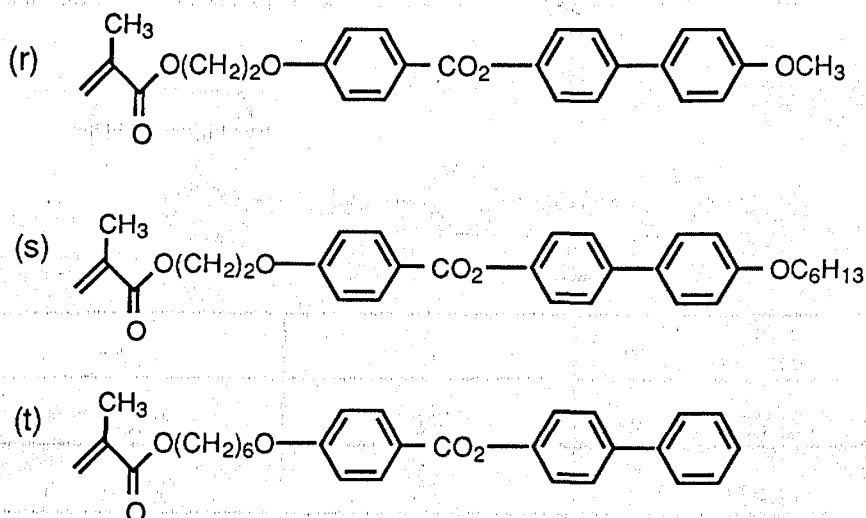
| | Transition Temperatures (°C) | |
System	Monomer	Polymer
(r)	K 97 Iso	g 101 N 121 Iso
(s)	K 47 N 53 Iso	g 60 S 115 Iso
(t)	K 64 S 68 N 92 Iso	g 132 S 164 N 184 Iso

Table 1.7 - Comparison of Phase Behaviour of Monomers with the Corresponding Mesogenic Polymers[65]

In principle, upon changing from monomer to polymer the chemical constitution of the system, polarisability, and form anisotropy should remain similar. Therefore, the strong shift of phase behaviour must be attributed to the restriction of translational, rotational and orientational motions of the mesogenic side chains.

Having established that polymerisation of the monomer stabilises the mesophase, it is now logical to examine the effect produced by variation of the molecular weight of the polymer. Portugall et al.[61] carried out such a study on the nematic acrylate polymer shown below and the results are shown in Table 1.8. Glass transition temperatures, isotropization temperature and the change in enthalpy at isotropization all increase up to a degree of polymerisation (n) of 114.
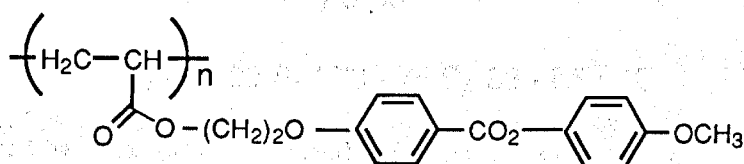
Mn	n	Transition Temperatures
4500	13	g 53 N 100 Iso
14000	41	g 59 N 114 Iso
39000	114	g 62 N 116 Iso

Table 1.8 - Influence of Molecular Mass on the Phase Transition Temperatures (°C) of a LC Polyacrylate [61]

1.9 FERROELECTRICITY AND ANTIFERROELECTRICITY IN SIDE CHAIN LIQUID CRYSTAL POLYMERS

The study of chiral smectic side chain liquid crystal polymers is still at a relatively early stage of investigation having only been reported for the first time in 1984 when Shibaev et al.[66] published results on the mesogenic methacrylate **P5*M** (Figure 1.34).

P5*M
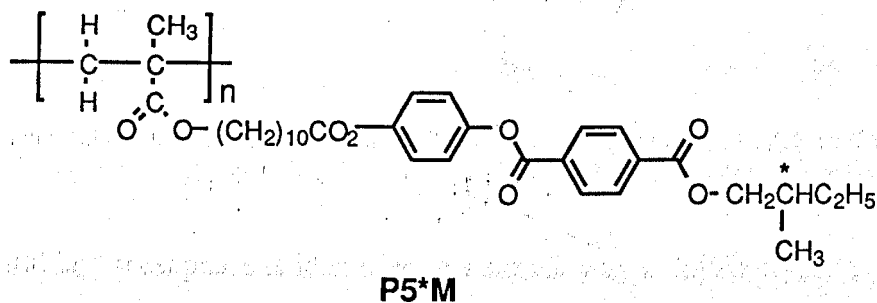
g 20 - 30 S_C* 73 - 75 S_A 83 - 85 I °C

Figure 1.34 - Structure and Transition Temperatures for the Polymer P5*M

Since then many structural modifications to this polymer have been made which have mainly been concerned with the polymer backbone (polyacrylate, polysiloxane) and with the mesogenic moiety. In many of the cases, the optically active centre located in the terminal group has been altered[67] (e.g., Figure 1.35) and the linking group between the phenyl rings has been changed.[68]

P6*M

$$g \xrightarrow{50} S_C^* \xrightarrow{79} I$$
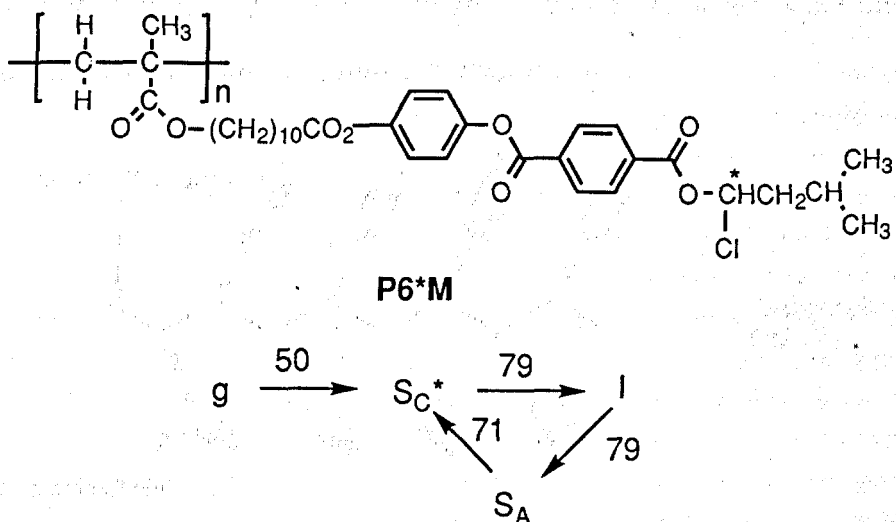
Figure 1.35 - Structure and Transition Temperatures (°C) of the SCLCP P6*M[58]

The chiral S_C^* mesophase is identified in a similar way in liquid crystal polymers and in low molar mass materials, that is by the use of thermal analysis, optical microscopy observations and X-ray measurements. X-ray investigations of SCLCPs have been obtained using powder samples or oriented fibres and it was while performing such observations on polymers shown in Figure 1.36 that Decobert et al.[69] noticed peculiar results.

R = H, CH₃
n = 2, 6
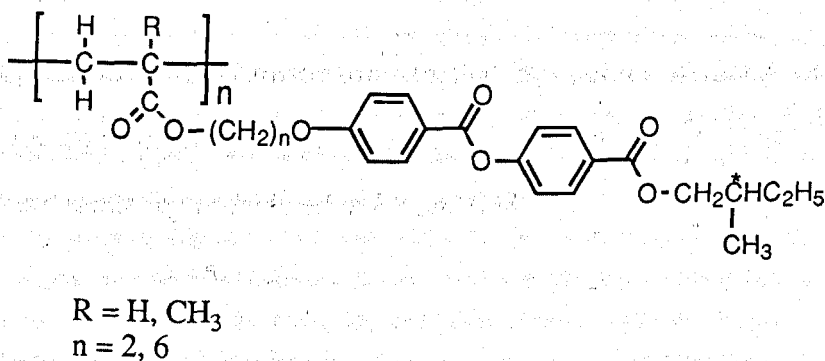
Figure 1.36 - SCLCPs studied by X-Ray Analysis by Decobert et al.[60]

Decobert et al. noted that the diffraction patterns were characteristic of a disordered lamellar structure, which would be expected for a smectic, but that below 110 °C three well-defined inner rings were observed corresponding to a Bragg spacing of 36-38 Å, which is less than twice the molecular length.

Decobert *et al.* proposed that the side chains within the layers were therefore oriented in one of the two ways shown in Figure 1.37.

Polymer Backbone

Mesogenic Side Chain

Antiferroelectric-like Ordering

+

Ferroelectric-like Ordering
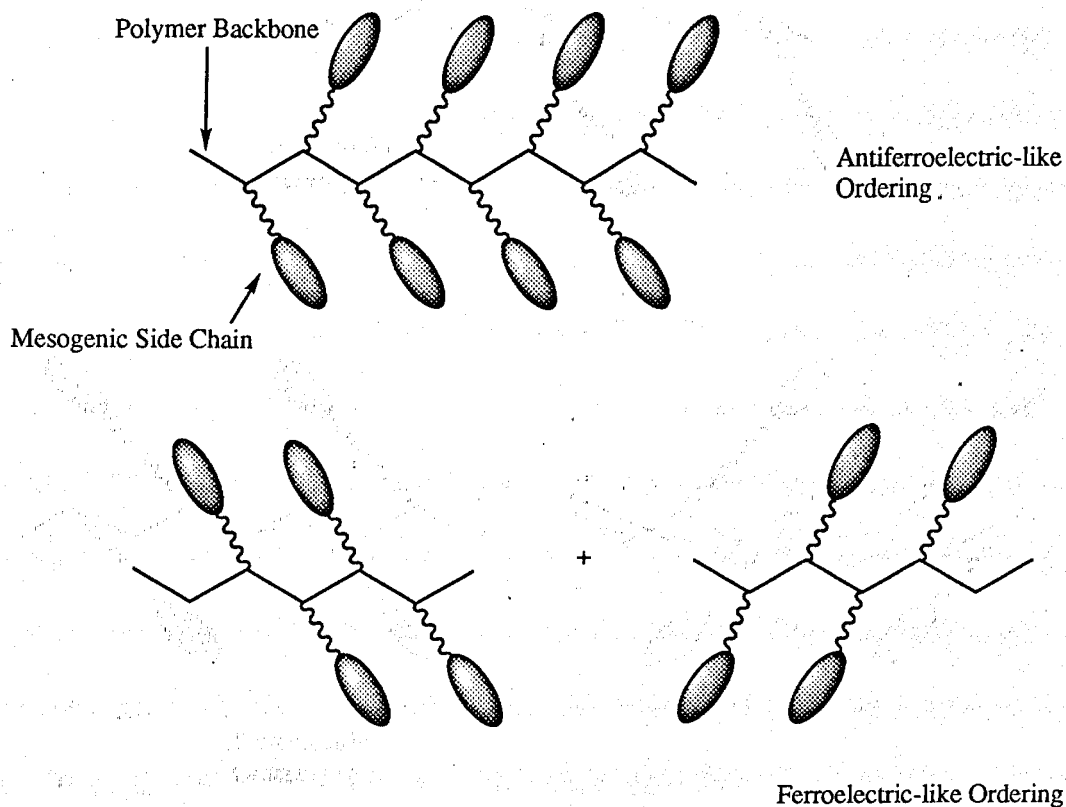
Figure 1.37 - Antiferroelectric and Ferroelectric Ordering in a SCLCP as Reported by Decobert et al.[69]

This diagram however is misleading in that the points of attachment of the pendant mesogenic groups appear to be on adjacent carbon atoms. A more accurate representation is depicted in Figure 1.38

Antiferroelectric
Ordering

+

Ferroelectric
Ordering
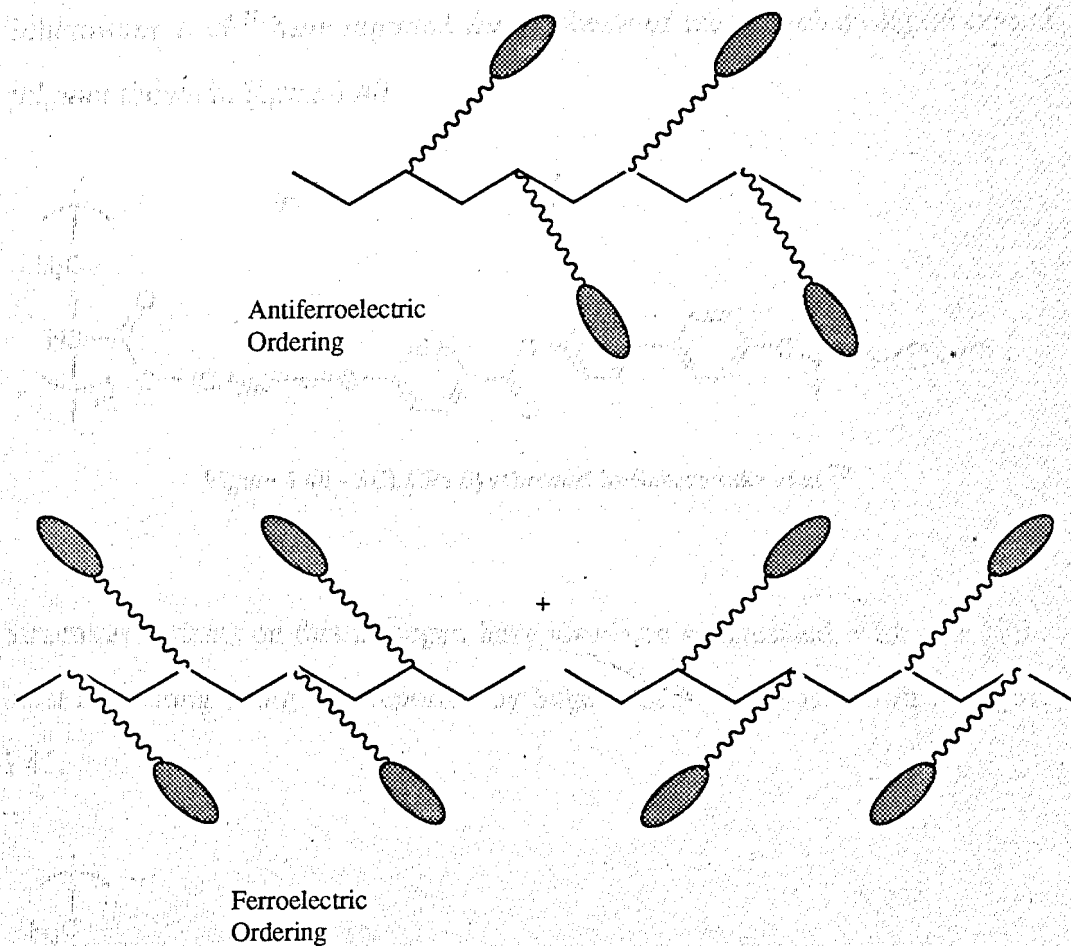
Figure 1.38 - Antiferroelectric and Ferroelectric Ordering in a SCLCP

Further SCLCPs which exhibit antiferroelectric ordering and tri-state switching
have been reported (Figure 1.38).[70, 71]
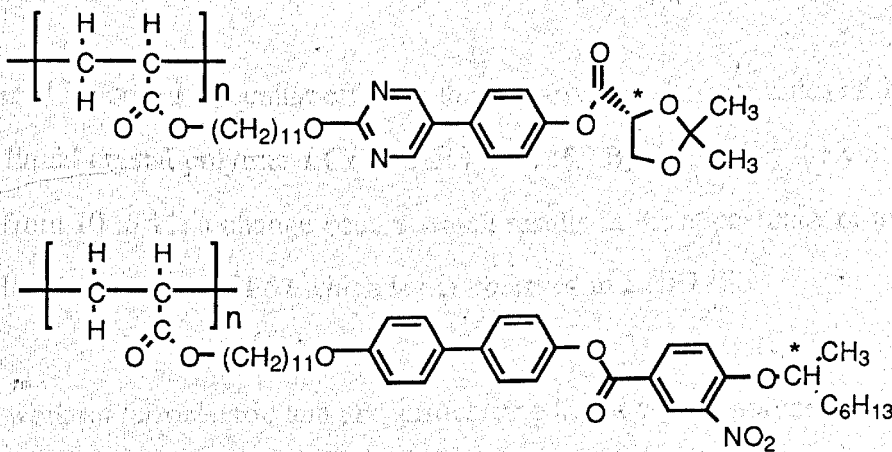
Figure 1.39 - SCLCPs Exhibiting Tri-State Switching

Scherowsky *et al.*[78] have reported the synthesis of the side-chain liquid crystal polymer shown in Figure 1.40
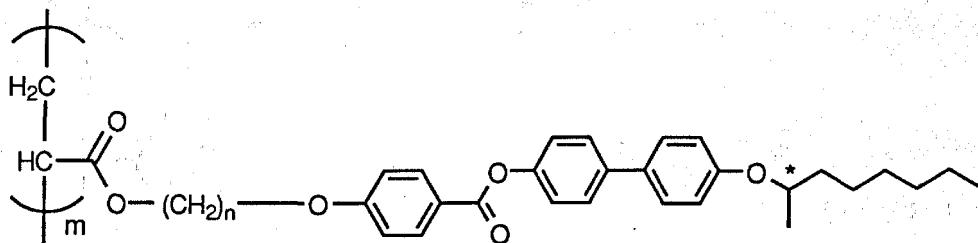
Figure 1.40 - SCLCPs Synthesised by Scherowsky *et al.*[78]

Structural variants on this mesogen have also been synthesised, with one of the most interesting being that reported by Sage *et al.*[79] which is shown in Figure 1.41.
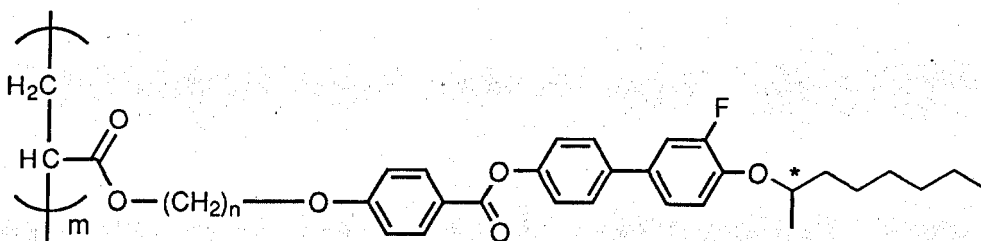
LCP67, n = 11
LCP145, n = 10

Figure 1.41 - Structures of LCP67 and LCP145

Sage *et al.*[79] noticed a peculiar effect in the electro-optic characteristics of the side chain liquid crystal polymer **LCP67** and **LCP145**. By increasing the value of n by 1, from 10 to 11, a change occurs which results in the appearance of an anti-ferroelectric phase in **LCP67** which is not observed in **LCP145**.

Other work on ferroelectric and antiferroelectric liquid crystal polymers has been reported by Nishiyama *et al.*[80] where low molar mass molecules known to exhibit

antiferroelectric properties have been incorporated into polymeric materials (see Figure 1.42).
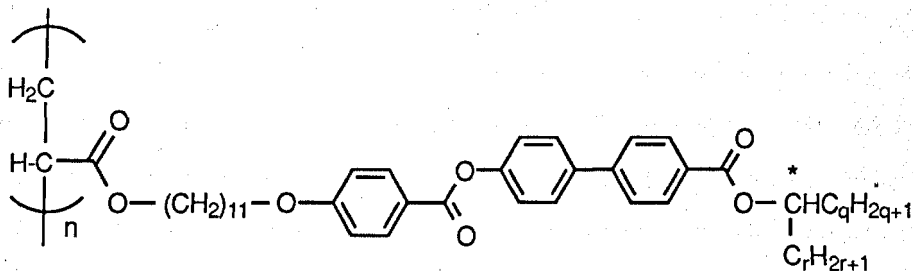
Figure 1.42 - SCLCPs reported by Nishiyama *et al.*[71]

These polymers retain the antiferroelectric phase exhibited in the monomeric material, however they do not exhibit the ferroelectric phase which is exhibited by the monomer.

CHAPTER 2
AIMS

AIMS

2.1 AIMS OF THE PROJECT

Chirality in liquid crystals has been of interest over the past 25 years,[72] first with the development of cholesteric liquid crystals for thermochromic applications,[73] then with the discovery of the Blue Phases,[74] and more recently with the use of ferroelectric smectogens in display applications.[75]

This project has focused on the synthesis of side chain liquid polymers which contain mesogenic side chains of similar structure to low molar mass materials known to exhibit smectic C phases having ferroelectric,[76] antiferroelectric[77] and ferrielectric[43] properties.

The main aim of this project is to synthesise side chain liquid crystal polymers whose structure was based on the structure of the first reported antiferroelectric liquid crystal **MHPOBC** (Figure 1.18) to determine whether the antiferroelectric properties would be retained in a polymeric material, and to examine the effect structural variations had on polymers similar in structure.

The first structural variation examined was the effect caused by insertion of a lateral fluoro substituent, in the final phenyl ring, on the liquid crystal properties of the mesogenic side chain liquid crystal polymers outlined in Figure 2.1.
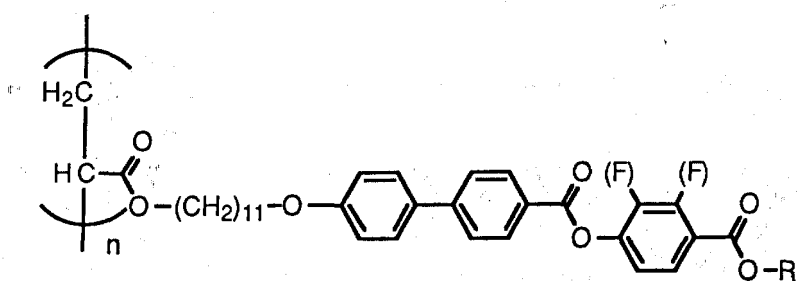
R = (R)-1-methylheptyl or 1-propylbutyl

Figure 2.1 - SCLCPs Prepared to examine the Effect of Fluoro Substitution on Liquid Crystal Properties

The next structural variation examined was the effect of altering the flexible spacer length of the SCLCP by one carbon unit (see Figure 2.2) would have on the liquid crystal properties, and to see if this was consistent with the results reported by Sage et al.[70] (Figure 1.41).
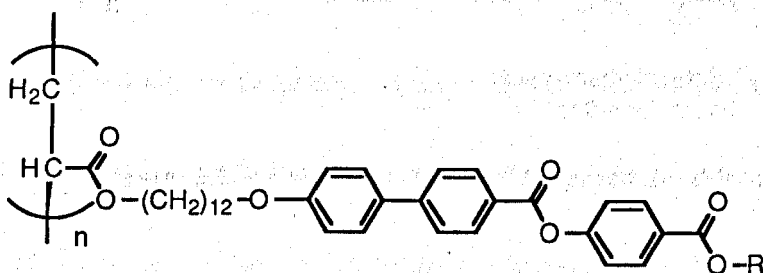
R = (R)-1-methylheptyl or 1-propylbutyl

Figure 2.2 - SCLCPs Prepared to Examine the Effect of Increasing the Flexible Spacer by one Carbon Atom

The first two series of polymers made were based upon an acrylate polymer backbone [Figure 2.3(a)]. Further series of polymers were prepared based upon allyl alcohol [Figure 2.3(b)] and α-hydroxymethylacrylonitrile [Figure 2.6(c)] in order to examine the effect the change of polymer backbone has upon the liquid crystal behaviour.
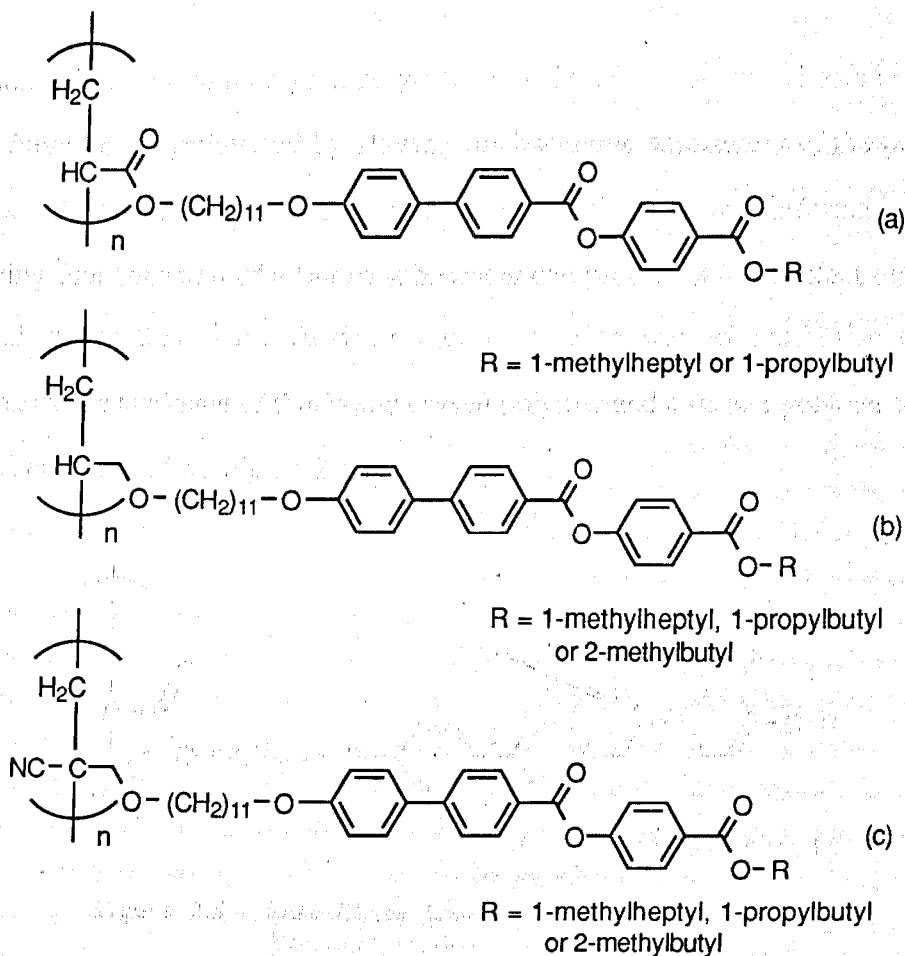
Figure 2.3 - Polymeric Systems Prepared in this Work

A fourth series of side chain liquid crystal polymers were synthesised with the aim of examining the effect of altering the method of attaching the mesogenic side chain and flexible space to the polymer backbone. The structure of these polymers can be seen in Figure 2.4.
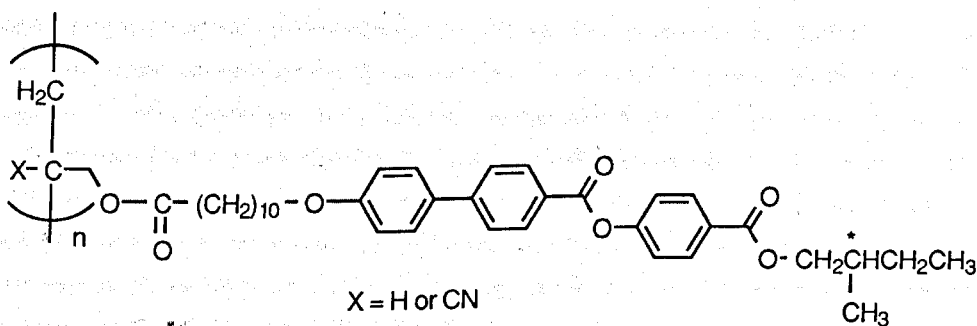
Figure 2.4 - SCLCPs Prepared to examine the Effect of Changing the Linking Moiety on the Liquid Crystal Properties

Various side chain liquid crystal polymers, based on the structures shown in Figure 1.41, have been synthesised by altering the backbone substituent of the polymer (*i.e.* acrylate, methacrylate and chloroacrylate).[81] With this information, and knowing that insertion of a fluoro substituent can produce a large effect on liquid crystal properties,[82] the final structural variation was to synthesise the α-fluoroacrylate analogue of this liquid crystal polymer and a further polymer with an achiral end group (see Figure 2.5).

R = octyl or 1-methylheptyl
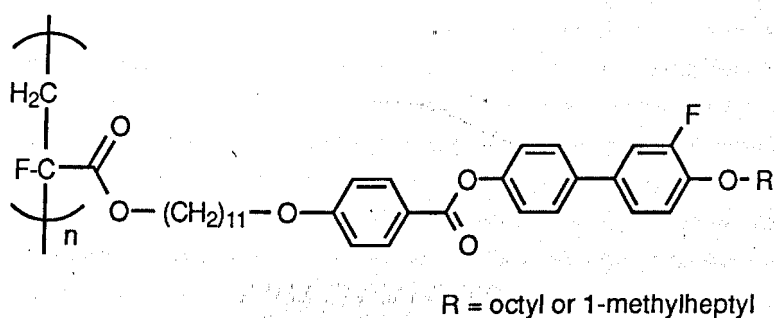
Figure 2.5 - Side Chain Liquid Crystal Fluoroacrylate Prepared in this work

CHAPTER 3
EXPERIMENTAL

EXPERIMENTAL

3.1 GENERAL NOTES

3.1.1 Purities of Materials Prepared

(a) Purification of the intermediate materials and the monomers was carried out by flash chromatography on silica gel (230 - 400 mesh, Merck Darmstadt) using the eluent described in the individual synthetic procedures, following the procedure outlined by Still, *et al.*[83] followed by recrystallisation from ethanol unless otherwise stated. Where necessary, the intermediates were further purified by short-path distillation using a modified vertical sublimation apparatus, consisting of a collecting vessel fitted to the bottom of a 'cold finger'. The temperature recorded was the temperature of the heating bath.

(b) The purity of the intermediate materials and the monomers prepared were checked using thin layer chromatography (tlc). The tlc plates used were Kieselgel 60 F_{254} (Merck Darmstadt) and dichloromethane was used as eluent. Detection of the products was achieved using UV radiation ($\lambda = 254$ and 365 nm).

(c) The reactions were monitored as appropriate using tlc, as described above, or by using Gas Chromatography (gc) using a Perkin-Elmer 8310 Gas Chromatograph attached to a Perkin-Elmer GP-100 graphics printer. A packed column (10% Silar 10C on 80-100 mesh Chromosorb W; 4 m column) or a capillary column (BP10, 0.25 mm film, 25 m column) was used with nitrogen as the carrier gas.

(d) The polymers were checked for low molar mass content, and their molecular weights and polydispersities were obtained by Gel Permeation Chromatography

(GPC) using 2 x 5 μm mixed D PLgel columns connected to an ERMA Inc. ERC 7510 RI detector and a Polymer Laboratories data station. Polystyrene was used as the standard.

3.1.2 Physical Properties of Intermediates, Monomers and Polymers

(a) Melting points and initial phase assignments, along with the corresponding transition temperatures, were determined by thermal optical microscopy using an Olympus BH-2 polarizing light microscope equipped with a Mettler FP82 hotstage and FP80 control unit. The heating and cooling rate were 2 °C min^{-1} with the temperatures quoted for phase transitions being the mean values for the heating and cooling cycles unless otherwise stated.

(b) Temperatures and enthalpies of transitions were investigated by differential scanning calorimetry (DSC) using a Perkin-Elmer PC Series DSC 7 calorimeter. An indium standard was used to calibrate the instrument (scanning rate of 10.0 °C min^{-1}). The measured latent heat was compared with the standard value for indium of 28.45 J g^{-1}[84]. The materials were studied at a scanning rate of 10.0 °C min^{-1} (or 20 °C min^{-1} for the initial heat and cool cycle on a polymeric sample) after being encapsulated in aluminium pans.

(c) The photomicrographs were obtained using the thermal optical microscopy apparatus as described previously in conjunction with a Hitachi FP7 colour video camera and Hitachi VY200-A colour video printer. The magnification used for the photomicrographs was x100 unless otherwise stated.

(d) Optical Rotations were determined using an AA10 automatic polarimeter at 22 °C using chloroform as solvent, unless otherwise stated.

3.1.3 Spectroscopic and Spectrometric Studies

(a)   Proton (^{1}H) and carbon 13 (^{13}C) nuclear magnetic resonance (Nmr) spectroscopy was carried out using a JEOL JNM-GX270 FT nuclear magnetic resonance spectrometer.   In the reporting of the Nmr data the following abbreviations have been used:

s	singlet,
d	doublet,
dd	doublet of doublets,
t	triplet,
q	quartet,
m	multiplet.

(b) Infra-red (Ir) spectroscopy was carried out using a Perkin-Elmer 783 infrared spectrophotometer.

(c) Mass spectrometry (Ms) was carried out using a Finnegan MAT 1020 automated GC / MS.

3.1.4 Drying and Purification of Solvents and Reagents

Commercially available starting materials were used as supplied by Aldrich Ltd.

The following solvents were dried in the way stated.

(a) Toluene was dried over sodium wire.

(b) Dichloromethane was distilled over phosphorus pentoxide.

(c) Tetrahydrofuran was distilled over sodium and benzophenone.

(d) Dimethylformamide was dried over molecular sieves.

(e) 1,2-Dichloroethane was dried over molecular sieves.

3.2 SYNTHETIC PROCEDURES

The synthetic routes to the molecules are outlined in the following schemes. The methods employed in the synthesis of these molecules are given after each scheme.

Phase identification of mesogenic intermediate materials was carried out using the optical microscopy setup as described in section 3.1.2 (c). Typical textures for these phases are given in Appendix 1.

Scheme 1
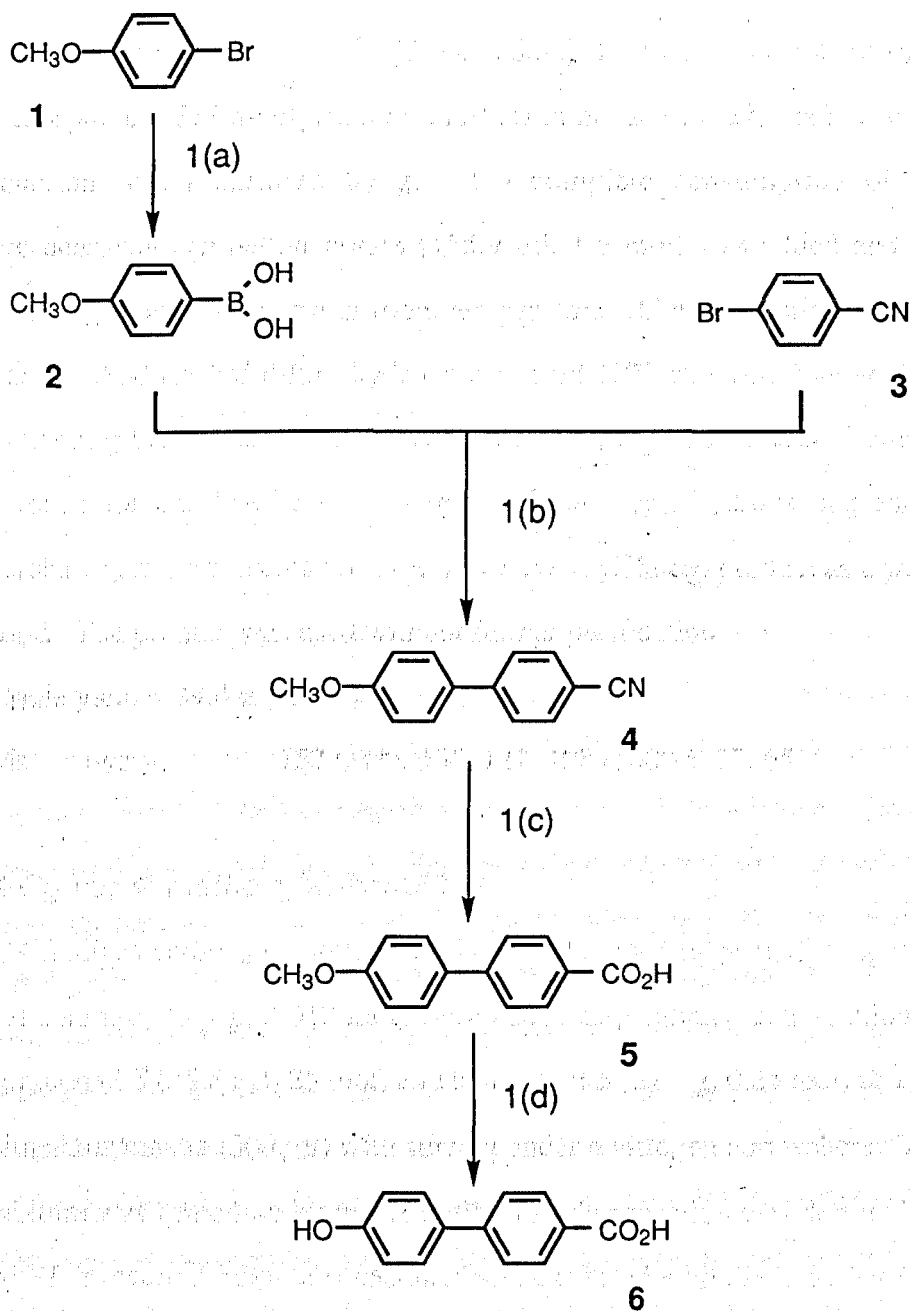
Reagents
1(a) ... i) n-Butyllithium, ii) trimethyl borate, iii) dil. HCl

1(b) ... Pd(PPh₃)₄, Na₂CO₃ (aq), DME

1(c) ... cH₂SO₄, acetic acid, water

1(d) ... 48% HBr, acetic acid

4-Methoxyphenylboronic acid (2)

To a solution of 4-bromoanisole (1) (46.8 g, 0.25 mol) in tetrahydrofuran (400 ml) maintained at -70 °C was added dropwise under a nitrogen atmosphere 2.5M n-butyllithium (110 ml in hexanes, 0.275 mol) and the reaction was monitored by gc. On complete consumption of the bromoanisole, trimethyl borate (155.9 ml, 1.5 mol) was added and the reaction allowed to warm to room temperature while being stirred for 12 hours. Addition of dilute hydrochloric acid (100 ml) was followed by extracting the solution with ether (3 x 100ml) and the organic fractions were combined. The fractions were then dried over anhydrous magnesium sulphate and the solvents removed *in vacuo* to yield the product as a waxy solid. The product was used without further purification.

Crude yield = 39.4 g (100%)

Ms   m/z =   152 (M$^+$), 135, 121, 108 (100%), 77, 65

4-Cyano-4'-methoxybiphenyl (4)

2M Sodium carbonate solution (200 ml) and tetrakis(triphenylphosphine) palladium(0) (3.5 g, 0.018 mol) were added sequentially to a solution of compound 3 (45.8 g, 0.25 mol) and compound 2 (39.4 g, 0.25 mol) in 1, 2-dimethoxyethane (500 ml) with stirring under a nitrogen atmosphere. The mixture was heated under reflux until no further reaction was detected by gc. The reaction mixture was cooled and extracted with diethyl ether (3 x 125 ml) and the ethereal solutions washed with water and dried over anhydrous magnesium sulphate, before the solvent was removed under reduced pressure. The pure product was obtained by column chromatography using 1:1 dichloromethane / petroleum ether (bp 40 - 60 °C) as eluent.

Yield = 37.8 g (72%)

mp = 99.7 - 99.9 °C

^{1}H Nmr (CDCl$_3$) δ   3.86 (3H, s), 7.01 (2H, d), 7.54 (2H, d),

         7.61 - 7.71 (4H, m)

Ir (KBr) ν$_{max}$ cm^{-1} 2920, 2450, 1410, 1210, 860

Ms   m/z =   209 (M$^+$, 100%), 194, 166, 140, 63, 51

4′-Methoxybiphenyl-4-carboxylic acid (5)

Compound **4** (30.0 g, 0.15 mol) was dissolved in glacial acetic acid (300 ml), concentrated sulphuric acid (60 ml) and water (60 ml), and the solution was heated under reflux for 8 hours. The solution was allowed to cool to room temperature before being poured into cold water and left to stand overnight. The resulting white precipitate was filtered off and recrystallised from glacial acetic acid.

Yield = 34.1 g (100%)

^{1}H Nmr (CDCl$_3$) δ   3.86 (3H, s), 7.01 (2H, d), 7.54 - 7.64 (4H, m),

         8.05 (2H, d), acid proton not detected

Ir (KBr) ν$_{max}$ cm^{-1} 3400, 3300, 1680, 1410, 1310, 830

Ms   m/z =   228 (M$^+$, 100%), 211, 185, 139, 63

4′-Hydroxybiphenyl-4-carboxylic acid (6)

Compound **5** (34.1 g, 0.15 mol) and 48% hydrobromic acid in water (200 ml) were dissolved in acetic acid (300 ml) and heated under reflux for 8 hours. The white product was filtered off, washed with water, and recrystallised from acetic acid before being dried overnight at 100 °C.

Yield = 31.6 g (98%)

mp = 295 °C

^{1}H Nmr (CDCl$_3$) δ   6.88 (2H, d), 7.56 - 7.77 (4H, dd), 7.91 (2H, d)

         9.70 (1H, s), 12.80 (1H, s)

Ir (KBr) ν$_{max}$ cm^{-1} 3600, 3400, 1680, 1410, 1310, 830

Ms   m/z =   214 (M$^+$), 185, 139(100%), 106, 63

Scheme 2
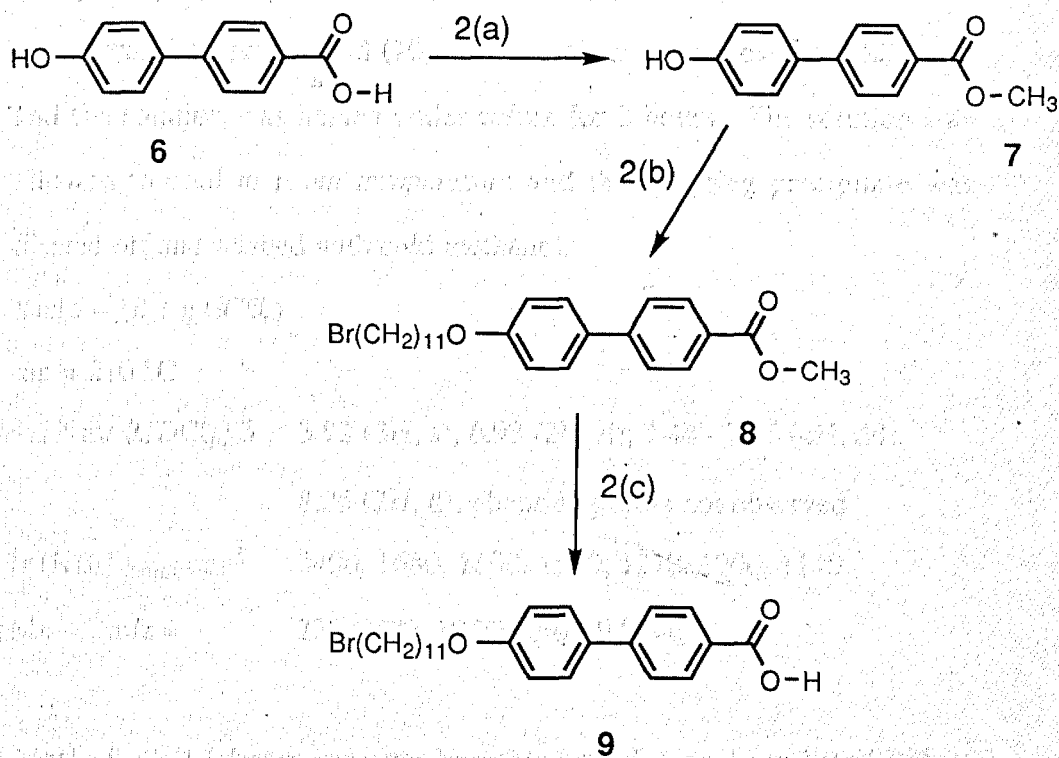
Reagents   2(a) ... cH₂SO₄, methanol

                  2(b) ... 11-bromoundecan-1-ol, DEAD, PPh₃, THF

                  2(c) ... (i) NaOH (aq), ethanol, (ii) dil. HCl

Methyl 4'-hydroxybiphenyl-4-carboxylate (7)

4'-Hydroxybiphenyl-4-carboxylic acid (6) (10.0 g, 0.047 mol) and concentrated sulphuric acid (10 ml) were dissolved in methanol (250 ml) and the solution was heated under reflux for 3 hours. The solution was allowed to cool to room temperature and the resulting precipitate was filtered off and washed with cold methanol.

Yield = 10.3 g (97%)

mp = 210 °C

^{1}H Nmr (CDCl$_3$) δ   3.92 (3H, s), 6.93 (2H, d), 7.44 - 7.65 (4H, dd),

           8.05 (2H, d), phenolic proton not observed

Ir (KBr) v_{max} cm^{-1} 3400, 1680, 1600, 1580, 1270, 1200, 1140

Ms   m/z =   228 (M$^+$), 197(100%), 94, 84, 58, 48

Methyl 4'-(11-bromoundecyloxy)biphenyl-4-carboxylate (8)[85]

Compound 7 (7.54 g, 0.033 mol), 11-bromoundecan-1-ol (8.29 g, 0.033 mol) and diethyl azodicarboxylate (DEAD) (5.74 g, 0.033 mol) were dissolved in tetrahydrofuran under a nitrogen atmosphere. Triphenylphosphine (9.51 g, 0.0363 mol) dissolved in tetrahydrofuran was added dropwise to this mixture and the mixture was stirred at room temperature until the reaction was complete, as observed on examination by tlc. The solvent was removed *in vacuo* and the resulting slurry was purified by column chromatography using petroleum ether (bp 40-60 °C) / dichloromethane 3:7 as eluent followed by recrystallisation.

Yield = 8.6 g (56%)

mp = 97 °C

^{1}H Nmr (CDCl$_3$) δ   1.21 - 1.53 (14H, m), 1.74 - 1.92 (4H, m),

           3.41 (2H, t), 3.93 (3H, s) , 4.00 (2H, t), 6.98 (2H, d),

           7.52 - 7.64 (4H, dd), 8.08 (2H, d)

Ir (KBr) v_{max} cm^{-1} 2920, 2840, 1740, 1280, 1200, 1120

Ms   m/z =   460 (M$^+$), 228, 197 (100%), 139, 69, 55

4'-(11-Bromoundecyloxy)biphenyl-4-carboxylic acid (9)

To a solution of compound 8 (4.30 g, 0.010 mol) dissolved in ethanol (100 ml) was added sodium hydroxide (6.50 g) dissolved in water (15 ml) and the resulting solution was heated under reflux for 1 hour before being allowed to cool to room temperature. The mixture was brought to pH2 by the addition of dilute hydrochloric acid and then stirred for a further 30 minutes. The resulting white precipitate was filtered off and recrystallised from acetic acid before being dried overnight at 100 °C.

Yield = 3.5 g (88%)

mp = 154 - 155 °C

^{1}H Nmr (CDCl$_3$) δ   1.21 - 1.58 (14H, m), 1.74 - 1.91 (4H, m),

3.42 (2H, t), 4.00 (2H, t), 6.99 (2H, d),

7.52 - 7.66(4H, dd) 8.08 (2H, d), acid proton not

detected

Ir (KBr) v_{max} cm^{-1} 3400, 2920, 2840, 1670, 1050, 1030, 1000

Ms   m/z =   446 (M$^+$), 412, 214, 197 (100%), 97, 55

Scheme 3
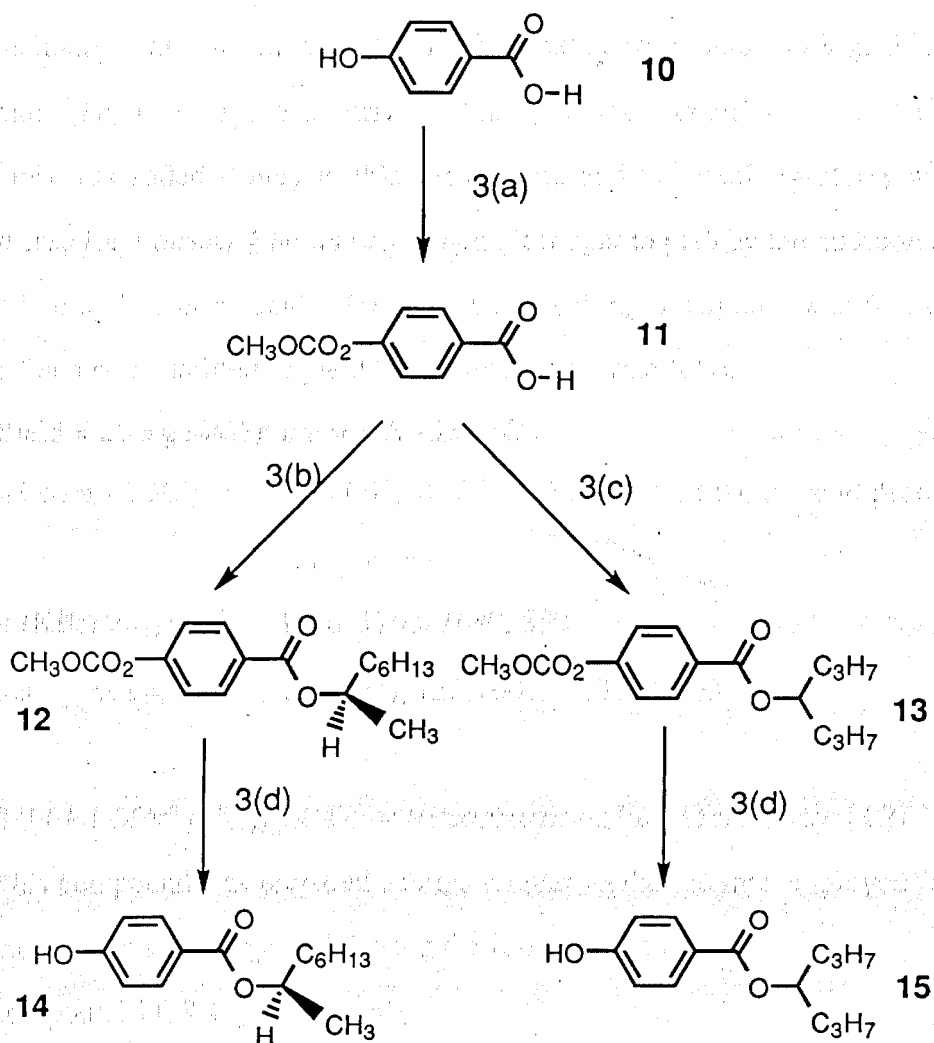
Reagents   3(a) ... methyl chloroformate, NaOH, water

                 3(b) ... (S)-(+)-octan-2-ol, DEAD, PPh₃, THF

                 3(c) ... heptan-4-ol, DEAD, PPh₃, THF

                 3(d) ... ethanol, NH₃ (aq)

4-(Methoxycarbonyloxy)benzoic acid **(11)**[86]

To a solution of sodium hydroxide (30.0 g, 0.75 mol) in water (800 ml), maintained at -10 °C, was added 4-hydroxybenzoic acid (35.8 g, 0.259 mol) **(10)** with vigorous stirring. Methyl chloroformate (40.0 g, 0.423 mol) was added slowly to this suspension, and the resulting slurry was stirred for a further 4 hours before being brought to pH5 by the addition of dilute hydrochloric acid (200 ml). The resulting precipitate was filtered off and recrystallised to yield the product as a white solid.

Yield = 21.6 g (44%); mp = 178 - 182 °C

^{1}H Nmr (CDCl$_3$) δ   3.86 (3H, s), 7.36 (2H, d), 8.01 (2H, d), acid proton
　　　　　　　　　　not detected

Ir (KBr) v_{max} cm^{-1} 1770, 1750, 1680, 850

Ms   m/z =   196 (M$^+$), 152(100%), 135, 92, 63, 59

(R)-(-)-1-Methylheptyl 4-(methoxycarbonyloxy)benzoate **(12)**

This compound was prepared using a similar method to that employed for the synthesis of compound **8** using the following charge;

compound **11**, 8.4 g (0.043 mol),

(*S*)-(+)-octan-2-ol, 5.6 g (0.043 mol),

diethyl azodicarboxylate, 7.5 g (0.043 mol),

triphenylphosphine, 12.4 g (0.0473 mol),

THF, 200 ml.

The pure product was obtained as a liquid by column chromatography [dichloromethane / petroleum ether (bp 40-60 °C) 3:7 as eluent].

Yield = 6.9 g (52%)

^{1}H Nmr (CDCl$_3$) δ   0.86 (3H, t), 1.21 - 1.44 (10H, m),
　　　　　　　　　　1.51 - 1.79 (3H, m), 3.88 (3H, s) 5.22 (1H, m),
　　　　　　　　　　7.25 (2H, d), 8.08 (2H, d)

Ir (neat) v_{max} cm^{-1} 2960, 2920, 1760, 1710, 1440, 860

Ms   m/z =   308 (M+), 197, 179, 135 (100%), 69, 55

Specific Rotation : $[\alpha]_D$ = -15.6 °

1-Propylbutyl 4-(methoxycarbonyloxy)benzoate **(13)**

This compound was prepared using a similar method to that employed for

the synthesis of compound **8** using the following charge;

compound **11**, 3.9 g (0.02 mol),

heptan-4-ol, 2.0 g (0.02 mol),

diethyl azodicarboxylate, 3.5 g (0.02 mol),

triphenylphosphine, 5.8 g (0.02 mol),

THF, 100 ml.

The pure product was obtained as a liquid by column chromatography [

dichloromethane / petroleum ether (bp 40-60 °C) 3:7 as eluent].

Yield = 3.6 g (62%)

^{1}H Nmr (CDCl$_3$) δ   0.88 (6H, t), 1.27 - 1.49 (4H, m),

1.51 - 1.76 (4H, m), 3.91 (3H, s) 5.18 (1H, m),

7.25 (2H, d), 8.08 (2H, d)

Ir (neat) ν$_{max}$ cm^{-1} 2960, 2940, 1770, 1720, 1440, 860

Ms   m/z =   294 (M+), 197, 179, 135 (100%), 98, 55

(R)-(-)-1-Methylheptyl 4-hydroxybenzoate **(14)**[86]

To a solution of compound **12** (5.1 g, 0.017 mol) dissolved in ethanol (100

ml) at room temperature was added 30% aqueous ammonia (50 ml). The

mixture was stirred at room temperature until no further reaction was

observed upon analysis by tlc. Ethanol and ammonia were removed by

evaporation under reduced pressure and the resulting slurry was purified

by column chromatography, using dichloromethane as eluent, to yield the

product as a liquid.

Yield = 4.0 g (95%)

^{1}H Nmr (CDCl$_3$) δ   0.88 (3H, t), 1.19 - 1.77 (13H, m), 5.18 (1H, m),

6.88 (2H, d), 8.08 (2H, d), phenolic proton not

detected

Ir (neat) ν$_{max}$ cm^{-1} 3400, 2960, 2920, 1720, 1450, 850

Ms   m/z =   250 (M$^+$), 138, 121, 93 (100%), 65, 55

Specific Rotation :   [α]$_D$ = -21.2 ° (24 °C)

1-Propylbutyl 4-hydroxybenzoate **(15)**

This compound was prepared using a similar method to that employed in

the synthesis of compound **14** using the following charge;

compound **13** 3.6 g (0.012 mol),

ethanol, 100 ml,

30% aqueous ammonia, 50 ml.

The pure product was obtained as a liquid by column chromatography

(dichloromethane as eluent).

Yield = 2.0 g (70%)

^{1}H Nmr (CDCl$_3$) δ   0.93 (6H, t), 1.25 - 1.49 (4H, m),

1.50 - 1.76 (4H, m), 5.18 (1H, m),

7.25 (2H, d), 8.09 (2H, d), phenolic proton not

detected

Ir (neat) ν$_{max}$ cm^{-1} 3350, 2940, 2920, 1740, 1440, 850

Ms   m/z =   236 (M$^+$), 139, 121, 98 (100%), 65, 55

Scheme 4
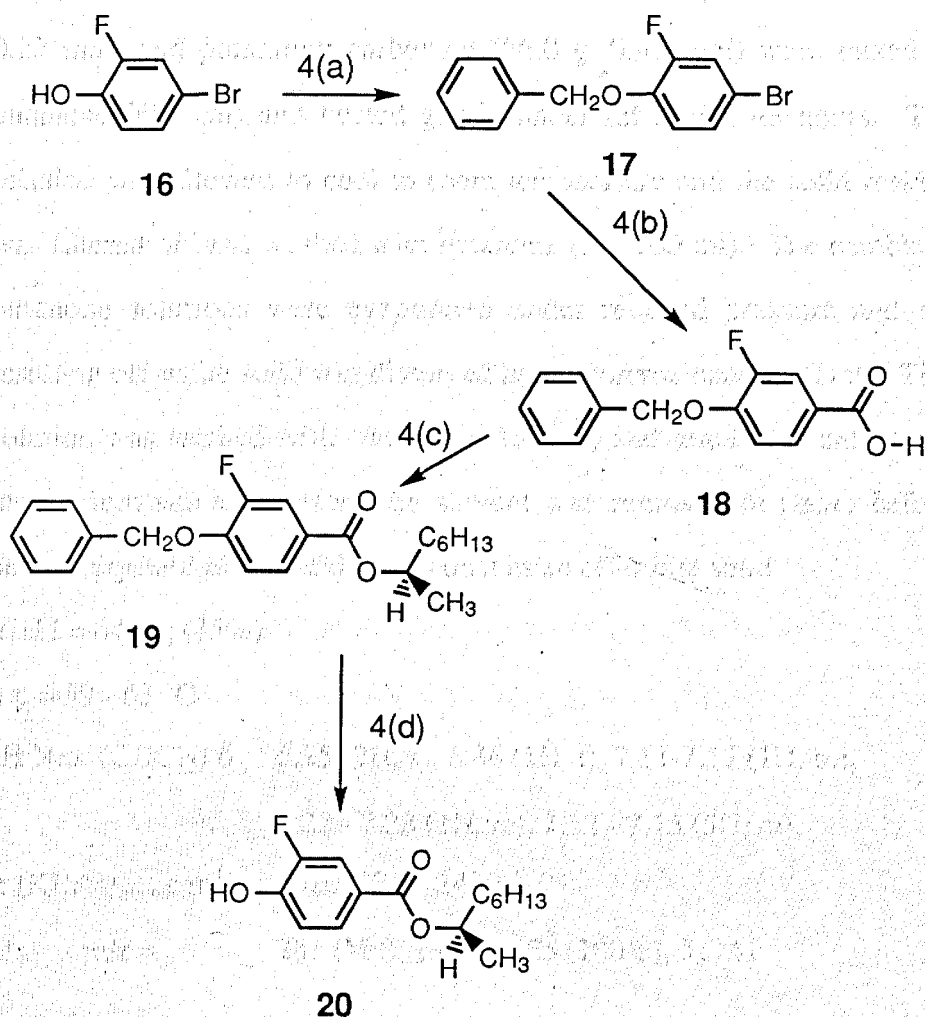
Reagents : 4(a) ... benzyl chloride, K_2CO_3, butanone

4(b) ... i) BuLi, ii) CO_2, iii) dil. HCl

4(c) ... (S)-(+)-octan-2-ol, DEAD, PPh_3, THF

4(d) ... Pd / C, H_2(g), ethyl acetate

1-Benzyloxy-4-bromo-2-fluorobenzene (17)

Benzyl chloride (37.6 g, 0.297 mol), 4-bromo-2-fluorophenol (16) (51.9 g, 0.27 mol) and potassium carbonate (56.0 g, 0.41 mol) were mixed in butanone (600 ml) and heated gently under reflux for 48 hours. The solution was allowed to cool to room temperature and the solid residue was filtered off and washed with butanone (3 x 100 ml). The combined butanone solutions were evaporated under reduced pressure and the resulting off-white solid was dissolved in dichloromethane (300 ml). This solution was washed with water (3 x 150 ml) and dried over anhydrous magnesium sulphate before the solvent was removed *in vacuo* before being recrystallised to yield the product as an off-white solid.

Yield = 64.8 g (85%)

mp = 59 - 63 °C

^{1}H Nmr (CDCl$_3$) δ   5.25 (2H, s), 6.86 (1H, t), 7.11-7.17 (1H, m),

7.22 - 7.28 (1H, m), 7.32 - 7.45 (5H, m)

Ir (KBr) v_{max} cm^{-1} 3020, 2960, 1490, 860

Ms   m/z =   281 (M$^+$), 199, 91, 65 (100%), 51, 41

4-Benzyloxy-3-fluorobenzoic acid (18)

To a solution of compound 17 (19.7 g, 0.07 mol), dissolved in THF (600 ml), under a nitrogen atmosphere maintained at -70 °C was added 10M butyllithium (7.7 ml in hexanes, 0.077 mol). The reaction was monitored by gc until the starting material was completely consumed and the mixture then allowed to warm to -30 °C. Carbon dioxide was bubbled through the mixture and the reaction was stirred for a further 12 hours. 2M Sulphuric acid (100 ml) was added and the mixture was washed with diethyl ether (3 x 200 ml). The organic layers were combined, dried over anhydrous magnesium sulphate and the solvents removed by evaporation under reduced pressure. The pure product was obtained as an off-white solid by

column chromatography using ethyl acetate / dichloromethane 1:1 as eluent follwed by recrystalisation from propan-2-ol.

Yield = 9.8 g (57%)

mp = 176 °C

^{1}H Nmr (CDCl$_3$) δ   5.23 (2H, s), 7.05 (1H, t), 7.31-7.48 (5H, m),

                          7.73 (1H, d), 7.75 - 7.32 (1H, m), acid proton not

                          detected

Ir (KBr) v_{max} cm^{-1} 3040, 2940, 1670, 1500, 850

Ms   m/z =   246 (M$^+$), 147, 91 (100%), 65, 51, 41

(R)-(-)-(1-Methylheptyl) 4-benzyloxy-3-fluorobenzoate (19)

This compound was prepared using a similar method to the one employed for the synthesis of compound **8** using the following charge;

compound **18**, 6.1 g (0.025 mol),

(S)-(+)-octan-2-ol, 3.3 g (0.025 mol),

diethyl azodicarboxylate, 3.8 g (0.02 mol),

triphenylphosphine, 5.3 g (0.02 mol),

THF, 100 ml.

The pure product was obtained as an oil by column chromatography [dichloromethane / petroleum ether (bp 40-60 °C) 3:7 as eluent].

Yield = 5.6 g (63%)

^{1}H Nmr (CDCl$_3$) δ   0.87 (3H, t), 1.12 - 1.44 (8H, m),

                          1.46 - 1.99 (5H, m), 5.10 (1H, m), 5.15 (2H, s),

                          7.05 (1H, t), 7.31-7.48 (5H, m),

                          7.73 (1H, d), 7.75 - 7.32 (1H, m)

Ir (neat) v_{max} cm^{-1} 2920, 1720, 1280, 1200, 860

Ms   m/z =   358 (M$^+$), 246, 229, 139, 91 (100%), 65

Specific Rotation : $[\alpha]_D = -23.6$ °

(R)-(-)-1-Methylheptyl 3-fluoro-4-hydroxybenzoate (20)

Compound **19** (5.5 g, 0.016 mol) and 10% Pd on charcoal (1.0 g) were dissolved in ethyl acetate and the vessel was evacuated. Once evacuation was complete, the vessel was filled with hydrogen. This process was repeated three times before finally being filled with hydrogen and stirred at room temperature until no further hydrogen was consumed. The mixture was passed through a bed of 'Hyflo Supercel' filter aid to remove the catalyst and the solvent removed *in vacuo*. The pure product was obtained as an oil by column chromatography using dichloromethane as eluent.

Yield = 2.4 g (56%)

^{1}H Nmr (CDCl$_3$) δ   0.87 (3H, t), 1.18 - 1.46 (8H, m),

        1.52 - 1.79 (5H, m), 5.12 (1H, m), 7.05 (1H, t),

        7.73 (1H, d), 7.75 - 7.32 (1H, m), phenolic proton

        not observed

Ir (neat) v_{max} cm^{-1} 3350, 2940, 2920, 2860, 1680, 1220, 950, 840

Ms   m/z =   268 (M$^+$), 156, 139, 112, 83(100%), 70

Specific Rotation : $[\alpha]_D$ = -19.2 °

Scheme 5
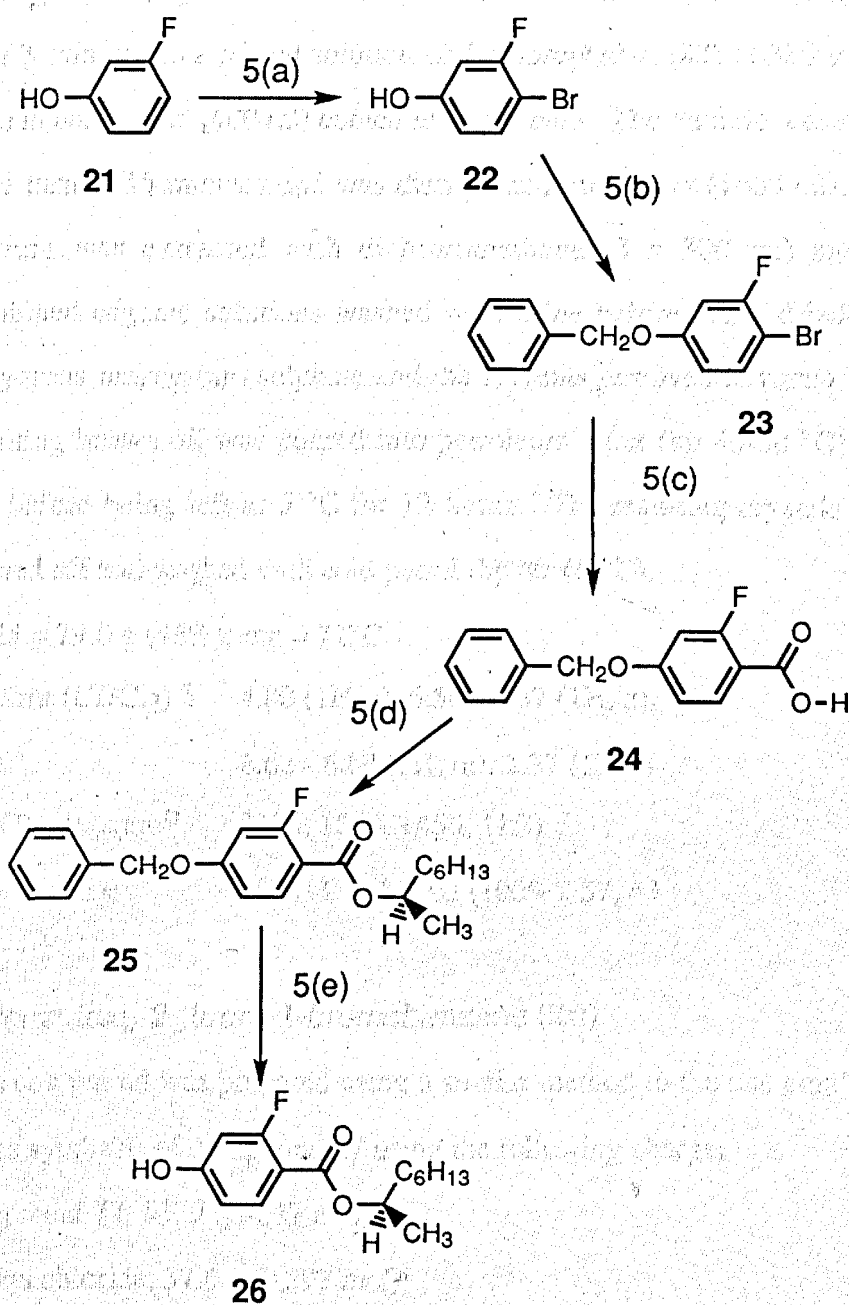
Reagents:

5(a) ... bromine, acetic acid

5(b) ... benzyl chloride, K$_2$CO$_3$, butanone

5(c) ... i) BuLi, ii) CO$_2$, (iii) dil. HCl

5(d) ... (S)-(+)-octan-2-ol, DEAD, PPh$_3$, THF

5(e) ... Pd / C, H$_2$(g), ethyl acetate

4-Bromo-3-fluorophenol (22)

Bromine (144.2 g, 0.90 mol) in acetic acid (80 ml) was added dropwise over 3 minutes to a stirred solution of 3-fluorophenol (21) (100.0 g, 0.90 mol) in acetic acid (400 ml) cooled in an ice bath. The mixture was stirred for a further 15 minutes and was then poured into water (1000 ml). The mixture was extracted with dichloromethane (3 x 300 ml) and the combined organic solutions washed with brine before being dried over anhydrous magnesium sulphate and the solvents removed *in vacuo*. The resulting brown oil was poured into petroleum ether (bp 40-60 °C) (200 ml) before being left at 5 °C for 12 hours. The resulting crystals were filtered off and washed with cold petrol (bp 40-60 °C).

Yield = 79.0 g (46%); mp = 71°C

^{1}H Nmr (CDCl$_3$) δ 4.80 (1H, s), 6.50 - 6.57 (1H, d),

6.62 - 6.69 (1H, m), 7.37 (1H, t)

Ir (KBr) ν_{max}cm^{-1} 3300, 1590, 1450, 1150

Ms   m/z =   190 (M$^+$), 83, 63 (100%), 57, 43

4-Benzyloxy 2-fluoro-1-bromobenzene (23)

This compound was prepared using a similar method to the one employed in the synthesis of compound 17 using the following charge;

compound 22, 51. 9 g (0.27 mol),

benzyl chloride, 37.6 g (0.297 mol),

potassium carbonate, 56.0 g (0.41mol),

butanone, 600 ml.

The Product was obtained as a liquid. Yield = 73.82g (97%)

^{1}H Nmr (CDCl$_3$) δ 5.00 (2H, s), 6.63 - 6.69 (1H, d),

6.72 - 6.78 (1H, m), 7.24 - 7.44 (6H, m)

Ir (neat) ν_{max}cm^{-1} 3040, 3020, 1600, 1480, 1170

Ms   m/z =   280 (M$^+$), 190, 91 (100%), 82, 66, 55

4-Benzyloxy-2-fluorobenzoic acid (24)

This compound was prepared using a similar method to the one employed in the synthesis of compound **18** using the following charge;

compound **23**, 19.7 g (0.070 mol),

10M butyllithium, 7.7 ml in hexanes (0.077 mol),

tetrahydrofuran, 600 ml.

The pure product was obtained as an off-white solid by column chromatography using ethyl acetate / dichloromethane 1:1 as eluent followed by recrystallisation from propan-2-ol.

Yield = 7.2 g (42%); mp = 147 °C

^{1}H Nmr (CDCl$_3$)	δ 5.20 (2H, s), 6.65 - 6.76 (1H, dd),
	6.77 - 6.82 (1H, dd) 7.30 - 7.46 (5H, m),
	7.93 (1H, t), acid proton not detected
Ir (KBr) v_{max}cm^{-1}	3010, 2980, 1700, 1610, 1240, 1270
Ms m/z =	246 (M$^+$), 168, 155, 138, 90 (100%), 65

(R)-(-)-1-Methylheptyl 4-benzyloxy-2-fluorobenzoate (25)

This compound was prepared using a similar method to the one employed in the synthesis of compound **19** using the following charge;

compound **24**, 6.1 g (0.025 mol),

(S)-(+)-octan-2-ol, 3.3 g (0.025 mol),

diethyl azodicarboxylate, 5.1 g (0.025 mol),

triphenylphosphine, 7.2 g (0.0275 mol),

tetrahydrofuran, 600 ml.

The pure product was obtained as a light brown oil by column chromatography using petroleum ether (bp 40-60 °C) / dichloromethane 1:1 as eluent.

Yield = 4.3 g (48%)

^{1}H Nmr (CDCl$_3$) δ 0.88 (3H, t), 1.20 - 1.41 (8H, m),

1.50 - 1.75 (5H, m), 5.05 - 5.19 (1H, m),

5.25 (2H, s), 6.64 - 6.72 (1H, m),

6.73 - 6.79 (1H, m), 7.28 - 7.41 (5H, m),

7.88 (1H, t)

Ir (neat) ν_{max}cm^{-1} 2920, 2880, 1720, 1280, 1200, 1120

Ms   m/z =   358 (M$^+$), 337, 247, 229, 138 (100%), 110

Specific Rotation : $[\alpha]_D$ = -17.2 °

(R)-(-)-1-Methylheptyl 2-fluoro-4-hydroxybenzoate (26)

This compound was prepared using a similar method to the one employed

in the synthesis of compound 20 using the following charge;

compound 25 2.3 g (6.5 mmol),

10% Pd on charcoal 1.0 g ,

ethyl acetate 100 ml.

The pure product was obtained as a light brown oil by column

chromatography using petroleum ether (bp 40-60 °C) / dichloromethane

1:1 as eluent.

Yield = 1.3 g (48%)

^{1}H Nmr (CDCl$_3$) δ   0.88 (3H, t), 1.19 - 1.41 (8H, m),

1.50 - 1.77 (5H, m), 5.05 - 5.19 (1H, m),

6.64 - 6.72 (1H, m), 6.73 - 6.79 (1H, m),

7.88 (1H, t), phenolic proton not detected

Ir (neat) ν_{max}cm^{-1} 3340, 2920, 2860, 1680, 1620, 1220, 1140, 1120

Ms   m/z =   268 (M$^+$), 246, 156, 139, 91(100%), 65

Specific Rotation : $[\alpha]_D$ = -24.8 °

Scheme 6
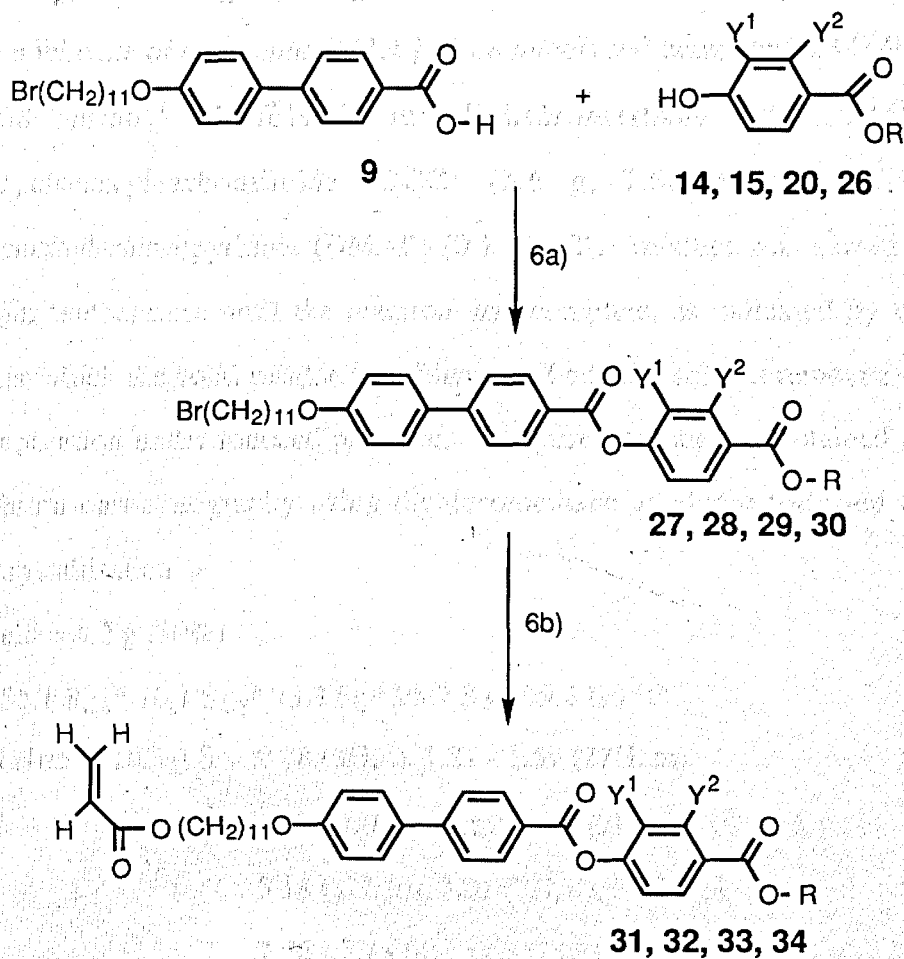
14, 27, 31, ; $Y^1 = Y^2 = H$, R = (R)-1-methylhepyl
15, 28, 32, ; $Y^1 = H$, $Y^2 = F$, R = (R)-1-methylheptyl
20, 29, 33, ; $Y^1 = F$, $Y^2 = H$, R = (R)-1-methylheptyl
26, 30, 34, ; $Y^1 = Y^2 = H$, R = 1-propylbutyl

Reagents: 6(a) ... DCC / DMAP, dichloromethane

6(b) ... Sodium acrylate, KI, HMPA

(R)-(-)-4-(1-Methylheptyloxycarbonyl)phenyl 4'-(11-bromoundecyloxy)biphenyl-4-carboxylate (**27**)[87]

To a mixture of compound **9** (3.4 g, 7.68 mmol) and compound **14** (1.9 g, 7.68 mmol) dissolved in dichloromethane was added dicyclohexylcarbodiimide (DCC) (1.6 g, 7.68 mmol) and 4-(dimethylamino)pyridine (DMAP) (0.1 g). The mixture was stirred at room temperature until the reaction was complete, as indicated by tlc, after which the solid residue was filtered off and the solvent removed by evaporation under reduced pressure. The pure product was obtained by column chromatography using dichloromethane as eluent followed by recrystallisation.

Yield = 4.2 g (80%)

K 55.1 S_{CA}* 70.1 $S_{C\gamma}$* 73.3 S_C* 95.7 S_A 109.4 Iso °C

^{1}H Nmr (CDCl$_3$) δ   0.88 (3H, t), 1.21 - 1.59 (27H, m),

1.72 - 1.93 (4H, m), 3.41 (2H, t), 4.02 (2H, t),

5.18 (1H, m), 7.01 (2H, d), 7.32 (2H, d),

7.56 - 7.78 (4H, dd), 8.13 (2H, d), 8.25 (2H, d)

Ir (KBr) ν_{max} cm^{-1} 2940, 2870, 1740, 1710, 1600, 1270, 1210, 1070

Ms   m/z =   678 (M$^+$), 431, 385, 197 (100%), 141, 69

Specific Rotation :   [α]$_D$ = -18.9 °

(R)-(-)-4-(1-Methylheptyloxycarbonyl)-3-fluorophenyl 4'-(11-bromoundecyloxy)biphenyl-4-carboxylate (**28**)

This compound was prepared using a similar method to that described for the preparation of compound **27** using the following charge;

compound **26**, 2.0 g (7.72 mmol),

compound **9**, 3.4 g (7.72 mmol),

dicyclohexylcarbodiimide, 1.59 g (7.7 mmol),

DMAP, 0.1 g,

dichloromethane, 100 ml.

Yield = 2.5 g (47%)

K 63.2 $S_{CA}*$ 78.9 $S_{C\gamma}*$ 79.7 S_C* 102.5 S_A 107.3 Iso °C

^{1}H Nmr (CDCl$_3$) δ   0.89 (3H, t), 1.23 - 1.62 (27H, m),

1.70 - 1.93 (4H, m), 3.41 (2H, t), 4.01 (2H, t),

5.19 (1H, m), 7.02 (2H, d), 7.06 - 7.14 (2H, m),

7.56 - 7.74 (4H, dd), 8.03 (1H, t), 8.22 (2H, d)

Ir (KBr) ν_{max}cm^{-1} 2920, 2850, 1750, 1710, 1600, 1240, 1210, 1060

Ms   m/z =   696 (M$^+$), 464, 335, 197 (100%), 141, 55

Specific Rotation :   [α]$_D$ = -15.6 °

(R)-(-)-4-(1-Methylheptyloxycarbonyl)-2-fluorophenyl 4'-

(11-bromoundecyloxy)biphenyl-4-carboxylate **(29)**

This compound was prepared using a similar method to that described for

the preparation of compound **27** using the following charge;

compound **20**, 2.0 g (7.0 mmol),

compound **9**, 3.4 g (7.0 mmol),

dicyclohexylcarbodiimide, 1.4 g (7.0 mmol),

DMAP, 0.1 g,

dichloromethane, 100 ml.

Yield = 2.2 g (44%)

K 44.8 $S_{CA}*$ 50.6 $S_{C\gamma}*$ 52.6 S_C* 53.8 S_A 86.6 Iso °C

^{1}H Nmr (CDCl$_3$) δ   0.89 (3H, t), 1.23 - 1.62 (27H, m),

1.70 - 1.93 (4H, m), 3.41 (2H, t), 4.01 (2H, t),

5.19 (1H, m), 7.02 (2H, d), 7.06 - 7.14 (2H, m),

7.56 - 7.74 (4H, dd), 8.03 (1H, t), 8.22 (2H, d)

Ir (KBr) ν_{max}cm^{-1} 2920, 2850, 1750, 1710, 1600, 1240, 1210, 1060

Ms   m/z =   696 (M$^+$), 464, 335, 197 (100%), 141, 55

Specific Rotation :   [α]$_D$ = -18.2 °

4-(1-Propylbutyloxycarbonyl)phenyl 4'-(11-

bromoundecyloxy)biphenyl-4-carboxylate (**30**)

This compound was prepared using a similar method to that described for

the preparation of compound **27** using the following charge;

compound **15**, 1.7 g (8.0 mmol),

compound **9**, 3.5 g (8.0 mmol),

dicyclohexylcarbodiimide, 1.7 g (8.0 mmol),

DMAP, 0.1 g,

dichloromethane 100ml.

Yield = 3.5 g (64%)

K 64.9 S_{CAlt} 74.7 S_A 78.9 Iso °C

^{1}H Nmr (CDCl$_3$) δ   0.89 (3H, t), 1.23 - 1.60 (25H, m),

1.72 - 1.93 (4H, m), 3.41 (2H, t), 4.01 (2H, t),

5.18 (1H, m), 7.02 (2H, d), 7.32 (2H, d),

7.56 - 7.74 (4H, dd), 8.13 (2H, d), 8.24 (2H, d)

Ir (KBr) v_{max}cm^{-1} 2920, 2850, 1750, 1710, 1600, 1260, 1200, 1070

Ms   m/z =   664 (M$^+$), 431, 385, 298, 197 (100%), 176, 91

(R)-(-)-11-{4'-[4-(1-Methylheptyloxycarbonyl)phenyloxycarbonyl]

biphenyl-4-yloxy}undecyl acrylate (**31**)

To a solution of compound **27** (1.0 g, 1.45 mmol) and sodium acrylate

(0.14 g, 1.46 mmol) dissolved in hexamethylphosphoramide (20 ml) was

added a small amount of potassium iodide (0.01 g) and the mixture was

stirred at room temperature. The reaction was monitored by tlc until the

reaction was complete whereupon the addition of dilute hydrochloric acid

(50 ml) afforded the crude product as a solid which was isolated by

filtration. The pure product was obtained by column chromatography

(dichloromethane / petroleum ether (bp 40-60 °C) 1:1 as eluent) and

recrystallisation.

Yield = 0.43 g (45%)

K 28.4 S_{CA}* 49.8 $S_{C\gamma}$* 50.3 S_C* 65.7 S_A 94.7 Iso °C

^{1}H Nmr (CDCl$_3$) δ   0.89 (3H, t), 1.21 - 1.59 (27H, m),

1.72 - 1.93 (4H, m) 4.02 (2H, t), 4.14 (2H, t),

5.20 (1H, m), 5.82 (1H, dd), 6.08 - 6.19 (1H, m),

6.37 - 6.44 (1H, dd), 7.02 (2H, d), 7.32 (2H, d),

7.56 - 7.74 (4H, dd), 8.13 (2H, d), 8.25 (2H, d)

Ir (KBr) v_{max} cm^{-1} 2920, 2850, 1750, 1710, 1600, 1240, 1210, 1060

Ms   m/z =   670 (M$^+$), 431, 214 (100%), 197, 69, 55

Specific Rotation :   [α]$_D$ = -12.9 °

(R)-(-)-11-{4'-[4-(1-Methylheptyloxycarbonyl)-3-fluorophenyloxy carbonyl]biphenyl-4-yloxy}undecyl acrylate (**32**)

This compound was prepared using a similar method to that described for

the preparation of compound **31** using the following charge;

compound **30**, 1.0 g (1.43 mmol),

sodium acrylate, 0.13 g (1.43 mmol),

potassium iodide, 0.01 g,

hexamethylphosphoramide, 20 ml

Yield = 0.57 g (57%)

K 14.8 S_{CA}* 41.8 $S_{C\gamma}$* 42.4 S_C* 58.6 S_A 90.4 Iso °C

^{1}H Nmr (CDCl$_3$) δ   0.89 (3H, t), 1.21 - 1.59 (27H, m),

1.72 - 1.93 (4H, m), 4.02 (2H, t), 4.12 (2H, t),

5.20 (1H, m), 5.84 (1H, dd), 6.08 - 6.17 (1H, m),

6.37 - 6.44 (1H, dd), 7.02 (2H, d),

7.06 - 7.14 (2H, m), 7.56 - 7.74 (4H, dd),

8.03 (1H, t), 8.22 (2H, d)

Ir (KBr) v_{max} cm^{-1} ·2970, 2860, 1720, 1690, 1610, 1250, 1200, 1060

Ms   m/z =   688 (M$^+$), 421, 395, 197, (100%) 97, 55

Specific Rotation : $[\alpha]_D = -21.1\ °$

(R)-(-)-11-{4'-[4-(1-Methylheptyloxycarbonyl)-2-fluorophenyl

oxycarbonyl]biphenyl-4-yloxy}undecyl acrylate (**33**)

This compound was prepared using a similar method to that described in

the preparation of compound **31** using the following charge;

compound **29**, 1.0 g (1.43 mmol),

sodium acrylate, 0.13 g (1.43 mmol),

potassium iodide, 0.01 g,

hexamethylphosphoramide 20 ml

Yield = 0.44 g (44%)

K 7.5 S_{CA}* 28.6 S_C* 33.2 S_A 78.7 Iso °C

^{1}H Nmr (CDCl$_3$) δ   0.89 (3H, t), 1.21 - 1.59 (27H, m),

1.72 - 1.93 (4H, m), 4.02 (2H, t), 4.12 (2H, t),

5.20 (1H, m), 5.84 (1H, dd), 6.08 - 6.17 (1H, m),

6.37 - 6.44 (1H, dd), 7.02 (2H, d),

7.06 - 7.14 (2H, m), 7.56 - 7.74 (4H, dd),

8.03 (1H, t), 8.22 (2H, d)

Ir (KBr) v_{max} cm^{-1} 2980, 2840, 1740, 1710, 1610, 1240, 1210, 1060

Ms   m/z =   688 (M$^+$), 421, 295, 214, (100%), 197, 97, 55

Specific Rotation : $[\alpha]_D = -25.1\ °$

11-{4'-[4-(1-Propylbutyloxycarbonyl)phenyloxycarbonyl]

biphenyl-4-yloxy}undecyl acrylate (**34**)

This compound was prepared using an identical method to that described

for the preparation of compound **31** using the following charge;

compound **28**, 1.0 g (1.45 mmol),

sodium acrylate, 0.14 g (1.45 mmol),

potassium iodide, 0.01 g,

hexamethylphosphoramide, 20 ml

Yield = 0.84g (85%)

K 38.4 $S_{C_{Alt}}$ 41.9 S_A 76.9 Iso °C

^{1}H Nmr (CDCl$_3$) δ   0.89 (3H, t), 1.23 - 1.60 (25H, m),

        1.72 - 1.93 (4H, m), 4.02 (2H, t), 4.12 (2H, t),

        5.20 (1H, m), 5.84 (1H, dd), 6.08 - 6.17 (1H, m),

        6.37 - 6.44 (1H, dd), 7.02 (2H, d),

        7.32 (2H, d), 7.56 - 7.75 (4H, dd), 8.14 (2H, d),

        8.25 (2H, d)

Ir (KBr) ν_{max} cm^{-1} 2940, 2860, 1740, 1720, 1610, 1240, 1200, 1060

Ms   m/z =   656 (M$^+$), 421, 295, 197 (100%), 97, 55

Scheme 7

37, 39 ; R = (R)-1-methylheptyl   **39, 40**
38, 40 ; R = 1-propylbutyl
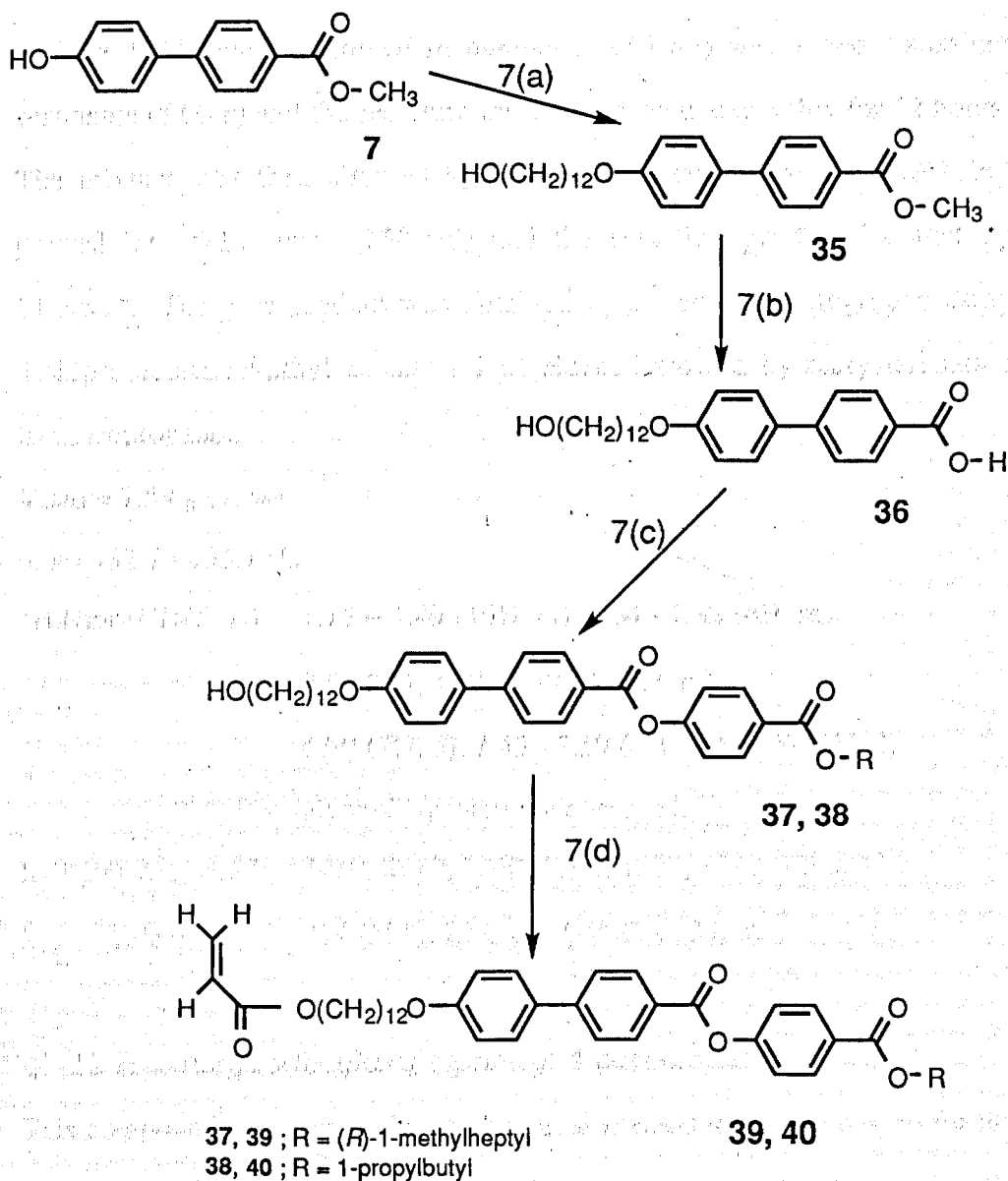
Reagents:

7(a) ... 12-bromododecan-1-ol, K_2CO_3, butanone,

7(b) ... (i) NaOH (aq), ethanol, (ii) dil. HCl

7(c) ... DCC , DMAP, dichloromethane, alcohol

7(d) ... acryloyl chloride, dichloromethane,

diisopropylamine

Methyl 4'-(12-hydroxydodecyloxy)biphenyl-4-carboxylate (**35**)

To a solution of 12-bromododecanol (5.00 g, 0.019 mol) and compound **7** (4.33 g, 0.019 mol) dissolved in butanone (150 ml) was added potassium carbonate (5.00 g) and the resulting mixture heated under reflux for 12 hours. The mixture was then allowed to cool to room temperature before being poured into cold water (150 ml) and the resulting product isolated by filtration. The pure product was obtained by colmn chromatography using dichloromethane / ethyl acetate 1:1 as eluent followed by recrystallisation from isopropanol.

Yield = 7.59 g (97%)

mp = 132.7 - 133.1 °C

^{1}H Nmr (CDCl$_3$) δ   1.15 – 1.49 (16H, m), 1.64 - 1.82 (4H, m),

3.84 (3H, s), 3.98 - 4.08 (4H, m),

6.90 (2H, d), 7.45 - 7.59 (4H, dd), 7.96 (2H, d),

alcoholic proton not observed.

Ir (KBr) v_{max} cm^{-1} 3410, 2910, 2860, 1740, 1280, 1210, 1200, 1120

Ms   m/z =   414 (M$^+$), 228, 197 (100%), 139, 69

4'-(12-Hydroxydodecyloxy)biphenyl-4-carboxylic acid (**36**)

This compound was prepared using a similar method to that employed for the preparation of compound **9** using the following charge;

compound **35**, 7.59 g (0.018 mol),

ethanol, 250 ml,

sodium hydroxide, 5 g,

water, 15 ml,

dilute hydrochloric acid. 200 ml.

Yield = 4.58 g (60%)

mp = decomposed above 300°C

^{1}H Nmr (CDCl$_3$) δ   1.15 – 1.49 (16H, m), 1.64 - 1.82 (4H, m),

3.98 - 4.08 (4H, m), 6.90 (2H, d),

7.45 - 7.59 (4H, dd), 7.96 (2H, d), acidic and

alcoholic protons not observed

Ir (KBr) v_{max} cm^{-1} 3400, 2920, 2840, 1670, 1100, 1000

Ms   m/z =   400 (M$^+$), 336, 214, 197 (100%), 69

(R)-(-)-4-(1-Methylheptyloxycarbonyl)phenyl 4'-(12-hydroxydodecyloxy)biphenyl-4-carboxylate **(37)**

This compound was prepared using an similar method to that employed for the preparation of compound **27** using the following charge;

compound **36**, 2.80 g (7.04 mmol),

compound **14**, 3.50 g (14.08 mmol),

dicyclohexylcarbodiimide, 1.46 g (7.04 mmol),

DMAP, 1.0 g,

dichlorormethane, 100 ml.

Yield = 1.68 g (38%)

K 53.6 S$_A$ 111.3 Iso °C

^{1}H Nmr (CDCl$_3$) δ   0.88 (3H, t), 1.01 - 1.96 (33H, m),

3.98 - 4.08 (4H, m), 5.13 (1H, m), 6.84 (2H, d),

6.92 (2H, d), 7.84 - 7.64 (4H, dd), 7.93 (2H, d),

8.08 (2H, d), alcoholic proton not observed

Ir (KBr) v_{max} cm^{-1} 3410, 2940, 2870, 1740, 1710, 1610, 1210, 1070

Ms   m/z =   630 (M$^+$), 430, 385, 214 (100%), 141, 55

Specific Rotation :   [α]$_D$ = -14.9 °

4-(1-Propylbutyloxycarbonyl)phenyl 4'-(12-hydroxydodecyloxy) biphenyl-4-carboxylate **(38)**

This compound was prepared using a similar method to that described for the preparation of compound **27** using the following charge;

compound **36**, 2.86 g (7.20 mmol),

compound **15**, 3.39 g (14.40 mmol),

dicyclohexylcarbodiimide, 1.48 g (7.20 mmol),

DMAP, 1.0 g,

dichlorormethane, 100 ml.

Yield = 1.44 g (33%)

K 46.7 S_A 99.3 Iso °C

^{1}H Nmr (CDCl$_3$) δ   0.88 (6H, t), 1.23 - 1.83 (28H, m),

3.98 - 4.08 (4H, m), 5.20 (1H, m), 7.02 (2H, d),

7.32 (2H, d), 7.56 - 7.74 (4H, m), 8.13 (2H, d),

8.24 (2H, d), alcoholic proton not observed

Ir (KBr) v_{max} cm^{-1} 3410, 2920, 2850, 1750, 1710, 1600, 1260, 1200,

Ms   m/z =   616 (M$^+$), 464, 335, 197 (100%), 141, 69, 55

(R)-(-)-12-{4'-[4-(1-Methylheptyloxycarbonyl)phenyloxycarbonyl]
biphenyl-4-yloxy}dodecyl acrylate **(39)**

To a solution of compound **37** (1.20 g, 4.08 mmol) and acryloyl chloride (0.36 g, 4.08 mmol) in dry dichloromethane (25 ml) was added dropwise diisopropylamine (1 ml) and the reaction stirred at room temperature. The reaction was monitored by tlc until complete whereupon the mixture was diluted with further dichloromethane (30 ml) and washed with 10% hydrochloric acid (50 ml) and water (2 x 50 ml) before being dried over anhydrous magnesium sulphate and the solvents removed *in vacuo*. The pure product was obtained by column chromatography using dichloromethane / petroleum ether (bp 40-60 °C) 1:1 as eluent and recrystallised from ethanol.

Yield = 0.68 g (48%)

K 52.6 S_{CA}* 87.3 $S_{C\gamma}$* 88.1 S_C* 97.3 S_A 103.6 Iso °C

^{1}H Nmr (CDCl$_3$) δ   0.88 (3H, t), 1.24 - 1.59 (29H, m),

1.72 - 1.93 (4H, m), 4.02 (2H, t), 4.11 (2H, t),

5.19 (1H, m), 5.84 (1H, dd), 6.08 - 6.17 (1H, m),

6.34 - 6.44 (1H, dd), 7.02 (2H, d), 7.32 (2H, d),

7.56 - 7.74 (4H, dd), 8.13 (2H, d), 8.25 (2H, d)

Ir (KBr) v_{max} cm^{-1} 2920, 2850, 1750, 1710, 1680, 1600, 1240, 1060

Ms   m/z =   684 (M$^+$), 431, 228, 197 (100%), 69, 55

Specific Rotation : $[\alpha]_D = -23.6\,^\circ$

12-{4'-[4(1-Propylbutyloxycarbonyl)phenyloxycarbonyl]biphenyl-4-yloxy}dodecyl acrylate **(40)**

This compound was prepared using a similar method to that described for the

preparation of compound **39** using the following charge;

compound **38**, 1.20 g (1.94 mmol),

acryloyl chloride, 0.36 g (4.08 mmol),

diisopropylamine, 1 ml,

dichloromethane, 25 ml.

Yield = 0.62 g (45%)

K 57.6 S$_{CA\text{lt}}$ 72.3 S$_A$ 87.5 Iso °C

^{1}H Nmr (CDCl$_3$) δ   0.88 (6H, t), 1.24 - 1.60 (24H, m),

1.72 - 1.93 (4H, m), 4.02 (2H, t), 4.11 (2H, t),

5.19 (1H, m), 5.84 (1H, dd), 6.08 - 6.17 (1H, m),

6.34 - 6.44 (1H, dd), 7.02 (2H, d), 7.32 (2H, d),

7.56 - 7.74 (4H, dd), 8.13 (2H, d), 8.25 (2H, d)

Ir (KBr) v_{max} cm^{-1} 2950, 2860, 1750, 1710, 1680, 1610, 1240, 1060

Ms   m/z =   670 (M$^+$), 422, 295, 214 (100%), 197, 97, 55

Scheme 8
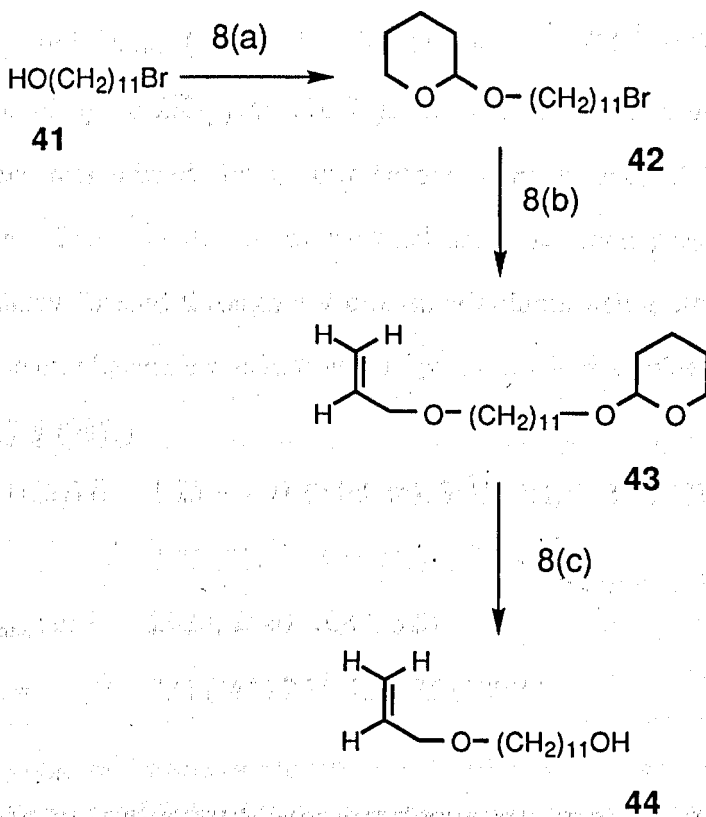
Reagents:

8(a) ... 3,4-dihydro-2*H*-pyran, *p*-toluenesulphonic acid, dichloromethane

8(b) ... allyl alcohol, NaH, THF

8(c) ... *p*-toluenesulphonic acid, dichloromethane

12-(11-Bromoundecan-1-oxy)tetrahydropyran (42)

To a solution of 11-bromoundecan-1-ol (41) (40.0 g, 0.160 mol) and *p*-toluenesulphonic acid (4.0 g) in dichloromethane (100 ml) was added dropwise 3,4-dihydro-2*H*-pyran (16.9 g, 0.2 mol) over 10 minutes at 0 °C. The mixture was stirred for 1 hour before being quenched with sodium bicarbonate. The solvent was evaporated under reduced pressure and the resulting slurry filtered through a 9 cm silica column using ethyl acetate as solvent. The ethyl acetate was removed *in vacuo* to yield a golden liquid.

Yield = 52.7 g (98%)

^{1}H Nmr (CDCl$_3$) δ   1.23 – 1.91 (24H, m), 3.35 (2H, t), 3.71 (2H, t),

        3.75 (2H, t), 4.58 (1H, t)

Ir (film) ν_{max} cm^{-1} 2920, 2840, 1080, 820

Ms   m/z =   334 (M$^+$) 253, 151, 85 (100%)

3-[11-(Tetrahydropyranyl-2-oxy)undecyloxy]prop-1-ene (43)

To a solution of allyl alcohol (1.1 g, 0.018 mol) dissolved in dry tetrahydrofuran (100 ml) was added sodium hydride (60% dispersion in mineral oil) (0.7 g, 0.018 mol). This mixture was stirred at room temperature while compound 42 (6.0 g, 0.018 mol) dissolved in tetrahydrofuran (50 ml) was added dropwise. The reaction mixture was stirred at room temperature until no further reaction was observed upon examination by tlc, whereupon the mixture was further diluted by the addition of THF (100 ml) before being washed with water (3 x 100 ml) and dried over anhydrous magnesium sulphate. The solvent was removed by evaporation under reduced pressure and the resulting slurry purified by column chromatography [dichloromethane in petroleum ether (bp 40-60 °C) 2:8 as eluent] to yield a colourless liquid.

Yield = 4.2 g (74%)

^{1}H Nmr (CDCl$_3$) δ   1.23 – 1.91 (26H, m), 3.35 (2H, t), 3.74 (2H, m),

3.96 (2H, m), 4.56 (1H, m), 5.12 - 5.33 (2H, m),

5.76 - 6.00 (1H, m)

Ir (film) ν$_{max}$cm^{-1} 2920, 2840, 1620, 1120, 1080, 820

Ms   m/z =   312 (M$^+$), 271, 228, 85 (100%), 55

3-(11-Hydroxyundecyloxy)prop-1-ene (44)

To a solution of compound **43** (4.1 g, 0.014 mol) dissolved in
dichloromethane (100 ml) was added *p*-toluenesulphonic acid (2.9 g, 0.0154
mol) and the resulting mixture stirred for 24 hours at room temperature. The
solid residue was filtered off and the filtrate extracted with dichloromethane (2
x 50 ml). The combined dichloromethane fractions were dried over
anhydrous magnesium suphate and removed on a rotary evaporator. The pure
product was obtained by distillation at 198 °C / 1 mm Hg to yield the product
as a colourless liquid.

Yield = 1.4 g (43%)

^{1}H Nmr (CDCl$_3$) δ   1.14 – 1.39 (14H, m), 1.50 - 1.64 (4H, m),

3.42 (2H, t), 3.62 (2H, t), 3.96 (2H, dt),

512 - 5.32 (2H, m), 5.76 - 6.00 (1H, m),

alcoholic proton not observed

Ir (film) ν$_{max}$cm^{-1} 3400, 2920, 2840, 1620, 1080, 820

Ms   m/z =   228 (M$^+$), 197, 155, 97, 85 (100%), 55

Scheme 9
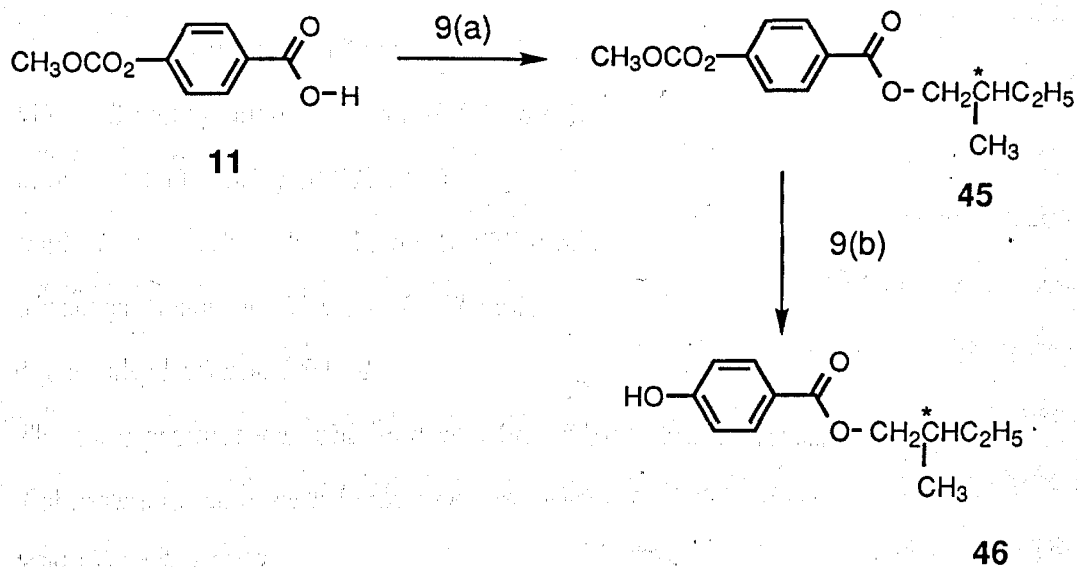
Reagents: 9(a) ... (S)-(-)-2-methylbutanol, DEAD, PPh₃, THF

9(b) ... NH₃(aq), ethanol

(R)-(+)-2-Methylbutyl 4-methoxycarbonyloxybenzoate (45)

This compound was prepared using a similar method to that employed in the synthesis of compound 12 using the following charge;

(S)-(-)-2-methylbutanol, 6.78 g (0.077 mol),

compound 11, 15.1 g (0.077 mol),

diethyl azodicarboxylate, 13.6 g (0.077 mol),

triphenylphosphine, 22.6 g (0.0847 mol),

dry tetrahydrofuran, 250 ml.

The pure product was obtained as a liquid by column chromatography using dichloromethane in petroleum ether (bp 40-60 °C) 3:7 as eluent.

Yield = 14.3 g (66%)

^{1}H Nmr (CDCl$_3$) δ   0.86 - 1.20 (6H, m), 1.21 - 1.36 (1H, m),

                1.44 - 1.60 (1H, m), 1.76 - 1.94 (1H, m),

                3.92 (3H, s), 4.06 - 4.24 (2H, m), 6.95 (2H, d),

                7.97 (2H, d)

Ir (neat) v_{max} cm^{-1} 2960, 2920, 1760, 1710, 1440, 860

Ms   m/z =   266 (M$^+$), 197, 179, 135 (100%), 69, 55

Specific Rotation :   [α]$_D$ = +19.4 °

(R)-(+)-2-Methylbutyl 4-hydroxybenzoate (46)

This compound was prepared using an identical method to the one employed in the synthesis of compound 14 using the following charge:

Compound 45, 14.3 g (0.051 mol),

30% aqueous ammonia, 50 ml,

ethanol, 150 ml.

The pure product was obtained as a liquid by column chromatography using dichloromethane as eluent.

Yield = 10.6 g (100%)

^{1}H Nmr (CDCl$_3$) δ   0.86 - 1.2o (6H, m), 1.21 - 1.36 (1H, m),

1.44 - 1.60 (1H, m), 1.76 - 1.94 (1H, m),

4.06 - 4.24 (2H, m), 6.95 (2H, d), 7.97 (2H, d),

phenolic proton not observed

Ir (neat) ν_{max} cm^{-1} 3410, 2960, 2920, 1760, 1440, 860

Ms   m/z =   208(M$^+$), 197, 179, 135 (100%), 69, 55

Specific Rotation : $[\alpha]_D$ = +21.1 °

Scheme 10
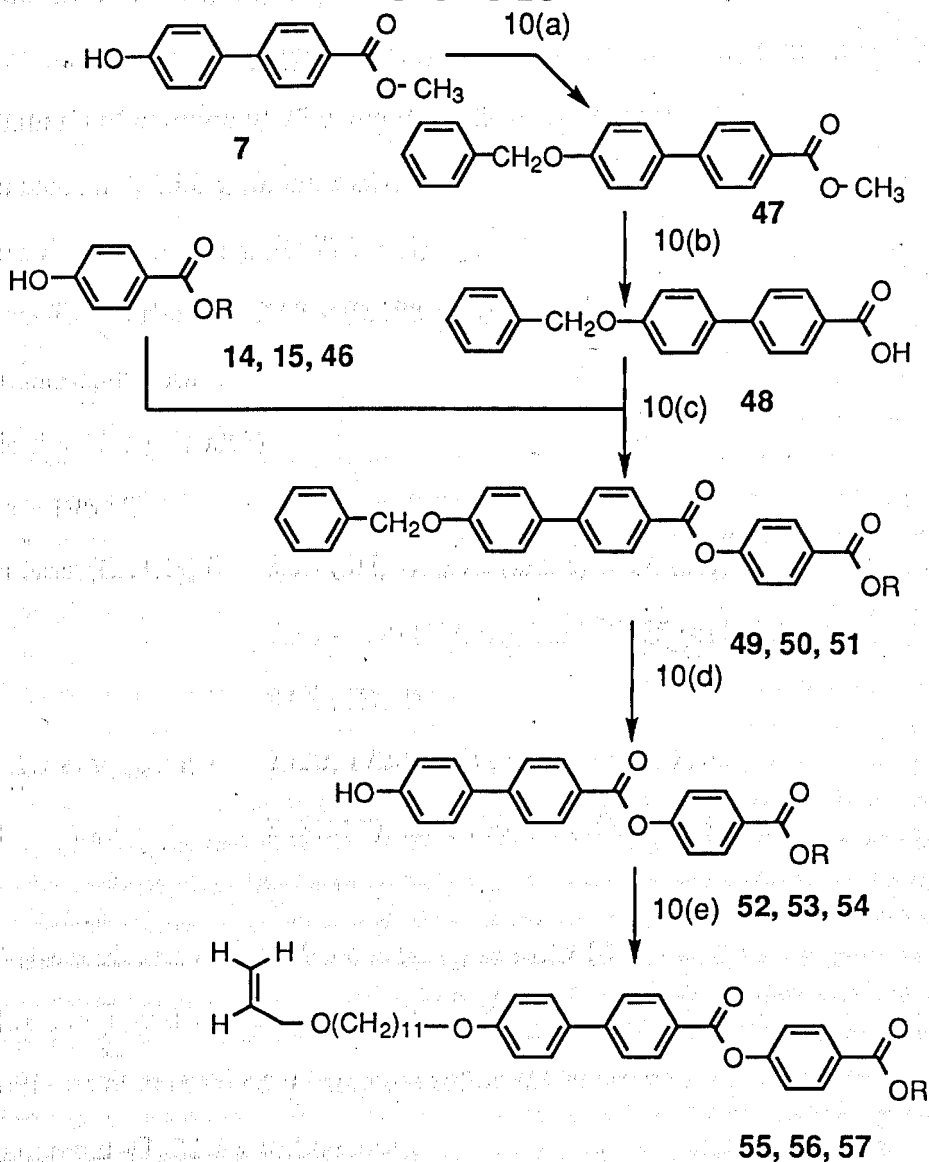
49, 52, 55 ; R = (R)-1-methylheptyl
50, 53, 56 ; R = 1-propylbutyl
51, 54, 57 ; R = (R)-2-methylbutyl

Reagents:

10(a) ... benzyl chloride, K_2CO_3, butanone

10(b) ... (i) NaOH(aq), ethanol (ii) dil. HCl

10(c) ... DCC / DMAP, dichloromethane

10(d) ... Pd / C, H_2(g), THF / ethanol

10(e) ... DEAD, PPh_3, THF, compound **44**

Methyl 4'-benzyloxybiphenyl-4-carboxylate (47)

This compound was prepared using a similar method to that employed in the

synthesis of compound 17 using the following charge;

compound 7, 15.0 g (0.066 mol),

benzyl chloride, 9.2 g (0.0726 mol),

potassium carbonate, 27.3 g (0.198 mol),

butanone, 400 ml.

Yield = 22.1 g (100%)

mp = 196 °C

^{1}H Nmr (CDCl$_3$) δ   3.93 (3H, s), 5.12 (2H, s), 7.06 (2H, d),

7.30 - 7.49 (5H, m), 7.54 - 7.65 (4H, dd),

8.08 (2H, d)

Ir (KBr) v_{max} cm^{-1} 2920, 1720, 1600, 1280, 1190, 770

Ms   m/z =   318(M$^+$), 227, 139, 91 (100%), 65

4'-Benzyloxybiphenyl-4-carboxylic acid (48)

This compound was prepared using a similar method to that employed in the

synthesis of compound 9 using the following charge;

compound 47, 22.1 g (0.066 mol),

sodium hydroxide, 13.0 g,

water, 30 ml,

ethanol, 200 ml,

dilute hydrochloric acid, 200 ml.

Yield = 20.8 g (98%)

mp = decomposed above 300 °C

^{1}H Nmr (CDCl$_3$ + D$_6$ DMSO) δ 5.12 (2H, s), 7.06 (2H, d), 7.30 - 7.49

(5H, m), 7.54 - 7.65 (4H, dd), 8.08 (2H, d), acid

proton not detected

Ir (KBr) v_{max} cm^{-1} 3040, 2920, 1740, 1600, 1280, 1190, 770

Ms   m/z =   304(M$^+$), 213, 139, 91(100%), 65

(R)-(-)-4-(1-Methylheptyloxycarbonyl)phenyl 4'-benzyloxy-biphenyl-4-carboxylate (49)

This compound was prepared using a similar method to that employed in the synthesis of compound **27** using the following charge;

compound **48**, 6.9 g (0.023 mol),

compound **14**, 5.7 g (0.023 mol),

dicyclohexylcarbodiimide, 4.7 g (0.023 mol),

DMAP, 0.1 g,

dichloromethane, 100 ml.

Yield = 5.5 g (44%)

K 186.5 S$_A$ 191.0 Iso °C

^{1}H Nmr (CDCl$_3$) δ   0.88 (3H, t), 1.08 - 1.42 (13H, m), 5.12 (2H, s),

          5.13 - 5.24 (1H, m), 7.10 (2H, d), 7.14 (2H, d)

          7.28 - 7.49 (5H, m), 7.58 - 7.73 (4H, dd),

          8.14 (2H, d), 8.23 (2H, d)

Ir (KBr) v_{max} cm^{-1} 2920, 2840, 1740, 1720, 1260, 1150, 760

Ms   m/z =   536 (M$^+$), 385, 287 (100%), 196, 91

Specific Rotation :   [α]$_D$ = -18.9 °

4-(1-Propylbutyloxycarbonyl)phenyl 4'-benzyloxybiphenyl-4-carboxylate (50)

This compound was prepared using a similar method to that employed in the synthesis of compound **27** using the following charge;

compound **48**, 6.9 g (0.023 mol),

compound **15**, 5.4 g (0.023 mol),

dicyclohexylcarbodiimide, 4.7 g (0.023 mol),

DMAP, 1.0 g,

dichloromethane, 100 ml.

Yield = 5.8 g (48%)

mp = 187 °C

^{1}H Nmr (CDCl$_3$) δ   0.95 (6H, t), 1.14 - 1.50 (4H, m),

                        1.50 - 1.80 (4H, m), 5.10 (2H, s),

                        5.11 - 5.24 (1H, m), 7.10 (2H, d), 7.14 (2H, d)

                        7.28 - 7.48 (5H, m), 7.58 - 7.73 (4H, dd),

                        8.14 (2H, d), 8.23 (2H, d)

Ir (KBr) ν$_{max}$ cm^{-1} 2920, 2850, 1740, 1720, 1280, 1150, 760

Ms   m/z =   526 (M$^+$), 385, 287 (100%), 196, 91

(R)-(+)-4-(2-Methylbutyloxycarbonyl)phenyl 4'-benzyloxy

biphenyl-4-carboxylate **(51)**

This compound was prepared using a similar method to that employed in the

synthesis of compound **27** using the following charge;

compound **48**, 6.9 g (0.023 mol),

compound **46**, 4.8 g (0.023 mol),

dicyclohexylcarbodiimide, 4.74 g (0.023 mol),

DMAP, 1.0 g,

dichloromethane, 100 ml.

Yield = 5.7 g (50%)

K 174.2 S$_A$ 184.5 Iso °C

^{1}H Nmr (CDCl$_3$) δ   0.93 - 1.07 (6H, m), 1.21 - 1.37 (1H, m),

                        1.47 - 1.62 (1H, m), 1.82 - 1.95 (1H, m),

                        4.10 - 4.27 (2H, m), 5.12 (2H, s), 7.10 (2H, d),

                        7.14 (2H, d), 7.28 - 7.49 (5H, m),

                        7.58 - 7.73 (4H, dd), 8.14 (2H, d), 8.23 (2H, d)

Ir (KBr) ν$_{max}$ cm^{-1} 2920, 2840, 1740, 1720, 1260, 1150, 760

Ms   m/z =   494 (M$^+$), 385, 287 (100%), 196, 91

Specific Rotation : $[\alpha]_D = +20.1\,^\circ$

(R)-(-)-4-(1-Methylheptyloxycarbonyl)phenyl 4'-hydroxy-biphenyl-4-carboxylate **(52)**

This compound was prepared using a similar method to that employed in the synthesis of compound **20**, using tetrahydrofuran / ethanol as the solvent, and the following charge;

compound **49**, 5.4 g (0.01 mol),

palladium on charcoal, 1.0 g,

tetrahydrofuran, 400 ml,

ethanol, 20 ml.

Yield = 4.4 g (98%)

mp = 140 - 141 °C

^{1}H Nmr (CDCl$_3$) δ   0.88 (3H, t), 1.08 - 1.42 (13H, m), 5.11 (1H, m),

7.10 (2H, d), 7.14 (2H, d), 7.58 - 7.73 (4H, dd),

8.14 (2H, d), 8.23 (2H, d),

phenolic proton not observed

Ir (KBr) ν_{max} cm^{-1} 3040, 2920, 2840, 1740, 1720, 1150, 760

Ms   m/z =   446 (M$^+$), 385, 287, 214, 196(100%), 91

Specific Rotation : $[\alpha]_D = -17.2\,^\circ$

4-(1-Propylbutyloxycarbonyl)phenyl 4'-hydroxybiphenyl-4-carboxylate **(53)**

This compound was prepared using a similar method to that employed in the synthesis of compound **20** using tetrahydrofuran / ethanol as the solvent, and the following charge;

compound **50**, 5.6 g (0.012 mol),

palladium on charcoal, 1.0 g,

tetrahydrofuran, 400 ml,

ethanol 20, ml.

Yield = 3.6 g (74%)

mp = 127 - 129 °C

^{1}H Nmr (CDCl$_3$) δ   0.95 (6H, t), 1.14 - 1.50 (4H, m),

1.50 - 1.80 (4H, m), 5.11 - 5.24 (1H, m),

7.10 (2H, d),, 7.14 (2H, d), 7.58 - 7.73 (4H, dd),

8.14 (2H, d), 8.23 (2H, d),

phenolic proton not observed

Ir (KBr) ν$_{max}$ cm^{-1} 3060, 2920, 2850, 1740, 1720, 1150, 760

Ms   m/z =   432 (M$^+$), 385, 287 (100%), 196, 91

(R)-(+)-4-(2-Methylbutyloxycarbonyl)phenyl 4'-hydroxy-biphenyl-4-carboxylate (**54**)

This compound was prepared using a similar method to that employed in the synthesis of compound **20** using tetrahydrofuran / ethanol as the solvent, and the following charge;

compound **50**, 5.6 g (0.012 mol),

palladium on charcoal, 1.0 g,

tetrahydrofuran, 400 ml,

ethanol 20, ml.

Yield = 4.1 g (86%)

mp = 128 - 129 °C

^{1}H Nmr (CDCl$_3$) δ   0.93 - 1.07 (6H, m), 1.21 - 1.37 (1H, m),

1.47 - 1.62 (1H, m), 1.82 - 1.95 (1H, m),

4.10 - 4.27 (2H, m), 7.10 (2H, d), 7.14 (2H, d),

7.58 - 7.73 (4H, dd), 8.14 (2H, d), 8.23 (2H, d),

phenolic proton not observed

Ir (KBr) ν$_{max}$ cm^{-1} 3040, 2920, 2840, 1740, 1720, 1260, 1150, 760

Ms   m/z =   404 (M$^+$), 385, 287 (100%), 196, 91

Specific Rotation : $[\alpha]_D = +11.3°$

(R)-(-)-3-(11-{4'-[4-(1-Methylheptyloxycarbonyl)phenyloxycarbonyl]
biphenyl 4-yloxy}undecyloxy)prop-1-ene **(55)**

This compound was prepared using a similar method to that employed in the
synthesis of compound **8** using the following charge;

compound **52**, 1.0 g (2.2 mmol),

compound **44**, 0.5 g (2.2 mmol),

diethyl azodicarboxylate, 0.4 g (2.2 mmol),

triphenylphosphine, 0.63g (2.42 mmol),

tetrahydrofuran, 60 ml.

The pure product was obtained by column chromatography using
dichloromethane / petroleum ether (bp 40-60 °C) 1:1 as eluent, followed by
recrystallisation.

Yield = 0.50 g (36%)

K 41.9 S_C* 65.9 S_A 106.8 Iso °C

^{1}H Nmr (CDCl$_3$) δ   0.88 (3H, t), 1.21 - 1.849 (31H, m),

                     3.98 - 4.08 (6H, m), 5.02 (1H, m),

                     5.11 - 5.33 (2H, m), 5.84 - 6.00 (1H, m),

                     7.01 (2H, t), 7.31 (2H, d), 7.56 - 7.74 (4H, dd),

                     8.13 (2H, d), 8.24 (2H, d)

Ir (KBr) v_{max} cm^{-1} 2920, 2850, 1760, 1740, 1600, 1260, 1240, 860

Ms   m/z =   656 (M$^+$), 407, 197 (100%), 139, 71, 55

Specific Rotation : $[\alpha]_D = -27.3°$

11-{4'-[4-(1-Propylbutyloxycarbonyl)phenyloxycarbonyl]biphenyl-
4yloxy}undecyloxyprop-2-ene **(56)**

This compound was prepared using a similar method to that employed in the
synthesis of compound **8** using the following charge;

compound **53**, 1.00 g (2.3 mmol),

compound **44**, 0.52 g (2.3 mmol),

diethyl azodicarboxylate, 0.41 g (2.3 mmol),

triphenylphosphine, 0.65 g (2.53 mmol),

tetrahydrofuran, 60 ml.

The pure product was obtained by column chromatography using dichloromethane / petroleum ether (bp 40-60 °C) 1:1 as eluent, followed by recrystallisation.

Yield = 0.54 g (36%)

K 42.4 S_{CAlt}* 71.6 S_A 113.2 Iso °C

^{1}H Nmr (CDCl$_3$) δ   0.92 (6H, t), 1.24 - 1.92 (26H, m),

3.97 - 4.08 (6H, m), 5.02 (1H, m),

5.13 - 5.23 (2H, m), 5.83 - 5.99 (1H, m),

7.01 (2H, d), 7.31 (2H, d), 7.56 - 7.74 (4H, dd),

8.13 (2H, d), 8.24 (2H, d)

Ir (KBr) ν_{max} cm^{-1} 2920, 2860, 1760, 1740, 1600, 1260, 1240, 850

Ms   m/z =   642 (M$^+$), 349, 196 (100%), 167, 104, 55

(R)-(+)-3-(11-{4'-[4-(2-Methylbutyloxycarbonyl)phenyloxycarbonyl]biphenyl-4-yloxy}undecyloxy)prop-1-ene **(57)**

This compound was prepared using a similar method to that employed in the synthesis of compound **8** using the following charge;

compound **54**, 1.00 g (2.2 mmol),

compound **44**, 0.50 g (2.2 mmol),

diethyl azodicarboxylate, 0.40 g (2.2 mmol),

triphenylphosphine, 0.63g (2.42 mmol),

tetrahydrofuran, 60 ml.

The pure product was obtained by column chromatography using dichloromethane / petroleum ether (bp 40-60 °C) 1:1 as eluent, followed by recrystallisation.

Yield = 0.48 g (34%)

K 44.6 S_C* 52.7 S_A 94.6 Iso °C

^{1}H Nmr (CDCl$_3$) δ	0.90 (3H, t), 1.24 - 1.99 (22H, m), 3.42 (2H, t),
	3.98 - 4.09 (6H, m), 4.10 - 4.28 (2H, m),
	5.13 - 5.23 (2H, m), 5.83 - 5.99 (1H, m),
	7.01 (2H, d), 7.31 (2H, d), 7.55 - 7.74 (4H, dd),
	8.13 (2H, d), 8.24 (2H, d)
Ir (KBr) cm^{-1}	2920, 2860, 1760, 1740, 1610, 1270, 1240, 860
Ms m/z =	614 (M$^+$), 351, 197 (100%), 107, 104, 69
Specific Rotation :	$[\alpha]_D$ = +6.1 °

Scheme 11
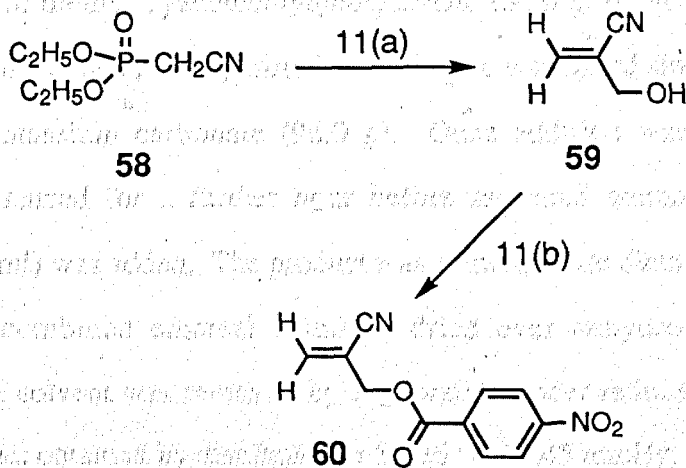
Reagents :

11(a) ... formaldehyde(aq), K_2CO_3, H_2O

11(b) ... 4-nitrobenzoic acid, DCC , DMAP,

dichlorormethane

α-(Hydroxymethyl)acrylonitrile (**59**)[88]

To a mixture of diethyl cyanomethylphosphonate (50.0 g, 0.280 mol) and 30% aqueous formaldehyde (110 ml) stirred at 1000 rpm, was added slowly a saturated solution of potassium carbonate (96.0 g). Once addition was complete the mixture was stirred for a further hour before saturated ammonium chloride solution (150 ml) was added. The product was extracted into diethyl ether (3 x 50 ml) and the combined ethereal solutions dried over anhydrous magnesium sulphate. The solvent was removed by evaporation under reduced pressure and the pure product obtained by distillation at 55-56 °C / 0.45 mmHg.

Yield = 12.2 g (53%)

^{1}H Nmr (CDCl$_3$) δ   3.71 (1H, s), 4.47 (2H, s), 6.05 (2H, m)

^{13}C Nmr (CDCl$_3$) δ   62.0 (CH$_2$), 117.0 (C≡N), 130.5, 122.3 (C=C)

Ms   m/z =   83 (M$^+$), 66, 64 (100%), 45

α-(4-nitrophenylcarbonyloxymethyl)acrylonitrile (**60**)

This compound was prepared using a similar method to that employed in the synthesis of compound **27** using the following charge;

compound **59**, 4.6 g (0.056 mol),

4-nitrobenzoic acid, 9.4 g (0.056 mol),

dicyclohexylcarbodiimide, 11.5 g (0.056 mol)

DMAP, 0.1 g,

dichloromethane 150 ml.

The pure product was obtained by column chromatography, using dichloromethane as eluent, followed by recrystallisation from ethanol.

Yield = 11.4 g (88%)

mp = 79 - 82 °C

^{1}H Nmr (CDCl$_3$) δ   4.99 (2H, t), 6.18 (1H, t), 6.23 (1H, t),

8.27 - 8.35 (4H, m)

Ir (KBr) cm^{-1} 2920, 2850, 2120, 1760, 1610, 1510, 1270, 850

Ms   m/z =   232 (M$^+$), 150 (100%), 134, 104, 82, 76

Scheme 12

14, 63, 67 ; R = (R)-1-methylheptyl
15, 64, 66 ; R = 1-propylbutyl
46, 65, 68 ; R = (R)-2-methylbutyl
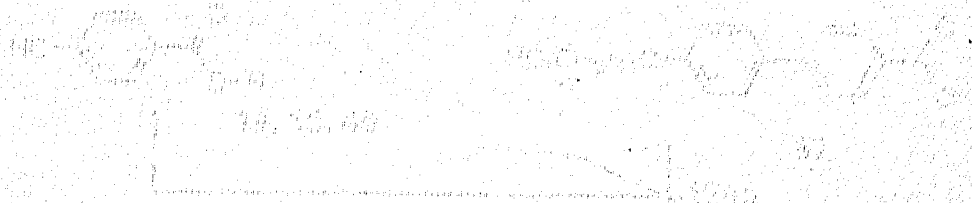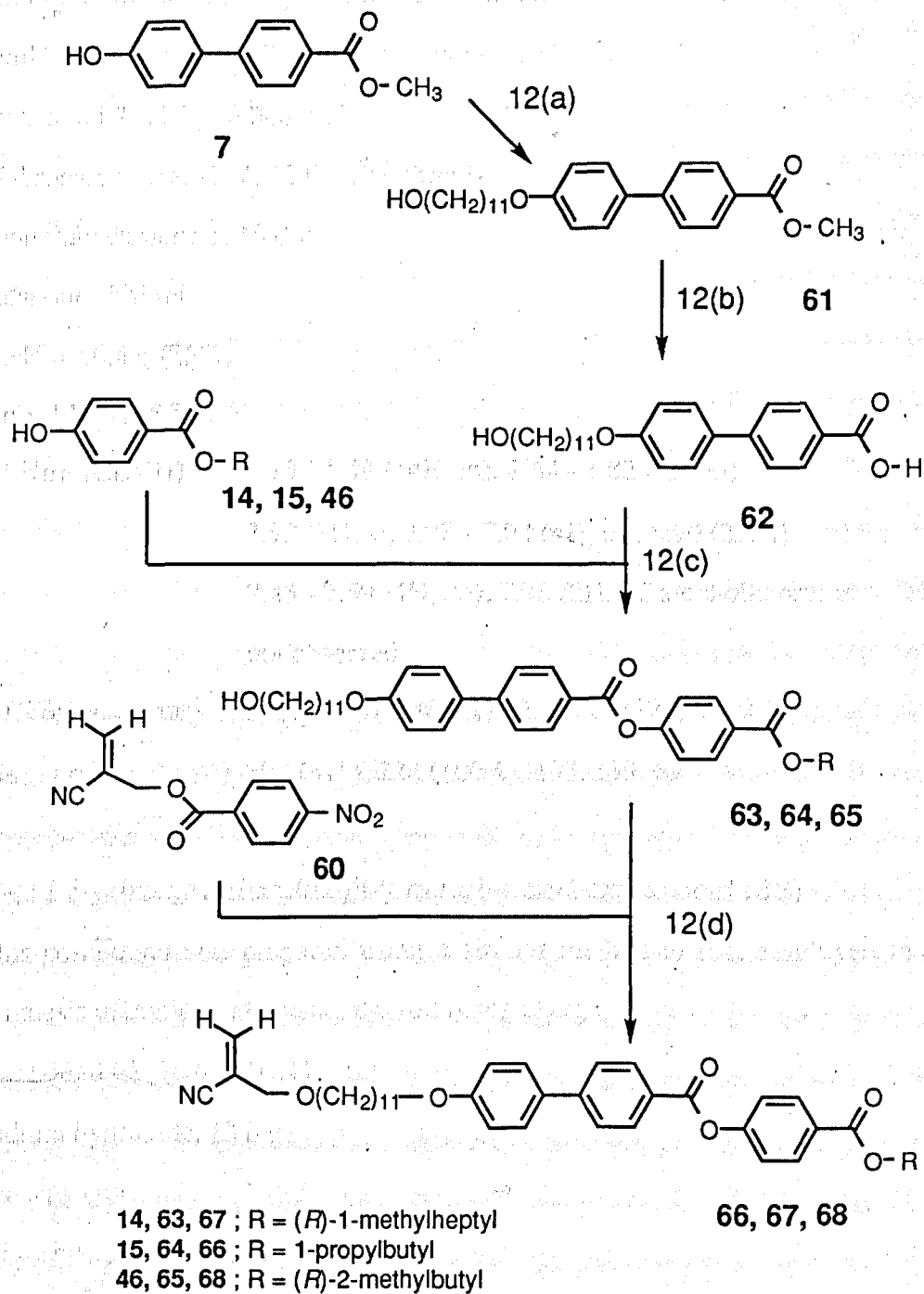
Reagents:

12(a) ... 11-bromoundecan-1-ol, K$_2$CO$_3$, butanone

12(b) ... (i) NaOH (aq), ethanol, (ii) dil. HCl

12(c) ... DCC , DMAP, dichloromethane

12(d) ... NaH, THF

Methyl 4'-(11-hydroxyundecyloxy)biphenyl-4-carboxylate (**61**)

This compound was prepared using a similar method to that employed in the synthesis of compound **35** using the following charge;

compound **7**, 11.0g (0.048 mol),

11-bromoundecan-1-ol, 12.0 g (0.048mol),

potassium carbonate, 10.0 g,

butanone, 500 ml.

Yield = 16.4 g (86%)

mp = 124 - 125 °C

^{1}H Nmr (CDCl$_3$) δ   1.15 - 1.49 (14H, m), 1.64 - 1.82 (4H, m),

                 3.92 (3H, s), 3.98 - 4.08 (4H, m), 6.90 (2H, t)

                 7.45 - 7.59 (4H, dd), 7.96 (2H, d), alcoholic proton

                 not observed

Ir (KBr) v_{max} cm^{-1} 3410, 2920, 2860, 1740, 1280, 1220, 1120

Ms   m/z =   398 (M$^+$), 228 (100%), 197, 139, 69

4'-(11-Hydroxyundecyloxy)biphenyl-4-carboxylic acid (**62**)

This compound was prepared using a similar method to that employed in the synthesis of compound **9** using the following charge;

compound **61**, 16.4 g (0.041 mol),

sodium hydroxide, 13.0 g,

water, 30 ml,

dilute hydrochloric acid, 200 ml.

Yield = 13.9 g (84%)

mp = decomposed above 300 °C

^{1}H Nmr (CDCl$_3$ + D$_6$ DMSO) δ 1.15 - 1.49 (14H, m), 1.64 - 1.82 (4H, m),

                 3.98 - 4.02 (4H, m), 6.90 (2H, t),

                 7.45 - 7.59 (4H, dd), 7.96 (2H, d), acidic and

                 alcoholic protons not observed

Ir (KBr) v_{max} cm^{-1} 3400, 2920, 2840, 1670, 1100, 1000

Ms   m/z =   384 (M$^+$), 336, 214 (100%), 197, 69

(R)-(-)-4-(1-Methylheptyloxycarbonyl)phenyl 4-(11-hydroxyundecyloxy)biphenyl-4-carboxylate (**63**)

This compound was prepared using a similar method to that employed in the synthesis of compound **27** using the following charge;

compound **62**, 1.9g (5.0 mmol),

compound **14**, 2.5 g (10.0 mmol),

dicyclohexyldicarbodiimide, 1.0 g (5.0 mmol),

DMAP, 0.1 g

dichloromethane 100ml.

The pure product was obtained by column chromatography using dichloromethane / ethyl acetate 1:1 as eluent, followed by recrystallisation from isopropanol.

Yield = 2.7 g (88%)

K 52.0 S$_A$ 106.2 Iso °C

^{1}H Nmr (CDCl$_3$) δ   0.89 (3H, t), 1.01 - 1.96 (31H, m),

3.98 - 4.08 (4H, m), 5.13 (1H, m), 7.01 (2H, d),

7.32 (2H, d), 7.56 - 7.74 (4H, dd), 8.13 (2H, d)

8.25 (2H, d), alcoholic proton not observed

Ir (KBr) v_{max} cm^{-1} 3420, 2960, 2880, 1740, 1710, 1600, 1270, 1070

Ms   m/z =   616 (M$^+$), 430, 385, 197 (100%), 151, 69

Specific Rotation : $[\alpha]_D$ = -24.0 °

4-(1-Propylbutyloxycarbonyl)phenyl 4'-(11-hydroxyundecyloxy)biphenyl-4-carboxylate (**64**)

This compound was prepared using a similar method to that employed in the synthesis of compound **27** using the following charge;

compound **62**, 1.9 g (5.0 mmol),

compound **15**, 2.3 g (10.0 mmol),

dicyclohexylcarbodiimide, 1.0 g (5.0 mmol),

DMAP 0.1 g

dichlorormethane, 100ml.

The pure product was obtained by column chromatography using 1:1 dichloromethane / ethyl acetate as eluent, followed by recrystallisation from isopropanol.

Yield = 2.2 g (72%)

K 49.7 S_A 101.0 Iso °C

^{1}H Nmr (CDCl$_3$) δ   0.89 (6H, t), 1.25 - 1.97 (26H, m),

3.98 - 4.10 (4H, m), 5.15 (1H, m), 7.02 (2H, d),

7.32 (2H, d), 7.54 - 7.74 (4H, dd), 8.13 (2H, d)

8.24 (2H, d), alcoholic proton not observed

Ir (KBr) v_{max} cm^{-1} 3410, 2960, 2890, 1750, 1710, 1610, 1270, 1070

Ms   m/z =   602 (M$^+$), 430, 385, 214 (100%), 151, 69, 55

(R)-(+)-4-(2-Methylbutyloxycarbonyl)phenyl 4'-(11-hydroxyundecyloxy)biphenyl-4-carboxylate **(65)**

This compound was prepared using a similar method to that employed in the synthesis of compound **27** using the following charge;

compound **62**, 1.9 g (5.0 mmol),

compound **46**, 2.1 g (10.0 mmol),

dicyclohexylcarbodiimide, 1.0 g (5.0 mmol),

DMAP 0.1 g

dichlorormethane, 100ml.

The pure product was obtained by column chromatography using dichloromethane / ethyl acetate 1:1 as eluent, followed by recrystallisation from isopropanol.

Yield = 2.0 g (68%)

K 48.6 S_A 99.2 Iso °C

^{1}H Nmr (CDCl$_3$) δ   0.90 (3H, t), 1.24 - 1.99 (24H, m),

3.98 - 4.08 (4H, m), 4.10 - 4.28 (2H, m),

7.01 (2H, d), 7.32 (2H, d), 7.56 - 7.74 (4H, dd),

8.13 (2H, d), 8.25 (2H, d), alcoholic proton not

observed

Ir (KBr) v_{max} cm^{-1} 3420, 2960, 2880, 1740, 1710, 1610, 1270, 850

Ms   m/z =   574 (M$^+$), 430, 385, 197 (100%), 151, 69

Specific Rotation :   [α]$_D$ = +16.6 °

(R)-(-)-α-(11-{4'-[4-(1-Methylheptyloxycarbonyl)phenyloxycarbonyl]
biphenyl-4-yloxy}undecyloxymethyl)acrylonitrile **(66)**

To a solution of compound **63** (2.7 g, 4.4 mmol) and sodium hydride (60%
dispersion in mineral oil) (0.2 g, 4.4 mmol) in tetrahydrofuran (50 ml) was added
compound **60** (1.0 g, 4.4 mmol) and the mixture stirred at room temperature until
no further reaction was observed upon examination by tlc. The mixture was then
diluted with tetrahydrofuran (50 ml) before being washed with water (2 x 25 ml)
and dried over anhydrous magnesium sulphate. The solvent was removed by
evaporation under reduced pressure and the pure product obtained by column
chromatography, using hexane as eluent, followed by recrystallisation.

Yield = 0.85g (29%)

K 52.2 S_{CA}* 63.4 S_A 89.7 Iso °C

^{1}H Nmr (CDCl$_3$) δ   0.88 (3H, t), 1.01 - 1.96 (31H, m),

3.98 - 4.19 (6H, m), 5.13 (1H, m),

6.15 - 6.23 (2H, m), 7.02 (2H, d), 7.30 (2H, d),

7.54 - 7.74 (4H, dd), 8.13 (2H, d), 8.25 (2H, d)

Ir (KBr) v_{max} cm^{-1} · 2940, 2920, 2850, 2120, 1740, 1720, 1600, 1260

Ms   m/z =   679 (M$^+$), 409 (100%), 196, 168, 138, 83, 68

Specific Rotation : $[\alpha]_D = -21.0\,^\circ$

α–(11{–4'-[4-(1-Propylbutyloxycarbonyl)phenyloxycarbonyl]biphenyl-4-yloxy}undecyloxymethyl)acrylonitrile (67)

This compound was prepared using a similar method to that employed in the synthesis of compound **66** using the following charge;

compound **64**, 2.1 g (3.6 mmol),

compound **60**, 0.84 g (3.6 mmol),

sodium hydride, 0.16 g,

tetrahydrofuran, 50 ml.

The pure product was obtained by column chromatography using hexane as eluent, followed by recrystallisation.

Yield = 0.65 g (27%)

K 49.7 S_{CA}* 56.5 S_A 79.4 Iso °C

^{1}H Nmr (CDCl$_3$) δ   0.90 (6H, t), 1.25 - 1.97 (26H, m),

   3.98 - 4.14 (6H, m), 5.13 (1H, m),

   6.15 - 6.23 (2H, m), 7.03 (2H, d),

   7.34 (2H, d), 7.54 - 7.74 (4H, dd), 8.14 (2H, d)

   8.25 (2H, d)

Ir (KBr) v_{max} cm^{-1} 2940, 2920, 2850, 2120, 1740, 1720, 1600, 1260

Ms   m/z =   667 (M$^+$), 409, 196, (100%), 168, 138, 83, 68,

(R)-(+)-α–(11–{4'-[4-(2-Methylbutyloxycarbonyl)phenyloxycarbonyl]biphenyl-4-yloxy}undecyloxymethyl)acrylonitrile (68)

This compound was prepared using a similar method to the one employed in the synthesis of compound **66** using the following charge.

Compound **65**, 1.95 g (3.4 mmol),

compound **60**, 0.79 g (3.4 mmol),

sodium hydride, 0.14 g

tetrahydrofuran, 50 ml.

The pure product was obtained by column chromatography using hexane as eluent, followed by recrystallisation.

Yield = 0.68 g (33%)

K 50.8 S_{CA}* 53.2 S_A 87.9 Iso °C
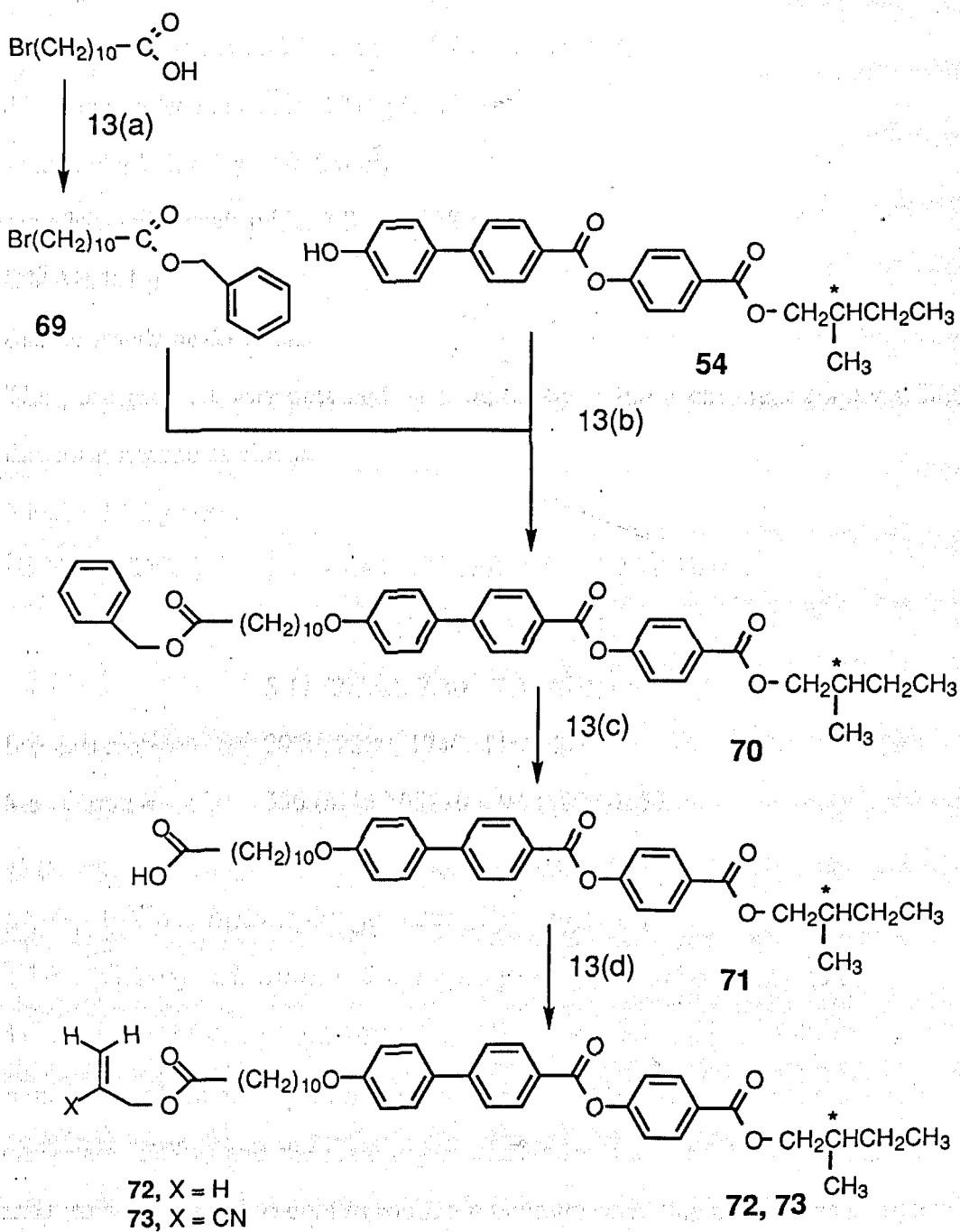
1H Nmr (CDCl3) δ 0.90 (3H, t), 1.24 - 1.99 (27H, m),

3.98 - 4.10 (4H, m), 4.10 - 4.28 (1H, m),

7.01 (2H, d), 6.15 - 6.24 (2H, m), 7.32 (2H, d),

7.56 - 7.74 (4H, dd), 8.13 (2H, d), 8.25 (2H, d)

Ir (KBr) ν_{max} cm^{-1} 2950, 2910, 2850, 2120, 1740, 1710, 1600, 1250

Ms m/z = 627 (M$^+$), 409, 214, 196, 68 (100%), 54

Specific Rotation : $[\alpha]_D$ = +14.8 °

Scheme 13

$Br(CH_2)_{10}-C\overset{O}{\underset{OH}{\lessgtr}}$

$\downarrow$ 13(a)

$Br(CH_2)_{10}-C\overset{O}{\underset{O}{\lessgtr}}$ —⟨benzyl⟩

69

54: HO—⟨biphenyl⟩—$C\overset{O}{\underset{O}{\lessgtr}}$—⟨phenyl⟩—$C\overset{O}{\underset{O}{\lessgtr}}$—$CH_2\overset{*}{C}HCH_2CH_3$ / CH_3

13(b)

$\downarrow$

⟨benzyl⟩—$O\overset{O}{\underset{}{\lessgtr}}$—$(CH_2)_{10}O$—⟨biphenyl⟩—$C\overset{O}{\underset{O}{\lessgtr}}$—⟨phenyl⟩—$C\overset{O}{\underset{O}{\lessgtr}}$—$O-CH_2\overset{*}{C}HCH_2CH_3$ / CH_3

70

13(c)

$\downarrow$

$HO\overset{O}{\underset{}{\lessgtr}}$—$(CH_2)_{10}O$—⟨biphenyl⟩—$C\overset{O}{\underset{O}{\lessgtr}}$—⟨phenyl⟩—$C\overset{O}{\underset{O}{\lessgtr}}$—$O-CH_2\overset{*}{C}HCH_2CH_3$ / CH_3

71

13(d)

$\downarrow$

$\underset{X}{\overset{H\quad H}{C=C}}-CH_2O\overset{O}{\underset{}{\lessgtr}}$—$(CH_2)_{10}O$—⟨biphenyl⟩—$C\overset{O}{\underset{O}{\lessgtr}}$—⟨phenyl⟩—$C\overset{O}{\underset{O}{\lessgtr}}$—$O-CH_2\overset{*}{C}HCH_2CH_3$ / CH_3

72, X = H
73, X = CN

72, 73

Reagents :

13(a) ... benzyl alcohol, DCC, DMAP, CH_2Cl_2

13(b) ... K_2CO_3, DMF

13(c) ... Pd / C, H_2 (g), ethyl acetate

13(d) ... DCC, DMAP, CH_2Cl_2

Benzyl -11-bromoundecanoate **(69)**

This compound was prepared using a similar method to that employed in the
synthesis of compound **27** using the following charge;

11-bromoundecanoic acid, 10.0 g (0.038 mol),

benzyl alcohol, 4.1 g (0.038 mol),

dicyclohexylcarbodiimide, 7.8 g (0.038 mol),

DMAP, 0.1 g,

dichloromethane, 200 ml.

The pure product was obtained as a liquid by column chromatography using
dichloromethane as eluent.

Yield = 12.0 g (89%)

^{1}H Nmr (CDCl$_3$) δ   1.21 - 1.44 (12H, m), 1.57 - 1.70 (2H, m),

1.77 - 1.89 (2H, m), 2.35 (2H, t), 3.38 (2H, t)

5.11 (2H, s), 7.30 - 7.37 (5H, m)

Ir (neat) cm^{-1} 2930, 2880, 1740, 1160, 700

Ms   m/z =   356 (M$^+$) 265, 108, 91 (100%), 55

(R)-(+)-4-(2-methylbutyloxycarbonyl)phenyl -4'-[

11-benzyloxycarbonyl)undecyoxy]biphenyl-4-carboxylate **(70)**

To a solution of compound **54** (3.2 g, 7.9 mmol) and compound **69** (2.7 g, 7.9
mmol) dissolved in dry dimethylformamide (200 ml) was added potassium
carbonate (5.00g) and the resulting mixture stirred at 60 °C for 8 hours. The
mixture was allowed to cool to room temperature once this period was complete
and the excess potassium carbonate removed by filtration. The solvent was
removed by evaporation under reduced pressure and the pure product obtained by
column chromatogrpahy using dichloromethane / hexane 1:1 as eluent, followed
by recrystallisation.

Yield = 2.4 g (45%)

K 44.8 S$_A$ 91.2 Iso °C

¹H Nmr (CDCl₃) δ   0.94 (3H, t), 1.24 - 1.90 (21H, m), 2.35 (2H, t),

                      4.00 (2H, t), 4.06 - 4.24 (2H, m), 5.12 (2H, s),

                      6.91 (2H, d), 6.98 (2H, d), 7.29 - 7.40 (5H, m),

                      7.51 - 7.63 (4H, dd), 7.99 (2H, d), 8.08 (2H, d)

Ir (KBr) cm⁻¹   2960, 2850, 1760, 1740, 1710, 1600, 1240, 850

Ms   m/z =   678 (M⁺), 409 (100%), 196, 169, 139, 55

Specific Rotation : $[\alpha]_D$ = +17.2 °

(R)-4'-[4-(2-Methylbutyloxycarbonyl)phenyloxycarbonyl]biphenyl -4-yloxy undecanoic acid (**71**)

This compound was prepared using a similar method to that used in the preparation of compound **20** using the following charge;

compound **70**, 2.4 g (3.53 mmol),

10% Palladium on charcoal, 1.0 g,

ethyl acetate, 100 ml.

Yield = 1.7 g (82%)

K 78.9 S$_A$ 102.3 Iso °C

¹H Nmr (CDCl₃) δ   0.94 (3H, t), 1.24 - 1.90 (21H, m), 2.35 (2H, t),

                      4.00 (2H, t), 4.06 - 4.24 (2H, m), 6.91 (2H, d),

                      6.98 (2H, d), 7.51 - 7.63 (4H, dd), 7.99 (2H, d),

                      8.08 (2H, d), acidic proton not observed

Ir (KBr) cm⁻¹   3400 - 3510, 2940, 2920, 2850, 1760, 1740, 1710,

                      1600, 1270

Ms   m/z =   588 (M⁺), 467, 452, 243, 228 (100%), 168, 82

(R)-(+)-{4'-[4-(2-Methylbutyloxycarbonyl)phenyloxycarbonyl]biphenyl -4-yloxydecyl}carbonyloxyprop-1-ene (**72**)

This compound was prepared using a similar method to that employed in the synthesis of compound **27** using the following charge;

compound **71**, 0.30 g (0.51 mmol),

allyl alcohol, 0.03 g (0.51 mmol),

dicyclohexylcarbodiimide, 0.11 g (0.51 mmol),

DMAP, 0.01 g,

dichloromethane 20 ml.

The pure product was obtained by column chromatography using dichloromethane / hexane 1:1 as eluent, followed by recrystallisation.

Yield = 0.30 g (94%)

K 47.6 S_A 96.6 Iso °C

^{1}H Nmr (CDCl$_3$) δ	0.94 (3H, t), 1.22 - 1.90 (21H, m), 2.35 (2H, t),
	4.00 (2H, t), 4.06 - 4.24 (2H, m),
	5.11 - 5.33 (1H, m), 6.15 - 6.23 (2H, m),
	6.91 (2H, d), 6.98 (2H, d), 7.51 - 7.63 (4H, dd),
	7.99 (2H, d), 8.08 (2H, d)
Ir (KBr) cm^{-1}	2940, 2920, 2850, 1760, 1740, 1710, 1600, 1280
Ms m/z =	628 (M+), 467, 450, 243, 228 197 (100%), 139, 82
Specific Rotation :	$[\alpha]_D$ = +13.6 °

(R)-(+)-{4'-[4-(2-Methylbutyloxycarbonyl]biphenyl-4-yloxydecyl}carbonyloxy methylacrylonitrile **(73)**

This compound was prepared using a similar method to that employed in the synthesis of compound **27** using the following charge;

compound **71**, 0.30 g (0.51 mmol),

compound **59**, 0.04 g (0.51 mmol),

dicyclohexyldicarbodiimide, 0.11 g (0.51 mmol),

DMAP, 0.01 g,

dichloromethane, 20 ml.

The pure product was obtained by column chromatography using dichloromethane / hexane 1:1 as eluent, followed by recrystallisation.
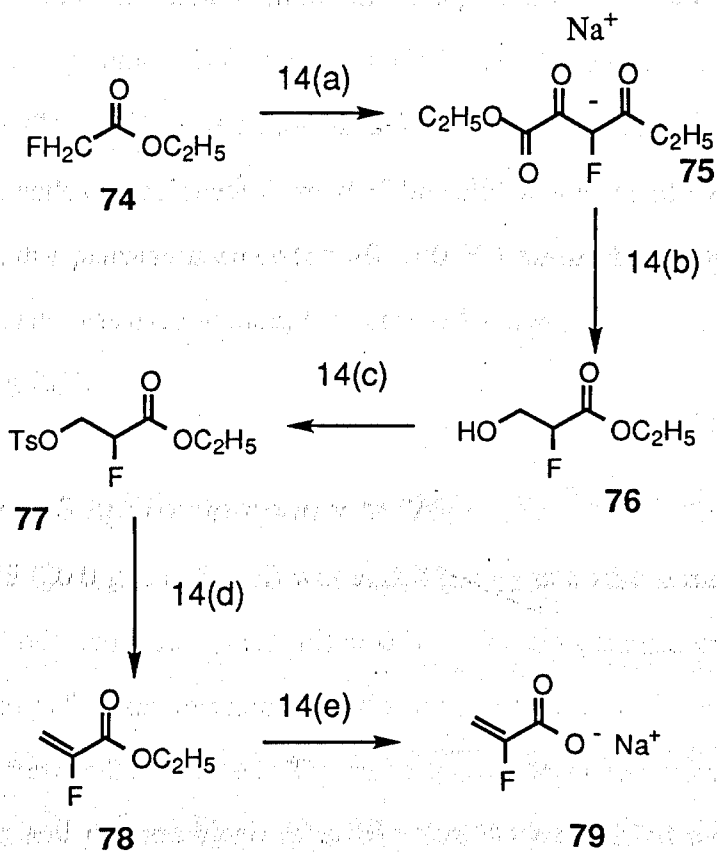
Yield = 0.28 g (84%)

K 66.2 S_A 117.3 Iso °C

^{1}H Nmr (CDCl$_3$) δ   0.94 (3H, t), 1.22 - 1.90 (21H, m), 2.35 (2H, t),

4.00 (2H, t), 4.06 - 4.24 (2H, m),

6.15 - 6.23 (2H, m), 6.91 (2H, d), 6.98 (2H, d),

7.51 - 7.63 (4H, dd), 7.99 (2H, d), 8.08 (2H, d)

Ir (film) cm^{-1} 2940, 2920, 2850, 2120, 1770, 1740, 1710, 1600,

Ms   m/z =   643 (M$^+$), 467, 452, 243, 228 (100%), 198, 139

Specific Rotation : $[\alpha]_D$ = +12.2 °

Scheme 14

Reagents:

14(a) ... sodium ethoxide, diethyl oxalate, diethyl ether

14(b) ... 40% formalin, H_2O

14(c) ... *p*-toluenesulphonyl chloride, pyridine

14(d) ... potassium phthalimide

14(e) ... 2N NaOH, ethanol

Sodium diethyl fluoro-oxaloacetate **(75)**

To a solution of alcohol-free sodium ethoxide prepared from sodium (4.6 g, 0.2 mol) in dry diethyl ether (100 ml) was added diethyl oxalate (30 ml) and ethyl fluoroacetate **(74)** (21.2 g, 0.2 mol) dropwise. The mixture was left overnight whereupon a yellow precipitate formed. The solid was isolated by filtration and washed with dry petroleum ether (bp 40 - 60 °C) before being dried *in vacuo*. This intermediate was used without further purification.

Yield = 71.6 g (63%)

Ethyl 2-fluoro-3-hydroxypropanoate **(76)**

Compound **75** (20.0 g, 0.088 mol) was added slowly to a stirred mixture of 40 % formalin (9.0 ml) and water (11.0 ml) at 0 °C. The temperature was maintained for 10 minutes before the mixture was allowed to warm to room temperature and stirred for a further 20 minutes. The mixture was extracted exhaustively with diethyl ether, and the combined ethereal solutions were dried over anhydrous magnesium sulphate and activated charcoal. The product was isolated from the solution by filtration, evaporation of the solvent and distillation of the product (112 °C / *ca.* 30 mmHg)

Yield = 13.8 g (46 %)

^{1}H Nmr (CDCl$_3$) δ   1.32 (3H, t), 3.15 (1H, s), 3.9-4.1 (2H, m),4.40 (2H, q),

                         4.8-5.2 (1H, m)

Ir (KBr) v_{max} cm^{-1} 3400, 2990, 1750, 1640, 1230

Ms   m/z =   136 (M$^+$), 121, 106, 91, 77, 61 (100%), 43

Ethyl 2-fluoro-3-p-toluenesulphonylpropanoate **(77)**

Compound **76** (7.4 g, 0.054 mol) was dissolved in pyridine (55.0 ml) and the solution was cooled to -10 °C. *p*-Toluenesulphonyl chloride (14.6 g, 0.077 mol) was added to the stirred solution over 45 minutes. The solution was then kept at -10 °C for a further 60 minutes and was left overnight at below 0 °C. The mixture

was then added to a stirred solution of concentrated sulphuric acid (15 ml) and water (150 ml) at a temperature of -8 °C. The product was then washed with ether, and the ethereal solution dried over anhydrous magnesium sulphate and charcoal. The product was isolated by filtration and evaporation of the solvent.

Yield = 15.84 g (39 %)

^{1}H Nmr (CDCl$_3$) δ   0.89 (3H, t), 2.46 (3H, s), 3.74 (2H, q),

        4.04 (2H, d), 4.82 - 5.23 (1H, m), 7.36 (2H, d),

        7.81 (2H, d)

Ir (KBr) ν$_{max}$ cm^{-1} 2990, 1750, 1640, 1610, 1230, 860

Ms   m/z =   290 (M$^+$), 185, 169, 105, 91 (100%), 77, 43

Ethyl α-fluoroacrylate (**78**)[89]

Compound **77** (9.72 g, 0.035 mol) was mixed dry with potassium phthalimide (19.7 g, 0.105 mol) and placed in a flat-bottomed reaction vessel. The mixture was rapidly heated to 100 °C and then more slowly heated to 120 °C *in vacuo* (*ca.* 10 mm Hg) whereupon the product was distilled out of the mixture and collected in a dry-ice trap. The fluoroacrylate ester was immediately stabilized with a few crystals of quinol, and the next stage in the reaction scheme was carried out immediately

Yield=3.2 g (86 %)

Sodium fluoroacrylate (**79**)

2N Aqueous sodium hydroxide was added dropwise to compound **78** (3.1 g, 0.027 mol) dissolved in ethanol (50 ml) until the ester was hydrolyzed quantitatively and the resultant solution gave a positive reaction with phenolphthalein. The sodium salt was then isolated by evaporation of the solvent.

Yield = 3.0 g (100 %)

^{1}H Nmr (CDCl$_3$) δ   5.18 (0.5H, d), 5.23 (0.5H, d), 5.36 (0.5H, d),

        5.53 (0.5H, d).

Scheme 15
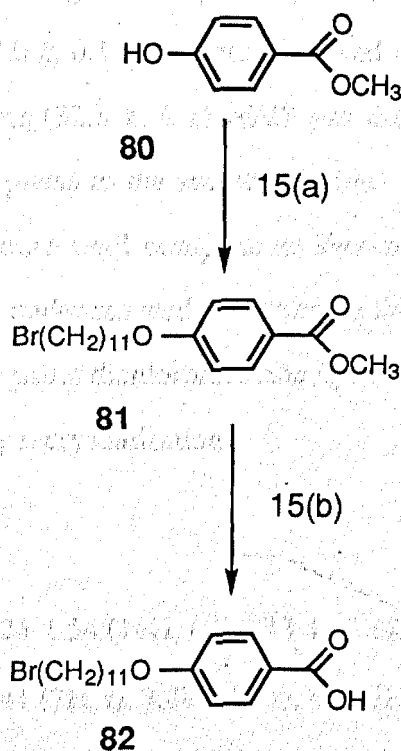
Reagents: 15(a) ... 11-bromoundecan-1-ol, DEAD, PPh$_3$, THF

15(b) ... (i) NaOH(aq), ethanol, (ii) dil. HCl

Methyl 4-(11-bromoundecyloxy)benzoate (81)

11-Bromoundecan-1ol (25.1 g, 0.1 mol), methyl 4-hydroxybenzoate (80) (15.2 g, 0.1 mol) and DEAD (14.0 g, 0.1 mol) were dissolved in dry tetrahydrofuran (500 ml). Triphenylphosphine (32.8 g, 0.11 mol) was dissolved in tetrahydrofuran (100 ml) and added dropwise to the stirred solution. The reaction mixture was stirred at room temperature until complete as shown by tlc. The solvent was removed by evaporation under reduced pressure and the pure product obtained by column chromatography using dichloromethane / petroleum ether (bp 40 - 60 °C) 1:1 as eluent followed by recrystallisation.

Yield = 25.2 g (65 %)

mp = 51 - 52 °C

^{1}H Nmr (CDCl$_3$) δ 1.24-1.54 (14H, m), 1.73-1.91 (4H, m),

                 3.41 (2H, t), 3.88 (3H, s), 4.0 (2H, t),

                 6.90 (2H, d), 7.98 (2H, d)

Ir (KBr) ν_{max} cm^{-1} 2930, 2920, 2850, 1720, 1600, 1250, 1170, 860

Ms   m/e =   386 (M$^+$), 262, 152 (100%), 121, 55, 41

4-(11-Bromoundecyloxy)benzoic acid (82)

Compound 81 (25.2 g, 0.065 mol) was dissolved in a mixture of sodium hydroxide (6.5 g) in water (15 ml) and ethanol (150 ml). The solution was heated under reflux for 8 hours. The mixture was acidified by the addition of dilute HCl followed by water. The resulting solid was isolated by filtration and washed with water. The product was purified by recrystallisation from acetic acid.

Yield = 24.2 g (100 %)

K 87.3 S$_A$ 99.8 N 107.7 Iso °C

^{1}H Nmr (CDCl$_3$ + D6 DMSO) δ1.24-1.54 (14H, m), 1.73-1.91 (4H, m),

                 3.40 (2H, t), 4.0 (2H, t), 6.90 (2H, d),

                 7.98 (2H, d), acidic proton not detected

Ir (KBr) ν_{max} cm^{-1} 3400, 2960, 2880, 1680, 1600, 1250, 850

Ms   m/z =   372 (M$^+$), 336, 289, 138, 121, 55 (100%)

(R)-(-)-4-Bromo-2-fluoro-(1-methylheptyoxy)benzene **(84)**

This compound was prepared using a similar method to that employed in the synthesis of compound **19** using the following charge;

compound **83**, 12.1 g (0.06 mol),

(*S*)-(+)-octan-2-ol 8.2 g (0.06 mol),

diethyl azodicarboxylate, 13.7 g (0.06mol),

triphenylphosphine, 18.2 g (0.0684 mol),

THF 250 ml.

The pure product was obtained by column chromatography using dichloromethane / petroleum ether (bp 40 - 60 °C) 1:1 as eluent to yield the product as a colourless liquid.

Yield = 16.3 g (84.6 %)

^{1}H Nmr (CDCl$_3$) δ 0.81 (3H, t), 1.35-1.50 (8H, m), 1.81 (4H, m), 4.32 (2H, t),

6.85 (1H, t), 7.10-7.30 (2H, m)

Ir (KBr) v_{max} cm^{-1} 2920, 2850, 1490, 1260, 850

Ms m/z = 304 (M$^+$), 190 (100%), 111, 83, 71, 55

Specific Rotation : $[\alpha]_D$ = -24.2 °

4-Bromo-2-fluoro-1-octyloxybenzene **(85)**

This compound was prepared using a similar method to that employed in the synthesis of compound **19** using the following charge;

compound **83**, 17.5 g (0.1 mol),

octan-1-ol 13.0 g (0.1 mol),

diethyl azodicarboxylate, 21.8 g (0.1mol),

triphenylphosphine, 36.0 g (0.11 mol),

THF 450 ml.

The pure product was obtained by column chromatography using dichloromethane / petroleum ether (bp 40 - 60 °C) 1:1 as eluent to yield the product as a colourless liquid.

Yield = 19.5 g (64.61 %)

^{1}H Nmr (CDCl$_3$) δ   0.85 (3H, t), 1.32-1.55 (8H, m), 1.82 (4H, m),

4.0 (2H, t,), 6.85 (1H, t), 7.11-7.30 (2H, d)

Ir (KBr) v_{max} cm^{-1} 2920, 2850, 1490, 1270, 860

Ms   m/z=   304 (M$^+$), 190 (100%), 138, 111, 71, 55

(R)-3-Fluoro-4-(1-methylheptyl)phenylboronic acid (86)

Compound 84 (6.0 g, 0.02 mol) was dissolved in tetrahydrofuran (300 ml) and cooled to below -70 °C under a nitrogen atmosphere. 10M Butyllithium (2.2 ml, 0.022 mol) was added dropwise through a syringe maintaining the temperature at -70 °C. The reaction was followed by gc to ensure complete reaction of compound 84. On completion, trimethyl borate (6.0 ml) was added and the reaction stirred overnight. Addition of dilute hydrochloric acid was followed by washing with ether (3 x 200ml). The combined ethereal solution was dried over anhydrous magnesium sulphate. The product was isolated by filtration and evaporation and used without further purification.

Crude yield = 7.9 g (100 %)

3-Fluoro-4-octyloxyphenylboronic acid (87)

This compound was prepared using a similar method to that employed in the synthesis of compound 86 using the following charge;

compound 85, 12.1 g (0.02 mol),

10 m butyllithium, 2.2 ml (0.022mol),

trimethyl borate, 6.0 ml

dil. HCl, 200 ml,

THF, 300 ml.

The product was not purified further.

Crude yield = 8.1 g (100 %)

1-Bromo-4-(tetrahydropyran-2-yloxy)benzene **(89)**

To a solution of 4-bromophenol **(88)** (10.0 g, 0.058 mol) in dichloromethane (50 ml) at 0 °C, 3,4-dihydro-2*H*-pyran (6.1 g, 0.073 mol) was added dropwise over a period of 10 minutes. The reaction was monitored by tlc until complete, whereupon the solution was quenched with sodium bicarbonate and the solvent evaporated under reduced pressure. The resulting slurry was dissolved in ethyl acetate and filtered through a 9 cm silica column. The solvent was removed under reduced pressure and the resulting liquid rapidly crystallised by cooling with liquid nitrogen. The solid was recrystallised from hexane.

Yield = 12.8 g (87 %); mp = 55 °C

^{1}H Nmr (CDCl$_3$) δ   1.51-2.13 (6H, m), 3.55 (2H, m), 3.92 (1H,t),

6.85 (2H, d), 7.44 (2H, d)

Ir (KBr) ν_{max} cm^{-1} 2940, 2880, 1580, 1470, 1240, 820

Ms   m/z =   256 (M$^+$), 171, 85 (100%), 64, 56

(R)-3-Fluoro-4-(1-methylheptyloxy)-4'-(tetrahydropyran-2-yloxy)biphenyl **(90)**

2M Sodium carbonate (60 ml) and tetrakis(triphenylphosphine)palladium(0) (0.35g, 1.8 mmol) were added sequentially to a solution of compound **89** (6.40 g, 0.025 mol) and compound **86** (7.90 g, 0.027 mol) in 1,2-dimethoxyethane (150 ml) with stirring under a nitrogen atmosphere. The mixture was heated under reflux until complete by gc. The mixture was washed with diethyl ether (3 x 125 ml) and the washings then washed with water and dried over anhydrous magnesium sulphate, before the solvent was removed under reduced pressure.

Crude yield = 9.5 g (100 %)

3-Fluoro-4-octyloxy-4'-(tetrahydropyran-2-yloxy)biphenyl **(91)**

This compound was prepared using a similar method to that employed in the synthesis of compound **90** using the following charge;

compound **89**, 6.4 g (0.025 mol),

compound **87**, 8.1 g (0.027 mol),

tetrakis(triphenylphosphine)palladium(0), 0.35 g (1.8 mmol),

2M sodium carbonate(aq), 60 ml,

1,2-dimethoxyethane, 150 ml.

The product was used without further purification.

Crude yield = 9.5 g (100 %)

(R)-(-)-3-Fluoro-4'-hydroxy-4-(1-methylheptyloxy)biphenyl (**92**)

Compound **90** (9.54 g, 0.025 mol) and *p*-toluenesulphonic acid (4.95 g, 0.0275 mol) were dissolved in dichloromethane and stirred at room temperature. The reaction was followed by tlc until no further reaction was observed and the solvent was then removed by evaporation under reduced pressure. The mixture was purified by column chromatography using dichloromethane as eluent to yield the pure product as a liquid.

Yield = 5.5 g (70 %)

^{1}H Nmr (CDCl$_3$) δ   0.90 (3H, t), 1.3-1.6 (9H, m),1.75 (4H, m),

                         4.4-4.5 (1H, m), 5.4 (1H, s), 6.9-7.0 (1H, m),

                         7.22-7.32 (4H, m), 7.55 (2H, d),

Ir (KBr) ν$_{max}$ cm^{-1} 3410, 2920, 2860, 1610, 1480, 1210, 860

Ms   m/z =   316 (M$^+$), 204 (100%), 175, 146, 127, 55

Specific Rotation :   [α]$_D$ = -7.9 °

3-Fluoro-4'-hydroxy-4-octoxybiphenyl (**93**)

This compound was prepared using a similar method to that employed in the synthesis of compound **92** using the following charge;

compound **91**, 9.5 g (0.025 mol),

p-toluenesulphonic acid, 4.9 g (0.0275 mol),

dichloromethane, 100 ml.

The pure product obtained by column chromatography using dichloromethane as eluent followed by recrystallisation.
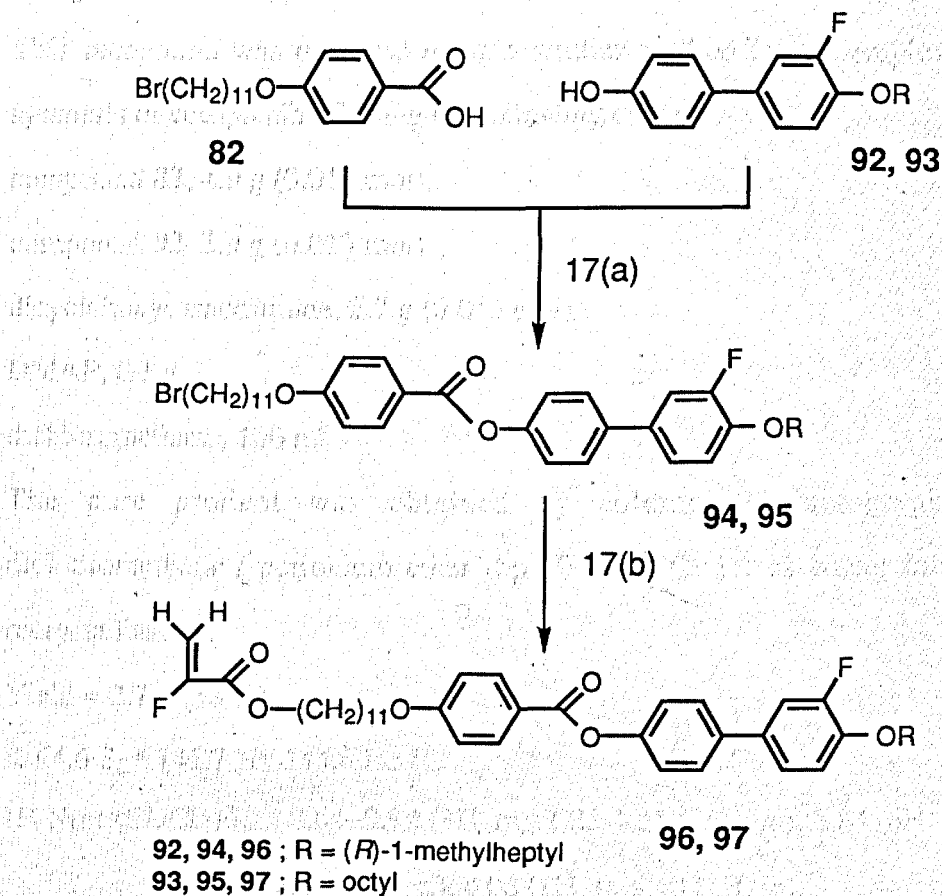
Yield = 5.1 g (64.89 %);

K 128.2 S_B 132.8 I °C

^{1}H Nmr (CDCl$_3$)δ	0.88 (3H, t), 1.28-1.61 (8H, m),1.75 (4H, m), 4.0 (2H, t),
	5.44 (1H, s), 6.9-7.0 (1H, m), 7.22-7.31 (4H, m),
	7.55 (2H, d),
Ir (KBr) ν_{max} cm^{-1}	3410, 2920, 2860, 1610, 1490, 1210, 850
Ms m/z =	316 (M$^+$), 204 (100%), 175, 146, 127, 55

Scheme 17

Br(CH$_2$)$_{11}$O—⟨ ⟩—COOH
82

HO—⟨ ⟩—⟨ ⟩—OR
92, 93

17(a)

Br(CH$_2$)$_{11}$O—⟨ ⟩—CO—O—⟨ ⟩—⟨ ⟩—OR
94, 95

17(b)

—O—(CH$_2$)$_{11}$O—⟨ ⟩—CO—O—⟨ ⟩—⟨ ⟩—OR
96, 97

92, 94, 96 ; R = (R)-1-methylheptyl
93, 95, 97 ; R = octyl

Reagents: 17a) ... DCC, DMAP, dichloromethane

        17b) ... sodium fluoroacrylate (**79**), HMPA

(R)-(-)-3'-Fluoro-4'-(1-methylheptyloxy)biphenyl-4-yl 4-(11-bromoundecyloxy)benzoate **(94)**

This compound was prepared using a similar method to that employed in the synthesis of compound **27** using the following charge;

compound **82**, 4.9 g (0.013 mol),

compound **92**, 3.9 g (0.013 mol),

dicyclohexycarbodiimide, 2.7 g (0.013 mol),

DMAP, 0.1 g,

dichloromethane, 100 ml.

The pure product was obtained by column chromatography using dichloromethane / petroleum ether (bp 40 - 60 °C) 1:1 as eluent followed by recrystallisation.

Yield = 2.7 g (30 %)

K 64.6 S_C* 141.7 N* 144.6 Iso °C

^{1}H Nmr (CDCl$_3$)δ   0.84–0.92 (3H, m), 1.25-1.55 (25H, m), 1.84 (6H, m),

3.40 (2H, t,), 4.06 (2H, t), 4.40 (1H, m),

6.98-7.06 (4H, m), 7.21-7.33 (3H, m), 7.55 (2H, d),

8.14 (2H, d).

Ir (KBr) v_{max} cm^{-1} 2920, 2840, 1740, 1600, 1500, 1290, 840

Ms   m/z =   670 (M$^+$), 355, 273, 203, 121(100%), 55

Specific Rotation : $[\alpha]_D$ = -3.4 °

3'-Fluoro-4'-octyloxybiphenyl-4-yl 4-(11-bromoundecyloxy)-benzoate **(95)**

This compound was prepared using a similar method to that employed in the synthesis of compound **27** using the following charge;

compound **82**, 4.9 g (0.013 mol),

compound **93**, 3.9 g (0.013 mol),

dicyclohexycarbodiimide, 2.7 g (0.013 mol),

DMAP, 0.1 g,

dichloromethane, 100 ml.

The pure product was obtained by column chromatography using dichloromethane / petroleum ether (bp 40 - 60 °C) 1:1 as eluent followed by recrystallisation.

Yield = 1.8 g (20 %)

K 68.2 S_C 126.9 N 135.3 Iso °C

^{1}H Nmr (CDCl$_3$) δ 0.84–0.94 (3H, m), 1.18-1.56 (24H, m), 1.82 (6H, m)

    3.42 (2H, t), 4.06 (4H, dd), 6.96-7.04 (4H, m),

    7.22-7.32 (3H, m), 7.55 (2H, d), 8.16 (2H, d).

Ir (KBr) v_{max} cm^{-1} 2920, 2840, 1750, 1600, 1500, 1290, 860

Ms m/z = 670 (M$^+$), 355, 273, 203, 121(100%), 55

(R)-(-)-11-{4-[3'-fluoro-4'-(1-methylheptyloxy)biphenyl-4-yloxycarbonyl]phenyloxy}undecyl 2-fluoroacrylate (**96**)

Sodium fluoracrylate (**79**) (0.44 g, 0.004 mol) and compound **94** (2.70 g, 0.004 mol) were dissolved in hexamethylphosphoramide (HMPA) (25 ml) and stirred at room temperature until the reaction was complete by tlc. Addition of water afforded the crude product which was isolated by filtration and washed with copious amounts of water. The pure product was isolated by column chromatography using dichloromethane / petroleum ether (bp 40 - 60 °C) 1:1 as eluent.

Yield = 1.33 g (51 %)

K 51.6 S_C* 58.2 S_A 104.9 Iso °C

^{1}H Nmr (CDCl$_3$) δ 0.84–0.92 (3H, m), 1.28-1.57 (23H, m), 1.84 (6H, m),

    3.22 (2H, t), 4.05 (2H, t), 4.40 (1H, m),

    5.28-5.76 (2H, dd), 6.95-7.15 (4H, m),

    7.22-7.32 (3H, m), 7.57 (2H, d), 8.15 (2H, d).

Ir (KBr) v_{max} cm^{-1} 2910, 2850, 1760, 1750, 1650, 1610, 1170, 840

Ms   m/z =   662 (M$^+$), 412, 355 (100%), 203, 121, 69

Specific Rotation : $[\alpha]_D$ = -4.4 °

11-{4-[3'-Fluoro-4'-octyloxybiphenyl-4-yloxycarbonyl]phenyloxy}undecyl 2-fluoroacrylate (97)

This compound was prepared using a similar method to that employed in the synthesis of compound **27** using the following charge;

compound **95**, 1.82 g (0.002 mol),

compound **79**, 0.22 g (0.002 mol),

HMPA, 15 ml.

The pure product was obtained by column chromatography using dichloromethane / petroleum ether (bp 40 - 60 °C) 1:1 as eluent.

Yield = 1.13 g (83 %)

K 64.8 S$_C$ 79.1 S$_A$ 109.6 Iso °C

^{1}H Nmr (CDCl$_3$) δ   0.86–0.93 (3H, m), 1.18-1.57 (24H, m), 1.84 (6H, m),

                3.22 (2H, t), 4.05 (2H, d), 4.40 (1H, m),

                5.28-5.75 (2H, dd), 6.95-7.06 (4H, m),

                7.22 - 7.32 (3H, m), 7.56 (2H, d), 8.15 (2H, d)

Ir (KBr) ν$_{max}$ cm^{-1} 2910, 2850, 1760, 1750, 1650, 1610, 1170, 840

Ms   m/z =   662 (M$^+$), 412, 355 (100%), 203, 121, 69

3.3 PREPARATION OF LIQUID CRYSTAL POLYMERS

Liquid Crystal Polymers were prepared from the monomer materials *via* one of the two following methods.

Method 1

Thermally initiated radical polymerisations were carried out using 5 mol % of 2,2'-azo-*bis*-isobutyronitrile (AIBN) as the initiating species in dry dichloroethane (4 ml per 500 mg of monomer) in a sealed glass tube under a nitrogen atmosphere for 48 hours at 65 °C. The polymer was obtained by precipitation induced by the addition of cold methanol to the cold reaction mixture. Purification of the polymer was carried out by dissolving the crude polymer in the minimum volume of dichloromethane followed by precipitation into ice cold methanol (25 ml). This process was then repeated until no further monomer was detected by tlc. The polymer was dissolved in the minimum volume of dichloromethane and the solution filtered through a 0.5 µm membrane filter and dried in a vacuum at room temperature.

Method 2

UV initiated radical polymerisations were carried out using 5 mol % Irgacure 184 as the initiating species. The monomeric material and initiator were dissolved in the minimum volume of dichloromethane and poured dropwise onto cold glass plates. The solvent was allowed to evaporate at room temperature before the resulting solid was dried in an oven at 40 °C. The plates were then sandwiched together and polymerised in bulk for 8 hours at 80 °C under a Philips Type HB 171 / A ultraviolet lamp. Purification of the polymers was carried out as described in Method 1.

Table 3.1 contains a summary of the monomers prepared and the polymerisation procedure followed in the production of the corresponding polymer. None of the polymers reported were polymerised by both methods. The polymers are subdivided according to the changes in molecular structure which have been examined.

Monomer	Polymer	Polymerisation Procedure
31	P31	Thermal (Method 1)
32	P32	Thermal
33	P33	Thermal
34	P34	Thermal
39	P39	Thermal
40	P40	Thermal
55	P55	UV (Method 2)
56	P56	UV
57	P57	UV
66	P66	UV
67	P67	UV
68	P68	UV
72	P72	UV
73	P73	UV
96	P96	Thermal
97	P97	Thermal

Table 3.1 - Method Employed in the Preparation of Side
Chain Liquid Crystal Polymers

The molecular weights of the polymers were determined by Gel Permeation Chromatography (GPC) [see section 3.1.1(d)] with a refractive index detector

(Gilson Model 131). Tetrahydrofuran was used as the solvent at a flow rate of 1 ml min^{-1}.

The number average molecular weight ($\overline{M}n$) and weight average molecular weight ($\overline{M}w$) were determined relative to polystyrene standards; $\overline{M}n$ and $\overline{M}w$ are defined in section 1.8.3. The polydispersity (γ) and number average degree of polymerisation ($\overline{X}n$) of the polymer sample were also calculated; polydispersity and number average degree of polymerisation are defined in sections 1.8.3 and 1.8.4 respectively.

The results obtained from the Gel Permeation Chromatography of the polymers defined in Table 3.1 are shown in Table 3.2.

POLYMER	($\overline{M}n$)	($\overline{M}w$)	(γ)	($\overline{X}n$)
P31	3900	4750	1.22	6
P32	4050	4940	1.22	6
P33	4240	4860	1.15	6
P34	4640	5430	1.17	7
P39	9640	10980	1.14	16
P40	7130	8280	1.16	12
P55	5060	9650	1.90	8
P56	6360	7210	1.13	10
P57	6580	7490	1.14	11
P66	6650	8900	1.34	10
P67	7230	9840	1.36	11
P68	6990	8280	1.19	11
P72	4120	6370	1.55	7
P73	4730	7110	1.50	8
P96	14800	21600	1.46	33
P97	10100	12400	1.23	19

Table 3.2 - GPC Results for Side Chain Liquid Crystal Polymers

CHAPTER 4
RESULTS AND DISCUSSION

RESULTS AND DISCUSSION

4.1 THE EFFECT OF THE POSITION OF LATERAL FLUORO SUBSTITUTION ON THE LIQUID CRYSTAL PROPERTIES OF SOME SIDE CHAIN LIQUID CRYSTAL ACRYLATES

4.1.1 Introduction

The monomeric compounds **31 - 34** [Figure 4.1(a)] and their corresponding polymers **P31 - P34** [Figure 4.1(b)] were prepared in order to investigate the influence of fluoro substitution on the generation of smectic phases which have alternating tilt direction in adjacent layers.
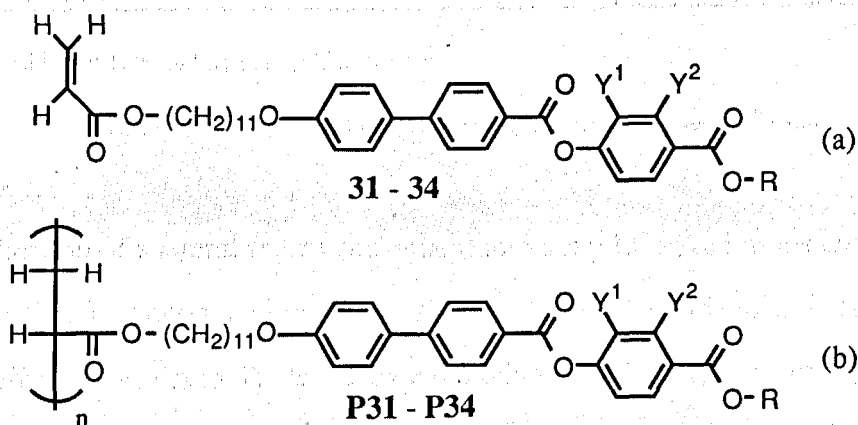
31, P31 ; Y^1, Y^2 = H, R = (*R*)-1-methylheptyl
32, P32 ; Y^1 = H, Y^2 = F, R = (*R*)-1-methylheptyl
33, P33 ; Y^1 = F, Y^2 = H, R = (*R*)-1-methylheptyl
34, P34 ; Y^1, Y^2 = H, R=1-propylbutyl

Figure 4.1 - Liquid Crystal Monomers and Polymers Prepared to Study the Effects of Fluoro Substitution

4.1.2 Transition Temperatures and Phase Behaviour of Monomeric Materials as Determined by Optical Microscopy

The phase sequences and the transition temperatures for the monomeric compounds **31 - 34** are listed in Table 4.1. The results are presented as a bar graph in Figure 4.2.

Cmpd	Iso - S_A	S_A - S_{C^*}	S_A - S_{CAlt}	S_{C^*} - $S_{C\gamma^*}$	$S_{C\gamma^*}$ - S_{CA^*}	S_{C^*} - S_{CA^*}	mp	Recryst[‡]
31	94.7	65.7	-	50.3	49.8	-	28.4	20.9
32	90.4	58.6	-	42.4	41.8	-	14.8[‡]	6.2
33	78.7	33.2	-	-	-	28.6	7.5[‡]	-19.4
34	76.9	-	41.9	-	-	-	38.4	-23.7

[‡]Obtained by Differential Scanning Calorimetry

Table 4.1 - Transition Temperatures (°C) for Compounds 31 -34

The insertion of a lateral fluoro substituent into a liquid crystal molecule can have a dramatic effect upon the liquid crystal properties of the molecule.[82] This can be seen from the results in Table 4.1 by examining the effect fluoro substitution has on the isotropization temperature of the mesogens. Fluoro substitution reduces the clearing point of the molecule significantly showing that the liquid crystallinity of the molecule has been diminished. This is seen to occur to the greatest extent when the fluoro substituent is 'facing inwards' (*e.g.* compound **33**, at the 2-position) which leads to the clearing point decreasing to 78.7 °C. The S_A - S_{C^*} transition temperature is also affected by the insertion of a fluoro substituent and once again the 2-fluoro substituent has the greatest effect. The most noticeable effect on phase behaviour is seen, however, at temperatures below the S_{C^*} phase. With the fluoro substituent facing outwards (*i.e.*, at the 3-position, compound **32**) both the ferroelectric-to-ferrielectric (S_{C^*} - $S_{C\gamma^*}$) and the ferrielectric-to-antiferroelectric ($S_{C\gamma^*}$ - S_{CA^*}) transition temperatures are lowered.

However, when the fluoro substituent is in the 2-position (compound **33**) the ferrielectric phase is eliminated from the phase sequence and instead a ferroelectric-to-antiferroelectric (S_C^* - S_{CA}^*) transition is observed at 28.6 °C. The melting points of all the molecules studied are also decreased by the insertion of a lateral fluoro substituent.
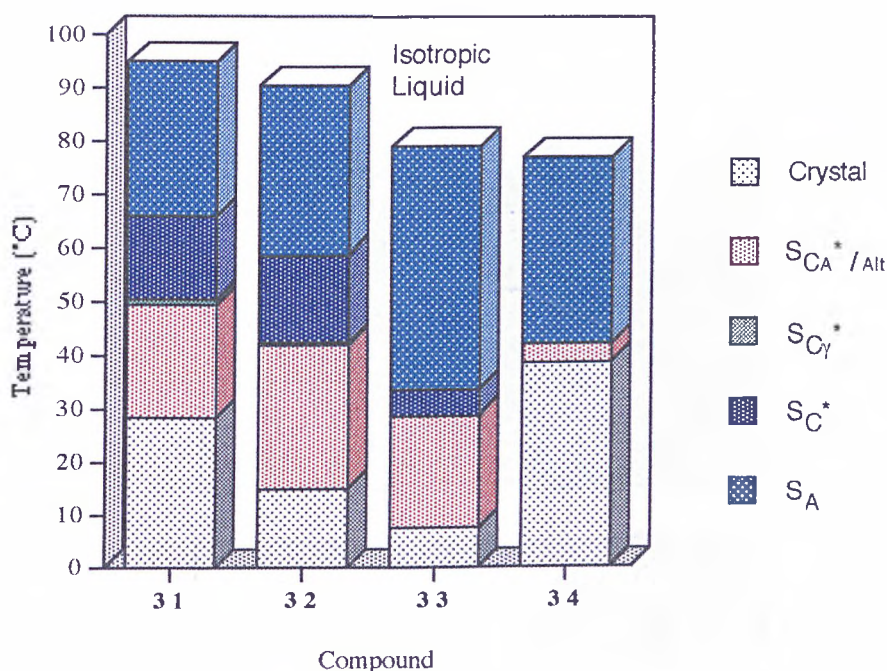
Figure 4.2 - Transition Temperatures (°C) and Phase Sequences for Compounds 31 - 34, as determined by Optical Microscopy

Photomicrographs of the textures shown by the S_A, S_C^*, $S_{C\gamma}^*$, and S_{CA}^* phases of compound **31** are given in Figure 4.3.

(a) S$_A$

(72.1 °C)

(b) S$_C$*

(59.3 °C)

(c) S$_{C\gamma}$*

(50.0 °C)

(d) S$_{CA}$*

(42.8 °C)
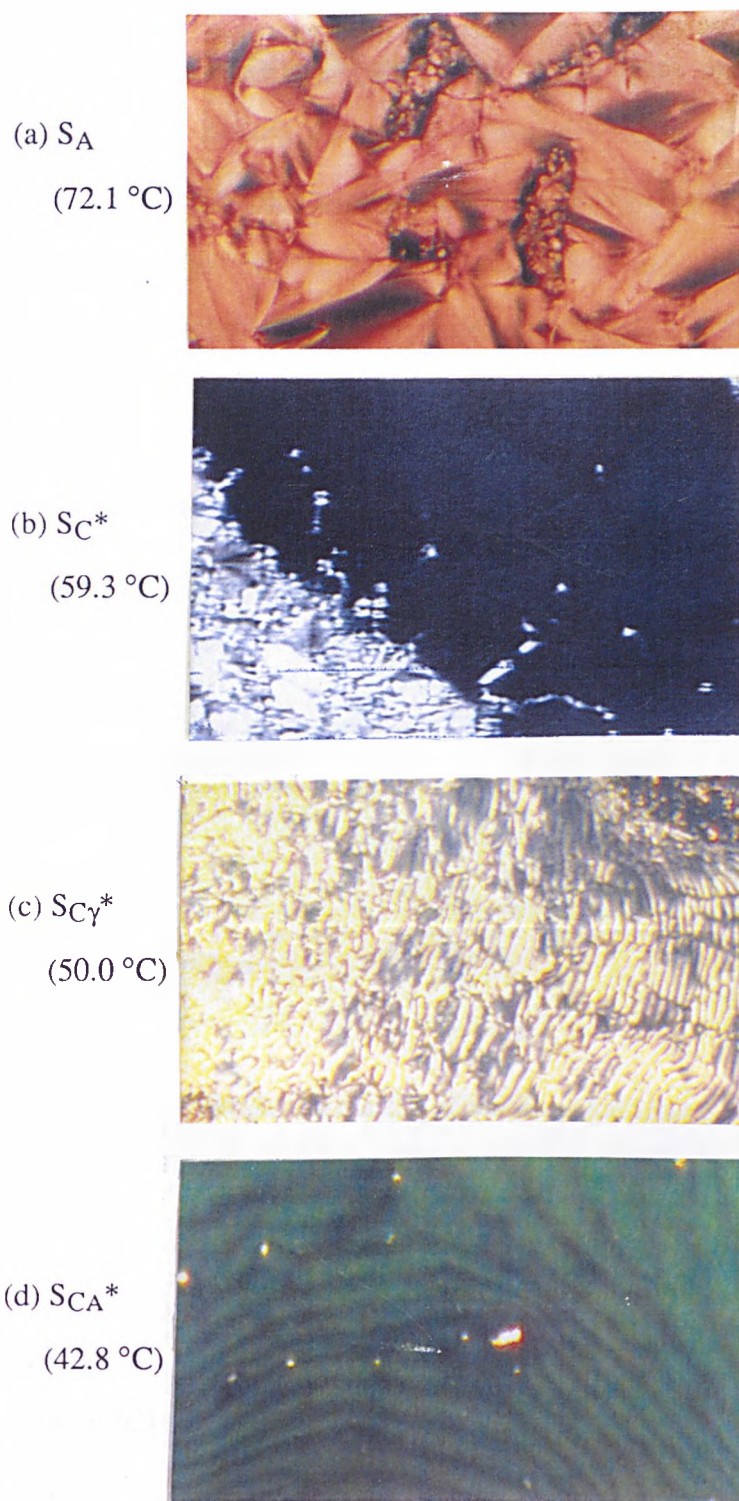
Figure 4.3 - Photomicrographs of the Textures obtained for the Phases Exhibited by Compound 31

When the optically active 1-methylheptyl end group of the monomeric molecule **31** is replaced with an achiral 1-propylbutyl group (which is known to be capable of generating an alternating phase in low molar mass materials[90]) to give compound **34**, again the isotropization temperature of the molecule is decreased. However, on reducing the temperature below the S_A phase, unlike the optically active analogue **31**, no ferroelectric or ferrielectric phases are observed and instead the molecule adopts a phase with an alternating structure at 41.9 °C. The textures exhibited by the S_A and S_{CAlt} phases of compound **34** can be seen in Figure 4.4.

(a) S_A
(66.3 °C)

(b) S_{CAlt}
(40.6 °C)
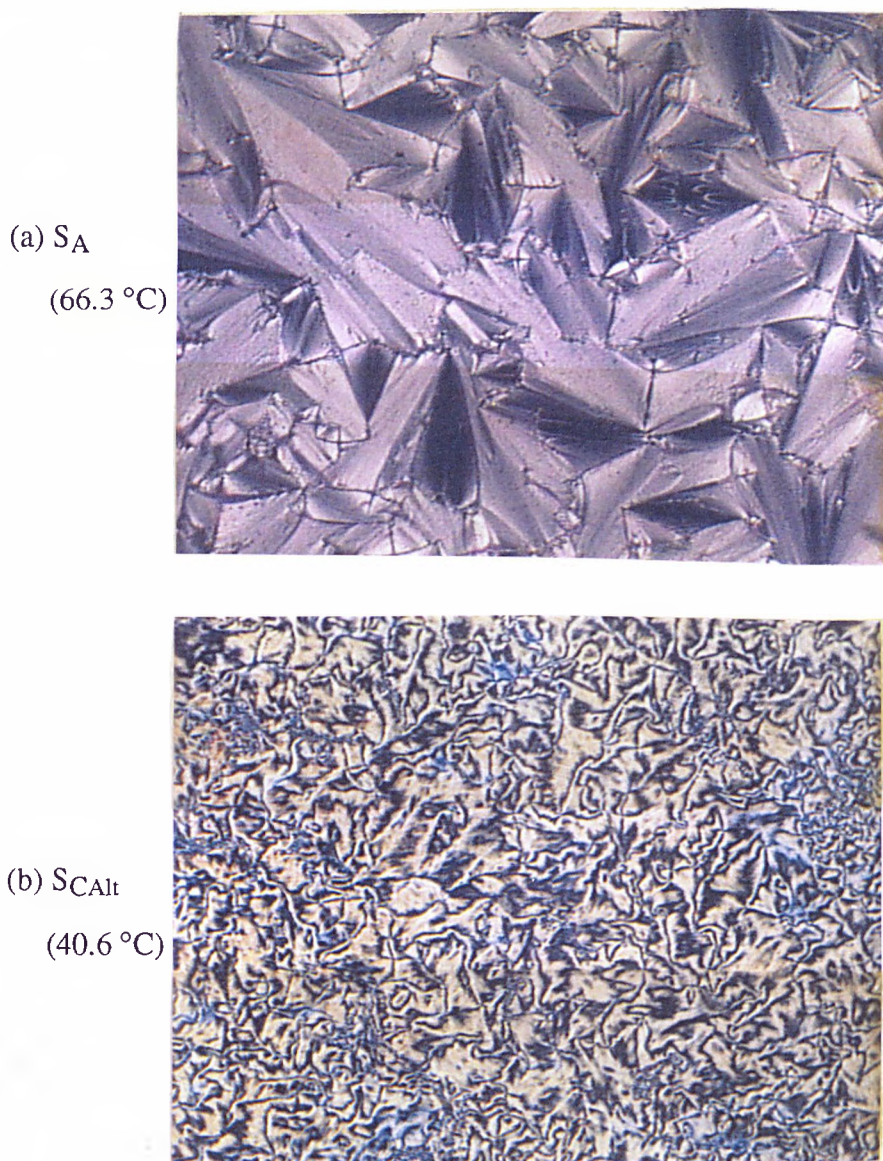
Figure 4.4 - Photomicrographs of the Textures obtained for the Phases Exhibited by Compound 34

4.1.3 Transition Temperatures and Phase Behaviour of the Monomeric Materials as Determined by Differential Scanning Calorimetry

Compounds **31 - 34** were examined by Differential Scanning Calorimetry (DSC) using the apparatus outlined in section 3.1.2(b). All DSC measurements were performed at a rate of 10 °C min^{-1} unless otherwise stated.

At the temperatures determined by optical microscopy for the ferroelectric-to-ferrielectric (S_C^* - $S_{C\gamma}^*$) and the ferrielectric-to-antiferroelectric ($S_{C\gamma}^*$ - S_{CA}^*) transitions for compounds **31** and **32**, peaks were not observed by DSC measurements. The liquid crystal transitions, and their associated enthalpies for compounds **31 - 34** are listed in Table 4.2. The DSC cooling thermograms for compounds **31** and **32** are shown in Figure 4.6.

Compound	Transition	Temperature	Enthalpy
31	Iso - S_A	93.6	4.12
	S_A - S_C*	66.6	0.44
	S_C* - $S_{C\gamma}*$	¶	¶
	$S_{C\gamma}*$ - $S_{CA}*$	¶	¶
	mp	29.9	53.52
32	Iso - S_A	88.7	3.70
	S_A - S_C*	60.1	0.39
	S_C* - $S_{C\gamma}*$	¶	¶
	$S_{C\gamma}*$ - $S_{CA}*$	¶	¶
	mp	14.8	49.76
33	Iso - S_A	76.3	1.99
	S_A - S_C*	31.6	0.42
	S_C* - $S_{CA}*$	27.2	0.11
	mp	7.5	32.61
34	Iso - S_A	79.8	1.91
	S_A - S_{CAlt}	44.9	0.70
	mp	39.9	63.11

¶ no peak observed using DSC .

Table 4.2 - Transition Temperatures (°C) and Enthalpies (kJ mol^{-1}) for Compounds 31 - 34 observed by DSC
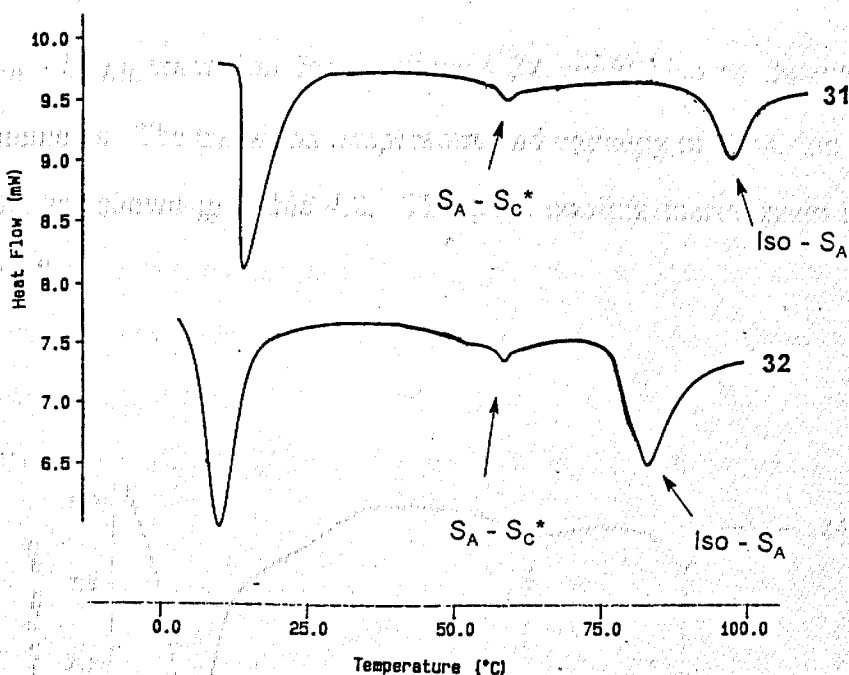
Figure 4.6 - DSC Cooling Thermograms for Compounds 31 and 32

The ferroelectric-to-antiferroelectric (S_C^* - S_{CA}^*) transition for compound **33** was detected by DSC measurements and this transition can be seen in the DSC cooling thermogram shown in Figure 4.7. The transition temperature and the value measured for the enthalpy of transition are shown in Table 4.2.
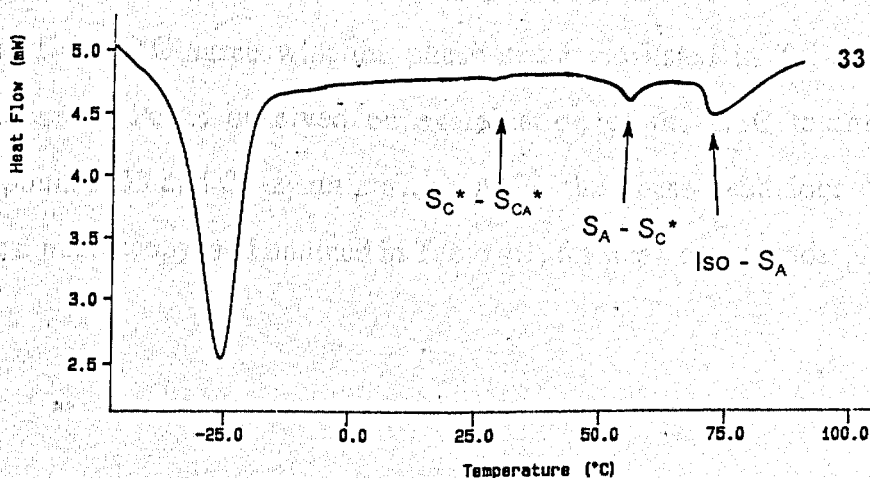
Figure 4.7 - DSC Cooling Thermogram for Compound 33

The S_A - $S_{CA\text{lt}}$ transition for compound **34** could also be detected by DSC measurements. The transition temperature and enthalpy of transition as observed by DSC are shown in Table 4.2. The DSC cooling thermogram is shown in Figure 4.8.
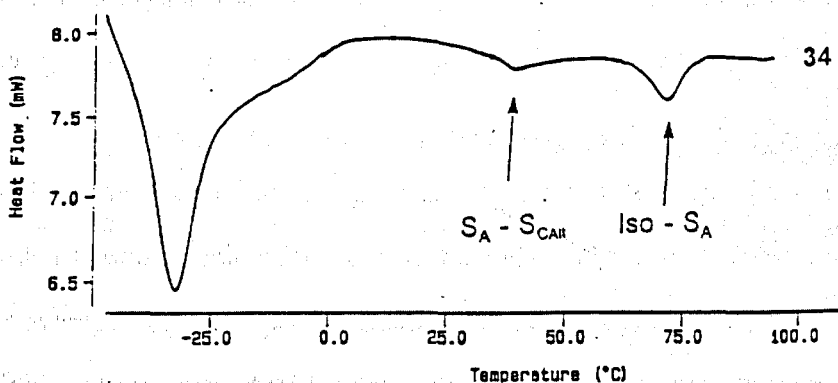
Figure 4.8 - DSC Cooling Thermogram for Compound 34

It can be seen from the DSC measurements that peaks observed for compound **31** at 29.9 °C, 66.6°C and 93.6 °C correspond to transitions observed during optical microscopy, thus confirming the phase behaviour outlined in Table 4.1. If the DSC thermogram for compound **32** (Figure 4.6) is examined then peaks at 88.7 °C and 60.1 °C agree with the phase sequence listed in Table 4.1 for this compound. Peaks observed on examination of the DSC thermograms for compounds **33** and **34** again correspond to the phase behaviour observed by optical microscopy, and outlined in Table 4.1, for these compounds.

4.1.4 Transition Temperatures and Phase Behaviour of Polymeric Materials as Determined by Optical Microscopy

Textural studies were carried out using a sample of the side chain liquid crystal poly(acrylate) sandwiched between a coverslip and a microscope slide. The polymer samples were annealed by heating to 20 °C above their isotropization temperature and the sample was cooled slowly at 0.2 °C min^{-1} until a few degrees into the liquid crystalline state and then left for 12 hours to allow a texture to develop.

Table 4.3 gives the transition temperatures obtained from optical microscopy and the number average molecular weight, the weight average molecular weight, the number average degree of polymerisation, and the polydispersity of the polymers **P31 - P34**. The results obtained from optical microscopy are displayed as a bar graph in Figure 4.9.

Polymer	Iso - S_A	S_A - S_{CA}* / Alt	mp‡	$\overline{M}n$	$\overline{M}w$	$\overline{X}n$	γ
P31	99.6	84.9	42.4	3900	4750	6	1.22
P32	113.4	84.7	66.6	4050	4940	6	1.22
P33	96.6	50.6	47.7	4240	4860	6	1.15
P34	111.6	78.6	55.9	4640	5430	7	1.17

‡ Obtained by DSC

Table 4.3 - Transition Temperatures (°C) Determined by Optical Microscopy and GPC data for Compounds P31 - P34
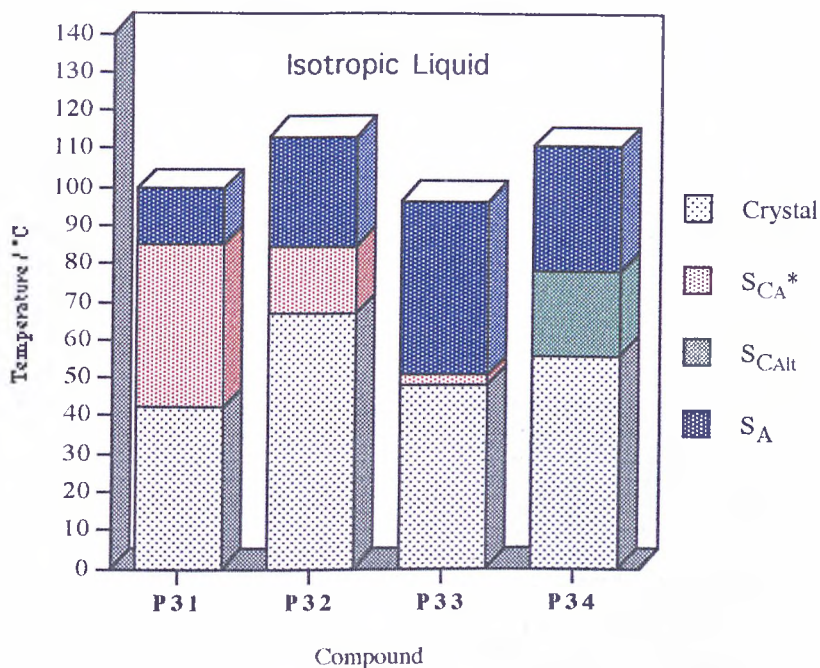
Figure 4.9 - Transition Temperatures (°C) for Compounds P31 - P34 as Determined by Optical Microscopy

Figure 4.9 shows the effect that insertion of a lateral fluoro substituent has on the incidence of an antiferroelectric phase in a liquid crystal poly(acrylate). In general, insertion of a fluoro substituent reduces the temperature range over which the antiferroelectric phase occurs and this is most noticeable when the substituent is in the 2-position (*i.e.* inner facing, polymer **P33**); the antiferroelectric phase then occurs only over a few degrees range. When the chiral 1-methylheptyl end group is replaced with the achiral 1-propylbutyl group the alternating structure of the antiferroelectric smectic C* phase is retained and an alternating smectic phase is obtained.

Each of the polymers **P31** - **P34** show a phase sequence of Iso $\Leftrightarrow$ S_A $\Leftrightarrow$ $S_{CA}*$ or S_{CAlt}. Photomicrographs for polymer **P31** are shown in Figure 4.10. Figure 4.10(a) shows the focal conic texture of the homogeneously aligned S_A phase. The dark region is due to homeotropic alignment. At 84.9 °C a phase transition occurs when the fans, characteristic of the focal conic texture of the S_A phase,

appear to break. The homeotropic areas also develop what appears to be small regions of schlieren texture [Figure 4.10(b)].

(a) S_A

(87.2 °C)
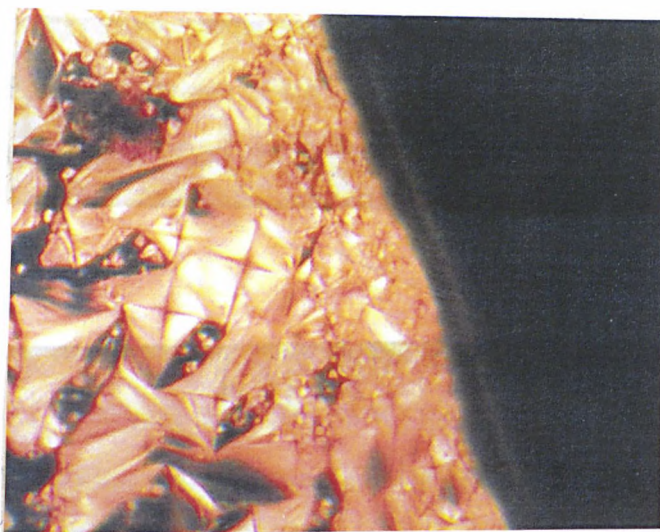
(b)S_{CA}*

(53.8 °C)
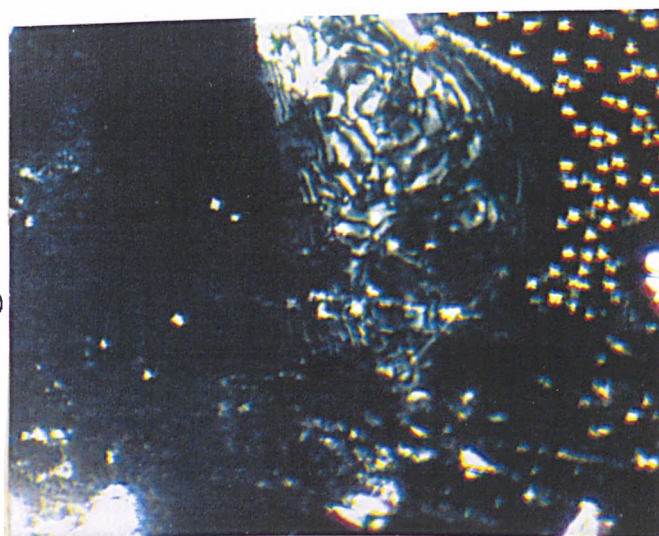
**Figure 4.10 - Photomicrographs of the Textures obtained for the
Phases exhibited by Compound P31**

Figure 4.11 shows the textures obtained during optical microscopy of polymer **P34**. The focal conic fan texture of the homogeneously aligned smectic A phase can again be seen. At 78.6 °C however, a four- and two-brush schlieren texture, characteristic of an alternating phase, is observed in the previously homeotropic areas.

The phase sequences observed by optical microscopy on the monomers (**31 - 33**) and polymers (**P31 - P33**) give results which show that the insertion of a lateral fluoro substituent has a marked effect on the liquid crystal properties of these materials. This is consistent with previous work reported.[73]

The existance of an antiferroelectric like phase in a non-chiral 'swallow-tailed' low molar mass material is consistent with the work reported by Nishiyama and Goodby,[90] however the existance of this phenomenon in a non-chiral 'swallow-tailed' polymeric material has not previously been reported.

(a) S_A

(103.6 °C)
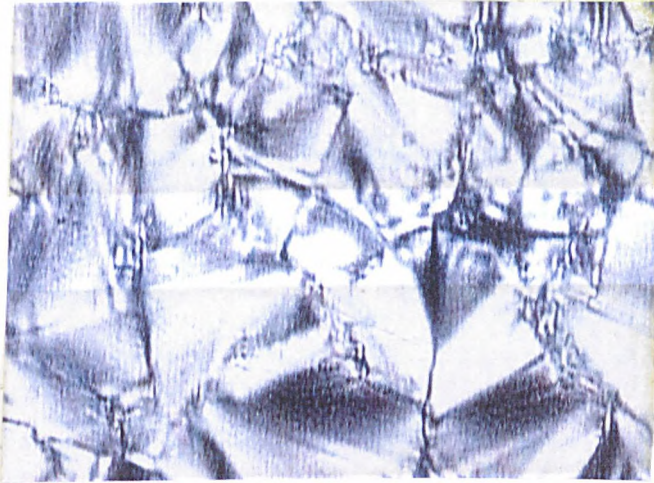
(b) S_{CAlt}

(62.3 °C)
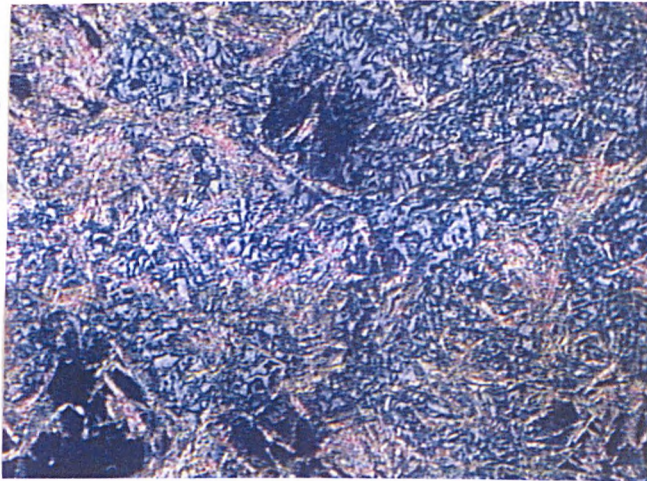
Figure 4.11 - Photomicrographs of the Textures Obtained for the Phases exhibited by Polymer P34

4.1.5 Transition Temperatures and Phase Behaviour of Polymeric Materials as Determined by Differential Scanning Calorimetry

Polymers **P31** - **P34** were examined by DSC. The transition temperatures obtained and the enthalpies associated with these transitions are given in Table 4.4

Compound	Transition	Temperature	Enthalpy
P31	Iso - S_A	103.2	4.59
	S_A - S_{CA}*	86.0	0.26
	mp	42.4	6.40
P32	Iso - S_A	113.4	8.01
	S_A - S_{CA}*	85.7	0.34
	mp	66.6	5.29
P33	Iso - S_A	96.6	12.27
	S_A - S_{CA}*	53.2	0.57
	mp	47.7	15.59
P34	Iso - S_A	113.3	8.01
	S_A - S_{CAlt}	78.5	0.60
	mp	55.9	15.92

Table 4.4 - Transition Temperatures (°C) and Enthalpies (J g^{-1}) for Polymers P31 - P34 Determined by DSC

The DSC thermograms for polymers **P31** and **P34** are shown in Figure 4.12.
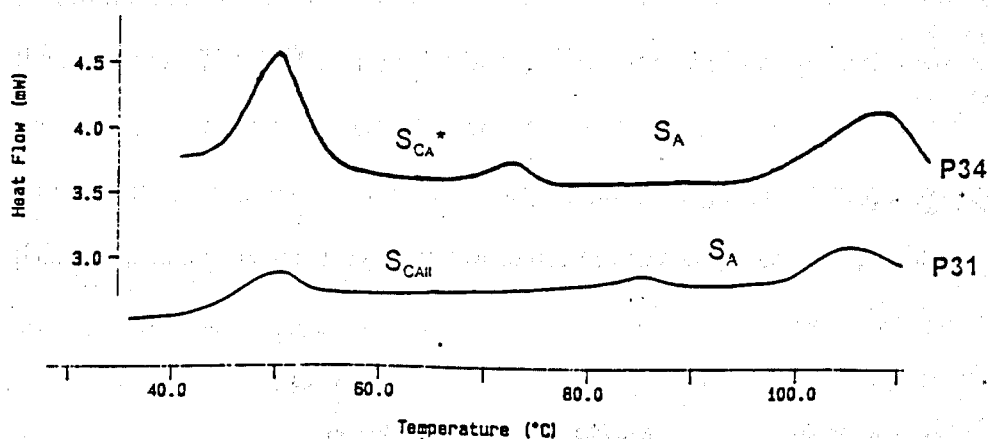
Figure 4.12- DSC Thermograms for Polymers P31 and P34

4.1.6 Miscibility Studies

In order to ascertain whether the antiferroelectric phases found in polymers **P31** -
P34 were of the same classification as those reported for low molar mass liquid
crystals, a miscibility test was carried out with the polymer and a standard low
molar mass material. Such miscibility studies have been previously reported for
mixtures of side chain liquid crystal polymers and low molar mass materials.[82]
The standard material used was (R)-[4-(1-methylheptyl)oxycarbonyl]phenyl 4'-
(11-undecyloxy)biphenyl-4-carboxylate (MHP11BC) and the structure and
transitions for this compound are shown in Figure 4.13.

Iso 147.9 S_A 120.2 S_C* 103.3 $S_{C\gamma}*$ 102.5 $S_{CA}*$ 57.13 K
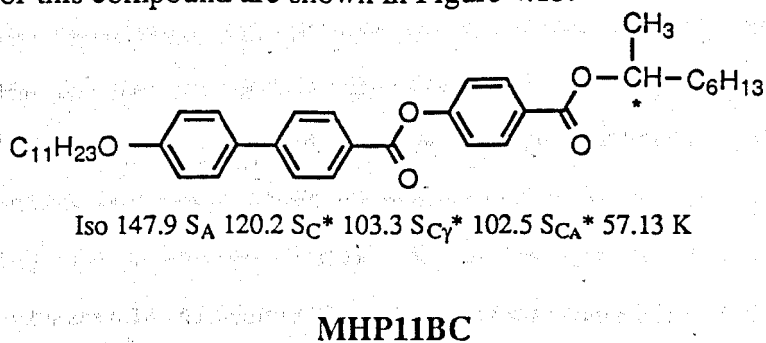
MHP11BC

Figure 4.13 - Structure and Transition Temperatures (°C) of (R)-[4-(1-
methylheptyl)oxycarbonyl]phenyl 4'-(11-undecyloxy)
biphenyl-4-carboxylate

Figure 4.14 shows the phase diagram for mixtures of polymer **P31** with the standard material **MHP11BC**. The phase diagram shows continuous miscibility across the full composition range for the $S_{CA}*$ and S_A phases of the polymer and the standard. The S_C* and $S_{C\gamma}*$ phases of the standard compound however, were found to disappear as the weight percentage of the test polymer **P31** increased to above approximately 45 and 25 weight percent polymer respectively, thus indicating that polymer **P31** does not exhibit either a S_C* or a $S_{C\gamma}*$ phase.
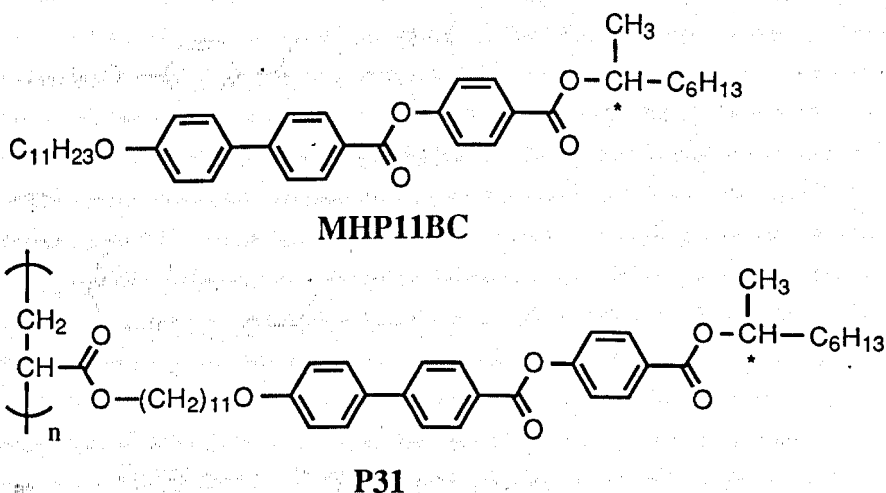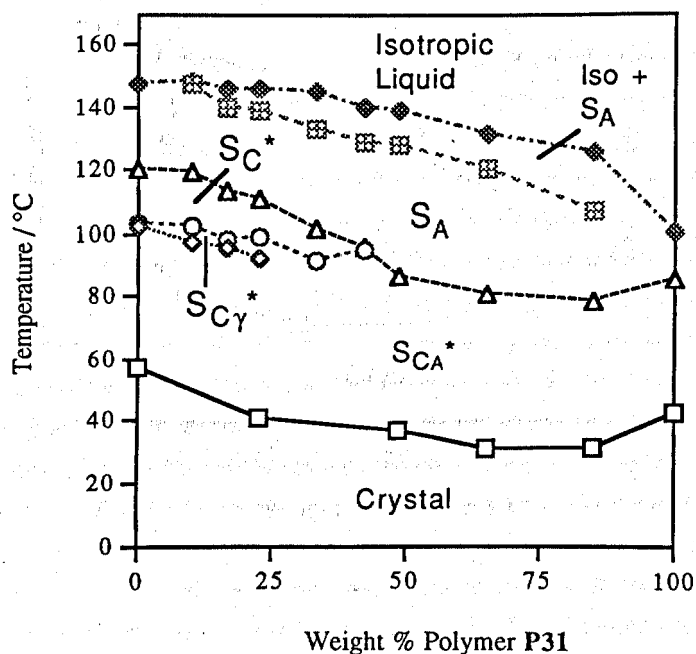
Figure 4.14 - Miscibility Phase Diagram for Polymer P31 and the
Standard Compound MHP11BC

Figure 4.15 shows a phase diagram between the test polymer material **P32** and the standard **MHP11BC**. Again the S_C* and $S_{C\gamma}*$ phases were found to disappear as the weight percentage of the test material rose above approximately 15%. The $S_{CA}*$ and S_A phases again showed complete miscibility throughout the entire composition range with the standard material.
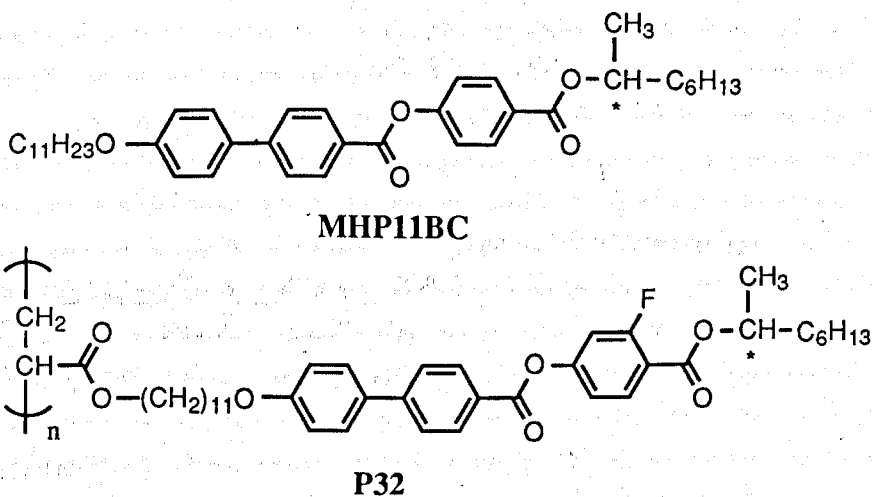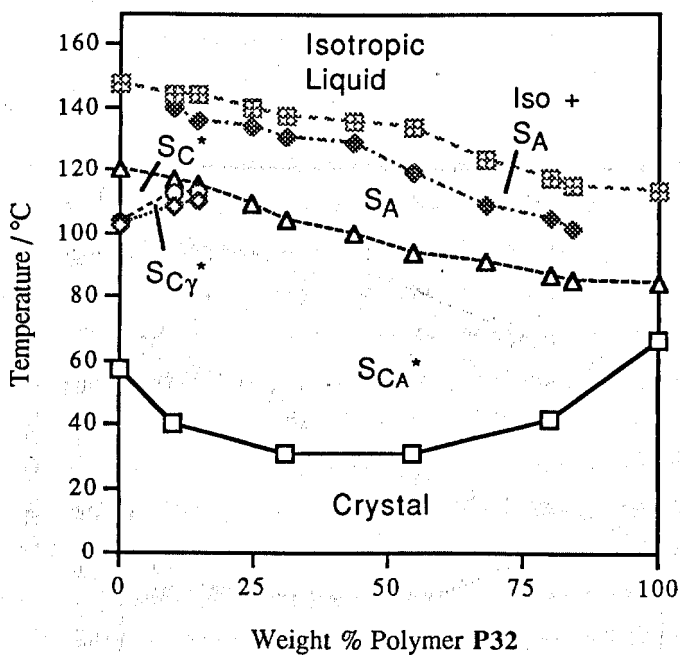
Figure 4.15 - Miscibility Phase Diagram for Polymer P32 and the Standard Compound MHP11BC

The binary miscibility diagram for polymer **P33** and the standard **MHP11BC** can be seen in Figure 4.16. The S_A and $S_{CA}*$ phases show complete miscibility throughout the entire composition range, although the temperature range in which the $S_{CA}*$ phase occurs diminishes when the composition of the mixture rises to above approximately 80 % polymer. The S_C* and $S_{C\gamma}*$ phases disappear above approximately 15 weight percent polymer showing that neither phase is present in the polymer.
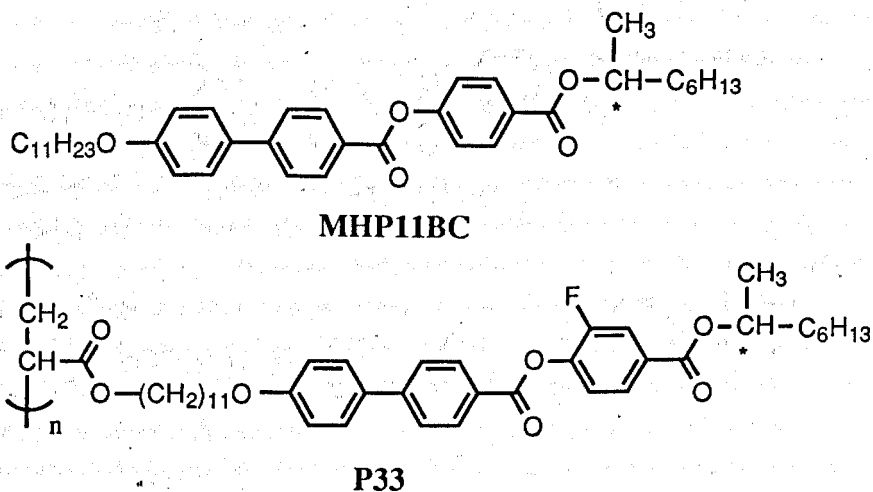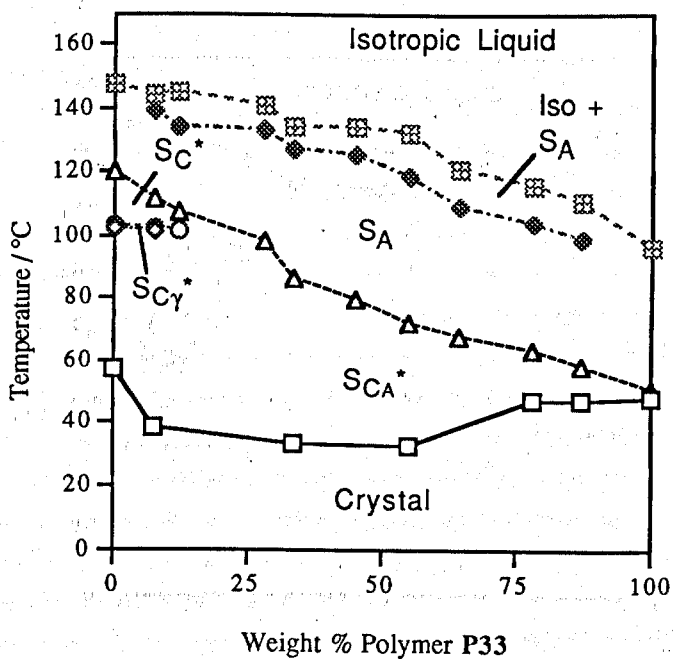
Figure 4.16 - Miscibility Phase Diagram for Polymer P33 and
the Standard Compound MHP11BC

Figure 4.17 shows the binary miscibility diagram for the standard material **MHP11BC** and the achiral polymer **P34**. The diagram shows that not only were the S_A phase of the standard material and the S_A phase of the polymer completely miscible, but that the alternating structure (obtained at lower temperatures for the polymer **P34**) and the $S_{CA}*$ phase of the standard were also completely miscible. The S_C* and $S_{C\gamma}*$ phases of the standard material disappeared over approximately 35 and 15 weight percent polymer respectively, indicating that these were not present in the polymer material alone.
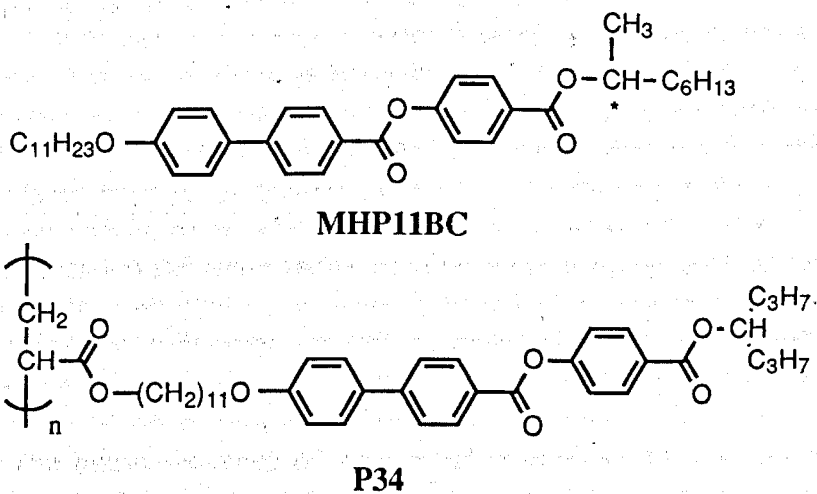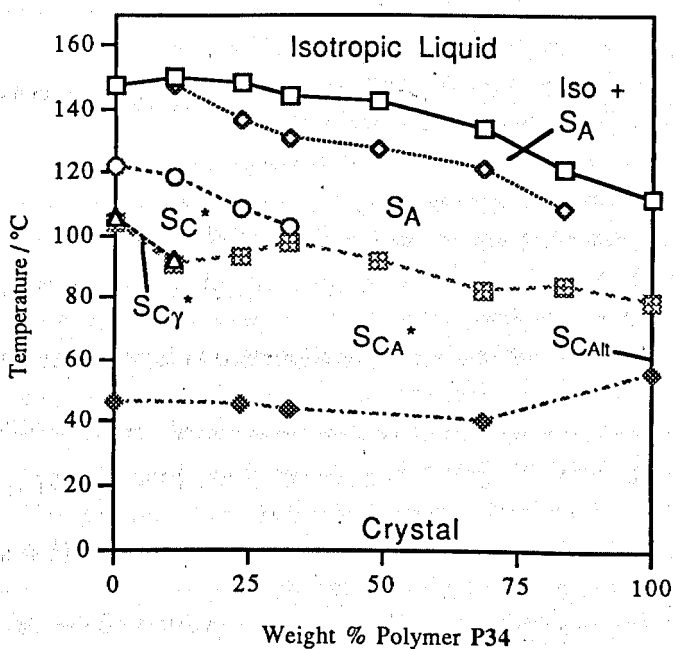
Figure 4.17 - Miscibility Phase Diagram for Polymer P34 and
the Standard Compound MHP11BC

An interesting effect can be seen when examining the miscibility diagrams for polymers **P31** - **P34**. The melting point to the $S_{CA}*$ phase of **MHP11BC** is depressed on addition of the side chain liquid crystal polymer, *i.e.*, the addition of 20 - 30 % of the appropriate polymer suppresses the melting point by approximately 25 °C. Concurrently the normal ferroelectric S_C* phase disappears and a direct S_A - $S_{CA}*$ transition is induced. Therefore when practical antiferroelectric liquid crystal mixtures are made, antiferroelectric side chain liquid crystal polymers could be a useful component to include for expanding the range of the $S_{CA}*$ phase.

4.1.7   Effect of Polymerisation on the Liquid Crystal Properties

It is already known that when a liquid crystalline material which can be polymerised, undergoes a polymerisation reaction then, in general, the liquid crystal phase of this material is thermally stabilised.[58] The transition temperatures and phase sequences of compounds **31** - **34** (listed in Table 4.1) and those for the corresponding polymers **P31** - **P34**, (listed in Table 4.3) are displayed as a bar graph in Figure 4.18, and it can be seen that the isotropization temperatures and melting points for the polymers **P31** - **P34** all increase with respect to the values for the monomers.

Closer examination of Figure 4.18 also shows another consequence of polymerisation. Examining the phase sequence of compounds **31** - **34**, and comparing these to the phase sequences obtained for polymers **P31** - **P34** then it can seen that in the polymeric materials the ferroelectric phases in compounds **31**, **32**, and **33**, and the ferrielectric phases observed in compounds **31** and **32** are absent. The phase sequence of the achiral monomer (**34**) remains unchanged when the material is polymerised (**P34**).
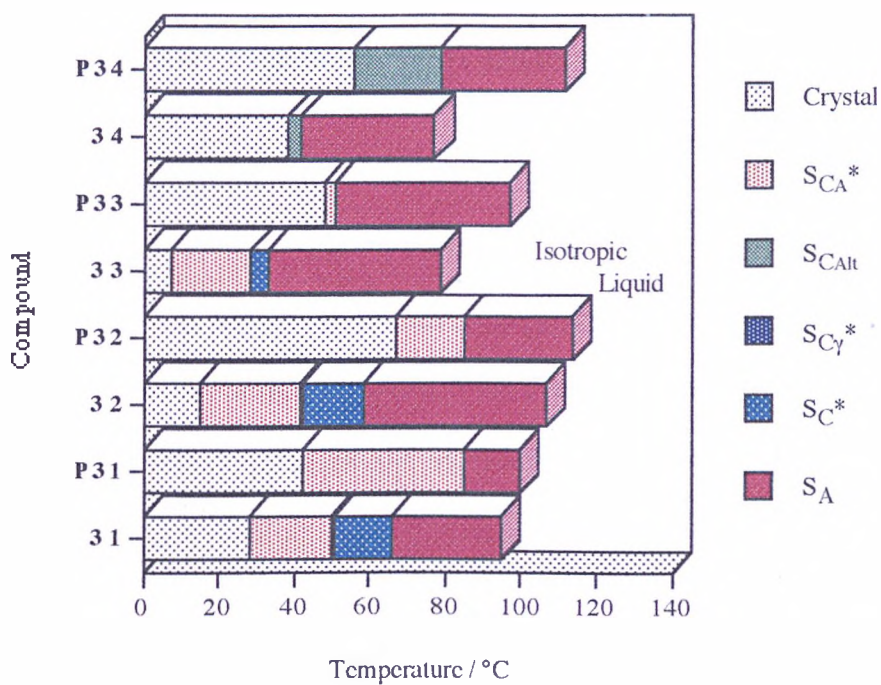
Figure 4.18 - Phase Behaviour of Compounds 31 - 34 and their Corresponding Polymers P31 - P34

4.2 THE EFFECT OF ALTERING THE FLEXIBLE SPACER LENGTH ON THE LIQUID CRYSTAL PROPERTIES OF SOME SIDE CHAIN LIQUID CRYSTAL ACRYLATES

4.2.1 Introduction

The monomeric compounds **39** and **40** [Figure 4.19(a)], and the corresponding polymers **P39** and **P40** [Figure 4.19(b)], were prepared and their liquid crystalline properties contrasted with the acrylic monomers, **31** and **34**, and polymers, **P31** and **P34**, described previously in section 4.1. This work was undertaken in order to examine the effect of increasing the flexible spacer length of polymers by one carbon atom on the liquid crystalline properties.

39, 40 (a)

P39, P40 (b)

39, P39 ; R = (R)-1-methylheptyl
40, P40 ; R = 1-propylbutyl
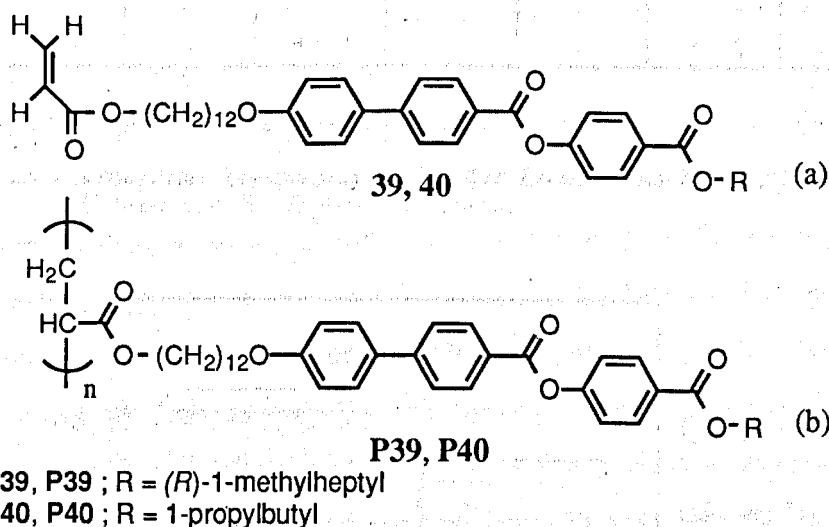
Figure 4.19 - **Liquid Crystal Monomers and Polymers with Dodecyloxy Spacers**

4.2.2 Transition Temperatures and Phase Behaviour of Monomeric Materials by Optical Microscopy

The phase sequences and the transition temperatures of the monomeric materials prepared, are listed in Table 4.5, with the results depicted as a bar graph in Figure 4.20. The transition temperatures and phase sequences for compounds **31** and **34** are repeated in Table 4.5.

Cmpd	Iso - S_A	S_A - S_{C^*}	S_A - S_{CAlt}	S_{C^*} - $S_{C\gamma^*}$	$S_{C\gamma^*}$ - S_{CA^*}	mp	Recryst[‡]
39	103.6	93.7	-	88.1	87.3	52.6	33.6
40	87.5	-	72.3	-	-	57.6	25.5
31	94.7	65.7	-	50.3	49.8	28.4	20.9
34	76.9	-	41.9	-	-	38.4	-23.7

[‡] Obtained by Differential Scanning Calorimetry

Table 4.5 - Transition Temperatures (°C) for Compounds 39, 40, 31 and 34 Determined by Optical Microscopy
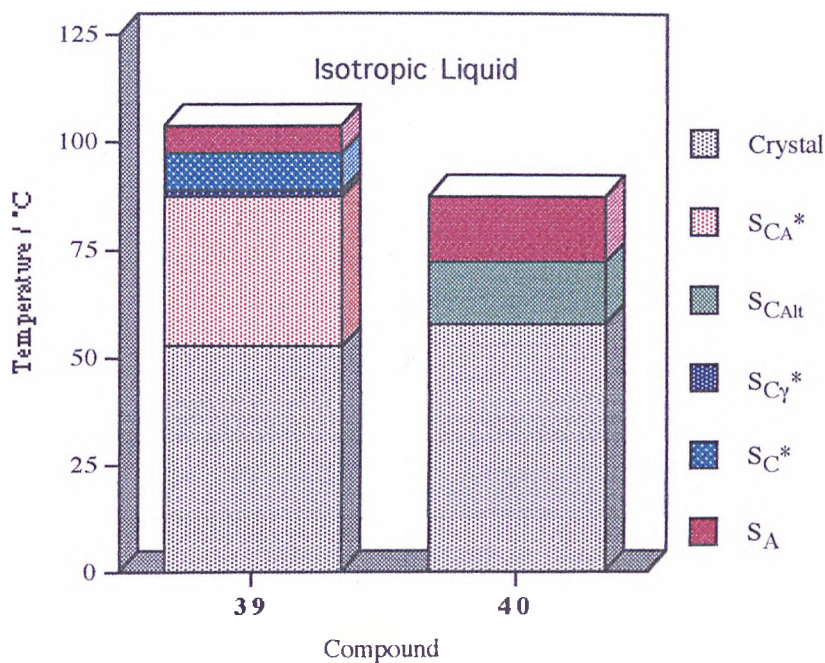
Figure 4.20 - Phase Behaviour for Compounds 39 & 40 Determined by Optical Microscopy

As can be seen from Table 4.5 increasing the spacer length of the acrylate monomer by one carbon unit has no effect on the phase sequence of the monomer. The optically active 1-methylheptyl monomeric compound **39** has a phase sequence of Iso $\Leftrightarrow$ S$_A$ $\Leftrightarrow$ S$_C$* $\Leftrightarrow$ S$_{C\gamma}$* $\Leftrightarrow$ S$_{CA}$* $\Leftrightarrow$ Cryst (*c.f.* compound **31** which has an identical phase sequence) and the achiral 1-propylbutyl compound **40** has a phase sequence of Iso $\Leftrightarrow$ S$_A$ $\Leftrightarrow$ S$_{CAlt}$ $\Leftrightarrow$ Cryst (*c.f.* compound **34** which also has this phase sequence) . The main difference in the two sets of compounds is that the addition of a further carbon to the terminal chain length has thermally stabilised the liquid crystalline state.

Photomicrographs of the textures obtained from the optical microscopy of compounds **39** and **40** can be seen in Figures 4.21 and 4.22 respectively.

(a) S_A

(96.6 °C)

(b) S_C*

(92.5 °C)

(c) $S_{C\gamma}*$

(87.9 °C)

(c) $S_{CA}*$

(74.1 °C)
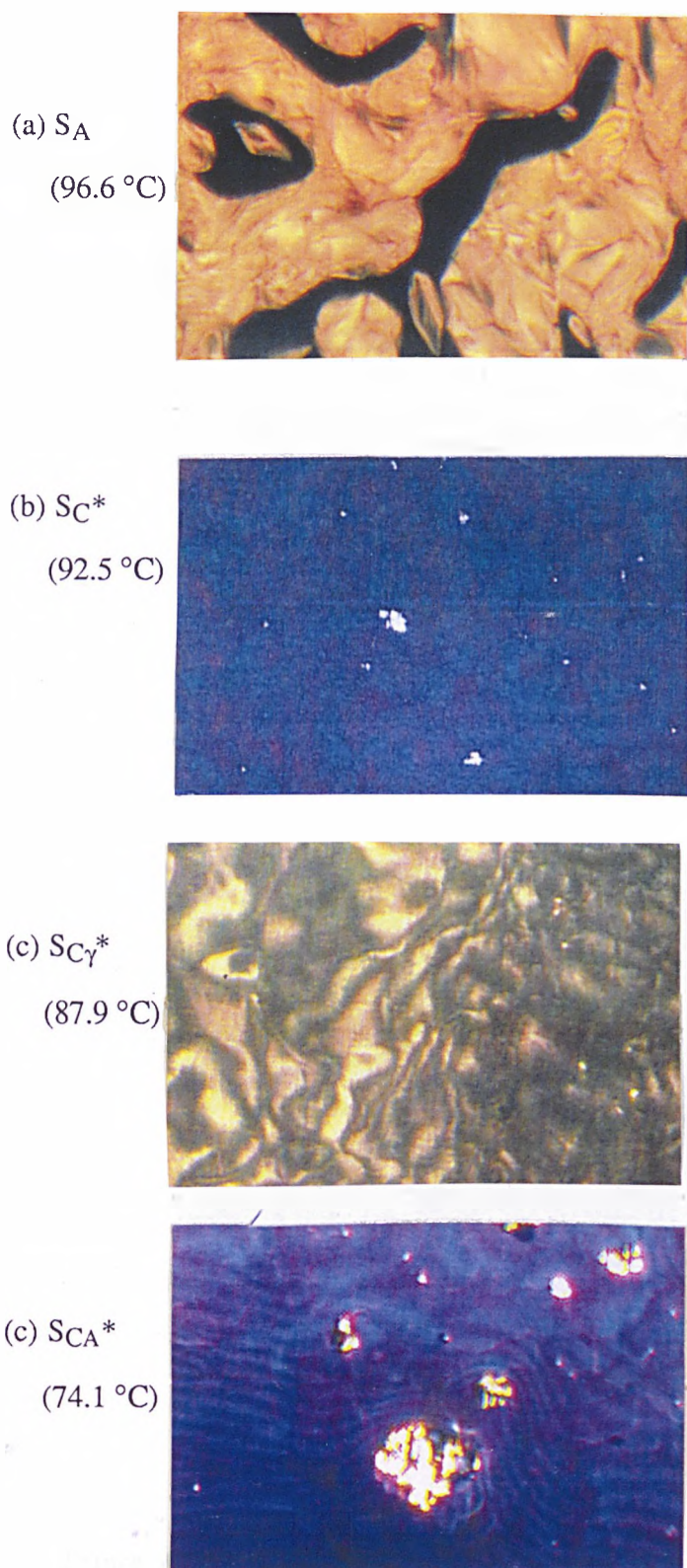
Figure 4.21 - Photomicrographs obtained during Optical Microscopy of Compound 39

(a) S$_A$

(79.3 °C)

(b) S$_{CAlt}$

(40.1 °C)
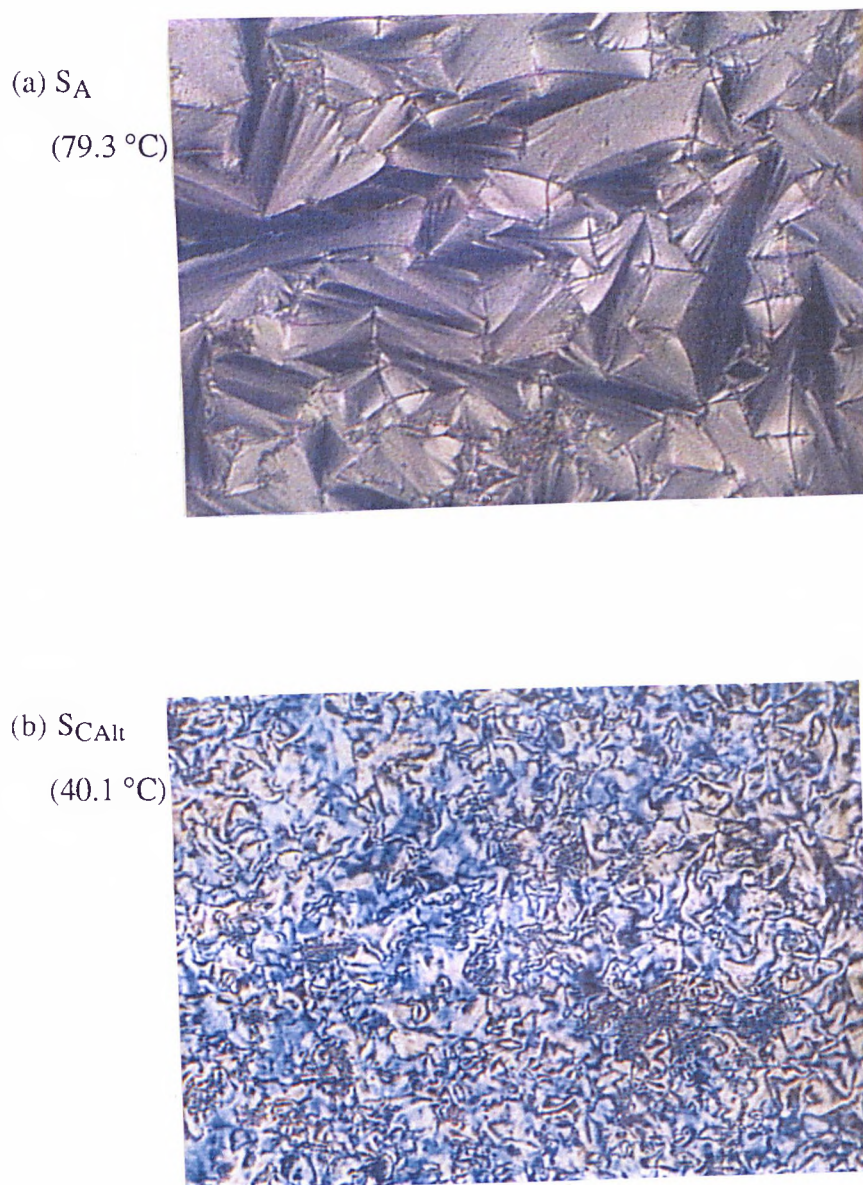
Figure 4.22 - Photomicrographs obtained during Optical
Microscopy of Compound 40

4.2.3 Transition Temperatures and Phase Behaviour of the Monomeric Materials as Determined by Differential Scanning Calorimetry

Compounds **39** and **40** were examined by DSC, using the apparatus outlined in section 3.1.2(b).

At the temperatures determined by optical microscopy for the ferroelectric to ferrielectric ($S_C* - S_{C\gamma}*$) and ferrielectric to antiferroelectric ($S_{C\gamma}* - S_{CA}*$) transitions for compound **39** no peaks could be observed by DSC. The isotropic liquid to S_A and $S_A - S_C*$ transitions were observed however, and the transition temperatures, obtained from the cooling cycle, and enthalpies associated with these transitions are listed in Table 4.6. The melting points were obtained from the heating cycle.

Compound	Transition	Temperature	Enthalpy
39	Iso - S_A	113.0	4.18
	S_A - S_C*	100.1	0.29
	recryst	33.6	1.06
	mp	56.3	20.18

Table 4.6 - Transition Temperatures (°C) and Enthalpies (kJ mol^{-1}) for Compound 39 observed by DSC

The DSC cooling thermogram for compound **39** is shown in Figure 4.23
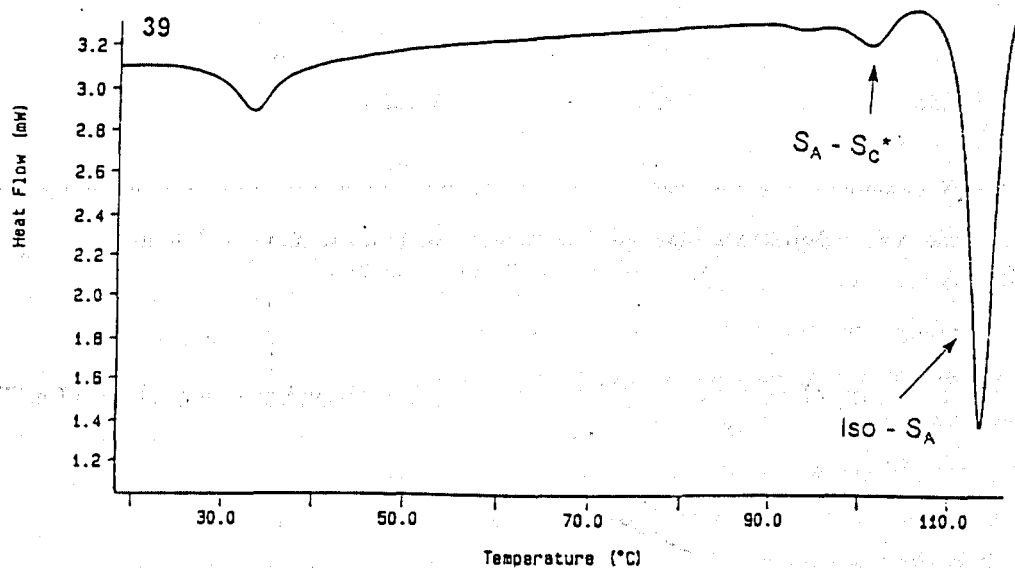
Figure 4.23 - Differential Scanning Calorimetry Thermogram for Compound 39

The DSC measurements on compound **40** showed both the isotropic-to-smectic A and S_A - S_{CAlt} transitions. The temperatures at which these transitions were observed on the cooling cycle, along with the enthalpies associated with these transitions are listed in Table 4.7. The melting point was obtained from the heating cycle.

Compound	Transition	Temperature	Enthalpy
40	Iso - S_A	85.4	1.74
	S_A - S_{CAlt}	77.1	0.16
	recryst	25.5	2.26
	mp	64.4	33.69

Table 4.7 - Transition Temperatures (°C) and Enthalpies (kJ mol^{-1}) for Compound 40 observed by DSC

The DSC heating thermogram for compound 40 is shown in Figure 4.24.
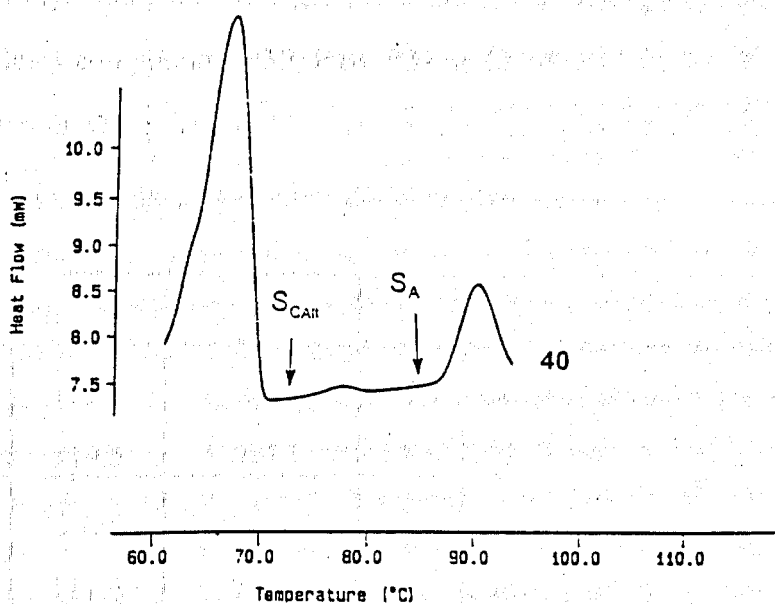
Figure 4.24 - Differential Scanning Calorimetry Thermogram for Compound 40

It can be seen from the DSC thermograms for compounds 39 and 40 that peaks are observed which correspond to the transitions observed by optical microscopy. This data can be used as evidence to confirm the phase behaviour and transition temperatures listed in Table 4.5 for compounds 39 and 40.

4.2.4 Transition Temperatures and Phase Behaviour of Polymeric Materials as Determined by Optical Microscopy

Textural studies were carried out on samples of the side chain liquid crystal poly(acrylate). The samples were prepared using a similar method to that described in section 4.1.4. The sample was then annealed for 12 - 18 hours to allow a texture to develop.

The phase sequence and accompanying transition temperatures, obtained from optical microscopy, the number average molecular weight, the weight average molecular weight, the number average degree of polymerisation and the polydispersity, obtained from gel permeation chromatography (GPC), for the poly(acrylate) compounds **P39**, **P40**, **P31** and **P34** are listed in Table 4.8. The results determined for the transition temperatures and phase behaviour for polymers **P39** and **P40** are displayed as a bar graph in Figure 4.25.

Polymer	Iso - S_A	S_A - $S_{C*/C}$	mp	$\overline{M}n$	$\overline{M}w$	$\overline{X}n$	γ
P39	116.3	98.9	46.4	9640	10980	16	1.14
P40	119.5	100.3	48.6	7130	8280	12	1.16
P31	99.6	84.9	42.4	3900	4750	6	1.22
P34	111.6	78.6	55.9	4640	5430	7	1.17

Table 4.8 - Transition Temperatures (°C) and GPC Data
for Compounds P39, P40, P31 and P34
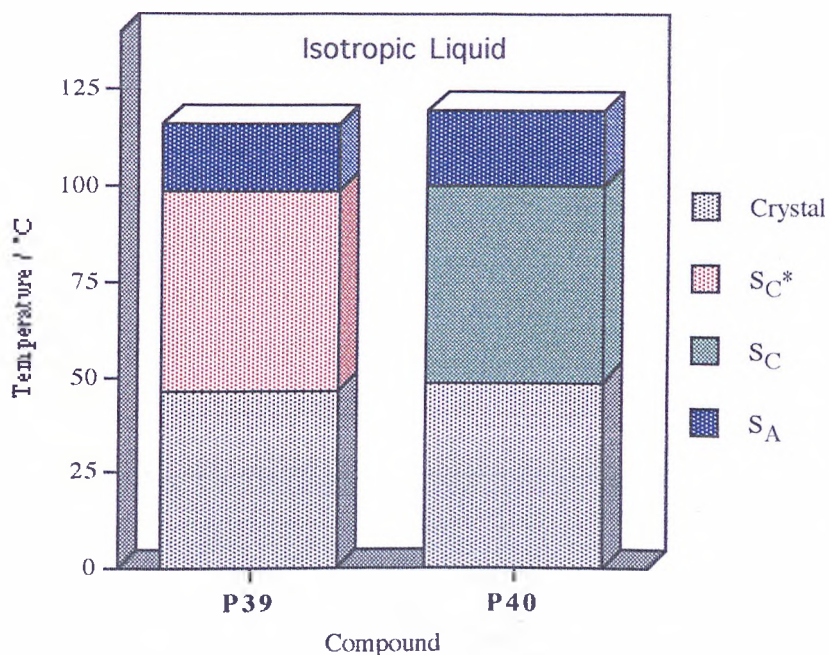
Figure 4.25 - Phase Behaviour of Compounds P39 and P40 by Optical Microscopy

Both of the polymers **P39** and **P40** show the phase sequence Iso $\Leftrightarrow$ S_A $\Leftrightarrow$ S_C (or S_C* when the material is chiral). Photomicrographs obtained for the smectic C phases given by **P39** and **P40** can be seen in Figure 4.26. Both polymeric materials show the focal conic fan texture of the homogeneously aligned S_A phase with the dark region being due to homeotropic alignment. On cooling, however a phase transition is observed when the focal conic fans appear to break and small areas of schlieren texture appear to form in the homeotropic areas

(a) **P39**

(78.3 °C)
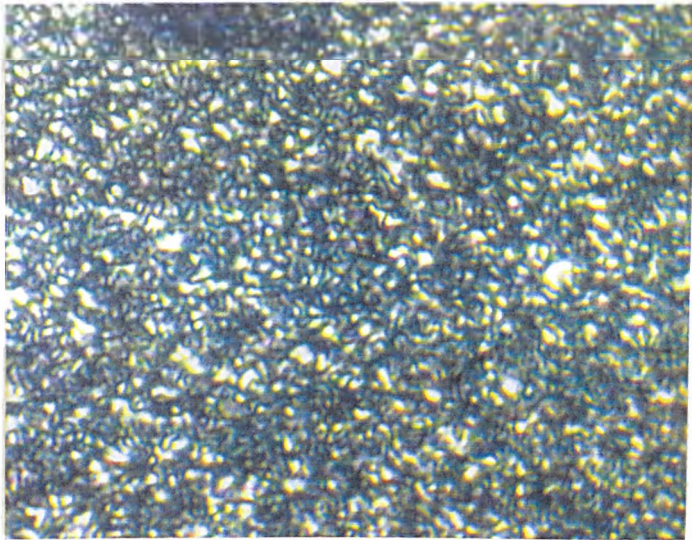
(b) **P40**

(82.2°C)
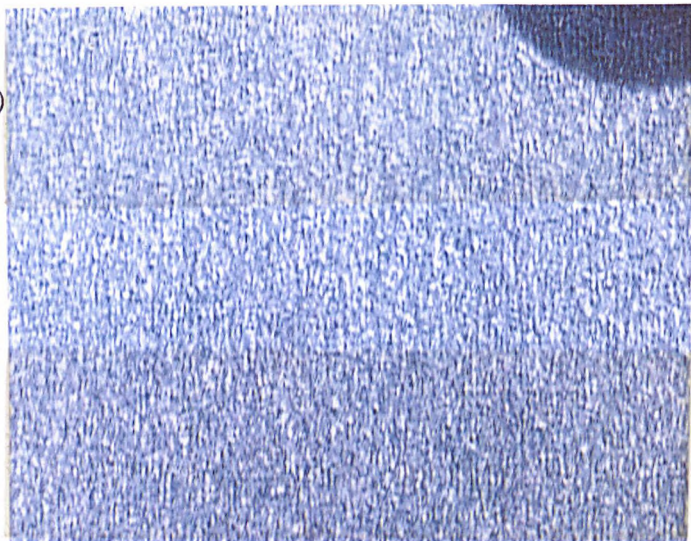
Figure 4.26 - Photomicrographs obtained from Optical Microscopy of Polymers P39 and P40

Comparison of the transition temperatures and phase sequences given in table 4.8 for polymers **P39** and **P40**, with those for polymers **P31** and **P34** allows the effect on the liquid crystal properties of altering the flexible spacer length in a liquid crystal polymer by one carbon unit to be seen. The liquid crystal mesophase has been thermally stabilised with both the isotropization temperature and the S_A - S_C transitions for both materials increasing. Closer examination, by miscibility studies (section 4.2.6), of the S_C phase, obtained in polymers **P39** and **P40** reveals that the structure of the molecules in adjacent layers in the S_C phase are not of alternating tilt. Thus altering the flexible spacer length of the liquid crystal polyacrylates by one unit determines whether a ferroelectric or antiferroelectric phase is obtained. This observation is consistent with those reported by *Sage et al.*[79]

4.2.5 Transition Temperatures and Phase Behaviour of Polymeric Materials Determined by Differential Scanning Calorimetry

Polymers **P39** and **P40** were also examined by DSC. Transition temperatures and the enthalpies associated with these transitions are listed in Table 4.9. DSC thermograms for polymers **P39** and **P40** are shown in Figure 4.27.
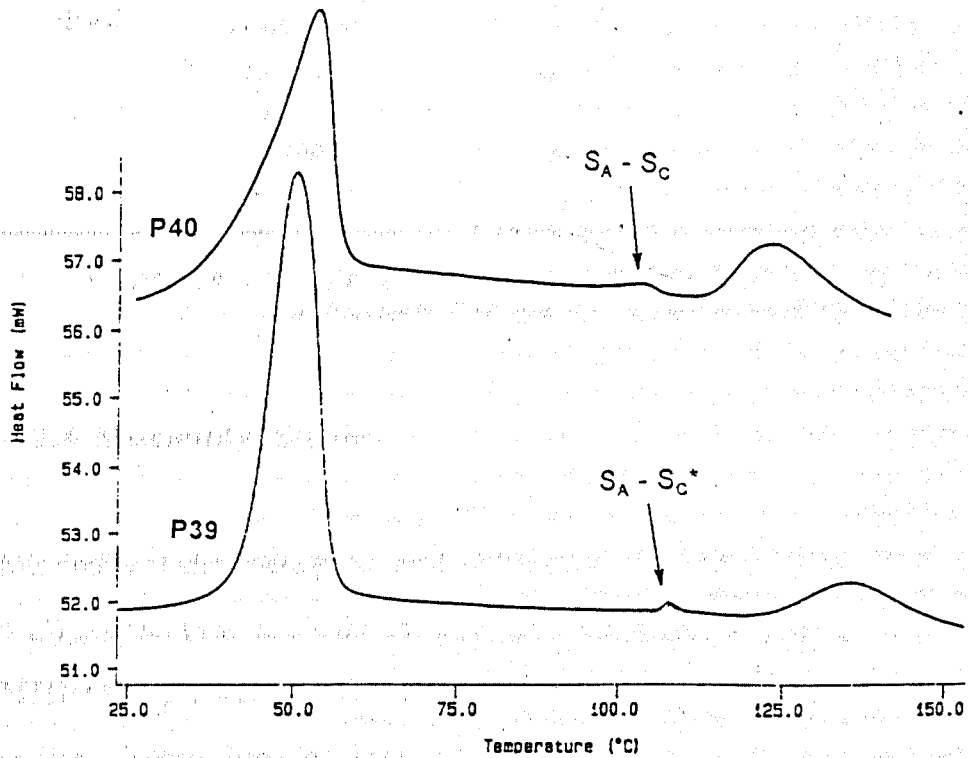
Figure 4.27 - DSC Thermograms for Polymers P39 & P40

Compound	Transition	Temperature	Enthalpy
P39	S_A - Iso	123.7	8.62
	$S_C{}^*$ - S_A	102.6	0.17
	mp	43.0	44.14
	recryst	17.1	15.09
P40	S_A - Iso	118.7	6.75
	S_C - S_A	101.1	0.35
	mp	47.4	23.05
	recryst	15.7	9.31

Table 4.9 - Transition Temperatures (°C) and Enthalpies ($J\ g^{-1}$)
for Polymers P39 and P40 as Determined by DSC

4.2.6 Miscibility Studies

Miscibility studies were performed with a standard compound **MHP11BC** (Figure 4.13) in order to ascertain the exact nature of the smectic C phase obtained. Using **MHP11BC** it was possible to determine whether the smectic C phase was antiferroelectric, ferroelectric or ferrielectric as the unidentified phase would show complete miscibility of the corresponding phase throughout the entire composition range for mixtures of the test polymer and standard material.

Figure 4.28 shows the binary miscibility diagram for mixtures between the standard compound **MHP11BC** and polymer **P39**. The $S_{CA}{}^*$ and $S_{C\gamma}{}^*$ phases were found to disappear once the composition of the binary mixture reached approximately 25 and 20 weight percent polymer respectively. The S_A and $S_C{}^*$ phases were found to show complete miscibility throughout the entire composition range indicating that these phases were present in the standard material and the test polymer.
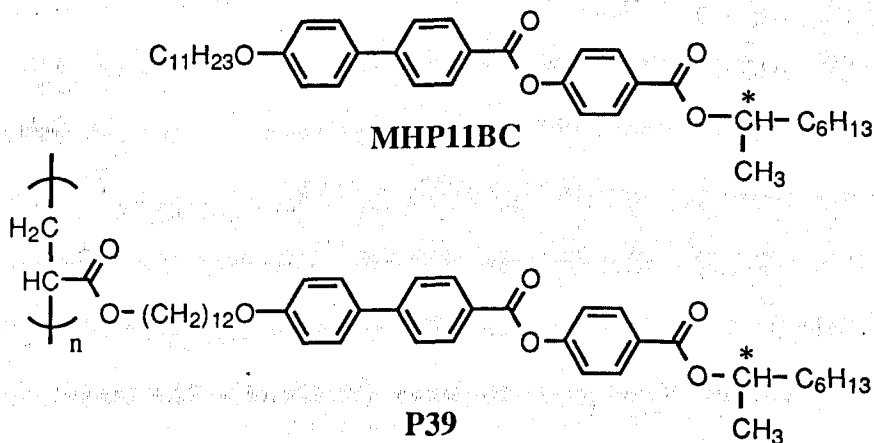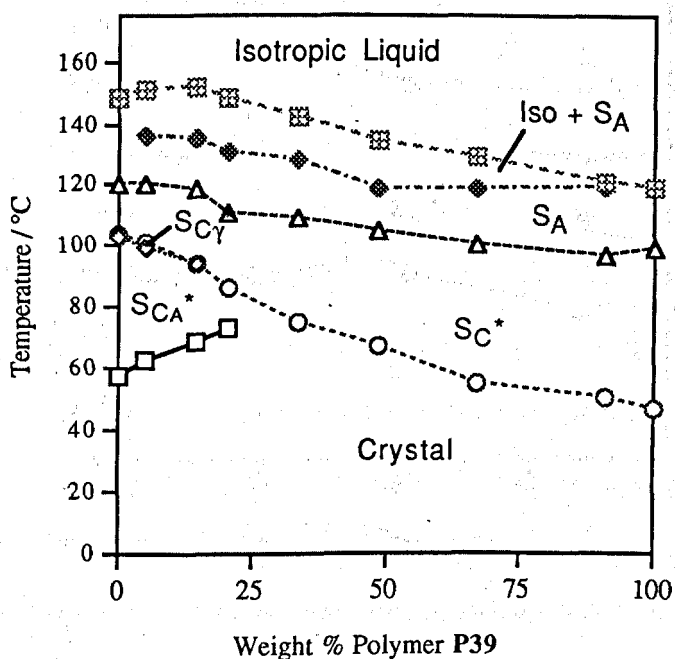
Figure 4.28 - Miscibility Phase Diagram for Polymer P39
and the Standard Compound MHP11BC

Figure 4.29 shows the binary miscibility diagram between the standard material
MHP11BC and the polymer **P40**. The S_A and S_C phases were found to show
complete miscibility throughout the entire composition range. The $S_{C\gamma}^*$ and S_{CAlt}
phases of the standard material and the polymer respectively were found to exist
until the composition of the binary mixture approached 15 and 45 weight percent
polymer respectively.
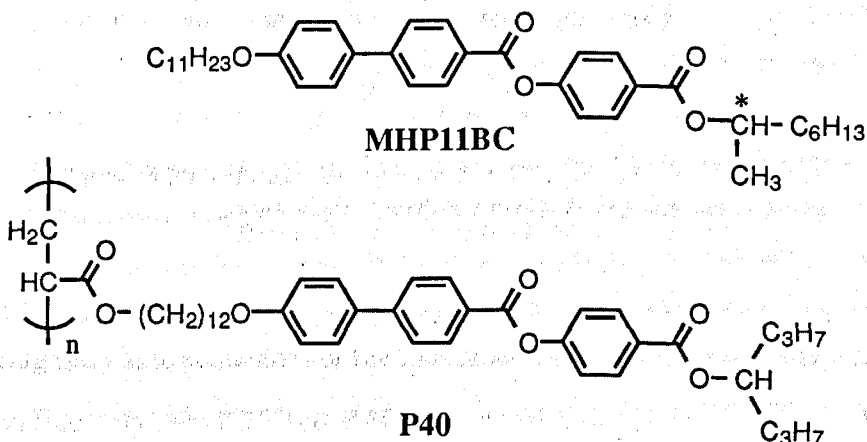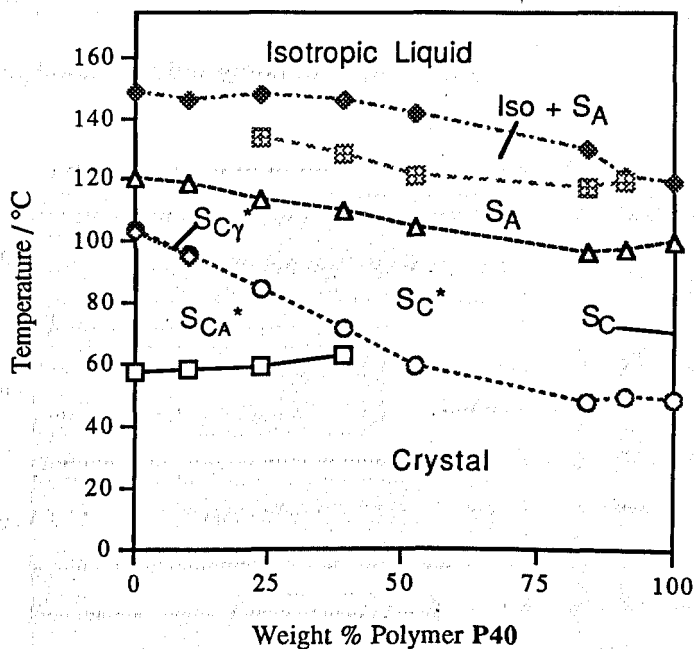
Figure 4.29 - Miscibility Phase Diagram for Polymer P40
and the Standard Compound MHP11BC

4.2.7 Effect of Polymerisation on the Liquid Crystal Properties

Examination of the transition temperatures and phase sequences listed in Table 4.5

for compounds **39** and **40** and comparison with the values listed in Table 4.8 for

the polymers **P39** and **P40** shows that polymerisation stabilises the liquid crystal

mesophase with the isotropization temperature and melting points being raised. The

values listed for compounds **39** and **40**, and their corresponding polymers **P39** and **P40** are displayed in a bar graph in Figure 4.30.
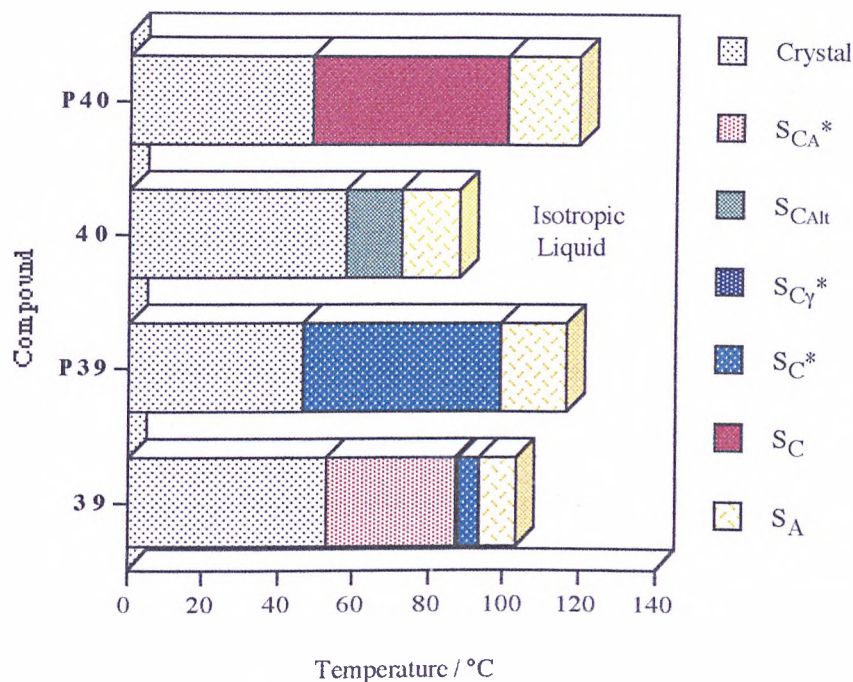
Figure 4.30 - Phase Behaviour for Compounds 39 and 40, and their Corresponding Polymers as Determined by Optical Microscopy

Comparing the phase sequences of the monomeric materials **39** and **40**, and their corresponding polymers **P39** and **P40** then, as with the compounds **31 - 33** and their corresponding polymers, the ferrielectric phase disappears in the polymeric materials. However, unlike the situation for compounds **31 - 33** and their corresponding polymers, the ferroelectric phase remains and the antiferroelectric phase disappears.

4.3   THE EFFECT OF CHANGE OF POLYMER BACKBONE ON THE LIQUID CRYSTAL PROPERTIES OF SOME SIDE CHAIN LIQUID CRYSTAL POLYMERS

4.3.1 Introduction

Previous liquid crystal polymers reported in this thesis have been based upon a poly(acrylate) polymer backbone. The effect of changing the polymer backbone is now investigated by altering the low molar mass molecule on which the polymer is based from an acrylate moiety to one based on allyl alcohol (see Figure 4.31). This change in molecular structure was made in order to ascertain whether the ester linking group used in a poly(acrylate) system has a marked effect upon the liquid crystal properties of a mesogenic acrylate polymer.

55, P55 ; R = (R)-1-methylheptyl
56, P56 ; R = 1-propylbutyl
57, P57 ; R = (R)-2-methylbutyl
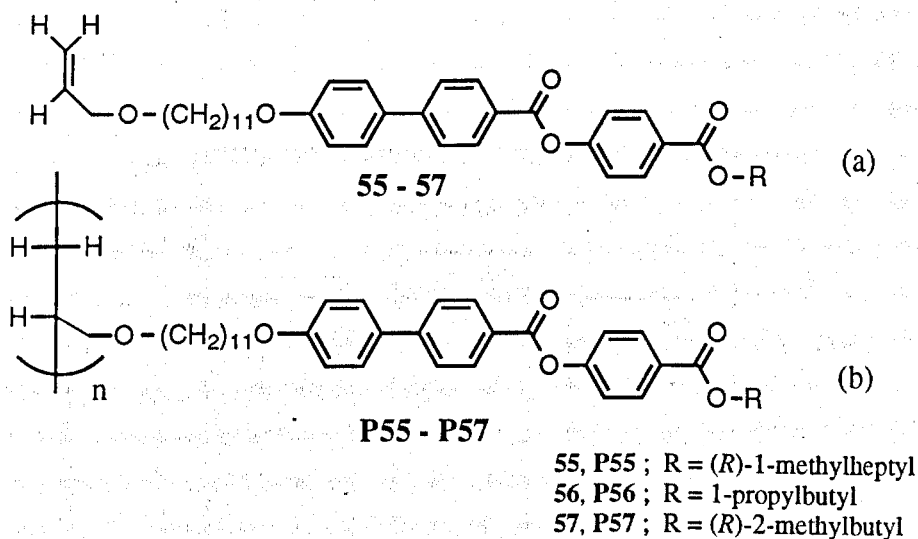
Figure 4.31 - Liquid Crystal Polymers and Monomers Studied to Examine the Effect of Change of Polymer Backbone

4.3.2 Transition Temperatures and Phase Behaviour of Monomeric Materials by Optical Microscopy

The phase sequences and accompanying transition temperatures for the monomeric compounds **55 - 57** as determined by optical microscopy, are listed in Table 4.10. The results are presented as a bar graph in Figure 4.32. .

Cmpd	Iso - S_A	S_A - S_{CA}^*	S_A - S_{CAlt}	mp	Recryst[‡]
55	106.8	65.9	-	41.9	4.5
56	113.2	-	71.6	42.2	-3.6
57	94.6	52.7	-	44.6	12.2

[‡] Obtained by DSC

Table 4.10 - Transition Temperatures (°C) and Phase Behaviour for Compounds 55 - 57 as Determined by Optical Microscopy
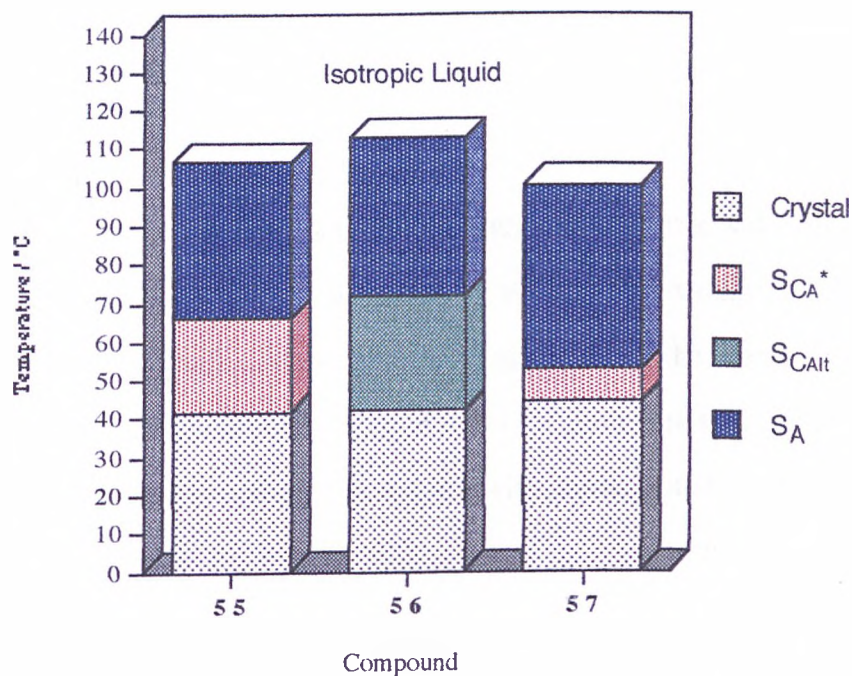
Figure 4.32 - Phase Behaviour for Compounds 55 - 57 as Determined by Optical Microscopy

It is well known for polymeric systems that changing the method of attachment of a lateral substituent onto a polymer backbone has an effect on the physical properties of the resulting polymer system.[92] If we consider the situation for the polymers poly(methyl acrylate) (PMA) [Figure 4.33(a)], poly(vinyl acetate) (PVA) [Figure 4.33(b)] and poly(but-1-ene) [Figure 4.33(c)] then it can be seen that by replacing the direct linkage used in poly(but-1-ene) by an ester group (PMA) increases the glass transition temperature. In addition, reversing the ester group used in PMA to attach the lateral methyl substituent to give the arrangement as in PVA, then the glass transition temperature is further raised to 301 K.

(a)　　　　(b)　　　　(c)

Tg = 276 K　　　Tg = 301 K　　　Tg = 233 K
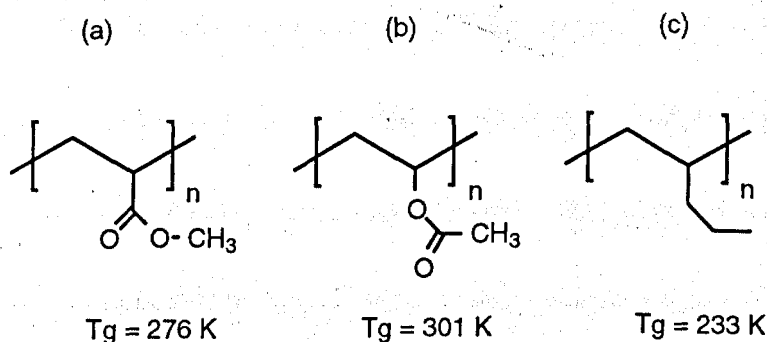
Figure 4.33 - Structures and Glass Transition Temperatures of Poly(methyl acrylate), Poly(vinyl acetate) and Poly(but-1-ene)[92]

Therefore, by altering the method of attaching a mesogenic side chain to the polymerisable unit in a side chain liquid crystal monomer we would expect to affect the liquid crystal properties of the material. This effect can be seen by examining the phase sequences and transition temperatures for compounds 55 and 56 listed in Table 4.10 and by comparing the values with those listed in Table 4.1 for compounds 31 and 34.

Looking initially at the phase sequences for the optically active materials 31 and 55, shows that by changing the linking function from the polymerisable moiety to the flexible spacer, from an ester to an ether group, that the S_C^* and $S_{C\gamma}^*$ phases have been eliminated from the phase sequence and a direct S_A - S_{CA}^* transition has

been induced; the phase sequence of the achiral materials **34** and **56** are the same. If we examine Figures 4.2 and 4.32, which show the phase sequences for compounds **31 - 34** and **55 - 57** respectively, then we see that by introducing an ether link into the molecule not only have the isotropization temperatures and the melting points of the molecules been increased and the thermal stability of the liquid crystal phase increased, but the temperature range over which the $S_{CA}{}^{*}$ phase occurs has also increased.

The textures obtained for the phases exhibited by compounds **55** and **56** are shown in Figures 4.34 and 4.35 respectively.

(a) S_A

(104.3 °C)

(b) $S_{CA}*$

(53.9 °C)
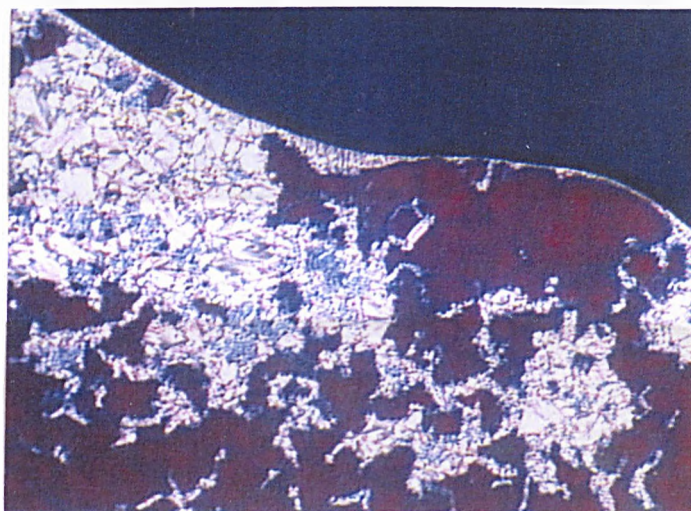
Figure 4.34 - Photomicrographs of the Textures Obtained for the Phases
Exhibited by Compound 55

(a) S_A

(92.1 °C)

(b) S_{CAlt}

(59.8 °C)

Figure 4.35 - Photomicrographs of the Textures Obtained for the Phases
Exhibited by Compound 56

4.3.3 Transition Temperatures and Phase Behaviour of the Monomeric Materials as Determined by Differential Scanning Calorimetry

Compounds **55 - 57** were examined by DSC using the apparatus outlined in section 3.1.2(b). All DSC measurements were performed at a rate of 10 °C min^{-1} unless otherwise stated.

Table 4.11 lists the transition temperatures, and the enthalpies associated with these transitions, observed on examination by DSC.

Compound	Transition	Temperature	Enthalpy
55	Iso - S_A	102.8	4.27
	S_A - S_{CA}*	60.2	0.21
	mp	39.9	14.46
56	Iso - S_A	111.7	3.66
	S_A - S_{CAlt}	67.4	0.39
	mp	44.5	17.73
57	Iso - S_A	93.1	4.69
	S_A - S_{CA}*	50.3	0.25
	mp	47.8	22.42

Table 4.11 - Transition Temperatures (°C) and Enthalpies (kJ mol^{-1}) for Compounds 55 - 57 as Observed by DSC

The DSC cooling thermograms for compounds **55 - 57** are shown in Figure 4.36.
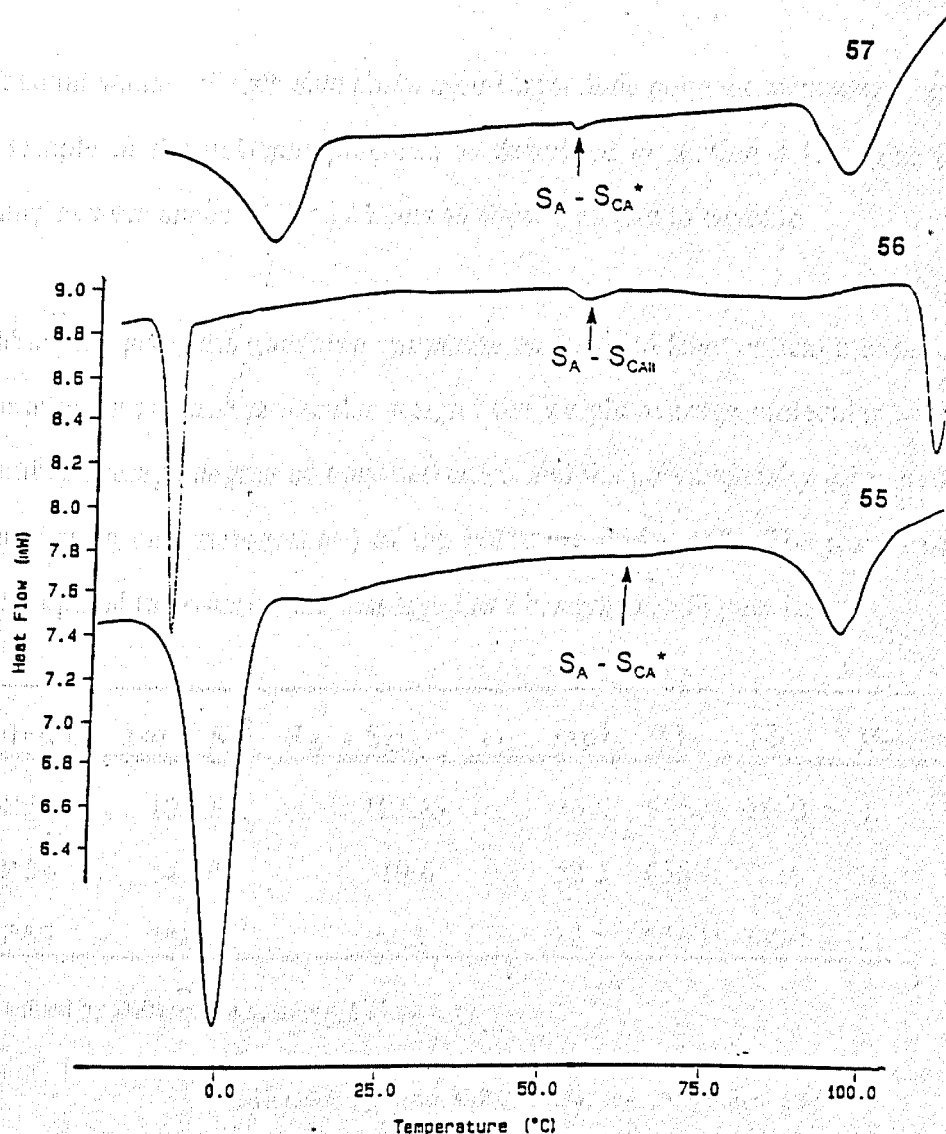
Figure 4.36 - DSC Cooling Thermograms Obtained for Compounds 55 - 57

By examining Table 4.11 and Figure 4.36 it can be seen that the transition temperatures and phase behaviour observed by optical microscopy are confirmed by DSC measurements. For example, if we examine the DSC thermogram for compound 55 we can see peaks at 102.8, 60.2 and 39.9 °C which correspond to the transitions observed by optical microscopy (Table 4.10) for the Iso - S_A, S_A - S_{CA}^* transitions and the melting point of the compound.

4.3.4 Transition Temperatures and Phase Behaviour of Polymeric Materials as Determined by Optical Microscopy

Textural studies of each side chain liquid crystalline polymer were carried out using a sample of the polymer prepared as described in section 4.1.4. The polymer samples were annealed for 12 hours to allow a texture to develop.

Table 4.12 gives the transition temperatures obtained from optical microscopy and the number average molecular weight, the weight average molecular weight, the number average degree of polymerisation and the polydispersity (obtained by gel permeation chromatography) of the polymers P55 - P57. The results obtained from optical microscopy are displayed as a bar graph in Figure 4.37.

Polymer	Iso - S_A	S_A - $S_{CA}*$ / $_{Alt}$	mp[‡]	$\overline{M}n$	$\overline{M}w$	$\overline{X}n$	γ
P55	124.5	105.8	36.6	5060	9560	8	1.90
P56	142.4	119.6	52.2	6360	7210	10	1.13
P57	99.6	74.3	32.5	6580	7490	11	1.14

[‡]Obtained by Differential Scanning Calorimetry

Table 4.12 - Transition Temperatures (°C) Determined by Optical Microscopy and GPC Data for Polymers P55 - P57
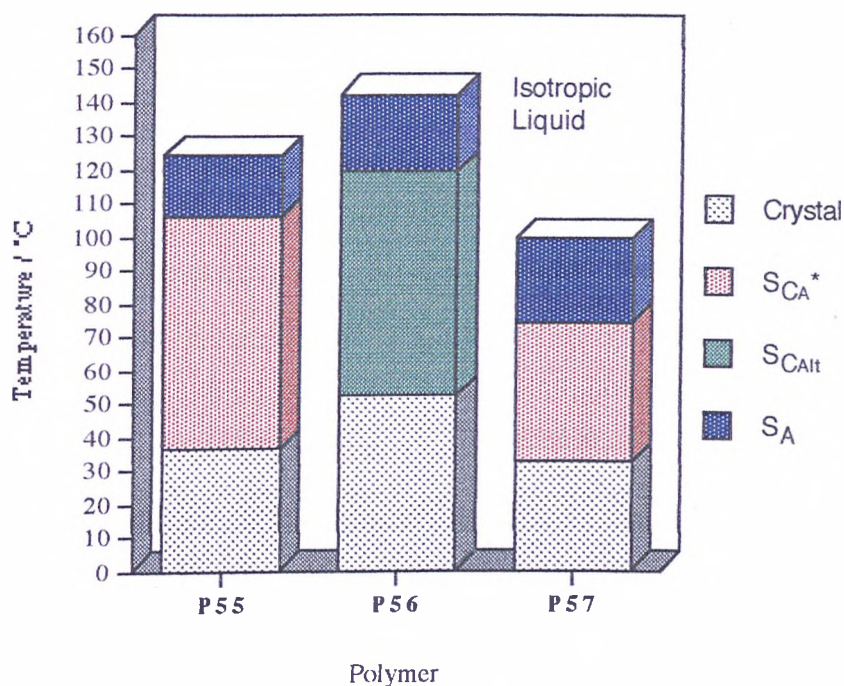
Figure 4.37 - Transition Temperatures (°C) and Phase Behaviour for Polymers P55 - P57 Determined by Optical Microscopy

The polymers **P55** - **P57** each show the phase sequence Iso $\Leftrightarrow$ S_A $\Leftrightarrow$ S_{CA}* (or S_{CAlt} when the material is achiral). Figures 4.38 and 4.39 show the textures obtained during the optical microscopy of compound **P55** and **P56** respectively. Each of the polymers show the characteristic fan texture associated with the homogeneous alignment of the smectic A phase [*e.g.*, see Figure 4.38 (a)] on cooling from the isotropic liquid state. This texture remains until the smectic A to smectic C transition whereupon the fans appear to break and the previously black homeotropic areas fill in with small areas of schlieren texture [*e.g.*, Figure 4.38 (b)].

Comparing the values listed in Table 4.12 for polymers **P55** and **P56**, and shown graphically in Figure 4.37, to the values listed in Table 4.3 for **P31** and **P34**, the effect of changing the linking moiety on the liquid crystal properties can be seen.

By replacing the ester group as the linkage to the flexible spacer in compounds **P31** and **P34**, with an ether group, then the ability of the polymer to form a smectic phase where the tilt direction of the molecules in adjacent layers alternates is not affected. However, as the change in structure has taken place close to the polymer backbone, then the transition temperatures in the phase sequence Iso $\Leftrightarrow$ S_A $\Leftrightarrow$ $S_{CA}*$ (or S_{CAlt}) have been affected and this can be clearly seen by comparing Figure 4.37 with Figure 4.9.

The melting points of polymers **P55** and **P56**, in comparison with those for polymers **P31** and **P34**, have remained at similar, if slightly lower, temperatures. However, if we look at the isotropization temperatures then an increase in the thermal stability of the materials is observed; that is, the liquid crystallinity of the polymers has increased. Similarly if we examine the $S_{CA}*$ (or S_{CAlt}) - S_A transition temperatures then it can be seen that the antiferroelectric phase has been thermally stabilised and occurs over a wider temperature range.

(a) S_A

(122.6 °C)
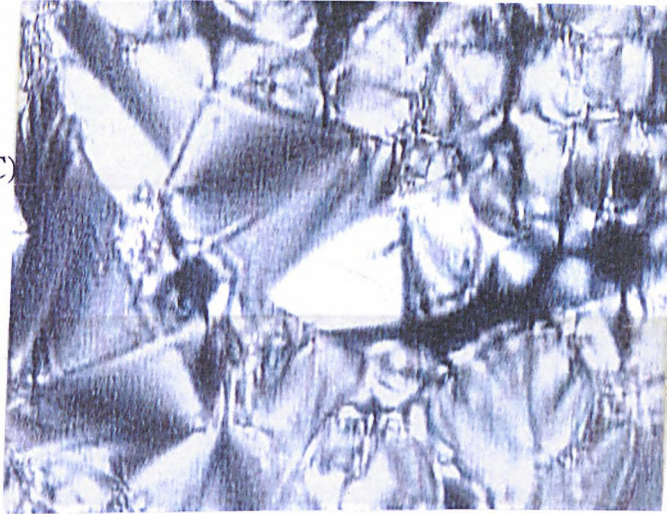
(b) $S_{CA}{}^*$

(99.6 °C)
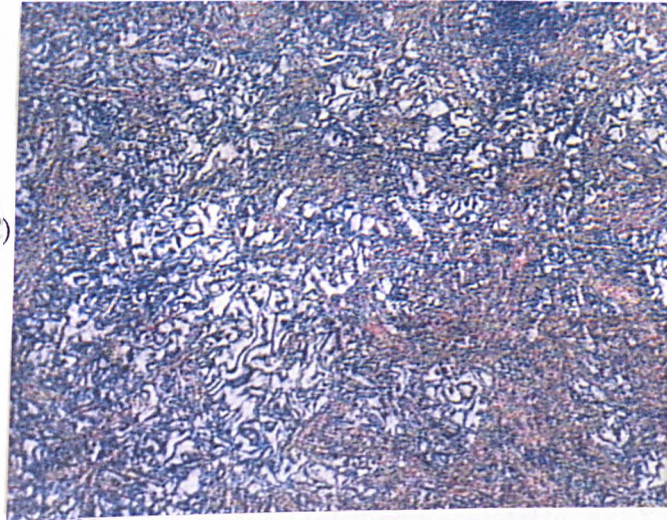
Figure 4.38 - Photomicrographs of the Textures Obtained for the Phases exhibited by Polymer P55

(a) S_A

(139.1 °C)

(b) S_{CAlt}

(106.8 °C)
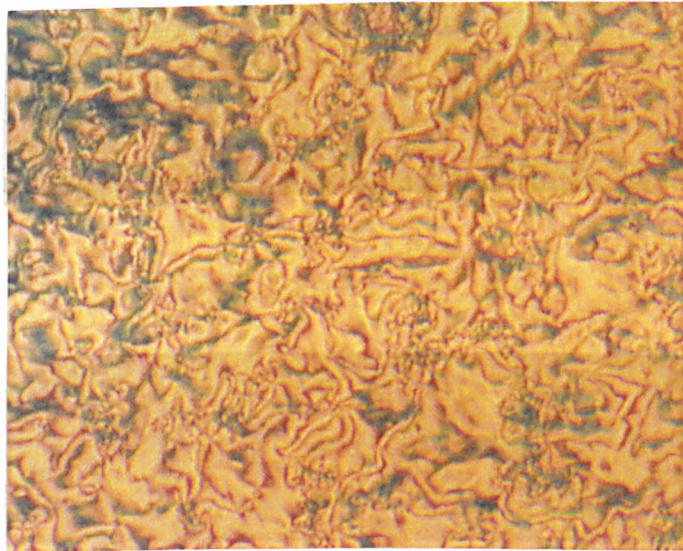
Figure 4.39 - Photomicrographs of the Textures Obtained for the Phases exhibited by Polymer P56

4.3.5 Transition Temperatures and Phase Behaviour of Polymeric Materials as Determined by Differential Scanning Calorimetry

Polymers **P55** - **P57** were also examined by DSC. The transition temperatures and enthalpies associated with these transitions are given in Table 4.13.

Polymer	Transition	Temperature	Enthalpy
P55	Iso - S_A	127.7	4.53
	S_A - S_{CA}*	107.3	0.18
	mp	36.6	13.39
P56	Iso - S_A	146.0	13.57
	S_A - S_{CAlt}	123.3	0.27
	mp	52.2	20.93
P57	Iso - S_A	105.0	2.98
	S_A - S_{CA}*	79.0	0.74
	mp	34.5	4.29

Table 4.13 - Transition Temperatures (°C) and Enthalpies ($J\ g^{-1}$) for Polymers P55 - P57

The DSC thermograms for polymers **P55** - **P57** are shown in Figure 4.40.
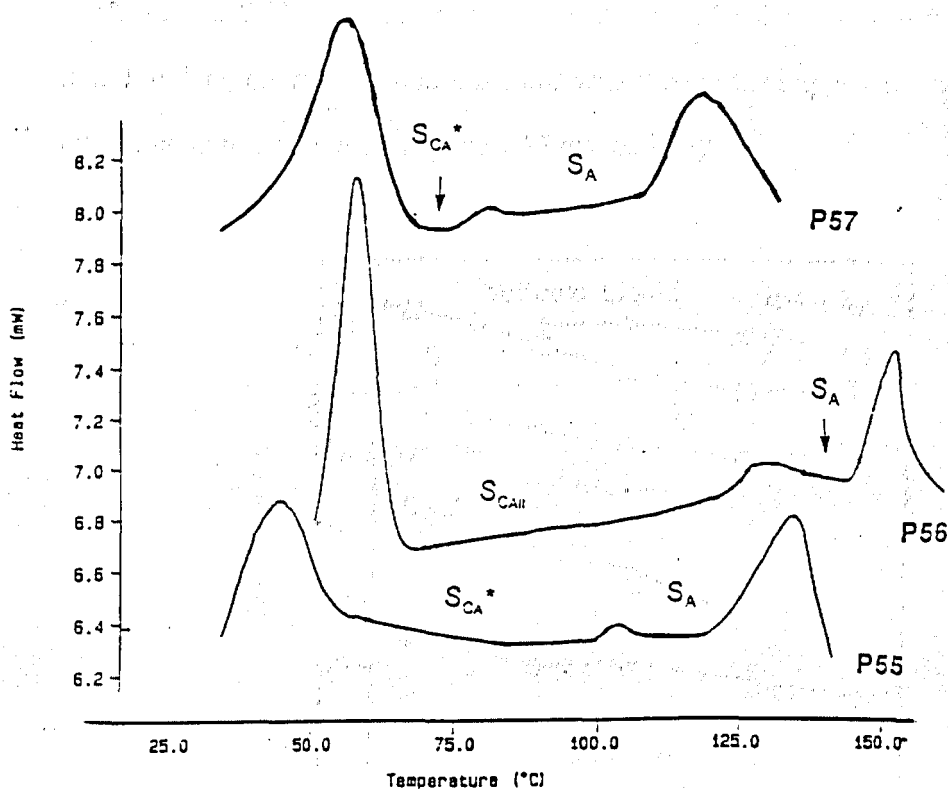
Figure 4.40 - DSC Thermograms for Polymers P55 - P57

4.3.6 Miscibility Studies

In order to confirm that the antiferroelectric phases found in polymers **P55 - P57** were of the same nature as those reported for low molar mass liquid crystals, a miscibility test was carried out with the polymer and a standard low molar mass liquid crystal. Such miscibility studies have been reported for mixtures of side chain liquid crystal polymers and low molar mass materials.[91] The standard material used was **MHP11BC** (see section 4.1.6). The structure and transitions for this compound are shown in Figure 4.13.

Figure 4.41 shows the binary miscibility diagram for the test polymer **P55** and the standard material **MHP11BC**. The S_A and $S_{CA}*$ phases are shown to exist throughout the entire composition range, therefore indicating that the

antiferroelectric phases exhibited by the standard compound **MHP11BC** and the test material **P55** were of the same structure. The $S_{C\gamma}*$ and S_C* phases were found to disappear above compositions which contained approximately 10 and 30 weight percent of the test polymer **P55** respectively.
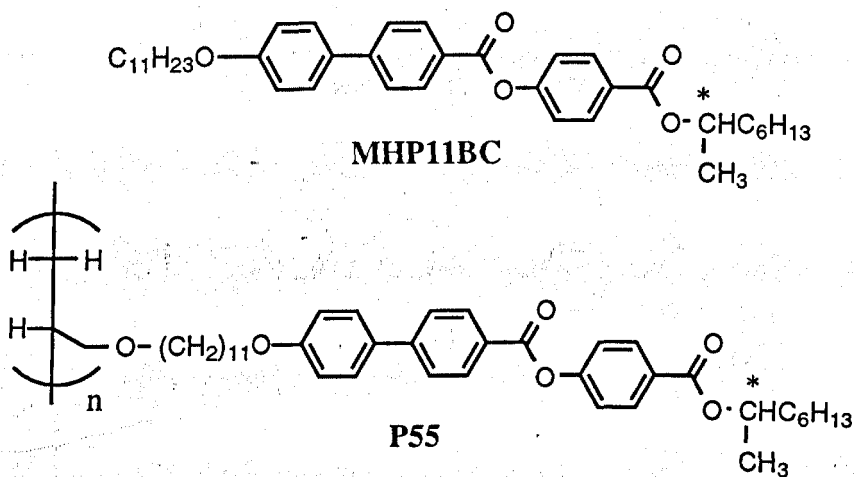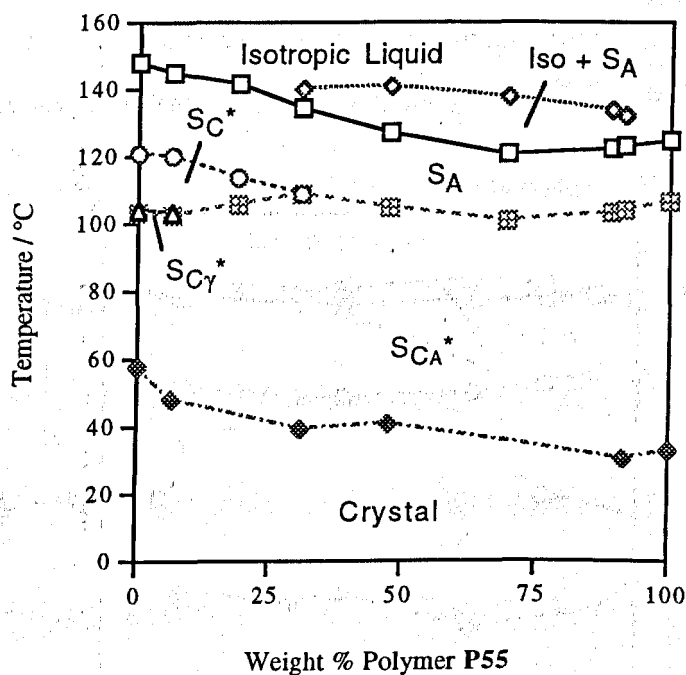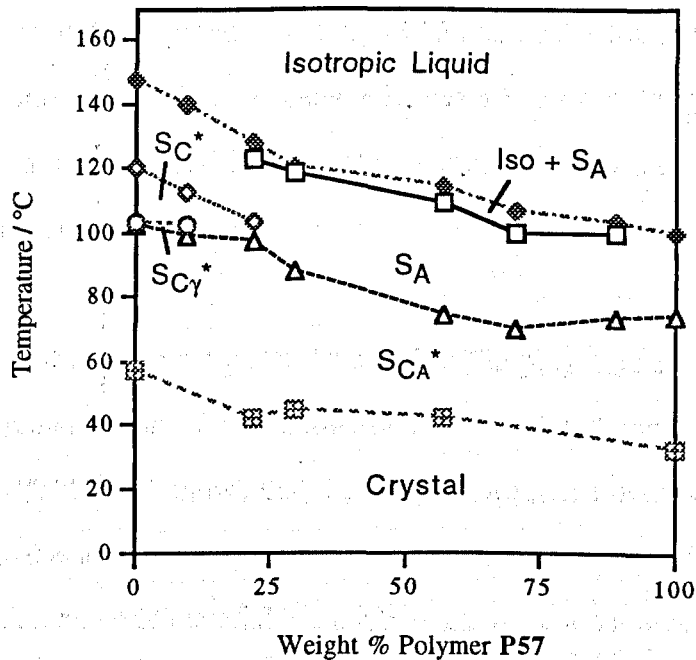

Figure 4.41 - Miscibility Phase Diagram for Polymer P55 and the Standard Compound MHP11BC

The binary miscibility diagram for the mixtures prepared containing the test polymer **P56** and the standard material **MHP11BC** is given in Figure 4.42. It can be seen

from this Figure that the S_A and S_{CA}^* phases show complete miscibility throughout the entire composition range indicating that again the phases obtained in the polymer **P56** are structurally the same as in the standard material. The S_C^* phase disappears at compositions above approximately 35 weight percent polymer. The $S_{C\gamma}^*$ phase does not appear at compositions above approximately 15 weight percent polymer. As no mixtures below this composition were made then its existence in mixtures of lower weight percent polymer cannot be discounted.

Weight % Polymer P56

MHP11BC

P56
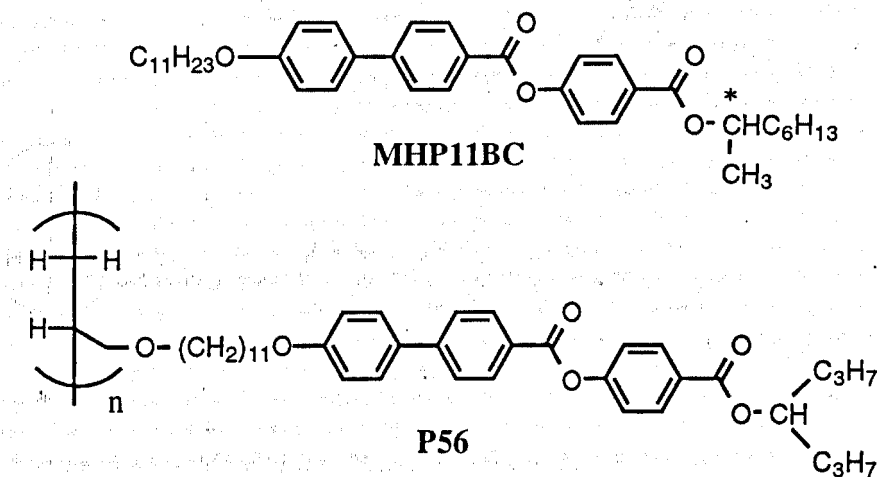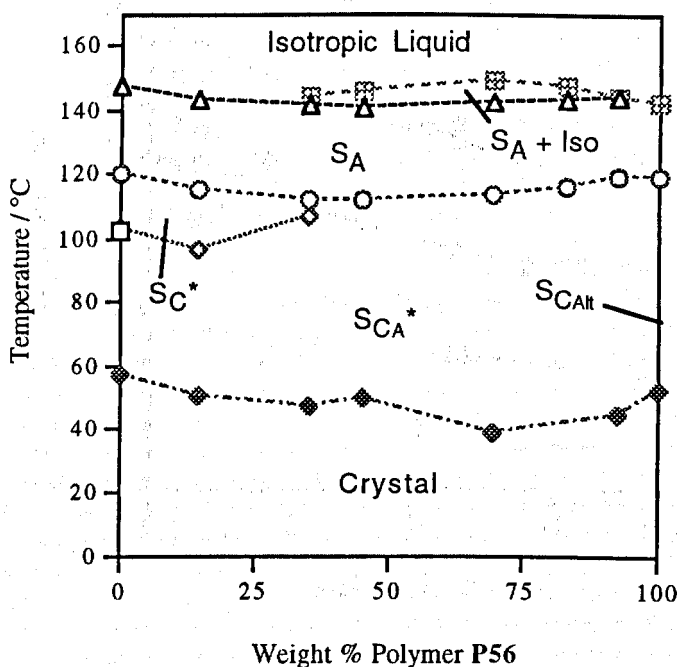
Figure 4.42 - Miscibility Phase Diagram for Polymer P56 and the Standard Compound MHP11BC

Figure 4.43 shows the binary miscibility diagram between the test polymer **P57** and the standard material **MHP11BC**. The $S_{C\gamma}*$ and S_C* phases were found to disappear above approximately 15 and 30 weight percent polymer respectively. The S_A and $S_{CA}*$ phases were found to exist throughout the entire composition range.
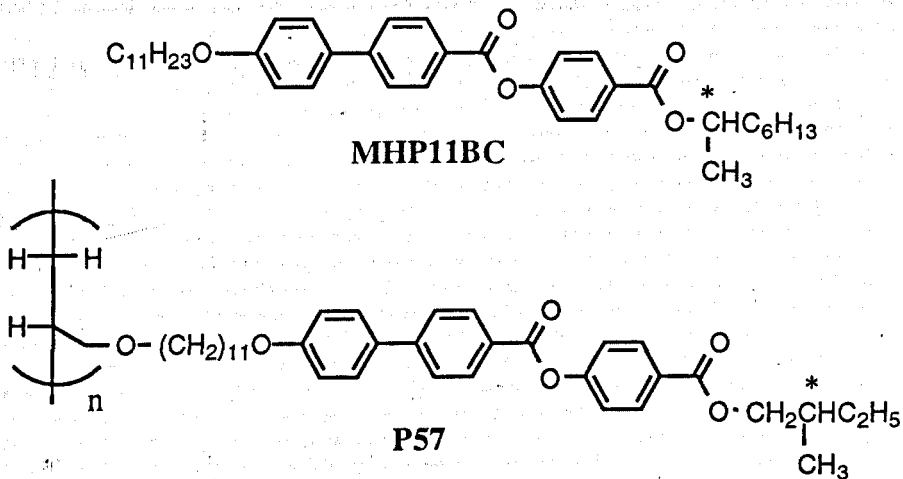
Figure 4.43 - Miscibility Phase Diagram for Polymer P57 and the Standard Compound MHP11BC

4.3.7 Effect of Polymerisation on the Liquid Crystal Properties

Examining the transition temperatures listed in Table 4.10 for the monomeric materials **55 - 57**, and comparing them with the values listed in Table 4.12 for the polymers **P55 - P57** then an unusual effect is observed. Unlike the previously reported monomeric materials **31 - 34, 39** and **40**, and their corresponding polymers where polymerisation thermally stabilises the liquid crystal mesophase, the melting point of the polymeric materials **P55** and **P57** is lower than that of the corresponding monomer. The polymer **P56** has a higher melting point than its corresponding monomer. The isotropization temperatures of all of the polymers **P55 - P57** has increased.

The resulting antiferroelectric phase obtained in the polymers **P55 - P57** is also affected by polymerisation. Examination of Table 4.12 and comparison with the values listed in Table 4.11 shows that the temperature range over which the S_{CA}^* (or S_{CAlt} when the material is achiral) phase occurs has increased. The phase sequence of the monomeric material has not been altered upon polymerisation.

The phase sequence for compounds **55 - 57** and their corresponding polymers **P55 - P57** is shown as a bar graph in Figure 4.44.
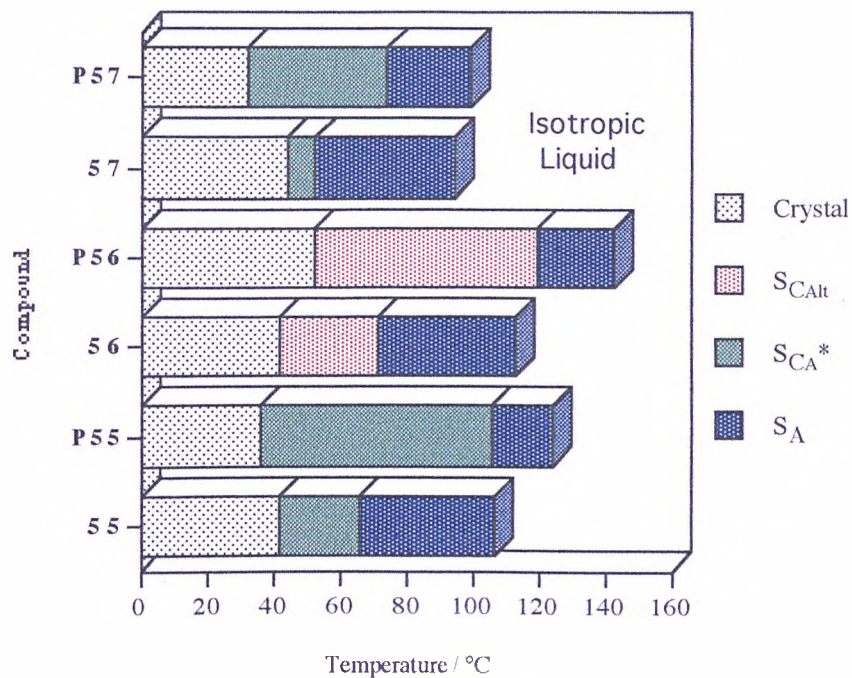
Figure 4.44 - Phase Behaviour for Compounds 55 - 57 and their
Corresponding Polymers P55 - P57

4.4 THE EFFECT OF ALTERING THE POLYMER BACKBONE SUBSTITUENT ON THE LIQUID CRYSTAL PROPERTIES OF SOME SIDE CHAIN LIQUID CRYSTAL POLYMERS

4.4.1 Introduction

It has previously been reported in this thesis (section 4.3.1) that the physical properties of polymers can be affected by molecular engineering changes in the polymer structure,[92] *i.e.* tacticity, backbone substituent and lateral substituent.

If we consider simple polymer systems based on acrylates and methacrylates then we see that altering the backbone substituent has an effect on the physical properties of the polymer material and this is illustrated by the data given in Figure 4.45.

Tg = 388 K   Tg = 276 K
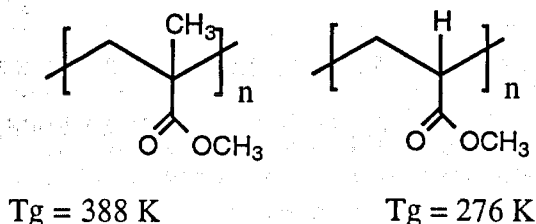
Figure 4.45 - Glass Transition Temperatures for Poly(methyl methacrylate) and Poly(methyl acrylate)[92]

In this section the backbone substituent of the polymer has been altered and a series of liquid crystal monomers [Figure 4.46(a)] has been synthesised based upon α-(hydroxymethyl)acrylonitrile along with the corresponding polymers [Figure 4.46(b)]. The physical properties of the monomers and polymers are compared with those of the monomers (compounds **55 - 57**) and polymers (**P55 - P57**) reported in section 4.3.

66, P66 ; R = (R)-1-methylheptyl
67, P67 ; R = 1-propylbutyl
68, P68 ; R = (R)-2-methylbutyl
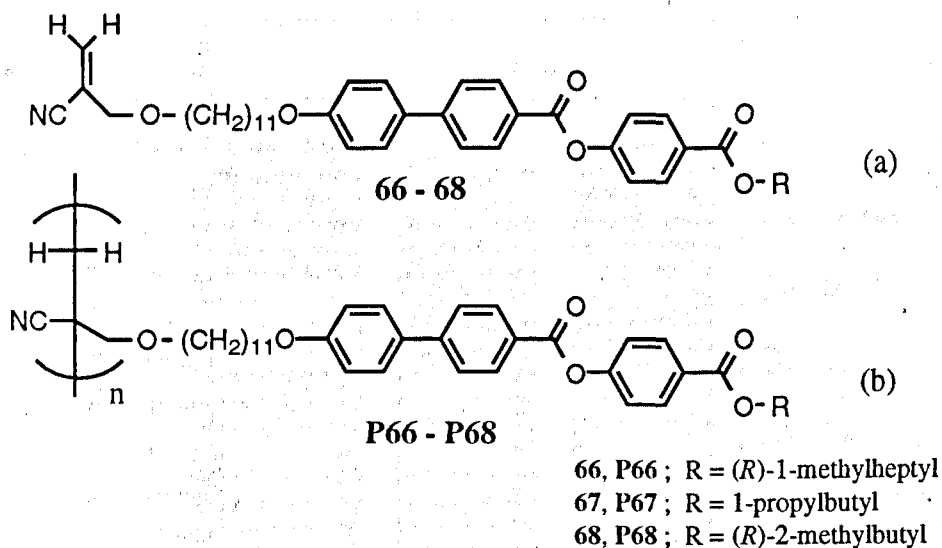
Figure 4.46 - Liquid Crystal Monomers and Polymers Prepared to Study the Effect of Changing the Backbone Substituent

4.4.2 Transition Temperatures and Phase Behaviour of Monomeric Materials as Determined by Optical Microscopy

The phase sequences and transition temperatures for the monomeric compounds **66** - **68** are listed in Table 4.14. The results are presented as a bar graph in Figure 4.47.

Cmpd	Iso - S_A	S_A - S_{CA}*	S_A - S_{CAlt}	mp	Recryst[‡]
66	108.8	71.1	-	47.9	20.61
67	93.6	-	58.6	52.4	23.50
68	96.6	55.4	-	50.2	16.66

[‡]Obtained by Differential Scanning Calorimetry

Table 4.14 - Transition Temperatures (°C) for Compounds 66 - 68 as Determined by Optical Microscopy
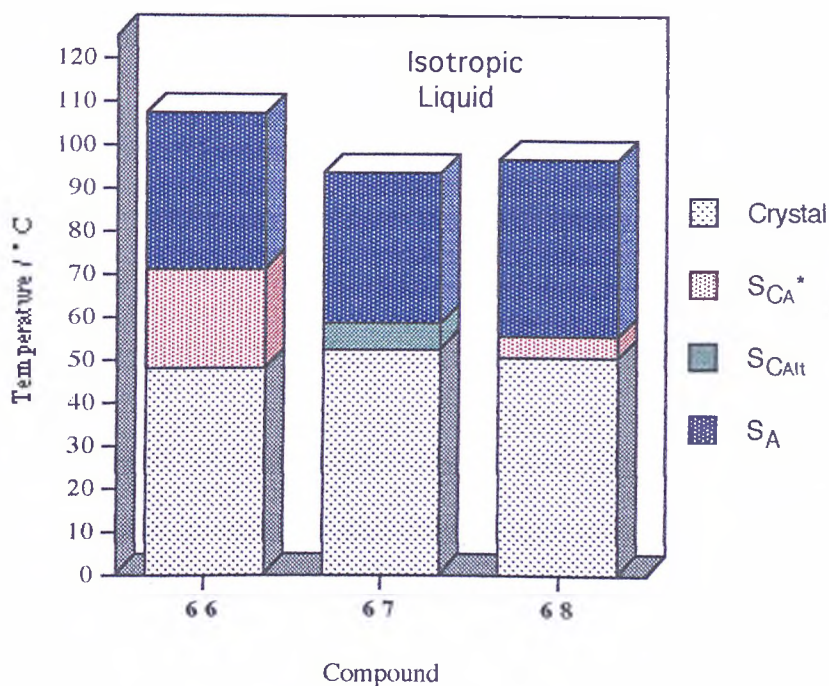
Figure 4.47 - Transition Temperatures (°C) and Phase Behaviour for Compounds 66 - 68 as Determined by Optical Microscopy

Photomicrographs of the textures exhibited in the phases shown by compound **66** are shown in Figure 4.48. A photomicrograph of the texture of the S_{CAlt} phase exhibited by compound **67** is shown in Figure 4.49.

It can be seen by examining the values listed in Table 4.14 for compounds **66 - 68** that all of the compounds exhibit the same phase sequence reported for compounds **55 - 57**, namely Iso $\Leftrightarrow$ S_A $\Leftrightarrow$ S_{CA}* (or S_{CAlt}) $\Leftrightarrow$ Crystal. Comparing these values to those listed in Table 4.10 for compounds **55 - 57** then the effect of increasing the size and polarity of the backbone substituent on the liquid crystal properties can be seen.

In all of the cases reported the melting point of the material has increased by inserting a cyano substituent. Examining the values given for the isotropization temperatures for the chiral compounds **55, 57** and comparing them to those for compounds **66** and **68** shows that the isotropization temperatures increases when

increases when the backbone substituent is a cyano group. However, when we examine the values given for the achiral compounds **56** and **67** then the isotropization temperature decreases. From these data it can be concluded that altering the 'backbone' substituent has no significant effect on the liquid crystal properties for the monomeric materials.

(a) S_A

(96.4 °C)

(b) $S_{CA}*$

(59.2 °C)
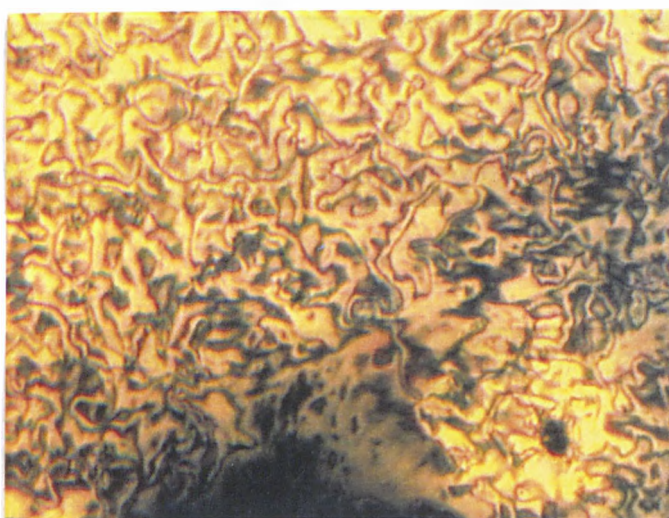
Figure 4.48 - Photomicrographs of the Textures Obtained for the Phases Exhibited by Compound 66

Figure 4.49 - Photomicrograph of the Texture Exhibited by the S_{CAlt} Phase Exhibited by Compound 67 at 56.8 °C

4.4.3 Transition Temperatures and Phase Behaviour of the Monomeric Materials as Determined by Differential Scanning Calorimetry

DSC was also used to determine the phase sequences and transition temperatures for compounds **66 - 68**. The liquid crystal transitions observed, and the enthalpies associated with these transitions, are listed in Table 4.15.

Compound	Transition	Temperature	Enthalpy
66	Iso - S_A	110.2	3.49
	S_A - S_{CA}^*	77.7	0.35
	mp	50.6	24.79
67	Iso - S_A	96.2	5.11
	S_A - S_{CAlt}	60.1	0.51
	mp	55.3	27.66
68	Iso - S_A	97.7	6.22
	S_A - S_{CA}^*	58.1	0.36
	mp	51.3	26.62

Table 4.15 - Transition Temperatures (°C) and Enthalpies (kJ mol^{-1}) for Compounds 66 - 68 as Observed by DSC

The DSC heating thermograms for compounds **66** -**68** are shown in Figure 4.50.

On examination of the DSC thermograms for compounds **66** - **68** shown in Figure 4.50 the S_{CA}^* / Alt - S_A transitions can clearly be seen. The temperatures at which these peaks occur are similar to the transition temperatures observed by optical microscopy, reported in Table 4.14.
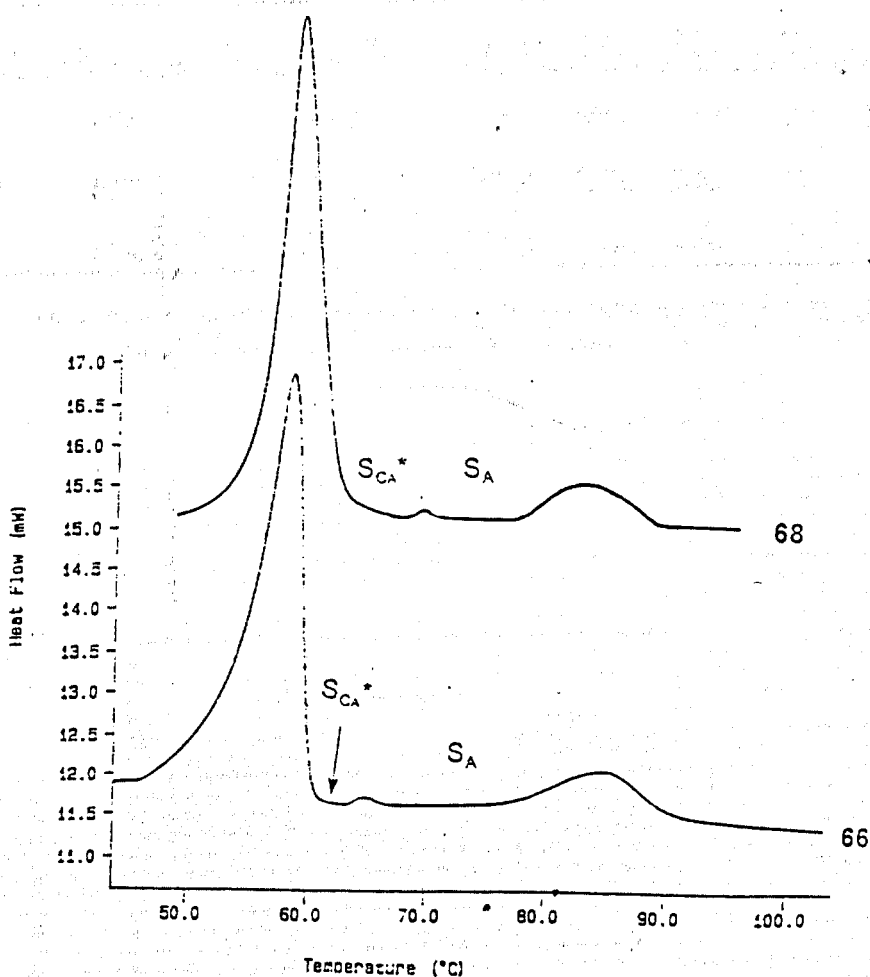
Figure 4.50 - DSC Heating Thermograms for Compounds 66 and 68

4.4.4 Transition Temperatures and Phase Behaviour of Polymeric Materials as Determined by Optical Microscopy

Textural Studies were carried out using a sample of the side chain liquid crystal polymer prepared as described in section 4.1.4. The polymer samples were annealed for 24 hours to allow a texture to develop.

Table 4.16 lists the values obtained for the transition temperatures as determined by optical microscopy, as well as the number average molecular weight, weight

average molecular weight, number average degree of polymerisation and polydispersity of each polymer sample. The results obtained from optical microscopy are displayed as a bar graph in Figure 4.51.

Polymer	Iso - S_A	S_A - S_{CA}*/Alt	mp	$\overline{M}_n$	$\overline{M}_w$	$\overline{X}_n$	γ
P66	112.6	82.2	55.7	6650	8900	10	1.34
P67	103.6	84.3	63.1	7230	9840	11	1.36
P68	118.4	82.1	63.3	6990	8280	11	1.19

Table 4.16 - Transition Temperatures (°C) Determined by Optical Microscopy and GPC Data for Polymers P66 - P68
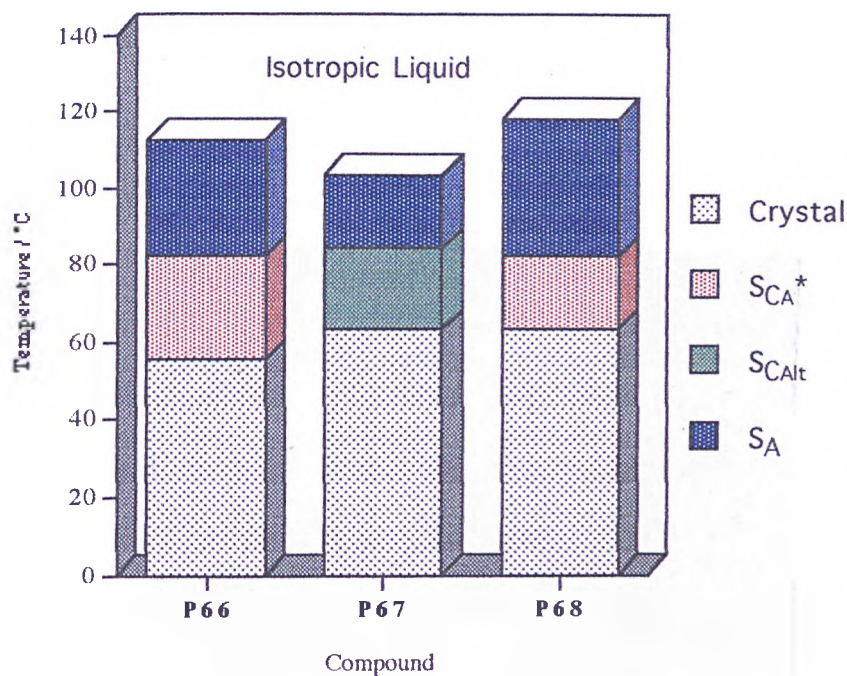
Figure 4.51 - Transition temperatures (°C) and Phase Behaviour for Polymers P66 - P68 as Determined by Optical Microscopy

The polymers **P66** - **P68** each show the phase sequence Crystal $\Leftrightarrow$ $S_{CA}*$ (or S_{CAlt}) $\Leftrightarrow$ S_A $\Leftrightarrow$ Iso (see Figure 4.51). Photomicrographs of the smectic C phases exhibited by polymers **P67** and **P68** are shown in Figure 4.52

(a) **P67**

(72.9 °C)
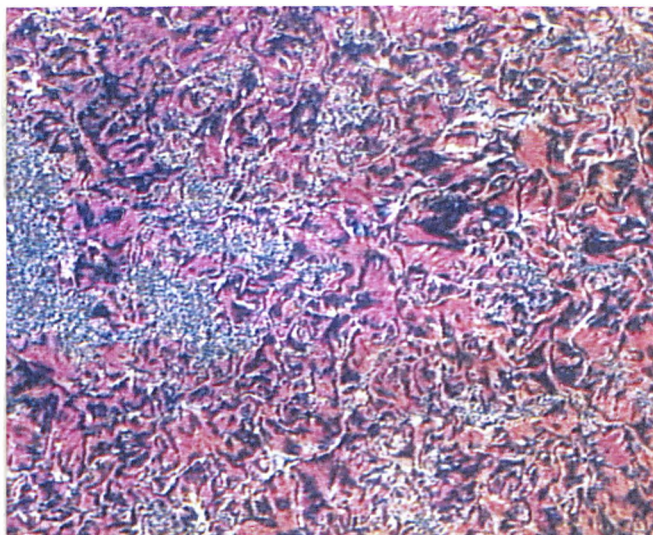
(b) **P68**

(79.6 °C)

Figure 4.52 - Photomicrographs of the Smectic C Phases Exhibited by P67 and P68

Comparing the values listed in Table 4.16 for polymers **P66 - P68** to those in Table 4.12 for polymers **P55 - P57**, then the effect of increasing the size and polarity of the backbone substituent on the liquid crystal properties can be seen. The values listed for the melting points of the polymers **P66 - P68** show that the melting point of each material has increased compared to polymers **P55 - P57**. Normally the melting point or Tg of a non-liquid crystalline polymer would be expected to increase as the size and polarity of the backbone substituent is increased. This is due to the backbone substituent affecting the ability of the polymer main chain to rotate due to the increased volume of this substituent, as well as the increased polarity and reduction in flexibility of the backbone substituent[92] This effect is also true for the SCLCPs reported here (see also section 4.7).

The isotropization temperatures and $S_{CA}*$ (or S_{CAIt}) - S_A transition appear to be unrelated to this change in structure and are generally lower than the corresponding values for polymers **P55 - P57**.

4.4.5 Transition Temperatures and Phase Behaviour of Polymeric Materials as Determined by Differential Scanning Calorimetry

Polymers **P66 - P67** where studied by DSC. The transition temperatures obtained and the enthalpies associated with these transitions are given in Table 4.17.

Compound	Transition	Temperature	Enthalpy
P66	S_A - Iso	116.9	17.50
	$S_{CA}*$ - S_A	91.3	0.14
	mp	56.5	2.25
P67	S_A - Iso	107.5	15.31
	S_{CAlt} - S_A	87.1	0.17
	mp	65.86	2.37
P68	S_A - Iso	115.5	17.32
	$S_{CA}*$ - S_A	77.1	0.16
	mp	68.3	4.44

Table 4.17 - Transition Temperatures (°C) and Enthalpies ($J\ g^{-1}$) for Polymers P66 - P68 as Determined by DSC

The DSC heating thermograms for polymers **P66** and **P68** are shown in Figure 4.53.
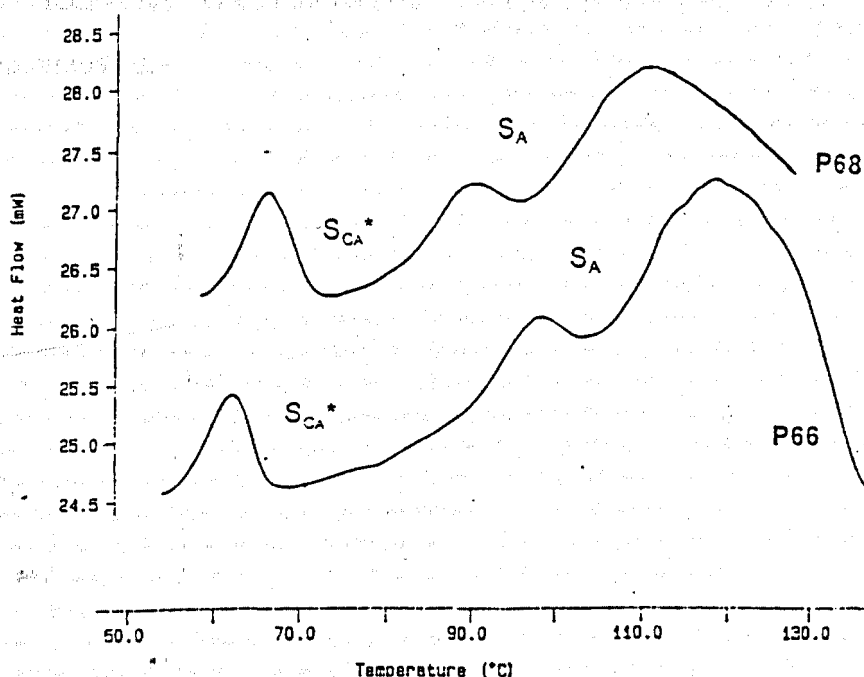
Figure 4.53 - DSC Heating Thermograms for Polymers P66 and P68

4.4.6 Miscibility Studies

Confirmation of the exact nature of the smectic phases found in polymers **P66** - **P68** was obtained by creating binary mixtures of the test polymer with the known standard **MHP11BC**. Its structure, phase behaviour and transition temperatures can be seen in Figure 4.13.

Figure 4.54 shows the binary miscibility diagram for the mixtures prepared from the test polymer **P66** and the standard material **MHP11BC**. It can be seen from this diagram that the S_A and $S_{CA}*$ phases show complete miscibility throughout the entire composition range indicating that the phases obtained in the test polymer are structurally the same as those shown by the standard material. The S_C* material exists for mixtures up to approximately 42 weight percent polymer, but is not exhibited in mixtures above this composition indicating that it is not present in the polymer **P66**. The $S_{C\gamma}*$ phase exhibited by **MHP11BC** was not observed in any of the mixtures prepared, however its existence in mixtures below approximately 15 weight percent polymer cannot be discounted as mixtures below this composition were not prepared.
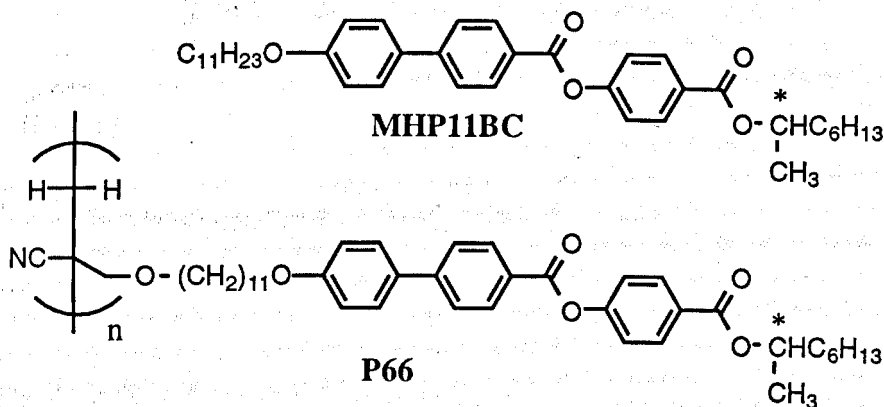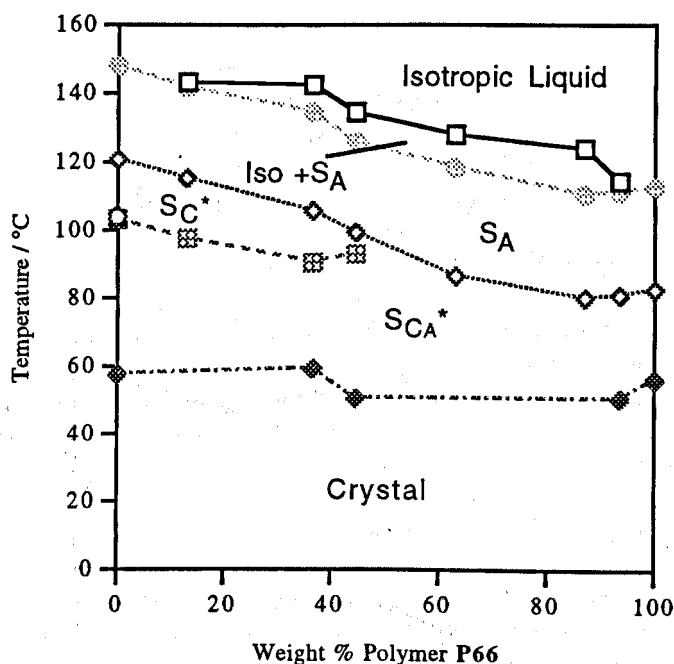
Figure 4.54 - Miscibility Phase Diagram for Polymer P66 and the Standard Compound MHP11BC

Figure 4.55 shows the binary miscibility diagram for the polymer **P67** and the standard material **MHP11BC**. The S_A and S_{CA}^* phases can be seen to exist throughout the entire composition range, therefore indicating that these phases are present in both the standard material and the test polymer. The S_C^* phase was found to disappear when the mixture contained greater than approximately 20 weight percent polymer. The $S_{C\gamma}^*$ phase was not found in any of the binary mixtures prepared, however its presence in mixtures which contain less than approximately 15 weight percent polymer cannot be discounted.
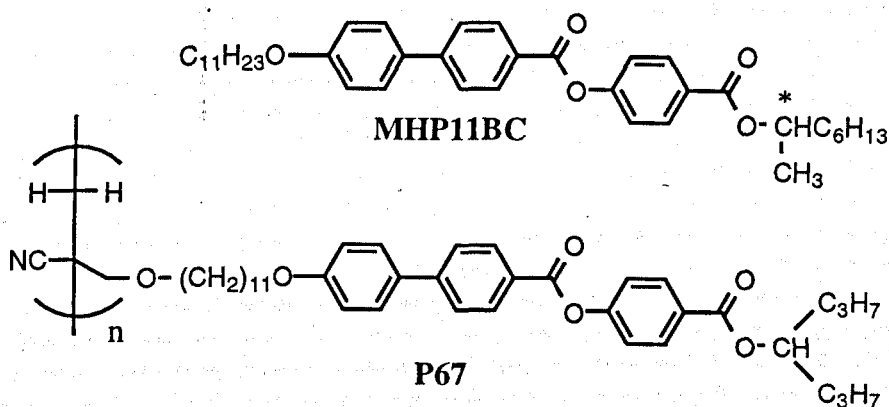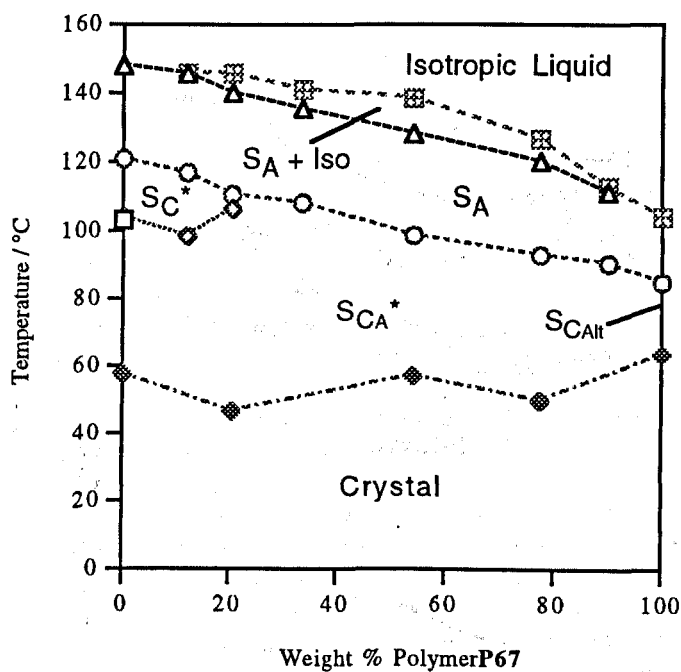
Figure 4.55 - Miscibility Phase Diagram for Polymer P67 and the Standard Material MHP11BC

The miscibility phase diagram for polymer **P68** and the standard material **MHP11BC** is given in Figure 4.56. The S_A and $S_{CA}*$ phases can be seen to exist throughout the entire composition range indicating their existence in both the test material and the standard material. The S_C* phase was found to disappear when the composition of the binary mixture rose to above approximately 25 weight percent polymer. The $S_{C\gamma}*$ phase present in the test material did not appear in any of the mixtures prepared.
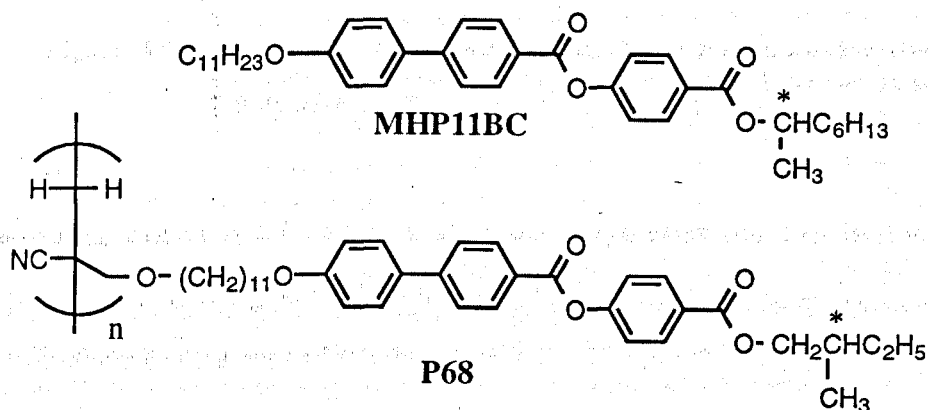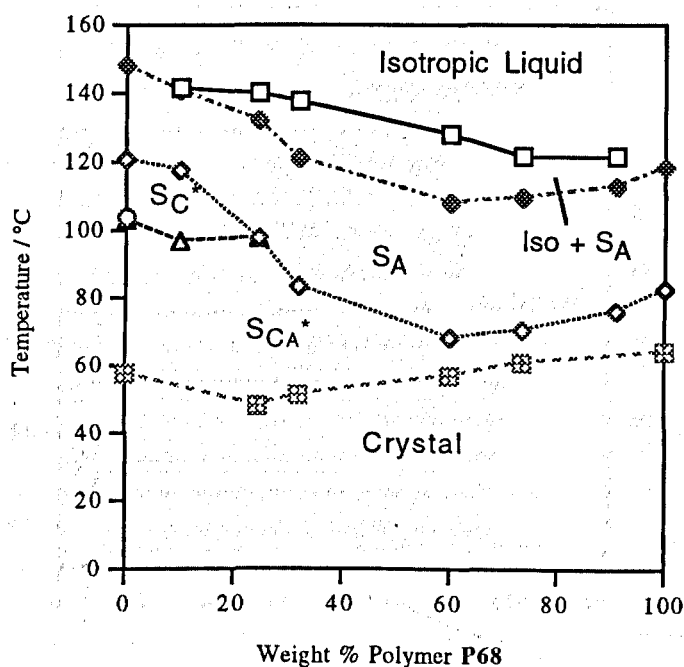
Figure 4.56 - Miscibility Phase Diagram for Polymer P68 and the Standard Compound MHP11BC

4.4.7 Effect of Polymerisation on the Liquid Crystal Behaviour

It has previously been stated in this thesis that polymerisation of a liquid crystal monomer to yield a liquid crystal polymer has the effect of stabilising the liquid crystal mesophase (e.g. section 4.1.7).[52] By consideration of the data listed in Table 4.14 for the monomeric materials, and comparison with the values listed in Table 4.16 for the polymeric materials, it can be seen that this holds true for the polymers P66 - P68. This data is represented as a bar graph in Figure 4.57.
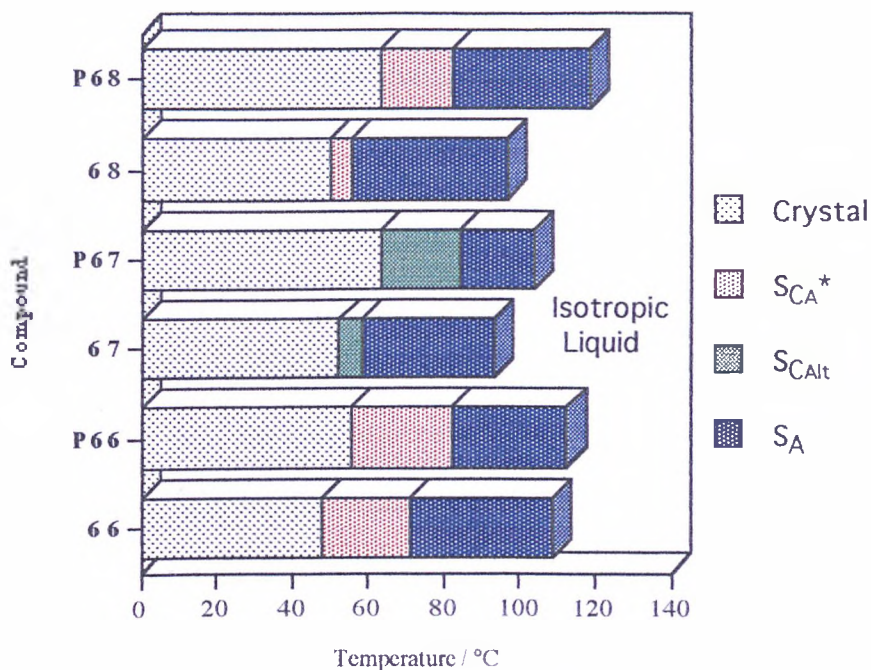
Figure 4.57 - Transition Temperatures and Phase Behaviour for the Monomeric Materials 66 - 68 and their Corresponding Polymers as Determined by Optical Microscopy

Examining Figure 4.57 shows that upon polymerisation the isotropization temperature and melting point of each material is increased. It can also be seen that the temperature range over which the alternating smectic C phase occurs increases when the material is polymerised.

4.5 THE EFFECT OF INSERTION OF A REVERSE ESTER IN THE FLEXIBLE SPACER ON THE LIQUID CRYSTAL PROPERTIES OF SOME SIDE CHAIN LIQUID CRYSTAL POLYMERS

4.5.1 Introduction

Previous work on the structure required to generate an antiferroelectric smectic C phase in a liquid crystal material has postulated that the ester groups within a molecule should be aligned in the same direction (see Figure 1.22).[43, 44] This section deals with some molecules which were synthesised with a reverse ester located at a position away from the rigid core of the mesogenic side chain. The monomeric materials synthesised, and their corresponding polymers, can be seen in Figure 4.58.

72, P72 ; X = H
73, P73 ; X = CN
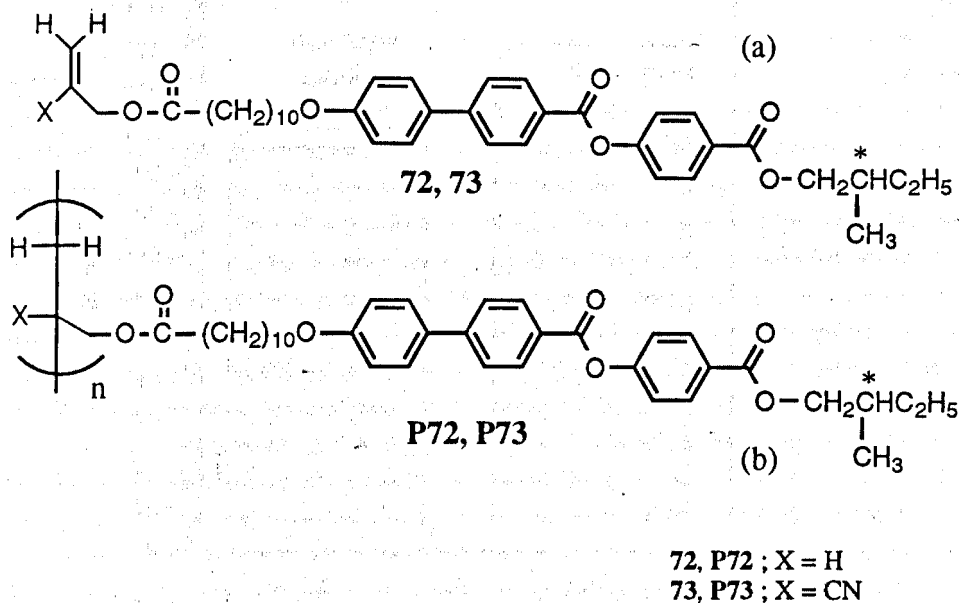
Figure 4.58 - Liquid Crystal Monomers and Polymers Containing a Reverse Ester Linkage in the Flexible Spacer

4.5.2 Transition Temperatures and Phase Behaviour of Monomeric Materials as Determined by Optical Microscopy

The phase sequences and transition temperatures of the monomeric materials **72** and **73** are listed in Table 4.18. The results are displayed as a bar graph in Figure 4.59.

Compound	Iso - S_A	mp	Recryst[‡]
72	96.6	47.6	12.9
73	117.3	66.2	22.0

[‡]Determined by Differential Scanning Calorimetry

Table 4.18 - Transition Temperatures (°C) and Phase Behaviour for Compounds 72 and 73
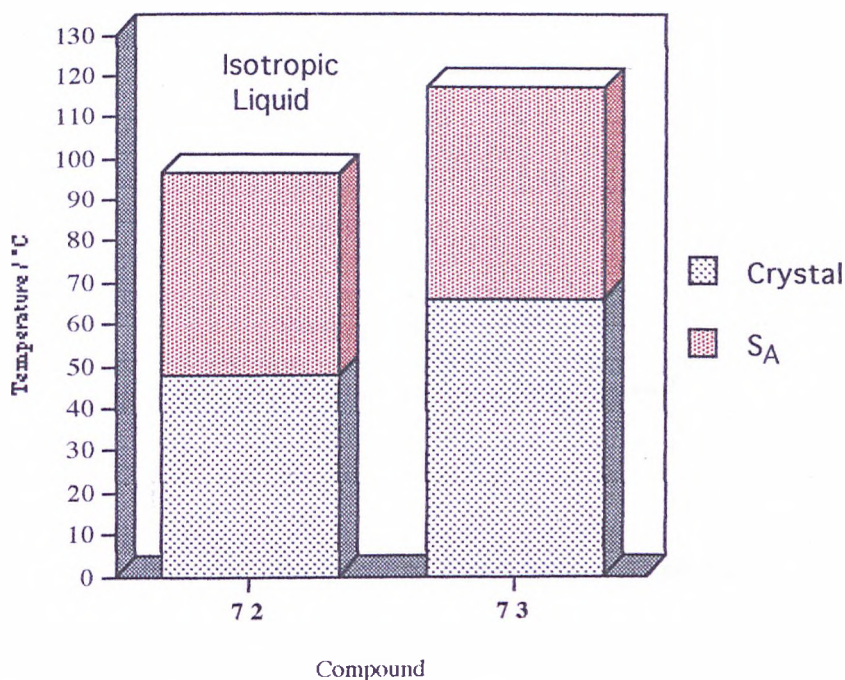
Figure 4.59 - Transition Temperatures (°C) and Phase Sequences for Compounds 72 and 73 as Determined by Optical Microscopy

Both the materials prepared exhibit the phase sequence Iso ⇔ S_A ⇔ Crystal. When the backbone substituent is changed from hydrogen (**72**) to cyano (**73**) then

the thermal stability of the liquid crystal mesophase increases. This is consistent with the results presented in section 4.4.

Comparing the values listed in Table 4.18 for compounds **72** and **73** with those for compounds **57** and **68** (Figure 4.60) listed in Table 4.19 then we see the effect of inserting a reverse ester link into the liquid crystal molecule.

Compound	Iso - S_A	S_A - S_{CA}*	mp
57	96.6	52.7	44.6
68	117.3	55.4	50.2

Table 4.19 - Transition Temperatures (°C) and Phase Behaviour for Compounds 67 and 68 as Determined by Optical Microscopy
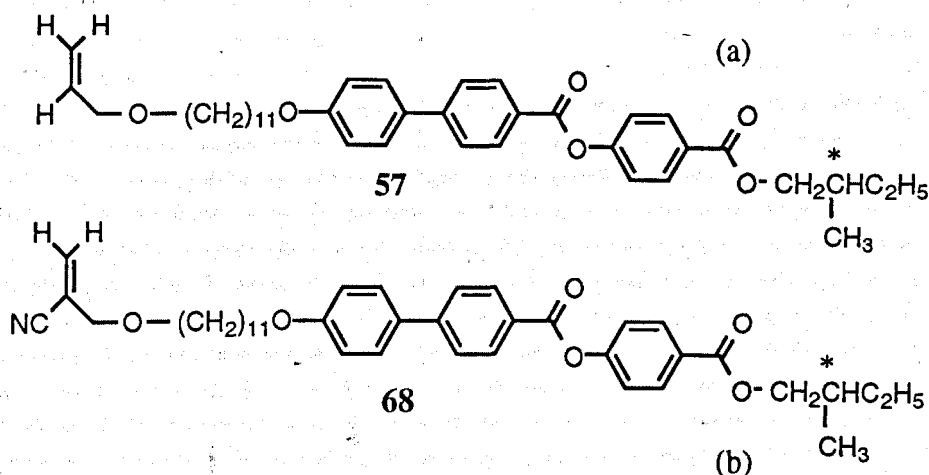
Figure 4.60 - Structure of Compounds 57 and 68

By comparing the phase sequences exhibited by compounds **72** and **73** with the phase sequences exhibited by compounds **57** and **68** then we see that compounds **72** and **73** do not exhibit a tilted smectic phase whereas compounds **57** and **68**, both exhibit a S_{CA}* phase. Previous work reported by Nishiyama[46] into the incidence of antiferroelectric phases in low molar mass materials has postulated that in materials which contain more than one ester group in the rigid core of the

molecule, the ester functionalities must be aligned in the same direction. Molecules in which one of the ester groups in the rigid core is oriented in the reverse direction (reverse esters) do not exhibit antiferroelectric phases. The data given in Table 4.18 suggests that this postulation is also true for materials where the reverse ester is situated away from the rigid core.

Photomicrographs of the S_A phases obtained for compounds **72** and **73** are given in Figure 4.61.

(a) **72**

(90.8 °C)
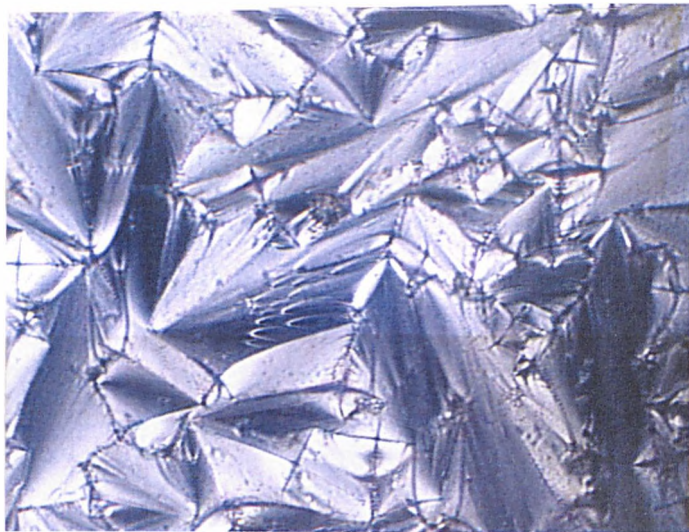
(a) **73**

(104.5°C)
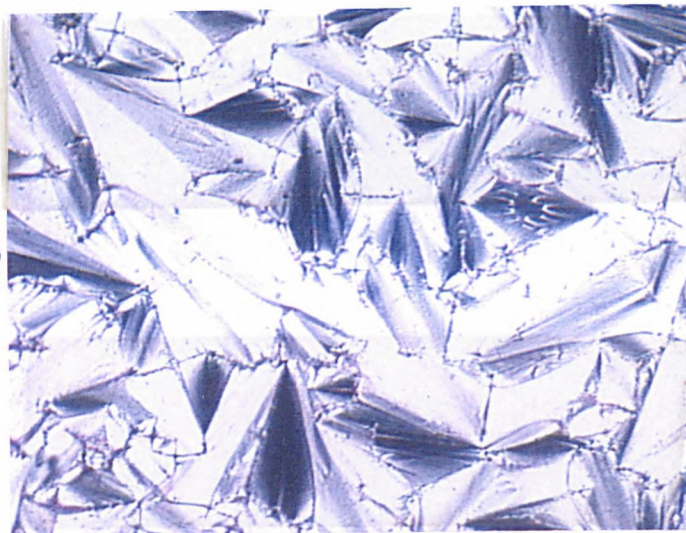
Figure 4.61 - Photomicrographs for the S_A Phases Exhibited by Optical Microscopy by Compounds 72 and 73

4.5.3 Transition Temperatures and Phase Behaviour of the Monomeric Materials as Determined by Differential Scanning Calorimetry

Compounds **72** and **73** were examined by DSC; the transitions observed, and the enthalpies associated with these transitions are given in Table 4.20.

Compound	Transition	Temperature	Enthalpy
72	Iso - S_A	99.2	7.23
	mp	49.9	47.63
	Recryst	12.9	36.49
73	Iso - S_A	118.8	6.86
	mp	68.0	40.09
	Recryst	22.0	37.73

Table 4.20 - Transition Temperatures (°C) and Enthalpies (kJ mol^{-1}) for Compounds 72 and 73 as Determined by DSC

The values listed in Table 4.20 for the melting points and isotropization temperatures of compounds **72** and **73** are similar to those listed in Table 4.18 which were obtained by optical microscopy. The DSC heating and cooling thermograms for compound **72** are given in Figure 4.62.
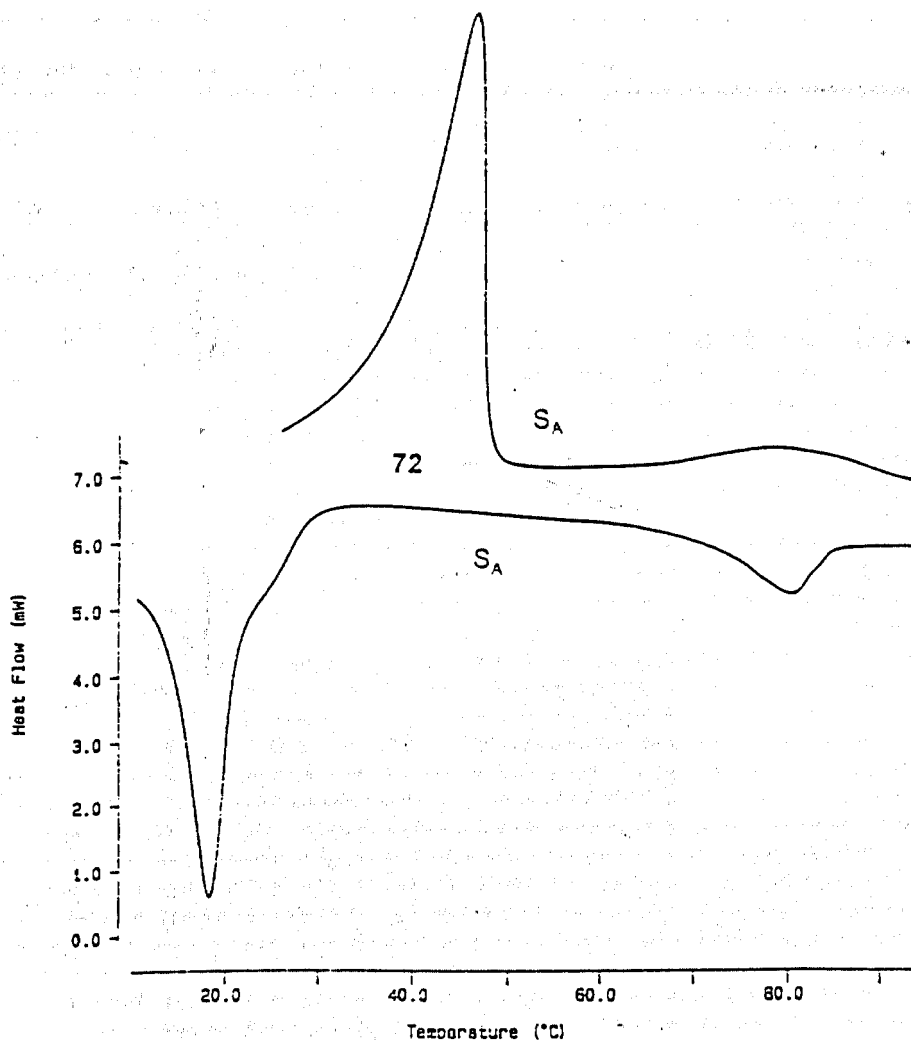
Figure 4.62 - Heating and Cooling DSC Thermograms Obtained
for compound 73

4.5.4 Transition Temperatures and Phase Behaviour of Polymeric Materials as Determined by Optical Microscopy

Textural studies were carried out on a sample of liquid crystal polymer as previously described (section 4.1.4).

Table 4.21 gives the transition temperatures obtained by optical microscopy for the polymers **P72** and **P73**. The number average molecular weight, weight average molecular weight, the number average degree of polymerisation and the

polydispersities of the polymer samples are also listed in Table 4.21. The results obtained from optical microscopy are displayed as a bar graph in Figure 4.63.

Polymer	Iso - S_A	$mp^{\ddagger}$	$\overline{M}n$	$\overline{M}w$	$\overline{X}n$	γ
P72	107.2	56.4	4120	6370	1.55	7
P73	126.6	70.1	4730	7110	1.50	8

‡Obtained by Differential Scanning Calorimetry

Table 4.21 - Transition Temperature (°C) Determined by Optical Microscopy and GPC data for Polymers P72 and P73
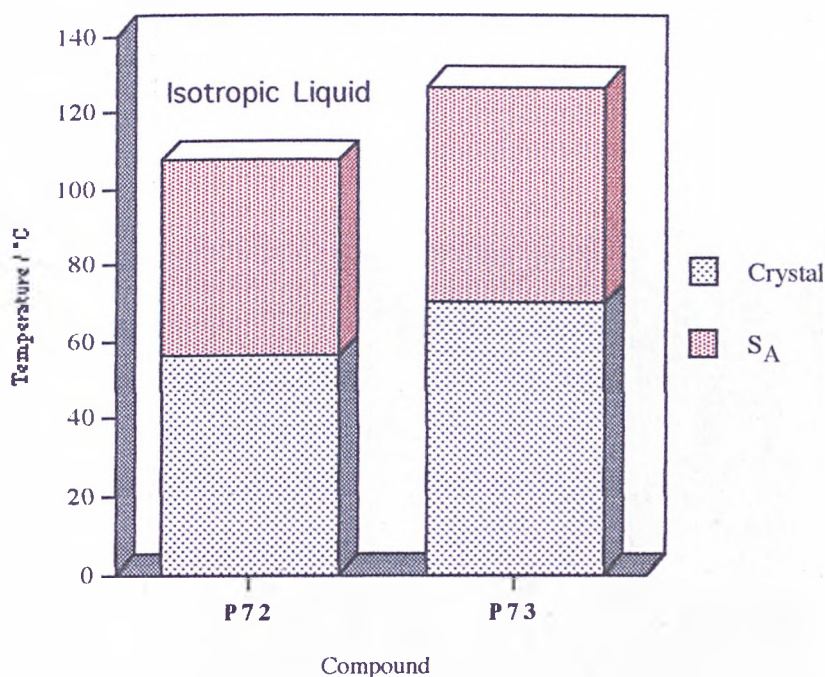
Figure 4.63 - Transition Temperatures (°C) and Phase Behaviour for Polymers P72 & P73

The polymers **P72** and **P73** show a phase sequence of Crystal $\Leftrightarrow$ S_A $\Leftrightarrow$ Iso. Photomicrographs of the S_A phase obtained for polymers **P72** and **P73** are given in Figure 4.64.

(a) **P72**

(93.5 °C)

(a) **P73**

(116.4 °C)

Figure 4.64 - Photomicrograph Obtained for the S_A
Phases of P72 and P73

4.5.5 Transition Temperatures and Phase Behaviour of Polymeric Materials as Determined by Differential Scanning Calorimetry

Polymers **P72** and **P73** were examined by DSC. The transition temperatures observed and the enthalpies associated with these transitions are listed in Table 4.22. The DSC thermograms for polymers **P72** and **P73** are shown in Figure 4.65.

Polymer	Transition	Temperature	Enthalpy
P72	Iso - S_A	109.6	7.33
	mp	58.2	30.16
P73	Iso - S_A	127.9	5.94
	mp	71.3	29.66

Table 4.22 - Transition Temperatures (°C) and Enthalpies (J g^{-1}) for Polymers P72 and P73 Determined by DSC
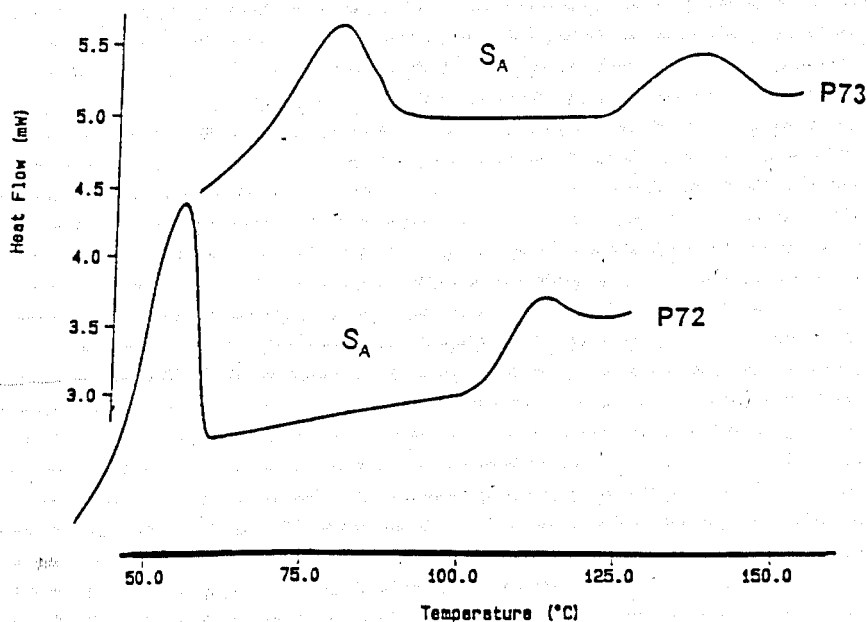
Figure 4.65 - DSC Heating Thermograms Obtained for Polymers P72 and P73

4.5.6 Miscibility Studies

Examination of the phase sequences listed in Tables 4.21 and 4.22 shows that polymers **P72** and **P73** do not exhibit a S_C phase. Studying the samples by optical microscopy clearly shows the characteristic focal conic fan texture associated with the S_A phase (Figure 4.64). There was therefore no need to perform miscibility studies on the samples.

4.5.7 Effect of Polymerisation on The Liquid Crystalline Properties

The transition temperatures and phase sequences for the low molar mass compounds **72** and **73** (Table 4.18) and their corresponding polymers **P72** and **P73** (Table 4.21) have been depicted as a bar graph in Figure 4.66. Examination of the values listed in these tables shows the effect that polymerisation has on these materials. It is clear that upon polymerisation the isotropization temperature and the melting point of the samples increase, thus thermally stabilising the liquid crystal phase.[52]
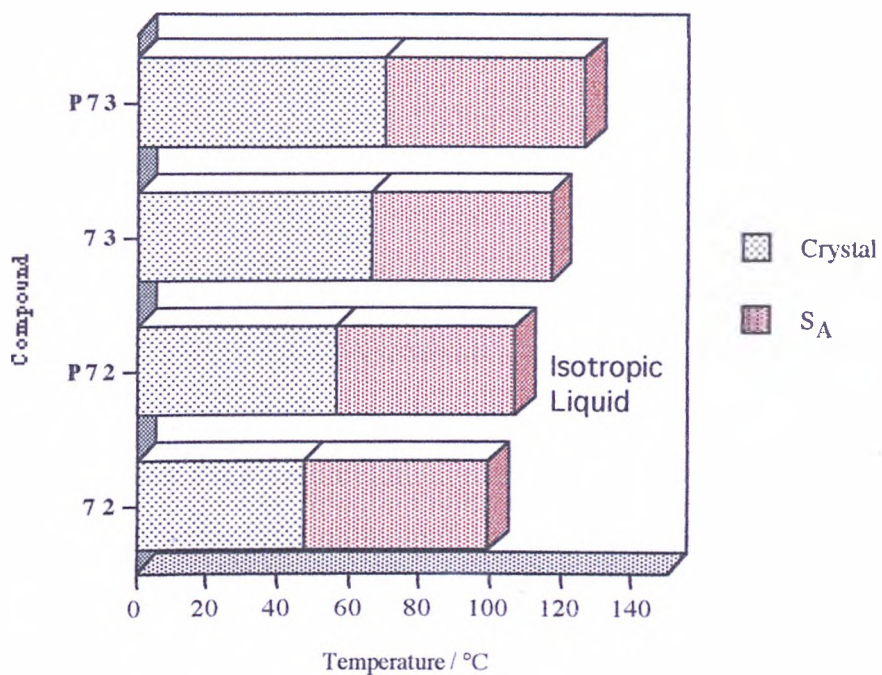
Figure 4.66 - Transition Temperatures and Phase Behaviour for the Monomeric Materials 72 and 73 and their Corresponding Polymers

4.6 EFFECT OF POLYMERISATION ON SOME LIQUID CRYSTALLINE α-FLUOROACRYLATES

4.6.1 Introduction

Previous work by Sage *et al.*[79] has shown the existence of an antiferroelectric phase in a liquid crystalline poly(acrylate) (Figure 1.41). The phase appeared at a relatively high temperature and it was deemed desirable to reduced the temperature of the appearance of the antiferroelectric phase. One way in which this could be done was to reduce the glass transition temperature of the polymer system by frustrating the packing of the polymer chains, thus reducing the crystallinity of the polymer.[92] It was thought that the insertion of a fluoro substituent onto the polymer backbone could have this effect.[82] The materials to be studied were prepared by taking the liquid crystal side chain used by Sage *et. al.* and attaching it it to sodium α-fluoroacrylate to give the fluoroacrylate monomers, **96** and **97**, shown in Figure 4.67(a). These monomers were subsequently polymerised to give the poly(fluoroacrylates), **P96** and **P97**, shown in Figure 4.67(b).

(a)

96, 97

(b)
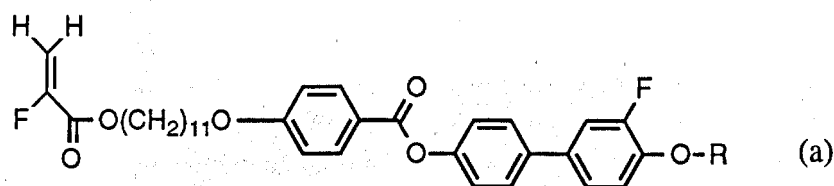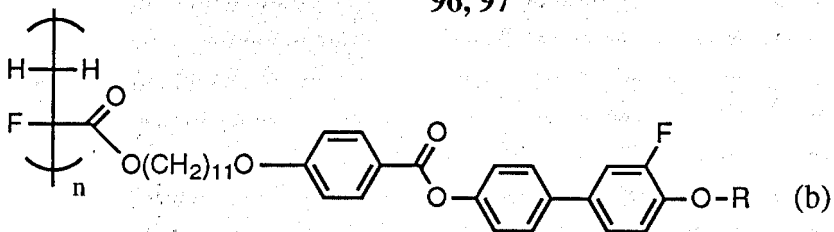
P96, P97

96, P96 ; R = (*R*)-1-methylheptyl
97, P97 ; R = 1-octyl

Figure 4.67 - Fluoroacrylate Monomers and Polymers Studied

4.6.2 Transition Temperatures and Phase Behaviour of α-Fluoroacrylate Monomers by Optical Microscopy

The phase sequences and accompanying transition temperatures for the α-fluoroacrylate compounds **96** and **97** are listed in Table 4.23. The results are presented as a bar graph in Figure 4.68.

Cmpd	Iso - S_A	S_A - S_C*	S_A - S_C	mp	Recryst[‡]
96	104.9	58.2	-	51.6	42.7
97	109.6	-	79.1	64.8	54.4

[‡] Obtained by Differential Scanning Calorimetry

Table 4.23 - Transition Temperatures (°C) and Phase Behaviour for Compounds 96 and 97
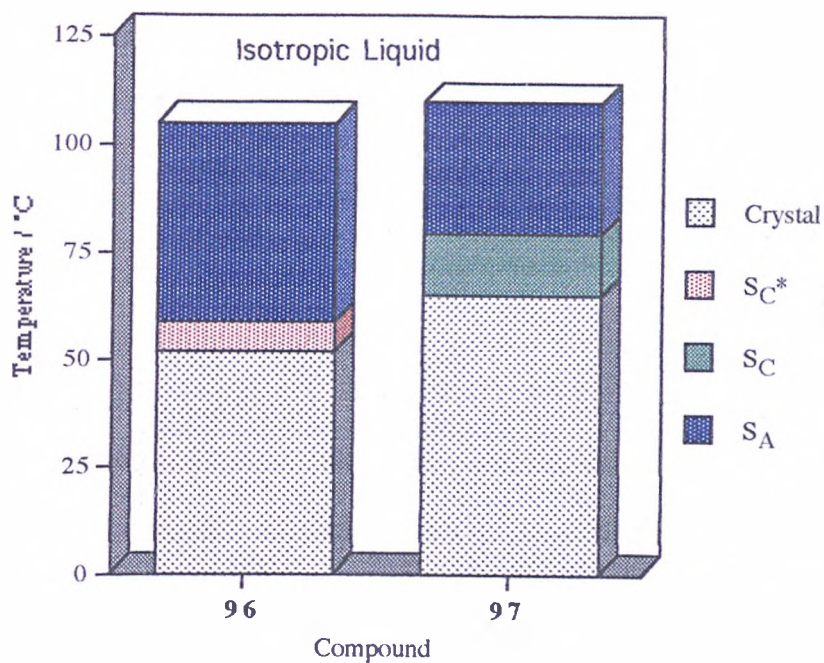
Figure 4.68 - Phase Behaviour of Compounds 96 and 97

Both compounds exhibit a phase sequence of Iso ⇔ S_A ⇔ S_C ⇔ crystal, with compound **96** displaying a S_C* phase due to its chiral nature. Compound **97** shows greater mesophase stability. This is probably due to the longer terminal chain of the molecule and the absence of branching in the terminal chain.

Textures exhibited by the S_A and S_C* phases of compound **96** and the S_C phase of compound **97** are shown in Figure 4.69.

(a) **96**, S_A

(91.1 °C)
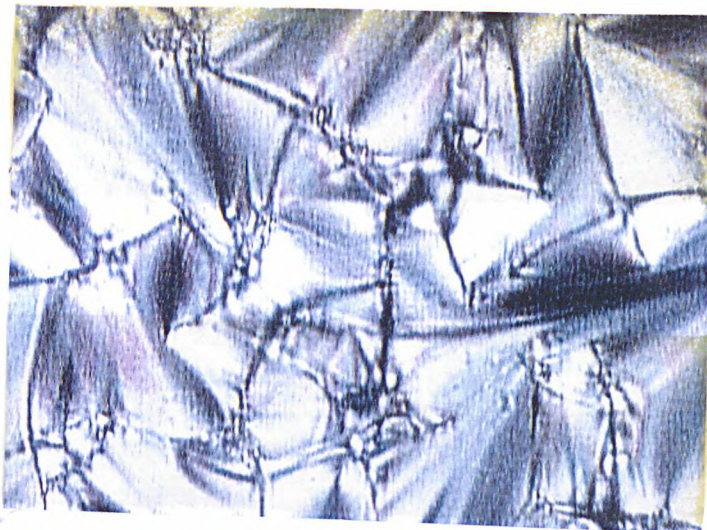
(b) **96**, S_C^*

(54.3 °C)
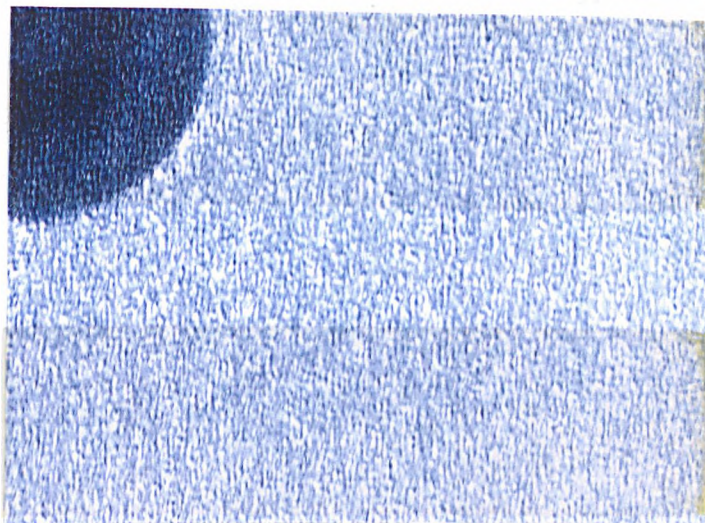
(c) **97**, S_C

(72.8 °C)
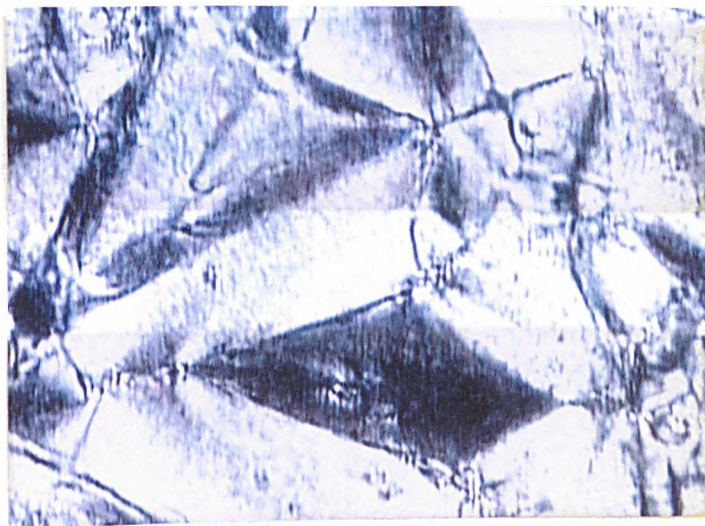
Figure 4.69 - Photomicrographs Obtained by Optical Microscopy
of Compounds 96 and 97
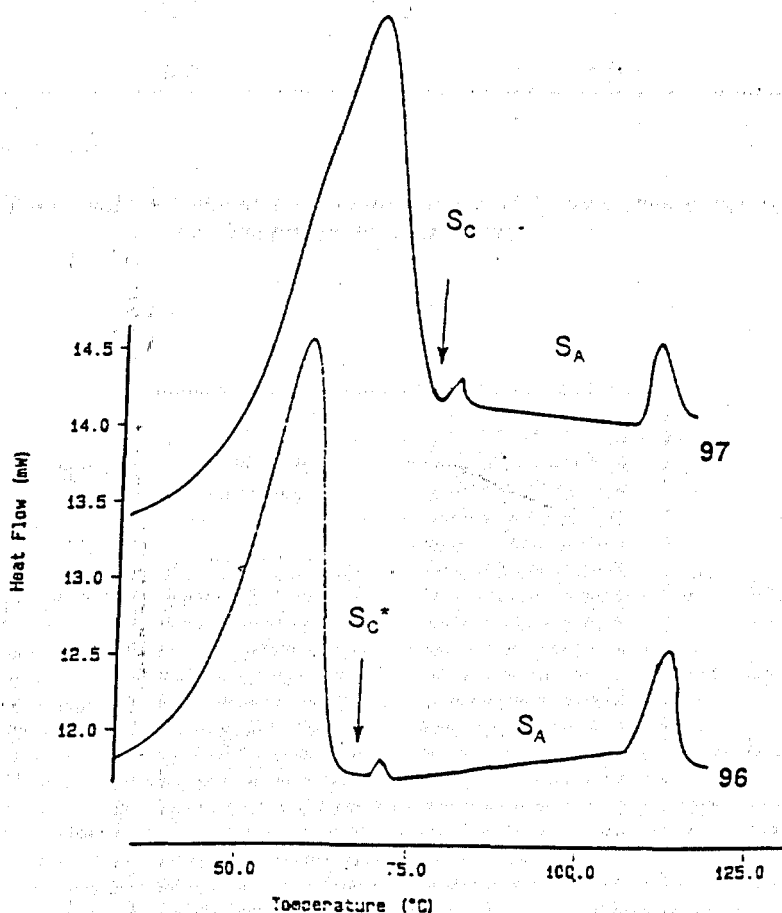
Figure 4.70 - DSC Heating Thermograms for Compounds 96 and 97

4.6.4 Transition Temperatures of Poly(α–fluoroacrylates) Studied by Optical Microscopy

Samples of poly(α-fluoroacrylate) were prepared for textural analysis by optical microscopy as described in section 4.1.4. The polymers were annealed for 72 hours.

The phase sequence and accompanying transition temperatures for the poly(α-fluoroacrylate) compounds **P96** and **P97** are listed in Table 4.25 with the results presented as a bar graph in Figure 4.71.

Polymer	Iso - S_A	S_A- S_C^*	S_A- S_E	T_g‡
P96	155.3	142.7	-	77.6
P97	209.1	-	195.6	102.3

‡Determined by DSC

Table 4.25 - Transition Temperatures (°C) and Phase Sequence for Polymers P96 and P97
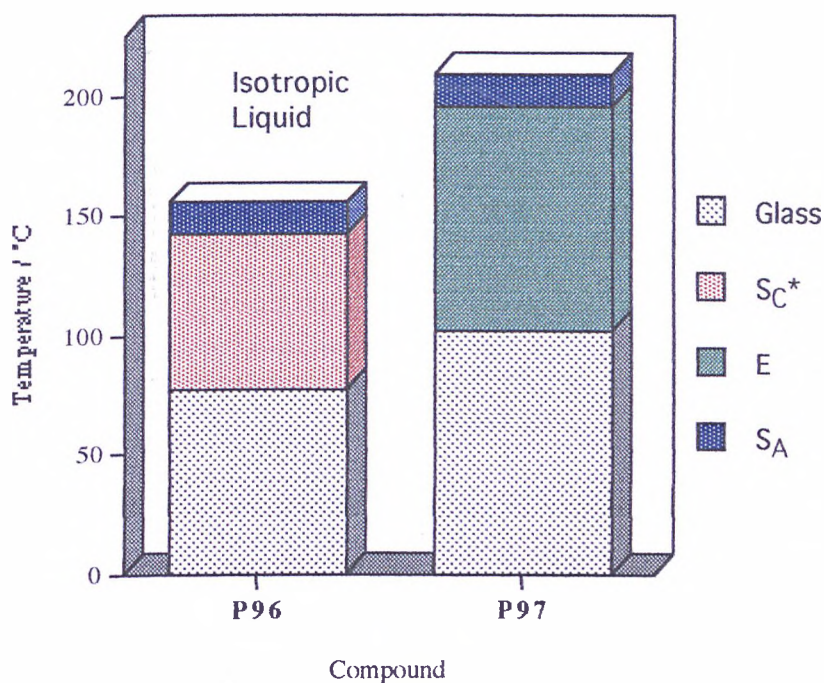
Figure 4.71 - Phase Sequences for Polymers P96 and P97

Examination of Figure 4.71 shows that by changing the nature of the end group of the polymer side chain the phase sequence of the polymer has been affected, *i.e.* by replacing the chiral 1-methylheptyl group in polymer **P96** with an achiral 1-octyl moiety (**P97**) the chiral S_C^* phase has disappeared. In its place a higher ordered crystal E phase (E) is observed. The higher temperature S_A phase is observed in both materials.

Photomicrographs of the phases observed for polymer **P96** and polymer **P97** are given in Figure 4.72.

(a) **P96**, S_A

(150.5 °C)

(b) **P96**, S_C*

(139.4 °C)
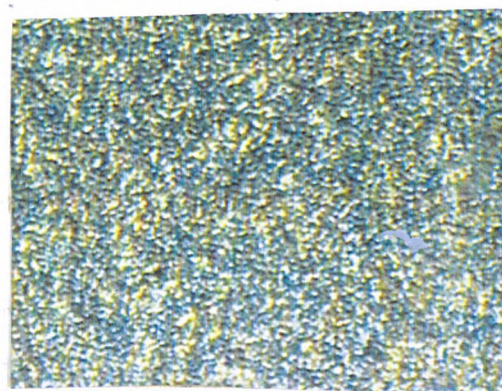
(a) **P97**, S_A

(202.6 °C)
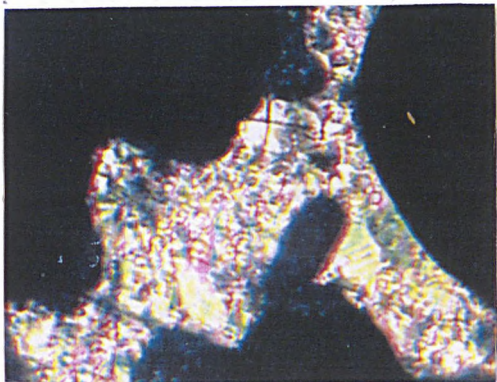
(a) **P97**, E

(187.6 °C)
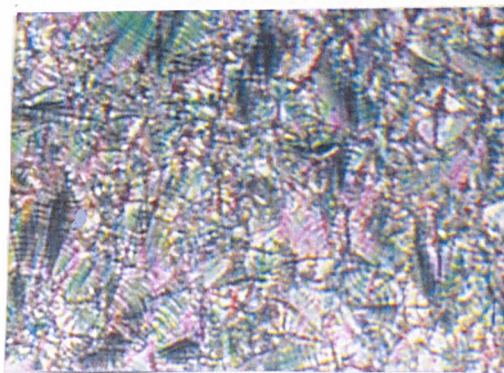
Figure 4.72 - Photomicrographs of the Textures Observed by Optical Microscopy of Polymers P96 and P97

4.6.5 Transition Temperatures and Phase Behaviour of Poly(α-Fluoroacrylate Materials Determined by Differential Scanning Calorimetry

Polymers **P96** and **P97** were studied by DSC and the transition temperatures obtained and enthalpies associated with these transitions are listed in Table 4.26.

Polymer	Transition	Temperature	Enthalpy
P96	Iso - S_A	149.6	2.27
	S_A - S_C*	141.7	1.68
	Tg	77.6	0.19
P97	Iso - S_A	204.5	7.62
	S_A - E	194.4	1.59
	Tg	99.7	0.16

Table 4.26 - Transition Temperatures (°C) and Enthalpies (J g^{-1}) for Polymers P96 and P97 as Determined by DSC

The DSC thermograms for polymers **P96** and **P97** are shown in Figure 4.73. The transitions observed are consistent with those obtained by optical microscopy.
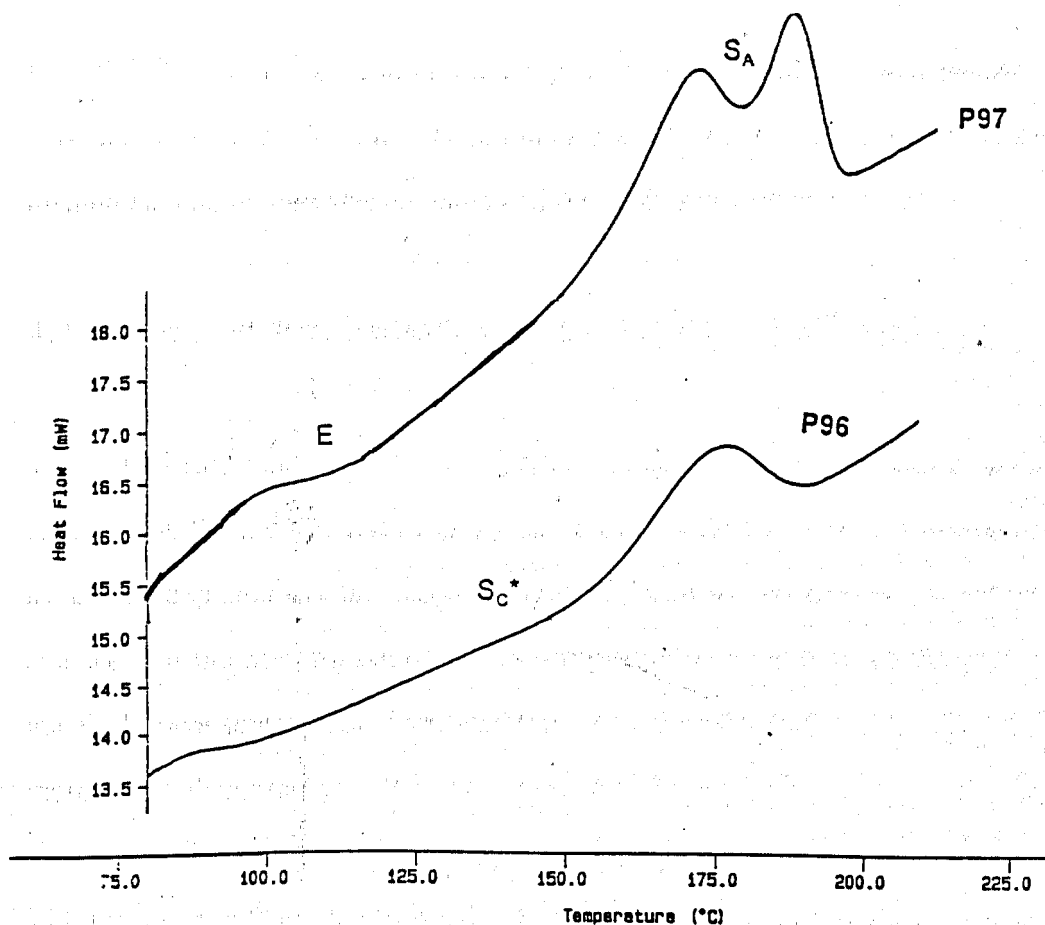
Figure 4.73 - DSC Thermograms for Polymers P96 and P97

4.6.6 Miscibility Studies

Textural studies performed upon the poly(α-fluoroacrylate) polymer **P96** showed the presence of a optically active smectic C phase. However, the exact nature of this phase was hard to determine by microscopy alone due to the very poor alignment obtained. Miscibility studies were therefore carried out on mixtures of the polymer **P96** and a standard low molar mass compound **MHP11BC** (Figure 4.13) with initial compositions of approximately 25, 50 and 75 weight percent polymer.

Textural studies performed on these mixtures proved initially inconclusive due to the very poor alignment obtained in all three compositions. The samples were then annealed by heating to 20 °C above their isotropization temperature and cooled at a

rate of 0.2 °C min^{-1} to a temperature just inside the liquid crystal phase. The samples were then left at this temperature for 48 hours, however again no distinguishable texture was obtained and the studies proved inconclusive.

4.6.7 Effect of Polymerisation on the Liquid Crystal Behaviour

The transition temperatures and phase sequences listed in Table 4.23 for compounds **96** and **97**, and those listed in Table 4.25 for polymers **P96** and **P97** have been depicted as a bar graph in Figure 4.74. If we examine this bar graph we can see that the melting points and isotropization temperatures of the polymeric materials have substantially increased (*i.e.*, the thermal stability of the molecule has increased substantially). It is also seen that by replacing the 1-methylheptyl terminal chain with a 1-octyl moiety affects the phase behaviour of the molecule, with the smectic C phase observed at lower temperatures in **P96** disappearing and an E phase being observed in **P97**.

Insertion of a fluoro substituent onto the polymer backbone increases the glass transition of the polymers obtained. This effect is observed in non-liquid crystalline polymers and is explained by the increased size and polarity of the fluoro backbone substituent causing restriction to the rotation of the polymer main chain[92]. High transition temperatures and very poor alignment indicate a more rigid backbone in the poly(α-fluoroacrylates) compared to the poly(acrylate) materials.[81]
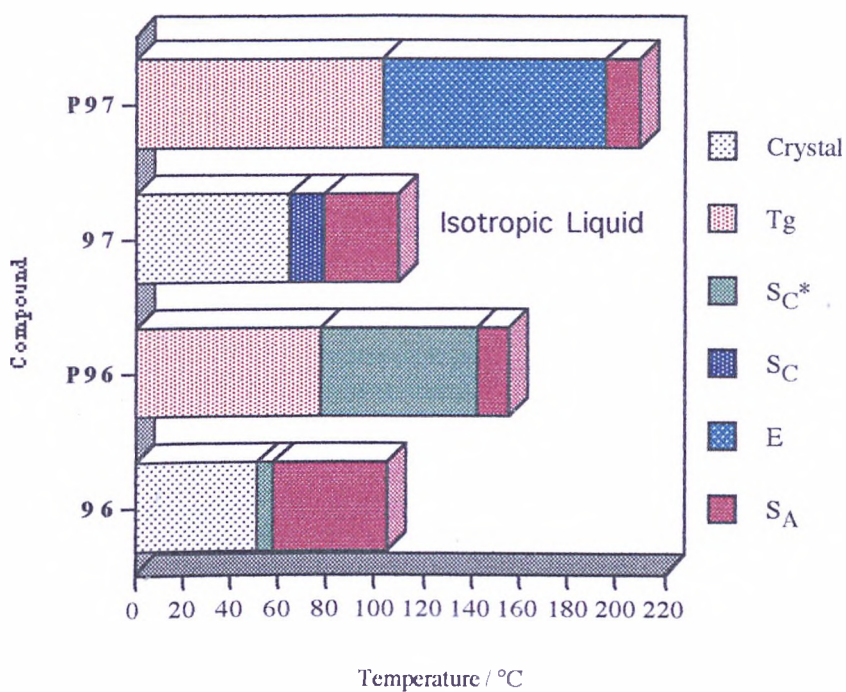
Figure 4.74 - Transition Temperatures and Phase Behaviour for Compounds 96 and 97 and Polymers P96 and P97

4.7 DISCUSSION OF THE SYNTHETIC ROUTES TAKEN TO THE TARGET MONOMERS

4.7.1 Introduction

The reactions reported in section 3 to obtain the target monomers are widely used in synthetic liquid crystal chemistry [*e.g.*, the protection of the hydroxy group of 4-hydroxycarboxylic acid with methyl chloroformate[86] (Scheme 3 and Scheme 9)] and do not require an extensive discussion. There are, however, some notable exceptions and these are discussed in the following section.

4.7.2 Synthesis of Laterally Fluoro Substituted Acrylates (Schemes 1 - 6)

The liquid crystal monomers described in this thesis all contain a biphenyl moiety as part of their rigid core. This biphenyl unit was synthesised *via* a palladium catalysed cross-coupling reaction (for example see Scheme 1). The mechanism for this reaction was proposed by Suzuki and is outlined in Figure 4.75.[93]

The mechanism for the cross-coupling reaction can be divided essentially into three steps. These are the oxidative addition of the palladium catalyst involving the aryl bromide, the transmetallation of the boronic acid and the reductive elimination of the catalyst complex.
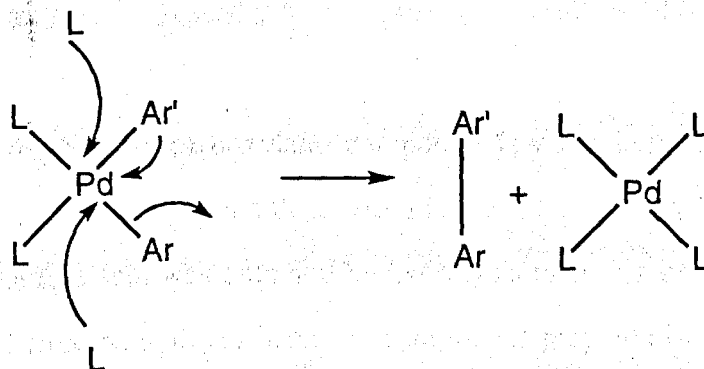
Step 1 - Oxidative Addition
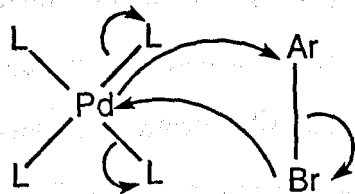
Step 2 - Transmetallation
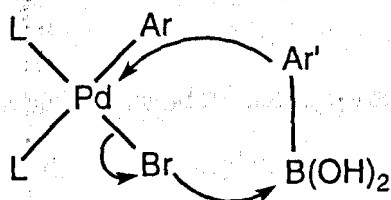
Step 3 - Reductive Elimination

L = PPh$_3$
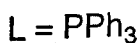
Figure 4.75 - Mechanism Proposed for a Palladium Catalysed Cross-Coupling Reaction[93]

The acid group of the biphenyl core was protected from further reaction by esterification with methanol, prior to the addition of the flexible spacer through a simple alkylation. The free acid was obtained by hydrolysis in strong base (Scheme 2).

Hydroxybenzoate esters (*e.g.*, compound **14**) were prepared by the widely used method outlined in Scheme 3.[86] Fluoro-substituted hydroxybenzoates (*e.g.*,

compound **20**) were prepared by the more complex routes outlined in Schemes 4 and 5. The bromo-substituted phenol was protected at the phenol moiety, with a benzyl group, before being treated with butyllithium followed by carbon dioxide and dilute acid to yield the corresponding carboxylic acids. These acids were then esterified using the Mitsunobu reaction[85] and the benzyl group was removed by catalytic hydrogenolysis (Schemes 4 and 5).

These substituted and unsubstituted hydroxybenzoates were then esterified (*e.g.*, Scheme 6) with the biphenyl acids[87] and the products from these reactions stirred at room temperature with sodium acrylate in hexamethylphosphoramide (HMPA) to yield the required monomeric materials.

4.7.3 Synthesis of C_{12} Spacer Acrylates (Scheme 7)

Methyl 4'-hydroxybiphenyl-4-carboxylate (compound **7**) was alkylated with 12-bromododecan-1-ol in order to attach the desired length of flexible spacer to the biphenyl core. The free acid was obtained by hydrolysis in strong base and this acid was esterified with the hydroxy benzoate compounds prepared in scheme 3. These compounds were reacted with acryloyl chloride, in the presence of an organic base, to yield the required acrylate materials.

4.7.4 Synthesis of Monomers Based on Allyl Alcohol (Schemes 8 - 10)

11-Bromoundecan-1-ol was protected at the alcohol group by reaction with 3,4-dihydro-2*H*-pyran and the product was then reacted with allyl alcohol *via* a Williamson style etherification to give compound **43**. The tetrahydropyranyl protecting group was removed by reaction with a molar equivalent of weak acid (Scheme 8) to give compound **44**.

Methyl 4'-hydroxybiphenyl-4-carboxylate (compound **7**, Scheme 10) was benzylated by reaction with benzyl bromide in the presence of a weak base and the resulting compound hydrolysed at the ester group. This acid was esterified with the hydroxybenzoate compounds prepared in schemes 3 and 9. The benzyl group was removed by catalytic hydrogenolysis and these products were reacted with compound **44** in a Mitsunobu reaction to give the required target molecules.

4.7.5 Synthesis of Acrylonitrile Monomers (Schemes 11 and 12)

α-Hydroxymethylacrylonitrile (**59**) was prepared *via* a Wittig-Horner reaction of the commercially available phosphonate ester with aqueous formaldehyde in basic conditions.[88] The product was esterified with 4-nitrobenzoic acid to produce a molecule with a good leaving group, as required in a subsequent reaction (Scheme 11).

The flexible spacer was attached to the rigid core and esterified with a hydroxybenzoate, in a similar manner to that described in section 4.7.3, to give compounds **63 - 65**. These compounds were treated with a strong base (sodium hydride) to give the alkoxide ion, and α-(4-nitrophenylcarbonyloxymethy)acrylonitrile, (**60**) was then added to yield the monomeric compounds **66 - 68** (Scheme 12).

4.7.6 Synthesis of Monomers Containing a Reversed Ester (Scheme 13)

11-Bromoundecanoic acid was esterified with benzyl alcohol and the ester was reacted with compound **54** under mildly basic conditions to give compound **70**. The benzyl group was removed by catalytic hydrogenolysis and the resulting carboxylic acid was esterified with either ally alcohol or α-hydroxymethylacrylonitrile to give the target monomers **72** and **73** (Scheme 13).

4.7.7 Synthesis of α-Fluoroacrylate Monomers
(Schemes 14 - 17)

α-Fluoroacrylic acid is not a commercially available material and its sodium salt was obtained by the synthetic route reported by Tolman et al.[89] (Scheme 14).

Compounds **92** and **93** (Scheme 16) were prepared by alkylation of 4-bromo-2-fluorophenol (**83**) using the Mitsunobu reaction, followed by the formation of a boronic acid, which was coupled with 1-bromo-4-(tetrahydropyran-2-yloxy)benzene (compound **89**) using the palladium catalysed cross coupling reaction outlined in Figure 4.75. The tetrahydropyranyl group was removed in acidic conditions.

The target monomers **96** and **97** were obtained by a similar route to that described in section 4.7.2 (Scheme 17).

CHAPTER 5
CONCLUSIONS

CONCLUSIONS

5.1 INTRODUCTION

In this thesis the effect of several structural variations in side chain liquid crystal polymers (SCLCPs) has been reported. Figure 5.1 gives a schematic representation of a side chain liquid crystal monomer, with particular emphasis on the structural changes which have been considered in this thesis. This section examines the effects of the structural variations systematically and draws conclusions from the results obtained.
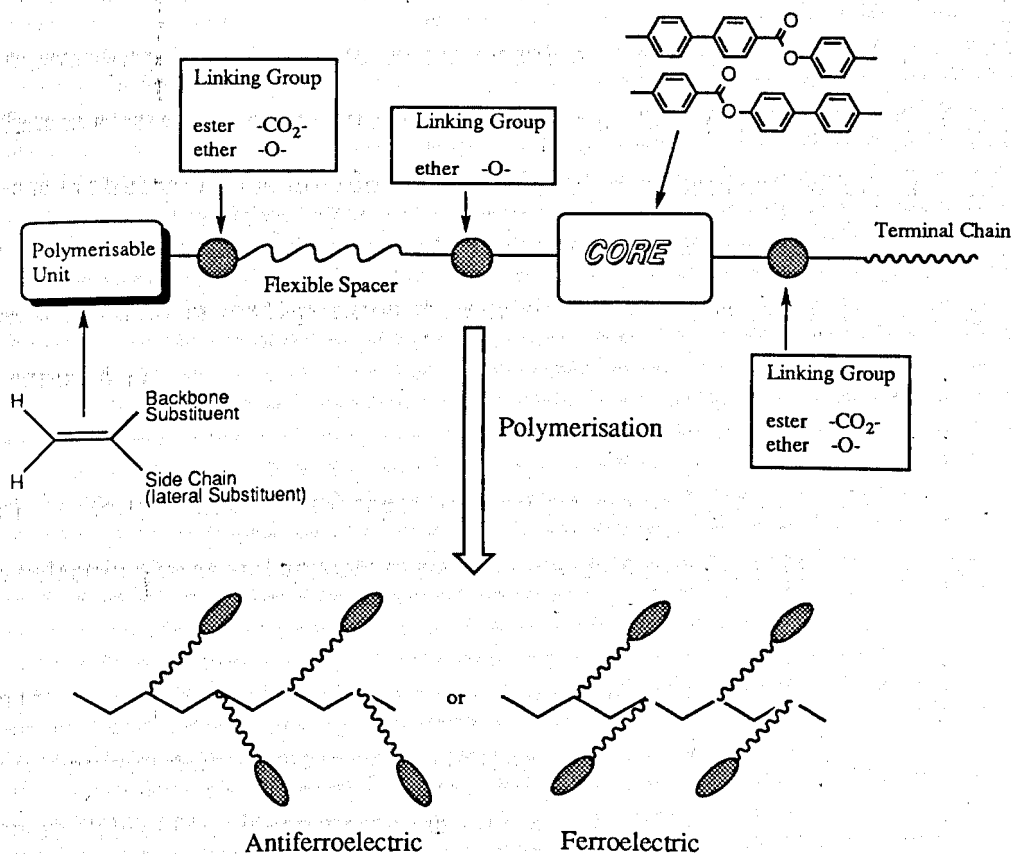

Figure 5.1 - Schematic Representation of the Generalised Molecular Structural Features Investigated in this Thesis

The results arising form the work reported in this thesis are as follows.

5.2 THE EFFECT OF LATERAL FLUORO SUBSTITUTION ON THE LIQUID CRYSTAL PROPERTIES OF SOME SIDE CHAIN LIQUID CRYSTALLINE ACRYLATES

(a)   The insertion of a lateral fluoro substituent into the rigid core of a liquid crystal acrylate and poly(acrylate) has the effect of reducing the transition temperatures of the monomeric and polymeric materials prepared (Section 4.1).

(b)   In the monomeric materials the isotropization temperatures and melting points of the materials decrease. This occurs to the greatest extent when the fluoro substituent is 'facing inwards' (in the 2-position). The S_A - S_C* transition temperature is also decreased by the insertion of a lateral fluoro substituent; the effect is greatest when the fluoro substituent is in the 2-position. The ferrielectric phase is affected by the insertion of a lateral fluoro substituent; with the substituent in the 3-position the temperature at which the phase occurs is decreased and with the substituent in the 2-position the ferrielectric phase is completely suppressed (Section 4.1).

(c)   Polymerisation of these monomers suppresses the ferroelectric and ferrielectric phases and appears to stabilise the antiferroelectric phase (Section 4.1).

(d)   Insertion of a lateral fluoro substituent into the rigid core of a liquid crystal poly(acrylate) reduces the temperature range over which the antiferroelectric phase occurs. This effect is most pronounced when the fluoro substituent is in the two-position (Section 4.1).

(e)   Liquid crystal acrylates and poly(acrylates) containing an achiral, swallow tailed terminal group have been prepared and they generate an antiferroelectric-like

structure. These molecules do not show ferroelectric or ferrielectric phases (Section 4.1).

5.3 THE EFFECT OF ALTERING THE FLEXIBLE SPACER LENGTH ON THE LIQUID CRYSTAL PROPERTIES OF SOME SIDE CHAIN LIQUID CRYSTAL ACRYLATES

(a)   Increasing the length of the flexible spacer (Figure 5.1) in a liquid crystal acrylate by one carbon unit (from C_{11} to C_{12}) has no effect on the phase sequence for the low molar mass materials; each of the monomeric C_{12} materials has identical phase sequences to those for the C_{11} analogues. The liquid crystal mesophases are, however, thermally stabilised by the increase in length of the spacer (Section 4.2).

(b)   Polymerisation of the monomers of increased spacer length (C_{12}) stabilises the ferroelectric phase and suppresses the ferrielectric and antiferroelectric phases, of the polymers and reveals an odd / even effect. That is, when the spacer length between the polymer main chain and the rigid core of the mesogen contains an odd number of carbons (C_{11}), the resulting smectic C phase is antiferroelectric, but when the spacer contains an even number of carbons (C_{12}) then the smectic C phase is ferroelectric (Section 4.2).

(c)   Liquid crystalline acrylates and poly(acrylates) containing an achiral, swallow tailed terminal group and a C_{12} flexible spacer have been prepared. The monomeric materials exhibit an antiferroelectric mesophase but no ferroelectric or ferrielectric properties. The polymeric materials show a ferroelectric phase but no antiferroelectric or ferrielectric phases (Section 4.2).

5.4 THE EFFECT OF CHANGING THE POLYMER BACKBONE ON THE LIQUID CRYSTAL PROPERTIES OF SOME SIDE CHAIN LIQUID CRYSTAL POLYMERS

(a) Changing the linking group between the flexible spacer and the polymerisable unit (Figure 5.1) in vinylic liquid crystalline materials, from an ester link to an ether link, affects the phase sequence of the resulting monomer. In optically active materials with an ether link, no ferroelectric and ferrielectric phases are observed (Section 4.3).

(b) Liquid crystal monomers containing an achiral, swallow tailed terminal group and an ether moiety linking the flexible spacer to the vinylic unit, have been prepared and these exhibit an antiferroelectric mesophase. These molecules show no ferroelectric or ferrielectric phases (Section 4.3).

(c) Insertion of an ether moiety as the linking unit between the flexible spacer and the polymerisable group appears to thermally stabilise the liquid crystal phase in the monomeric material when compared to acrylate materials of similar structure. In addition the tendency of an antiferroelectric phase to form is increased (*i.e.*, the temperature range over which the phase occurs is increased) (Section 4.3).

(d) Polymerisation of monomers where the linking group is an ether moiety increases the isotropization temperatures, but lowers the melting point in the case of the optically active materials.(Section 4.3).

5.5 THE EFFECT OF ALTERING THE POLYMER BACKBONE SUBSTITUENT ON THE LIQUID CRYSTAL PROPERTIES OF SOME SIDE CHAIN LIQUID CRYSTAL POLYMERS

(a)   Increasing the size and polarity of the backbone substituent

(i)   has no effect on the ability on the formation of an antiferroelectric mesophase (Section 4.4).

(ii)   suppresses the formation of ferroelectric or ferrielectric mesophases (Section 4.4).

(iii)   increases the thermal stability of the liquid crystalline phase slightly (Section 4.4).

(iv)   does not affect the formation of an antiferroelectric mesophase, in materials with a 'swallow-tailed' terminal chain (Section 4.4).

(b)   Polymerisation of materials with a cyano backbone substituent and an ether link to the flexible spacer results in polymers with an identical phase sequence to the monomeric materials. The thermal stability and the temperature range over which the alternating phases of the materials occur is increased. Increasing the size and polarity of the backbone substituent increases the thermal stability of the polymeric materials (Section 4.4).

5.6 THE EFFECT OF INSERTION OF A REVERSED ESTER IN THE FLEXIBLE SPACER ON THE LIQUID CRYSTAL PROPERTIES OF SOME SIDE CHAIN LIQUID CRYSTAL POLYMERS

(a) Insertion of a 'reversed ester', at a point away from the rigid core, in the monomeric material suppresses the formation of a smectic C phase. Polymerisation of these materials gives polymers where the formation of tilted smectic phases is suppressed. The mesophase obtained for the polymer material is thermally stabilised with respect to the monomeric material (Section 4.5).

5.7 THE EFFECT OF POLYMERISATION ON THE LIQUID CRYSTAL PROPERTIES OF SOME SIDE CHAIN LIQUID CRYSTAL α-FLUOROACRYLATES

(a) Liquid crystal poly(α-fluoroacrylate) materials appear to contain a high degree of rigidity in the polymer backbone, which appears to suppress alignment of the polymer side chains (Section 4.6).
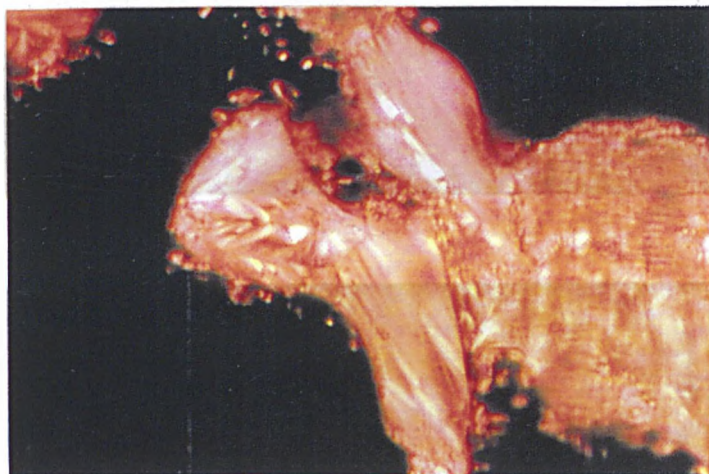
APPENDIX

APPENDIX

Plate 1 - Smectic A Texture Exhibited by Compound 27 (104.4 °C)

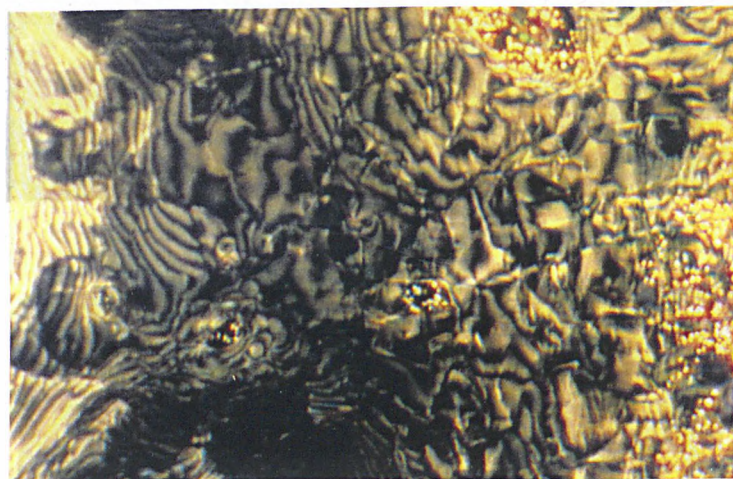Plate 2 - Smectic C_A* Texture Exhibited by Compound 29 (53.1 °C)

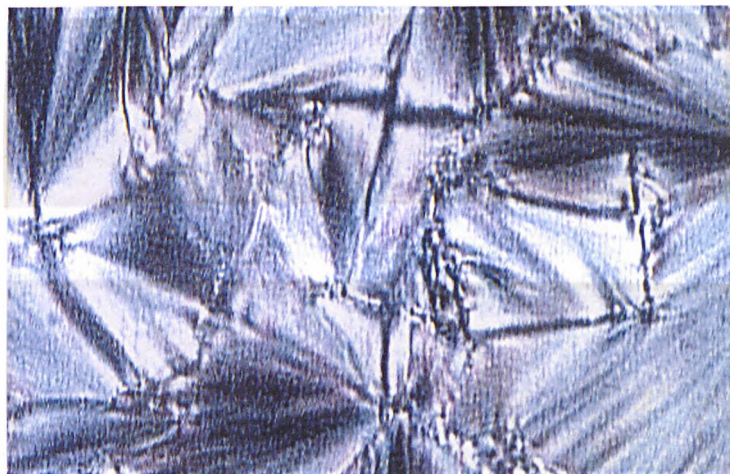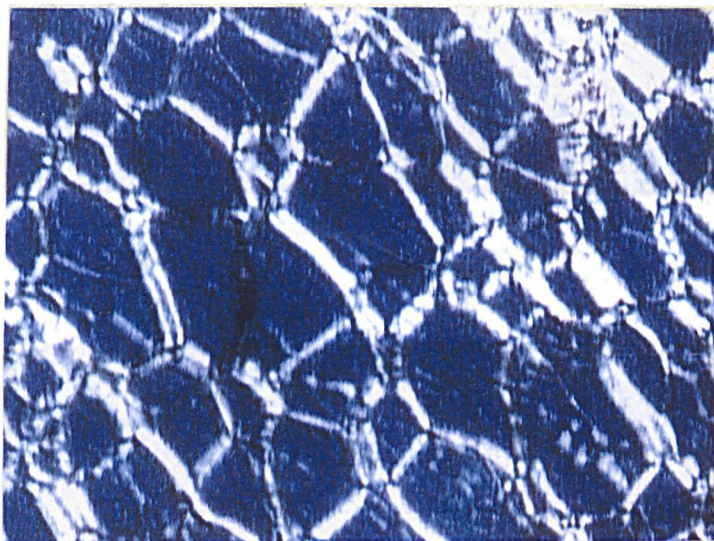Plate 3 - Smectic Cγ Texture Exhibited by Compound 30 (79.2 °C)

Plate 4 - Smectic A Texture Exhibited by Compound 51 (176.6 °C)

Plate 5 - Chiral Nematic Texture Exhibited by Compound 94 (142.2 °C)

REFERENCES

REFERENCES

1) F. Reinitzer, *Monatsch. der Weiner Chem. Ges.*, **9**, 421 (1888)

2) O. Lehmann, *Z. Physik. Chem. (Leipzig)*, **4**, 462 (1889)

3) G. Friedel, *Ann. Phys.*, **18**, 273 (1922)

4) a) R. Williams, *Nature*, **199**, 273 (1963)

   b) R. Williams, *J. Phys. Chem.*, **39**, 384 (1963)

5) G.H. Heilmeyer, L.A. Zanoni and L.A. Barton, *Proc. IEEE*, **56**, 1162 (1968)

6) M. Schadt and W. Helfrich, *Appl. Phys. Lett.*, **18**, 127 (1971)

7) T.J. Scheffer and J. Nehring, *Appl. Phys. Lett.*, **45**, 1021 (1984)

8) Idemitsu Display demonstrated at Fourth International Conference of Ferroelectric Liquid Crystals, 28th September to 1st October, Tokyo, Japan (1993)

9) E.B. Priestly, *"Introduction to Liquid Crystal Phases"*, Ed P.J. Wojkawicz and E.B. Priestly, Plenum Press, London (1979)

10) N. Boden, R.J. Bushby, J. Clements, M.V. Jesudason, P.F. Knowles and G. Williams, *Chem. Phys. Lett.*, **152**, 94 (1988)

11) G.W. Gray, *"Molecular Structure and the Properties of Liquid Crystals"*, Academic Press, London (1962)

12) H. Finkelmann, *Philos. Trans. R. Soc. London*, **A309**, 105, (1983)

13) G.W Gray and J.W. Goodby, *"Smectic Liquid Crystals"*, Leonard Hill, London (1984)

14) D. Coates and G.W. Gray, *Phys. Lett.*, **45A**, 115 (1973)

15) N. Hiji, A.D.L. Chandani, S. Nishiyama, Y. Ouchi, H. Takezoe and A. Fukuda, *Ferroelectrics*, **85**, 99 (1988)

16) A. Fukuda, Y. Takanishi, T. Isozaki, K. Ishikawa and H. Takezoe, *J. Mater. Chem.*, **4**, 997 (1994)

17) J.F. Johnson and R.F. Porter, *Analytical Calorimetry*, Plenum Press, New

York (1968)

18)   J. Valasek, *Phys. Rev.*, **17**, 475 (1921)

19) a) R.B. Meyer, *Mol. Cryst. Liq. Cryst.*, **40**, 33 (1977)

   b) R.B. Meyer, L. Liebert, L. Strzelecki and P. Keller, *J. Phys. (Lett.)*, **30**, L69 (1975)

20)   P.G. de Gennes, *"The Physics of Liquid Crystals"*, OUP, Oxford, (1974)

21)   J.S. Patel and J.W. Goodby, *Opt. Eng.*, **26**, 373 (1987)

22)   G.W. Gray and D.G. McDonnell, *Mol. Cryst. Liq. Cryst. Lett.*, **34**, 211 (1977)

23)   J.W. Goodby and E. Chin, *J. Am. Chem. Soc.*, **108**, 4736 (1986)

24)   J.S. Patel and J.W. Goodby, *Mol. Cryst. Liq. Cryst.*, **144**, 117 (1987)

25)   J.W. Goodby, J.S. Patel and E. Chin, *J. Phys. Chem.*, **91**, 5151 (1987)

26)   K. Yoshino, M. Ozaki, T. Sakurai, K. Sakamoto and M. Honma, *Jpn. J. Appl. Phys.*, **23**, L175 (1984)

27)   C. Bahr and G. Heppke, *Mol. Cryst. Liq. Cryst.*, **148**, 29 (1987)

28)   M. Kawada, Y. Uesugi, K. Matusumura, Y. Sudo, K. Kondo and T. Kitamura, *Abst. 16th Jpn. Liq.Cryst. Conf*, Hiroshima (1990)

29)   M. Koden, T. Kuratate, F. Funada, K. Awane, K. Sakaguchi, Y. Swiomi, and T. Kitamura, *Jpn. J. Appl. Phys.*, **29**, L981, (1990)

30)   N.A. Clark and S.T. Lagerwall in *"Liquid Crystals of One and Two Dimensional Order"*, Ed W. Helfrich and G. Heppke, Springer-Verlag, Berlin (1980)

31)   G.W. Gray, M. Hird, D. Lacey and K.J. Toyne, *Mol. Cryst. Liq. Cryst.*, **191**, 1 (1990)

32)   P. Martinot-Lagarde, R. Duke and G. Durand, *Mol. Cryst. Liq. Cryst.*, **75**, 249 (1981)

33)   J.S. Patel and J.W. Goodby, *Philos. Mag. Lett.*, **55**, 283 (1987)

34)   N.A. Clark and S.T. Lagerwall, *Appl. Phys. Lett.*, **36**, 899 (1980)

35)   B. Urbanc and B. Zecks, *Liq. Cryst.*, **5**, 1075 (1989)

36) H. Stegemeyer, R. Meister, U. Hoffmann and W. Kuczynski, *Liq. Cryst.*, **10**, 295 (1991)

37) J.W. Goodby, E. Chin, J.M. Geary, J.S. Patel and P.L. Finn, *J. Chem. Soc. Faraday Trans 1*, **83**, 3429 (1987)

38) N. Mikami, R. Higuchi, T. Sakurai, M. Ozaki and K. Yoshino, *Jpn. J. Appl. Phys.*, **25**, L833 (1986)

39) K. Furukawa, K. Terashima, M. Ichihashi, S. Saitoh, K. Miyazawa and T. Inukai, *Ferroelectrics*, **85**, 63 (1988)

40) A.D.L. Chandani, T. Hagiwara, Y. Suzuki, Y. Ouchi, H. Takezoe and A. Fukuda, *Jpn. J. Appl. Phys.*, **27**, L729 (1988)

41) A.D.L. Chandani, Y. Ouchi, H. Takezoe, A. Fukuda, K. Terashima, K. Furukawa and A. Kishi, *Jpn. J. Appl. Phys.*, **28**, L1261 (1989)

42) M. Fukui, H. Orikawa, Y. Yamada, N. Yamamoto and Y. Ishibashi, *Jpn. J. Appl. Phys.*, **28**, L849 (1989)

43) E. Gorecka, A.D.L. Chandani, Y. Ouchi, H. Takezoe and A. Fukuda, *Jpn. J. Appl. Phys.*, **29**, 131 (1990)

44) A. Suzuki, H. Orihari, Y. Ishibashi, Y. Yamada, N. Yamamoto, K. Mori K. Nakamura, T. Hariwari, I. Kawamura, and M. Fukuda, *Jpn. J. Appl. Phys.*, **29**, L336 (1990)

45) M. Yamawaki, Y. Yamada, N. Yamamoto, K. Mori, H. Hayashi, Y. Suzuki, Y.S. Negi, T. Hagiwari, I. Kawamura, H. Orihari and Y. Ishibashi, Proc. 9th Int Disp. Res. Conf., p26, Kyoto, Japan (1989)

46) I. Nishiyama, A. Yoshizawa, M. Fukumasa and T. Hirai, *Jpn. J. Appl. Phys.*, **28**, L2248 (1989)

47) a) T. Hagiwari, Y. Suzuki, Y. Arihari, Y. Sadamune, Y.S. Negi, I. Kawamura, Y. Yamada, N. Yamamoto and K. Mori., Abst. 15th Jpn. Liq. Cryst. Conf., p304, Osaka (1989)

b) H. Takeda, H. Miyabe, S. Takenaka and S. Kusabayashi, Abst, 16th Jpn. Liq. Cryst. Conf. p134, Hiroshima (1990)

48) S. Inui, S. Kawano, M. Saito, H. Iwane, Y. Takamishi, K. Hiraoka, Y. Ouchi, H. Takezoe and A. Fukuda, *Jpn. J. Appl. Phys.*, **29**, 987 (1990)

49) H. Takezoe, J. Lee, A.D.L. Chandani, E. Gorecka, Y. Ouchi, A. Fukuda, K. Terashima and K. Furukawa, *Ferroelectrics*, **114**, 187 (1991)

50) W.H. Carothers, *J. Am. Chem. Soc*, **51**, 2548 (1929)

51) J.F. Johnson and R.F. Porter, *Analytical GPC*, John Wiley and Sons, New York (1968)

52) B. Reck and H. Ringsdorf, *Makromol. Chem. Rapid. Commun.*, **6**, 291 (1985)

53) B. Reck and H. Ringsdorf, *Makromol. Chem. Rapid. Commun.*, **7**, 359 (1986)

54) J. Watanabe, M. Goto and T. Nagase, *Macromolecules*, **20**, 298 (1987)

55) W.J. Jackson and H. F. Kuhfuss, *J. Polym. Sci.:Polym. Chem. Ed.*, **14**, 2043 (1976)

56) F.E. McFarlane, V.A. Nicely and T.C. Davis in "*Contemporary Topics in Polymer Science* ", Ed. E.M. Pearce and J.R. Schaefgen, vol **2**, p109, New York (1977)

57) B.P. Griffin and M.K. Cox, *Brit. Polym. J.*, **12**, 147 (1980)

58) A. Roviello and A. Sirigu, *J. Polym. Sci.: Polym. Lett. Ed.* , **13**, 455 (1975)

59) a) H. Finkelmann, *Angew. Chem. Int. Edn. Engl.*, **26**, 816 (1987)

   b) H. Finkelmann, H. Ringsdorf, W. Siol and J.H. Wendorff in , *Mesomorphic Order in Polymers and Polymerisation in Liquid Crystalline Media*, ACS Symp. Ser., **74**, ed. A. Blumstein, American Chemical Society, Washington DC (1978)

60) J. Horvath, F. Cser and G. Hardy, *Prog. Coll. Polym. Sci.*, **71**, 59 (1985)

61) M.D. Portugall, H. Ringsdorf and R. Zentel, *Makromol. Chem.*, **183**, 2311, (1982)

62) M.A. Apfel, H. Finkelmann, G.M. Janini, R.J. Lamb, B.H. Luhmann, A. Price, W.L Robers, T.J. Shaw and C.A. Smith, *Anal. Chem.*, **57**, 651

(1985)

63) B.A. Newmann, V. Frosini and P.L. Maganini in *"Mesomorphic Order in Polymers"* Ed. A. Blumstein, A.C.S. Symposium Series, **74**, 71 (1978)

64) B. Hahn, J.H. Wendorff, M.D. Portugall and H. Ringsdorf, *Colloid Polym. Sci.*, **259**, 875

65) A. Frosini, G. Levita, G. Lupinacci and P.L. Maganini, *Mol. Cryst. Liq. Cryst.*, **66**, 21

66) V.P. Shibaev, M.V. Kozlovsky, L.A. Beresnev, L.A. Blinov and N.A. Platé, *Polym. Bull.*, **12**, 299, (1984)

67) V.P. Shibaev, M.V. Kozlovsky, N.A. Platé, L.A. Beresnev and L.A. Blinov, Vysokomol. Soedin, **29**, 1470 (1987)

68) J.M. Guglielminetti, G. Decobert and J.C. Dubois, *Polym. Bull.*, **16**, 411 (1986)

69) G. Decobert, J.C. Dubois, S. Esselin and C. Nöel, *Liq. Cryst.*, **1**, 307, (1986)

70) G. Scherowsky, K. Kuhnpast and J. Springer, *Makromol. Chem. Rapid Commun.*, **12**, 381 (1991)

71) K. Skarp, G. Andersen, S.T. Lagerwall, H. Kapitsa, H. Poths and R. Zentel, *Ferroelectrics*, **122**, 127 (1991)

72) J.W. Goodby, *J. Mater. Chem.*, **1**, 307 (1991)

73) J.G. Grabmaier, *in "Application of Liquid Crystals"*, Ed. G. Meier, E. Sackmann and J.G. Grabmaier, Springer-Verlag, Berlin-New York, pp83 - 160 (1975)

74) P.P. Crooker, *Liq. Cryst.*, **5**, 751 (1989)

75) a) K. Yoshino, S. Kishio, M. Ozaki, T. Sakurai, N. Mikami and M. Honma, *Jpn. J. Appl. Phys.*, **25**, L416 (1986)

   b) K. Yoshino and M. Ozaki, *Jpn. J. Appl. Phys.*, **24**, 130 (1985)

76) *"Ferroelectric Liquid Crystals - Principles Properties and Applications"*, R. Blinc, N.A. Clark, J.W. Goodby, S.T. Lagerwall, M.A. Osipov, S.A.

Pikin, T. Sakurai, K. Yoshino, and B. Zeks, Gordon and Breach, Philadelphia and Reading (1991)

77) A.D.L. Chandani, E. Gorecka, Y. Ouchi, H. Takezoe and A. Fukuda, *Jpn. J. Appl. Phys.*, **28**, L1265 (1989)

78) G. Scherowsky, K. Kuhnpast and J. Springer, *Makromol. Chem. Rapid Commun.*, **12**, 381 (1991)

79) I. Sage, D.G. McDonnell, K.P. Lymer, K.M. Blackwood, J.M. Blackmore, D. Coates, D.R. Beattie, M. Verrall, J.W. Goodby and M.J. Watson, to be published

80) I. Nishiyama and J.W. Goodby, *J. Mater. Chem.*, **3**, 169 (1994)

81) M. Verrall, Private Communication (1995)

82) G.W. Gray, M. Hird and K.J. Toyne, *Mol. Cryst. Liq. Cryst.*, **204**, 43 (1991)

83) W.C. Still, M. Kahn and A. Mitra, *J. Org. Chem.*, **23**, 2923 (1978)

84) *"CRC Handbook of Physics and Chemistry"*, ed. R.C. Weast, 67th Edition, CRC Press (1988)

85) O. Mitsunobu, *Synthesis*, 1 (1981)

86) E. Chin and J.W. Goodby, *Mol. Cryst. Liq. Cryst.*, **141**, 311 (1986)

87) M. Smith, J.G. Moffat and H.G. Khorana, *J. Am. Chem. Soc.*, **80**, 6204 (1958)

88) M. Ueda, K. Kawaguchi and M. Mano, *J. Polym. Sci. Part A. Polym. Chem.*, **27**, 737 (1989).

89) V. Tolman and P. Spronglova, *Coll. Czech. Chem. Commun.*, **48**, 319 (1983)

90) I. Nishiyama and J.W. Goodby, *J. Mater. Chem.*, **2**, 1015 (1994)

91) C. Nöel, *"Side Chain Liquid Crystal Polymers"*, Ed. C.B. McArdle, Blackie, Glasgow and London, 1980, p. 180 and references therein

92) J.M.G. Cowie, *"Polymers : Chemistry and Physics of Modern Materials"*, Intertext, p202 (1973)

93) a) M. Miyaura, T. Yanagi and A. Suzuki, *Synth. Comm.*, **11**, 513 (1981)

b) G.B. Smith, G.C. Dezeny, D.L. Hughes, A.O. King and T.R. Verhoeven, *J. Org. Chem.*, **59**, 8151 (1994)

c) A.R. Martin and Y. Yang, *Acta Chem. Scand.*, **47**, 221 (1993)